The Second International Conference

on

The Chemistry and Physics of the Transactinide Elements

Honoring the Scientific Achievements of Darleane C. Hoffman

Napa, California, USA
November 16-20, 2003

www.tan03.lbl.gov

— EXTENDED ABSTRACTS —

[This page was left blank intentionally.]

Conference Chairpersons

Prof. H. Nitsche (Berkeley)
Dr. K.E. Gregorich (Berkeley)
Dr. K.J. Moody (Livermore)

International Advisory Committee

Prof. H.W. Gäggeler (Bern)
Prof. B. Fricke (Kassel)
Prof. D.C. Hoffman (Berkeley)
Dr. S. Hofmann (Darmstadt)
Prof. U. Kaldor (Tel Aviv)
Prof. J.-V. Kratz (Mainz)
Prof. M. Leino (Jyväskylä)
Prof. W.D. Loveland (Corvallis)
Prof. G. Münzenberg (Mainz)
Dr. Y. Nagame (Tokai)
Prof. H. Nakahara (Tokyo)
Prof. W. Nazarewicz (Knoxville)
Prof. Yu.Ts. Oganessian (Dubna)
Dr. V. Pershina (Darmstadt)
Prof. P. Pyykkö (Helsinki)
Dr. M. Schädel (Darmstadt)
Prof. A. Sobiczewski (Warsaw)
Dr. N. Trautmann (Mainz)
Prof. A. Türler (Munich)
Dr. V.K. Utyonkov (Dubna)

Local Organizing Committee

Dr. Ch.E. Düllmann (Berkeley)
Mr. C.M. Folden III (Berkeley)
Ms. D. Jacobs (Berkeley)
Dr. J.B. Patin (Livermore)
Ms. L.Y. Planka (Berkeley)
Dr. D.A. Shaughnessy (Livermore)
Ms. A.M. Smith (Berkeley)
Dr. M.A. Stoyer (Livermore)
Dr. R. Sudowe (Berkeley)
Dr. J.F. Wild (Livermore)
Mr. P.M. Zielinski (Berkeley)

TAN 03 was organized by:

Nuclear Science Division, Lawrence Berkeley National Laboratory
The Glenn T. Seaborg Institute, Lawrence Livermore National Laboratory

Conference Address

TAN 03
c/o Lawrence Berkeley National Laboratory
Mailstop 70R0319
One Cyclotron Road
Berkeley, CA 94720-8169 USA

Contact Information

Phone: +1-510-486-7535
Fax: +1-510-486-7444
E-mail: tan03@lbl.gov

Conference Website

www.tan03.lbl.gov

Program and Table of Contents

Nuclear Structure Theory and Experiment 1

Oral Contributions

NS-P The structure of superheavy nuclei 3
P.H. Heenen

NS-1 Structure of nuclei in the mass 250 region.....4
I. Ahmad

NS-2 Nuclear structure investigations of heavy actinide and trans-actinide isotopes.....7
F.P. Hessberger

NS-3 Spectroscopy of the heaviest elements.....12
R. Julin

NS-4 Properties of superheavy nuclei 13
R. Smolanczuk

NS-5 Structure of superheavy elements with meson field theory.....14
W. Greiner

NS-6 Limits of stability, formation mechanism and structure of shell-stabilzed heavy nuclei 15
T.L. Khoo, P. Reiter, A. Afanasjev, I. Ahmad, A. Heinz, T. Lauritsen, C.J. Lister, D. Seweryniak, N. Amzal, P.A. Butler, M.P. Carpenter, A.J. Chewter, J.A. Cizewski, C.N. Davids, S. Frauendorf, P.T. Greenlees, K. Helariuta, R.D. Herzberg, G. Jones, R.V.F. Janssens, R. Julin, H. Kankaanpää, H. Kettunen, F. Kondev, P. Kuusiniemi, G.A. Lalazissis, M. Leino, A.A. Sonzogni, S. Siem, I. Wiedenhöver, J. Uusitalo

Poster Contributions

NS-A Charge and mass renormalization in no-photon QED.....19
H. Siedentop, C. Hainzl

NS-B Conversion electron measurement for the α decay of ^{257}No.....20
M. Asai, K. Tsukada, S. Ichikawa, Y. Nagame, T. Ishii, I. Nishinaka, K. Akiyama, A. Osa, M. Sakama, Y. Oura, K. Sueki, M. Shibata

NS-C Pairing correlations in superheavy nuclei.....23
Z. Patyk

NS-D Investigation of the decay property of extremely low-lying isomer ^{229m}Th 24
Y. Kasamatsu, H. Kikunaga, K. Takamiya, T. Mitsugashira, T. Nakanishi, T. Ohtsuki, H. Yuki, W. Sato, H. Yamana, Y. Ohkubo, H. Kimura, S. Shibata, Y. Kawase, A. Shinohara

NS-E Super- and hyperdeformed isomeric states and long-lived superheavy elements 31
A. Marinov, S. Gelber, D. Kolb, R. Brandt, R.V. Gentry, A. Pape

Nuclear Reaction Theory..... 35

Oral Contributions

NT-P Theoretical predictions of residue cross-sections for the superheavy elements.....37
Y. Abe, B. Bouriquet, G. Kosenko, C. Shen

NT-1 The physics of nucleus-nucleus fusion 41
W. Swiatecki

NT-2 Production of spherical super-heavy nuclei 42
K.H. Schmidt, A. Heinz, A.R. Junghans

NT-3 Open

NT-4 Fusion-fission dynamics and perspectives of superheavy element formation.....45
V.I. Zagrebaev

NT-5 The cold formation and decay of superheavy nuclei including the orientation degree of freedom.....50
R.K. Gupta, M. Balasubramaniam, R. Kumar, N. Singh

Poster Contribution

NT-A Four-dimensional dynamical approach to the multi-modal fission.....55
T. Wada, T. Asano, M. Ohta

Chemical Experiments 57

Oral Contributions

CE-P Current status and future of transactinide heavy element chemistry...59
A. Türler

CE-1 Gas phase chemistry of bohrium (element 107) 63
R. Eichler

CE-2 Chemical investigations of element 108, hassium (Hs).....67
Ch.E. Düllmann

CE-3 Chemical properties of element 112.....73
A. Yakushev

CE-4 Anion-exchange behavior of rutherfordium and dubnium in pure HF solution.....78
K. Tsukada, H. Haba, M. Asai, K. Akiyama, A. Toyoshima, I. Nishinaka, M. Hirata, K. Hashimoto, S.I. Ichikawa, Y. Nagame, K. Yasuda, Y. Miyamoto, Y. Tani, H. Hasegawa, W. Sato, A. Shinohara, S.I. Goto, M. Ito, J. Saito, H. Ishizu, H. Kudo, Y. Oura, K. Sueki, H. Nakahara, N. Kinoshita, H. Kikunaga, A. Yokoyama, M. Sakama, M. Schädel, J.V. Kratz

CE-5 Current status of transactinide research with the liquid-liquid extraction system SISAK.....81
J.P. Omtvedt, J. Alstad, D. Polakova, G. Skarnemark, L. Stavsetra, L. Zheng

CE-6 X-ray absorption fine structure spectroscopy of Zr and Hf in HCl solution for chemical characterization of Rf 85
H. Haba, K. Akiyama, K. Tsukada, M. Asai, A. Toyoshima, T. Yaita, M. Hirata, K. Sueki, Y. Nagame

Poster Contributions

CE-A First results of the CALLISTO-experiment: evidence for the formation of a hassate(VIII) 88
A. von Zweidorf, R. Angert, W. Brüchle, S. Bürger, K. Eberhardt, R. Eichler, H. Hummrich, E. Jäger, R. Jera, H.O. Kling, J.V. Kratz, U. Krille, B. Kuczewski, G. Langrock, G. Lehr, M. Mendel, A. Nähler, A. Peil, V. Pershina, U. Rieth, M. Schädel, B. Schausten, E. Schimpf, H.J. Schött, E. Stiel, P. Thörle, N. Trautmann, K. Tsukada, N. Wiehl, G. Wirth

CE-B Gas phase studies of volatile group 4 metal complexes using the BGS - test experiments with Zr and Hf 92
Ch.E. Düllmann, G.K. Pang, C.M. Folden III, K.E. Gregorich, D.C. Hoffman, H. Nitsche, R. Sudowe, P.M. Zielinski

CE-C Simultaneous measurement of volatility of Zr, Hf and Rf 96
T. Kaneko, K. Tsukada, K. Akiyama, M. Asai, H. Haba, A. Toyoshima, S. Ono, T. Hirai, S. Goto, S. Ichikawa, Y. Nagame, H. Kudo

CE-D Electrochemistry at the tracer scale - an approach to aqueous superheavy element chemistry 100
H. Hummrich, U. Rieth, J.V. Kratz, G. Lehr, M. Mendel, P. Thörle

CE-E Ion exchange and extraction chromatographic studies with homologs of seaborgium (element 106) in HNO_3-HF medium 103
P. Mohapatra, R. Tripathi, J.V. Kratz, A. Kronenberg, B.S. Tomar, A.V.R. Reddy, G. Pfrepper

CE-F A liquid-liquid extraction system suitable for studying the chemistry of rutherfordium with SISAK 105
D. Poláková, G. Skarnemark, J. Alstad, L. Stavsetra, L. Zheng, J.P. Omtvedt

CE-G Evidence for a very noble element 112 108
S. Soverna, R. Eichler, H.W. Gäggeler, F. Haenssler, Z. Qin, B. Eichler, R. Dressler, D. Piguet, W. Brüchle, E. Jäger, H.-J. Schött, M. Schädel, B. Schausten, E. Schimpf, K. Eberhardt, J.V. Kratz, P. Törle, N. Trautmann, A. von Zweidorf, A. Türler, P. Wilk, A.B. Yakushev, C.E. Düllmann, C.M. Folden III, K.E. Gregorich

CE-H Investigation of alpha-electron coincidences in data from liquid scintillation detection 113
L. Stavsetra, J. Alstad, H. Nitsche, D.C. Hoffman, J.P. Omtvedt

CE-I Suitability of extraction systems with macrocyclic ligands for the study of rutherfordium.....117
R. Sudowe, C.E. Düllmann, C.M. Folden III, K.E. Gregorich, D.C. Hoffman, P.M. Zielinski, H. Nitsche

CE-J Development of a selective separation method for element 107 – bohrium – based on fast liquid-liquid extractions 120
B. Wierczinski, K.J. Volkers

CE-K The new isotopes of element 107: Bh-266 and Bh-267 and the chemistry of bohrium 124
P.A. Wilk, J.L. Adams, W. Brüchle, R. Dressler, C.E. Düllmann, B. Eichler, R. Eichler, H.W. Gäggeler, K.E. Gregorich, D.C. Hoffman, S. Hübener, D.T. Jost, U.W. Kirbach, M.R. Lane, C.A. Laue, V.M. Lavanchy, D.M. Lee, H. Nitsche, J.B. Patin, D. Piguet, M. Schädel, D.A. Shaughnessy, D.A. Strellis, S. Taut, L. Tobler, Y.S. Tsyganov, A. Türler, A. Vahle, A.B. Yakushev

Nuclear Reaction Experiments 129

Oral Contributions

NE-P The current status and future of transactinide heavy element production.....131
Yu.Ts. Oganessian

NE-1 Reaction studies and the synthesis of superheavy elements at GSI 132
D. Ackermann

NE-2 Status and future of transactinide reaction experiments at RIKEN 137
K. Morita

NE-3 Sub-barrier fusion in the $^{48}Ca + ^{208}Pb$ reaction.....138
W.D. Loveland, J.B. Patin, D. Peterson, K.E. Gregorich, N. Myers, P. Miranda, T.N. Ginter, K. Aleklett

NE-4 Production and study of super-heavy nuclei at GANIL.....143
J. Péter, A. Drouart, C. Stodel

NE-5 Status and future of the RIA project viz. transactinide elements 144
D.J. Morrissey

NE-6 The RIA project and heavy element physics.....148
J.A. Nolen

Poster Contributions

NE-A Synthesis and mass determination of heavy and superheavy nuclei at separator VASSILISSA 149
A.V. Yeremin, Y.T. Oganessian, A.G. Popeko, O.N. Malyshev, A.V. Belozerov, V.I. Chepigin, M.G. Itkis, A.P. Kabachenko, R.N. Sagaidak, A.V. Shutov, A.I. Svirikhin, S. Hofmann, S. Saro

NE-B Spectroscopy of the transfermium nuclei ^{251}Md 154
A. Chatillon

NE-C Experimental study on photofission of ^{242}Pu, ^{238}U, ^{235}U and ^{232}Th in giant dipole resonance region 155
T.D. Thiep, N.V. Do, N.N. Son, T.T. An

NE-D Synthesis of new heavy nuclei using RNBs 158
W.D. Loveland, M. Cloughesy

NE-E Novel isomer spectroscopy and quasiparticle configurations in ^{254}No.....162
G.D. Jones for the Anglo-Finnish-French S.H.E. collaboration

NE-F Investigation of the 5n and α4n channels in the ^{20}Ne on ^{244}Pu reaction 163
R. Dressler, B. Eichler, D. Piguet, R. Eichler, H.W. Gäggeler, F. Haenssler, S. Soverna, M. Schädel, E. Schimpf, K. Eberhardt, P. Thörle, N. Trautmann

NE-G The search for ^{271}Mt via the reaction ^{238}U + ^{37}Cl.....165
P.M. Zielinski, K.E. Gregorich, Ch.E. Düllmann, C.M. Folden III, P.K. Gupta, D.C. Hoffman, W. Loveland, H. Mahmud, D. Peterson, M. Schädel, J.M. Schwantes, R. Sudowe, H. Nitsche

NE-H Random probability analysis of recent ^{48}Ca experiments 169
J.B. Patin, K.J. Moody, J.H. Landrum, C.A. Laue, D.A. Shaughnessy, M.A. Stoyer, J.F. Wild, V.K. Utyonkov, Y.T. Oganessian

NE-I Structure effects in photofission 170
N.N. Son, T.D. Thiep, P.V. Cuong

Chemical Theory 171

Oral Contributions

CT-P Progress in heavy-element research: results from relativistic quantum theory.....173
V. Pershina

CT-1 Improved density-functional calculations for molecules and calculation of adsorption of the heaviest elements on surfaces 177
B. Fricke

CT-2 Electronic properties for the superheavy elements 111 to 119 from relativistic ab-initio calculations 179
P. Schwerdtfeger, M. Seth

CT-3 High-accuracy calculations for heavy and superheavy elements.....180
U. Kaldor, E. Eliav, A. Landau

CT-4 Spin-orbit coupling in transactinide chemistry: secondary periodicity and effects in high-symmetry ligand fields 182
C.S. Nash

CT-5 Valence-shell QED effects in heavy-element compounds 183
P. Pyykkö

CT-6 Electronic structure of molecules containing very heavy & superheavy elements 184
K. Balasubramanian

Poster Contributions

CT-A Relativistic effects on the electronic structure and volatility of the group-8 tetroxides MO_4 (M=Ru, Os and Hs).....185
T. Bastug, V. Pershina

CT-B Ionic radii of heavy actinide(III) cations 186
A. Bilewicz

CT-C Adsorption of element 112 on Au surface.....191
C. Sarpe-Tudoran, J. Anton, W. Sepp, B. Fricke, V. Pershina

CT-D Relativistic mixed-sector intermediate hamiltonian coupled cluster method: theory and applications 192
E. Eliav, U. Kaldor, A. Landau

Methods and Future Developments..... 193

Oral Contributions

MD-P Physical and chemical techniques to investigate the heaviest elements – Presence and future 195
H.W. Gaeggeler

MD-1 Ion source developments for heavy element research 197
D. Leitner

MD-2 Recoil separator capabilities for heavy element research and an opportunity for second generation chemistry studies 198
K.E. Gregorich

MD-3 Heavy element research with laser spectroscopy and traps.....199
H. Backe

MD-4 Status and future developments in the aqueous heavy element chemistry 200
J.V. Kratz

MD-5 The status and future of heavy element research at Dubna 204
S.N. Dmitriev, Yu.Ts. Oganessian, M.G. Itkis

MD-6 Development of an on-line hot catcher for volatile species 205
Z. Qin, R. Eichler, H. Gaeggeler, F. Haenssler, S. Soverna, R. Dressler, B. Eichler, A. Hohn, D. Piquet

Poster Contributions

MD-A Application of artificial neural networks in LSC for transactinide research 210
N. Wiehl, G. Langrock, K. Eberhardt, H.O. Kling, J.V. Kratz, M. Mendel, A. Nähler, U. Tharun, N. Trautmann

MD-B Perspectives of the some computer methods using for the transactinide experimental and theory data treatment 215
M. Myagkova-Romanova, L.L. Makarov

MD-C Optical spectroscopy of the heaviest elements 218
M. Sewtz, H. Backe, A. Dretzke, W. Lauth, P. Schwamb, K. Eberhardt, P. Thörle, N. Trautmann, P. Kunz, G. Passler, S. Fritzsche, R.G. Haire

MD-D Development of a plutonium ceramic target for the MASHA separator 221
D.A. Shaughnessy, K.J. Moody, J.M. Kenneally, J.F. Wild, M.A. Stoyer, J.B. Patin, R.W. Lougheed, A.V. Yeremin, Y.T. Oganessian

Author Index 222

[This page was left blank intentionally.]

Nuclear Structure Theory and Experiment

[This page was left blank intentionally.]

The structure of superheavy nuclei

P.H. Heenen[1]

[1] U.L.B. Bruxelles, Belgium

phheenen@ulb.ac.be

Super-heavy nuclei represent a tough challenge for nuclear theoreticians. These nuclei are indeed far from stability and from the region where the ingredients of nuclear models have been adjusted. Their existence is related to shell effects, whose prediction is thus crucial for the understanding of their structure. But due to the large number of nucleons, the level density is particularly high and the shell effects are more sensitive to the parameters of the model used to describe super-heavy nuclei than in any other regions of the mass table.

It is therefore particularly important to apply to the study of super-heavy nuclei models with the largest possible generality. In the last decade, several microscopic mean-field models have been applied to this region of the mass table. They share the property that their only phenomenological ingredient is an effective interaction which has been adjusted on very general properties of nuclei. Three main families of models have been used: Hartree-Fock-Bogoliubov methods with either a Skyrme interaction [1] or the Gogny force [2] and relativistic Hartree Bogoliubov (usually called relativistic mean-field) methods with an effective Lagrangian [3].

I shall review these methods and their particularities. I shall first focus on how they have been tested on nuclei close to the super-heavy region. The recent experimental results for the Nobelium isotopes ^{252}No and ^{254}No [4,5] are in this respect of particular importance. They bring data in a region close to the domain of super-heavy nuclei, where our knowledge of single-particle spectra and of pairing correlations is particularly limited. All three families of mean-field methods have been applied to these nuclei [5-7] and I shall compare their results.

I shall finally present some recent applications. I will stress the importance of a correct treatment of paring correlations; I will also focus on the different ways odd nuclei are described and on the influence of the polarization effects due to the unpaired nucleon.

References

[1] S. Cwiok *et al*. Phys. Rev. Lett. **83**, 1108 (1999).
[2] J. Dechargé *et al*. Phys. Lett. **B451**, 275 (1999).
[3] M. Bender, Phys. Rev. C **61**, 031302(R) (2000).
[4] P. Reiter *et al*. Phys. Rev. Lett. **84**, 3542 (2000).
[5] P. A. Butler *et al*. Phys. Rev. Lett. **89**, 202501 (2002).
[6] M. Bender *et al*. Nucl. Phys. **A273**, 354 (2003).
[7] J. L. Egido *et al*. Phys. Rev. Lett. **85**, 1198 (2000).
[8] A. V. Afanasjev *et al*. Phys. Rev. C **67**, 024309 (2003).

Structure of nuclei in the mass 250 region

I. Ahmad[1]

[1] Argonne National Laboratory, USA

ahmad@phy.anl.gov

The nuclear structure of superheavy elements plays a very important role in the understanding and prediction of their nuclear properties. However, only few atoms of these nuclides can be produced because of the extremely low production cross sections. Thus, their structure must be deduced from systematics, using the information obtained on the structure of lower-mass nuclei. It is therefore essential to fully characterize the single-particle orbitals in nuclei that are available in sufficient quantities for such studies. The largest amount of the heaviest isotopes can be produced in the High Flux Isotope Reactor (HFIR) at Oak Ridge National Laboratory. This year we obtained extremely pure samples of ^{255}Fm, ^{253}Es and ^{251}Cf and studied their decay properties.

Extensive measurements of α-particle, conversion electron and γ-ray spectra have been performed with high-resolution semiconductor detectors. Alpha-particle spectra were measured by 25 mm^2 Passivated, Implanted, Planar Silicon (PIPS) detectors with resolutions (FWHM) of 9.2 keV. The α-particle energies directly provided the level energies in the daughter ^{247}Cm. More precise level energies were determined from the γ-ray spectra measured with a Low Energy Photon Spectrometer (LEPS). Conversion electron spectra measured with a 6-mm x 6-mm PIN diode of 0.3 mm thickness provided the transition multipolarities. Half-lives of the 227.4- and 404.9-keV levels were measured by the alpha-gamma delayed coincidence technique. Gamma-ray spectra were also measured in prompt and delayed coincidence with α particles. From the results of these measurements, the level scheme shown in Fig. 1, has been constructed [1] and spins, parities and Nilsson state assignments have been deduced. We have established the following single-particle states: $9/2^-$[734], 0 keV; $5/2^+$[622], 227.4 keV; $7/2^+$[624], 285.1 keV; $1/2^+$[620], 404.9 keV; $1/2^+$[631], 518 keV. The experimental E2 transition rate between the $1/2^+$[620] and $5/2^+$[622] state was found to be ~100 times faster than the rate calculated with single-particle wavefunctions [2] and pair occupation probabilities [3]. The E2 matrix element is extremely sensitive to the pairing term because the $1/2^+$[620] orbital is a particle state and the $5/2^+$[622] orbital is a hole state. Thus the observed discrepancy could be either due to the incorrect pairing term and/or due to the admixture of the $1/2^+$[620] wavefunction in the $5/2^+$[622] state. Also, the E3 transition rate was measured between the $5/2^+$[622] and $9/2^-$[734] levels to be 5 Weisskopf units (W.u). This clearly demonstrates octupole mixing in the $5/2^+$[622] level. Similar octupole mixing was observed in the $5/2^+$[622] level in the isotone ^{249}Cf [4].

The decay of ^{255}Fm ($t_{1/2}$=20.1 h) was studied in 1998 and 2000 to investigate the level structure of ^{251}Cf, and the results from the 1998 study, which included gamma-gamma coincidence measurements with Gammasphere, were published [5] in 2000. In that study we were able to establish the assignment of the $1/2^-$[750] Nilsson orbital to the 632-keV level. In addition, a $K^P=3/2^-$ and a $7/2^+$ bands were identified at 982 and 1078 keV, respectively. The former was interpreted as the 2^- octupole band coupled to the $7/2^+$[613] orbital and the latter was interpreted as the β band coupled to the $7/2^+$[613] configuration. We have measured the γ-singles spectra with a new source this year, which had less Es and other contaminants than previous samples. Also, gamma-gamma coincidence measurements were performed with Gammasphere. The results of these measurements confirm our earlier published results.

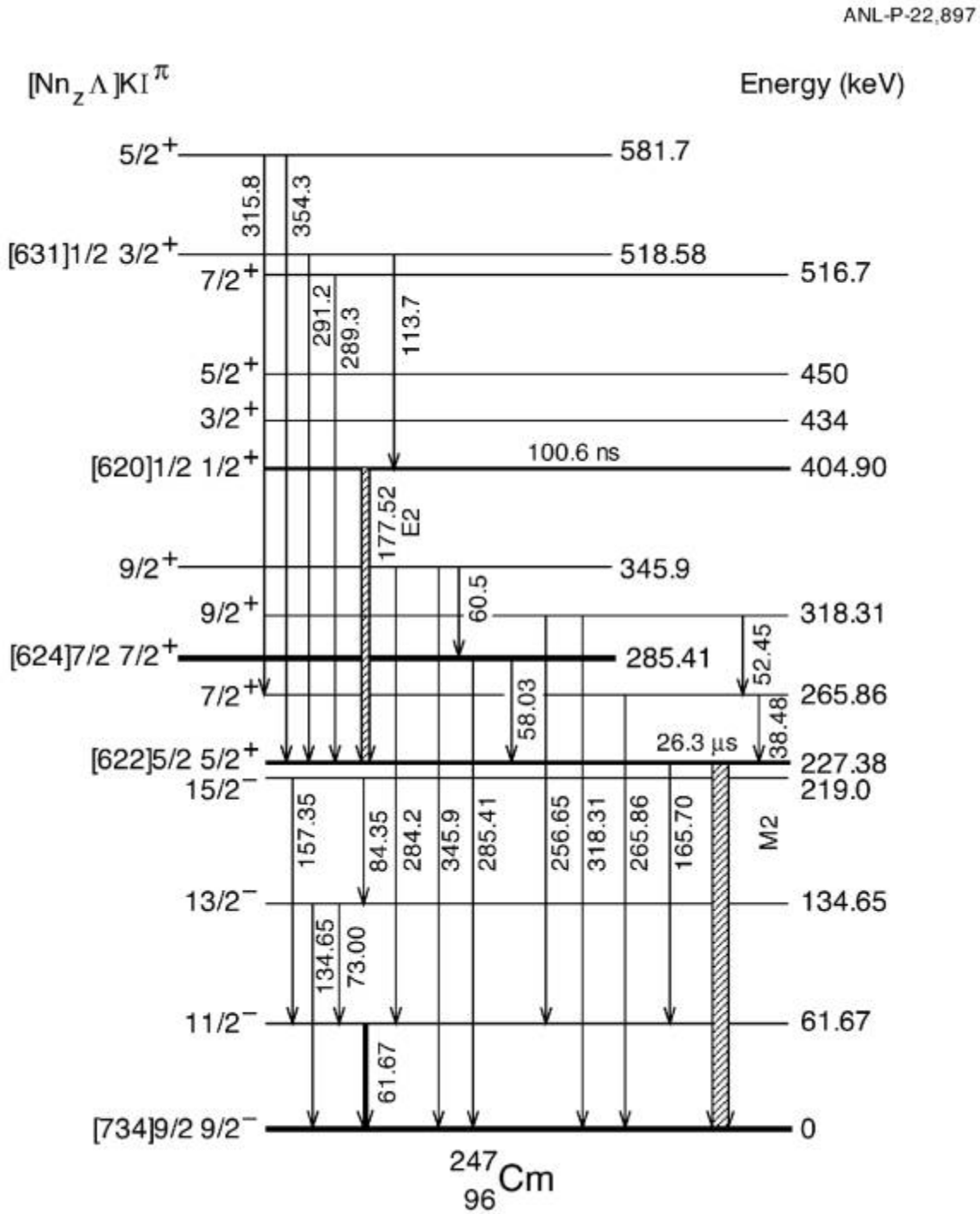

Figure 1. Level scheme of ^{247}Cm deduced from the study of ^{251}Cf alpha decay.

To investigate proton levels in ^{249}Bk we have used 1 mg ^{253}Es ($t_{1/2}$=20.47 d) for γ-singles and gamma-gamma coincidence measurements. This sample had an order of magnitude less ^{254}Es than any previous sample. This has allowed us to detect low-intensity γ rays. By following the decay of the γ-ray lines we have been able to assign gamma rays to ^{253}Es decay. Gamma-gamma coincidence measurements were performed with Gammasphere using 1 mg source. Data were accumulated for 5 days and are being

analyzed. By combining the results of the present investigation with (α,t) and (^{3}He,d) reaction spectroscopy data [6], we hope to make a definite identification of the $1/2^-$[521], $7/2^-$[514] and $9/2^+$[624] Nilsson orbitals in ^{249}Bk.

Calculations of single-particle spectra were made using a Woods-Saxon potential and pairing interaction [3] and these are in fair agreement with the observed level energies.

Acknowledgements

This work was supported by the U. S. Department of Energy, Division of Nuclear Physics, under contract No. W-31-109-ENG-38.

References

[1] I. Ahmad *et al*., Phys. Rev. **C**, to be published.
[2] R. R. Chasman, Phys. Rev. **C3**, 1806 (1971).
[3] R. R. Chasman, I. Ahmad, A. M. Friedman, and J. R. Erskine, Rev. Mod. Phys. **49**, 833 (1977).
[4] I. Ahmad, R. K. Sjoblom, and P. R. Fields, Phys. Rev. **C14**, 218 (1976).
[5] I. Ahmad *et. al*., Phys. Rev. **C62**, 064302 (2000).
[6] J. R. Erskine, G. Kyle, R. R. Chasman, and A. M. Friedman, Phys. Rev. **C11**, 561 (1975).

Nuclear structure investigations of heavy actinide and trans-actinide isotopes

F.P. Hessberger[1]

[1] Gesellschaft für Schwerionenforschung, Germany

F.P.Hessberger@gsi.de

Introduction

Approximately 35 years ago the search for superheavy elements (SHE) was initiated by extrapolations of the nuclear shell model into regions far above the heaviest nuclei (Z=103) known at that time. The next (spherical) closed proton and neutron shells above the doubly magic nucleus ^{208}Pb were predicted at Z=114 and N=184 [1]. A large number of new nuclides having Z > 100 was identified since then, but for most of them only some basic decay properties could be measured due to low production rates. Significant enhancement of the experimental sensitivity during the past years now allows detailed decay studies for numerous isotopes up to Z=108. Those results deliver valuable information on the nuclear structure of these nuclei or their decay products, thus forming a framework for further developments of enhanced theoretical predictions of properties of still unknown superheavy nuclides.

Experimental Procedure

Information on the structure of transfermium nuclei can be obtained so far as well by decay spectroscopy as by in-beam spectroscopy. In the latter case detectors suited to measure radiation (γ-rays, conversion electrons(CE)) emitted during the deexcitation process of the compound nucleus are placed close to the target position. It delivers information on nuclear levels populated during the deexcitation process after particle emission, i.e. information on the structure of the evaporation residue (ER). In-beam spectroscopy of transfermium nuclei so far has been performed at the RITU separator, Jyväskylä (Finland) and the AMS, Argonne (USA) to investigate isotopes of nobelium [2,3,4] and fermium [3].

Most of the information on the nuclear structure of transfermium isotopes, however, has been obtained by means of decay spectroscopy. In most of the set-ups used presently [5,6] the isotopes of interest are separated in-flight from the projectile beam and are implanted into an arrangement of Si-detectors ('stop detector'), used to measure the α-decay energies. γ-rays emitted in coincidence to α-particles are measured with Ge-detectors mounted directly behind the Si-detectors, while CE may be measured in a 'box' of Si-detectors surrounding the 'stop detector'.

We will report here (part of) the results from recent nuclear structure investigations performed at SHIP (GSI Darmstadt). The isotopes ^{254,253}Lr, $^{251-253}$No, ^{246,247}Md have been produced in bombardments of ^{206,207}Pb, ^{209}Bi with ^{48}Ca or ^{209}Bi with ^{40}Ar projectiles. Their radioactive decays as well as those of their daughter products have been investigated by means of α- and α-γ-coincidence spectroscopy. Data analysis is still in progress, so the results have to be regarded as preliminary.

Experimental Results

Low Spin Isomeric States in Odd Mass Nuclei

Detailed investigation of the decay properties of transfermium nuclei in the vicinity of N=152 during the past years has shown that the occurrence of isomeric states decaying by α-emission with half-lives typically in the order of (0.1-10) s is a widespread phenomenon. According to Weisskopf estimations a spin difference of at least $\Delta I=3$ between the isomeric state and subjacent levels is necessary in order that α-emission can compete with internal transitions in the range of those half-lives. In principle, two combinations, low spin ground state - high spin isomeric state or high spin ground state – low spin isomeric state are possible. An example for the first possibility is ^{257}Rf, where an 11/2$^-$[725] – isomeric state at E*=118 keV above the 1/2$^+$[620] – ground state was identified [7]. More frequent, however, appear low spin isomeric states above high spin ground states. Isomeric states in ^{257}Db and ^{253}Lr [6] as well as a spontaneous fission activity of $T_{1/2}$=0.23 s observed in the reaction ^{40}Ar + ^{209}Bi and attributed to ^{247m}Md [8] had been interpreted in this way. In our recent irradiation of ^{209}Bi with ^{40}Ar an α-emitter of E_α=8785 keV with a half-life of $T_{1/2}$=(0.26 ±0.6) s was observed, representing the α-decay branch of ^{247m}Md. In back dated measurements α-decay from isomeric states, e.g. ^{257}Rf, ^{257}Db, ^{253}Lr, often was not recognized due half-lives similar to that of the ground state decay. Higher production rates, allowing more precise half-life measurements and resulting in higher numbers of α-α- correlations, thus giving observation or non-observation of (correlated) α-lines a higher statistical significance, have solved this problem in several cases (see above). In our recent experiments we confirmed α - decay from an isomeric stats in ^{255}Lr [9] and identified an isomeric state in ^{251}No ($T_{1/2}$=0.93 s). The corresponding α-line of E_α =8665 keV had been already reported by Ghiorso et al.[10], but was never observed within the α-decay chain of ^{255}Rf [6,7]. A direct production by ^{206}Pb(^{48}Ca,3n)^{251}No clearly showed in addition to the E_α=8610 keV – transition an α-line of 8665 keV, correlated to an α-decay of E_α=8170 keV, $T_{1/2}$=4.3 s (see fig. 1).The latter activity had already been observed in irradiations of ^{239}Pu with ^{12}C and was attributed to the decay of an isomeric state in ^{247}Fm [11].

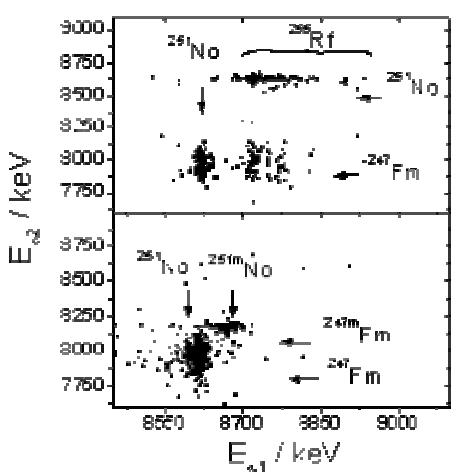

Figure 1. α-α correlation plot for a) evaporation residues produced in the reaction ^{50}Ti + ^{207}Pb at E = (4.77-4.86) AMeV, b) ^{48}Ca + ^{206}Pb at E = 4.81 AMeV.

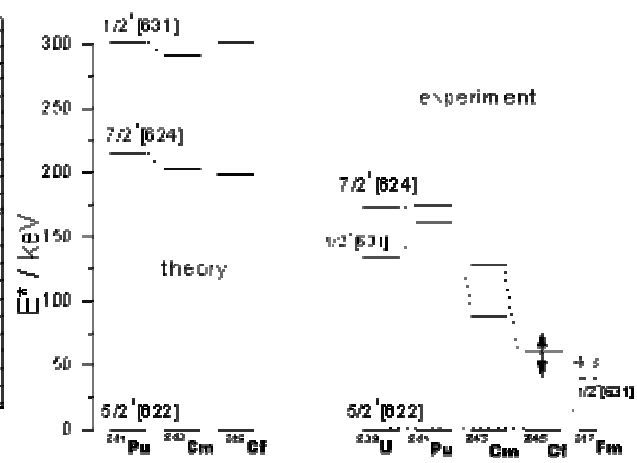

Figure 2. Comparison of calculated [14] and experimental Nilsson levels of N=147 isotones.

Nilsson Levels in Odd Mass Even Z Nuclei

In even Z – isotopes similarities in α-decay properties and nuclear structure are known for isotonic odd mass nuclei. These correlations have been used to explain the α-spectra of ^{257,255}Rf, ^{253}No [6,7,12,13] and to construct partial level schemes for the daughter nuclei. The recent experiments at SHIP delivered enhanced decay data for ^{249}Fm, ^{251}No and thus allowed to extend such comparisons to the N=149 – isotones and their N=147 - decay products. Level predictions of Cwiok et al. [14] for the N=147 – isotones are compared with experimental results in Fig. 2. Cwiok et al. predict the $5/2^+$[622] – Nilsson level as the ground-state of these nuclei, which is in line with the (older) experimental assignments, and rather stable excitation energies for the $7/2^+$[624] – level, which is assigned to the ground-state of the N=149 – mother nuclei, and the $1/2^+$[631] –level. Experimental assignments, however, place the $1/2^+$[631] below the $7/2^+$[624] – level and exhibit for both levels a drastic decrease of the energies from ^{241}Pu to ^{243}Cm [15].

In our experiments ^{249}Fm was produced by ^{207}Pb(^{48}Ca,2n) ^{253}No - α -> ^{249}Fm. Its α-line was significantly broader than that of ^{250}Fm, which was produced in the same irradiation by α-decay of ^{254}No. No γ-rays were observed in coincidence with α-decays of ^{249}Fm. Using the line width of ^{250}Fm, the ^{249}Fm, the α-spectrum was disentangled into two components of E_α=(7559±10) keV and E_α=(7583±10) keV. This line form was interpreted as due to energy summing of α-particles with conversion electrons either being stopped in the detector or leaving it. Taking into account that difference, maximum and minimum energy shifts of α-particles of $\Delta E_{max}=E^*-8$ keV and ΔE_{min}=21 keV, as obtained from α-γ-coincidence measurements of ^{253}No, we obtain an excitation energy of the level populated by the α-decay of E^*=(53±10) keV. Non-observation of γ-rays in coincidence with α-particles indicates that this value is already an upper limit. Respecting the number of observed α-decays and the efficiency of the Clover detector we obtain a lower limit for the conversion coefficient $\alpha_L > 50$, which refers to γ – energies $E_\gamma < 50$ keV for an M1 – transition [16].

For ^{251}No we observed a single narrow α-line of E_α=(8110 ± 10) keV (FWHM=21 keV). No γ – events in coincidence with α-particles were observed. Thus it is seemingly not influenced by energy summing K- or L- conversion electrons, which indicates that the $7/2^+$[624] – level in ^{247}Fm is already located below the L-electron binding energy ($E^* < 20$ keV). The observation of an isomeric state ^{247m}Fm ($1/2^+$[631]) decaying by α-emission with a half-life of 3 s, however, suggests that the $7/2^+$[624] – level already forms the ground state since a γ- decay life-time > 1s is rather expected for a $\Delta I=3$ – transition (M3), than for a $\Delta I=2$ – transition (E2) expected for $1/2^+$[631] -> $5/2^+$[622].

Nilsson Levels in Odd Mass Odd Z Nuclei

In odd Z nuclei similarities in α-decay properties and nuclear structure are known for isotopic odd mass nuclei. These correlations can be used to explain the α-spectra and to construct partial level schemes for the daughter nuclei. On the other hand, changes in the decay pattern may reveal a change of the ground state configuration of the daughter nuclei. Our investigations so far concentrated on the nuclei in the range Z=(99-105) characterised by T_z=45, 47, 49. Partial level schemes for these nuclides as derived on the basis of recent experiments at SHIP and literature data are shown in fig. 3.

The decay scheme of ^{257}Db has been discussed in detail in ref. [6]. Ground state was assigned as $9/2^+$[624] as predicted by Cwiok [14], isomeric state as $1/2^+$[521]. Isomeric decay populates an isomeric state in ^{253}Lr, decaying into $1/2^-$ - state in ^{249}Md. Whether this state decays by α-emission is presently still unclear.

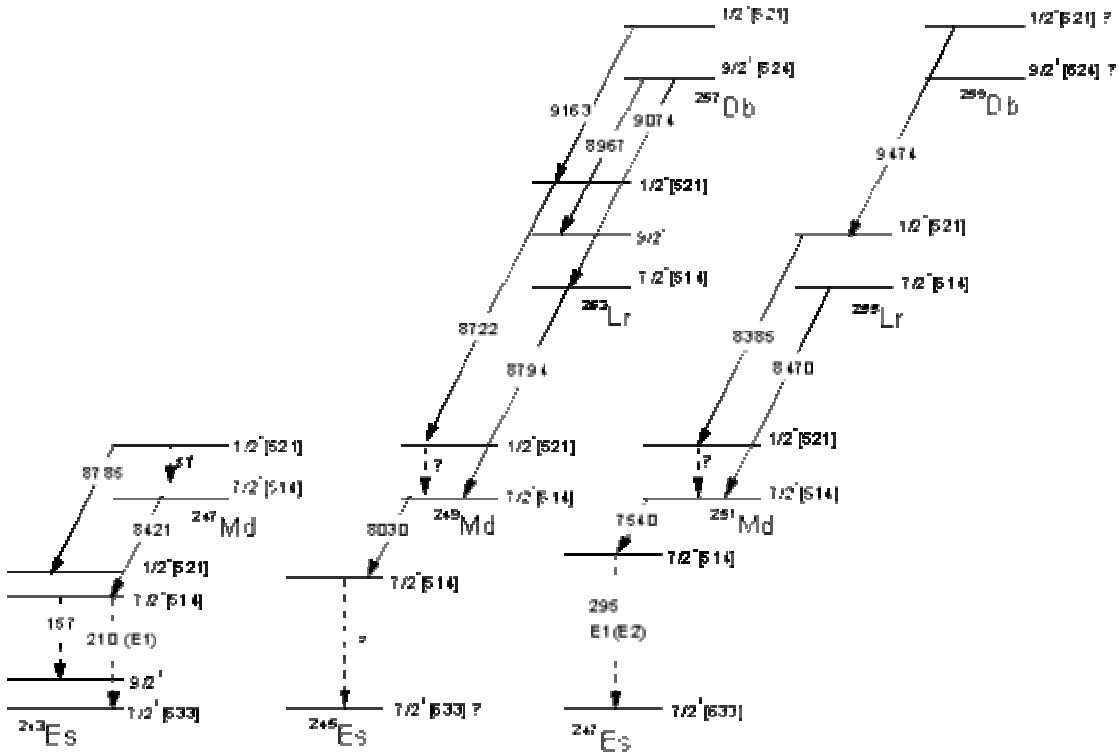

Figure 3. Adopted decay schemes for T_z=45, 47, 49 – odd Z isotopes. Level schemes and decay data are partly tentative and preliminary.

No statistically significant difference in α-decays of ^{249}Md following either ^{253m}Lr or ^{253}Lr have been observed so far. It was argued, however, that the decay pattern of ^{257m}Db and ^{257}Db exclude the 1/2$^-$[521] Nilsson level as ground-state of ^{249}Md as predicted [14], but favour the 7/2$^-$[514] level.

Similarities for the neighbouring T_z=49 – isotopes are evident. The two α-lines of ^{255}Lr are found to have different half-lives and thus represent the decay from different levels: ^{255m}Lr (E_α=8470 keV, $T_{1/2}$=2.1 s), ^{255}Lr (E_α=8375 keV, $T_{1/2}$=16.4 s). In analogy to the case of ^{253,253m}Lr the α-line of the higher energy has been attributed to the decay of the isomeric state. For the mother nucleus, ^{259}Db, only one α-lines has been reported so far [17]. The α-α-correlations observed by Gan et al. [17] suggest an assignment to an isomeric state similar to ^{257}Db. No statistically significant differences in the α-energy of ^{251}Md events following α -decays of either ^{255}Lr or ^{255m}Lr are observed. Also no γ-decays in coincidence with each of these lines were registered, while in coincidence with α-decays of ^{251}Md a 295.1 keV – γ-line as well as some Es-x-ray – events were observed. The ratio Σx-rays / $\Sigma\gamma$ suggest an E1-transition, which corroborates the ground-state level assignment 7/2$^-$[514] and 7/2$^+$[633] for ^{251}Md and ^{247}Es, respectively.

For the T_z=45 – members only α-decay of ^{247}Md and ^{243}Es was measured so far. The α-line at E_α 8421 keV was found in coincidence with a γ-line of 210 keV [12]. On the basis of coincidences with K-x-rays and an energy shift of the α-line due to energy summing with conversion electrons it was concluded that the γ-line represents rather an E1 – transition, which excludes a level assignment 3/2$^-$[521] for the ground-state of ^{243}Es [18], but an E2 – transition, which would favour the latter assignment could not be excluded [12]. A repetition of this measurement clearly proved the E1 – character, suggesting 7/2$^+$[633] as the

ground-state level of ^{243}Es. In addition an α-γ – coincidence E_α=8471 keV – E_γ=157 keV was observed. It is tentatively assigned to γ-decay from the $7/2^-$[514] – level into the first excited member of the ground state rotational band ($9/2^+$) of ^{243}Es.

Acknowledgements

The experiments were performed within our experimental program 'Nuclear Structure Investigations of Transfermium Isotopes' by the 'SHIP collaboration' presently consisting of S.Hofmann, F.P.H, D. Ackermann, H.-G. Burkhard, P. Cagarda, B. Kindler, I. Kojouharov, P. Kuusiniemi, B. Lommel, R. Mann, G. Münzenberg, H.J. Schött (GSI), M. Leino, J. Uusitalo (Univ. Jyväskylä, Finland), S. Antalic, P I.Brida, S. Saro (Univ. Bratislava, Slovakia), A.G. Popeko, A.V. Yeremin (FLNR JINR Dubna, Russia).

The author expresses his gratitude to the UNILAC staff for delivering the high intensity beams and to the staff of GSI target laboratory, W. Hartmann, J. Klemm and J. Steiner for the skilful preparation of the large area lead and bismuth targets.

References

[1] H. Meldner, Arkiv för fysik **36,** 593 (1967)
[2] M. Leino et al., Eur. Phys. J. A **6**, 63 (1999)
[3] R.-D. Herzberg et al., Phys. Rev. C **65,** 014303 (2001)
[4] P. Reiter et al., Phys. Rev. Lett. **82**, 509 (1999)
[5] S. Hofmann et al., Z. Phys. A **350**, 277 (1995)
[6] F.P. Heßberger et al., Eur. Phys. J. A **12**, 57 (2001)
[7] F.P. Heßberger et al., Z. Phys. A **359**, 415 (1997)
[8] S. Hofmann et al., GSI Scientific Report 1993, **GSI-94-1**, 64 (1994)
[9] P. Greenlees, private comm. 2003
[10] A. Ghiorso et al., Phys. Rev. Lett. **118**, 401 (1967)
[11] Flerov, G.N. et al., Atomnaya Energiya **22**, 343 (1967)
[12] F.P. Heßberger, Proc. Symp. 'Nucl. Clusters: From Light Exotic to Superheavy Nuclei', Rauischholzhausen,Germany, 5-9 Aug. 2002, eds. R.Jolos, W.Scheid, EP Systema Debrecen, Hungary, 439 (2003)
[13] F.P. Heßberger, Nucl. Phys. **A719**, 185c (2003)
[14] S. Cwiok et al., Nucl. Phys. **A573**, 356 (1995)
[15] R. Firestone et al. (eds.), Table of Isotopes (1996)
[16] R.S. Hager, E.C. Seltzer, Nucl. Data A **4** (1968)
[17] Z.G. Gan et al., Eur. Phys. J A **10**, 21 (2001)
[18] Y. Hatsukawa et al., Nucl. Phys. **A500**, 90 (1989)

Spectroscopy of the heaviest elements

R. Julin[1]

[1] JYFL University of Jyvaskyla, Finland

rauno.julin@phys.jyu.fi

The anomalously high production cross-section of about 2 microbarn for the cold fusion reaction ^{208}Pb(^{48} Ca,2n)^{254}No was utilized in the in-beam gamma-ray studies of ^{254}No, where the Gammasphere array was combined with the Fragment-Mass-Analyzer (FMA) at Argonne [1] and the Ge clover array (SARI) was combined with the RITU-gas-filled-separator at JYFL in Jyväskylä [2]. By employing the recoil- gating and recoil-decay-tagging (RDT) techniques the yrast line of ^{254}No was identified revealing that the ^{254}No nucleus is deformed with a deformation parameter, b_2=0.27(2).

For further studies of ^{254}No, the SACRED magnetic solenoid electron spectrometer was combined with RITU for in-beam electron RDT measurements. In a careful analysis of resulting prompt recoil-gated electron-electron coincidence spectra of ^{254}No it was found that a broad distribution under the discrete electron lines arising from transitions within the ground state band in ^{254}No is not due to random events but consists of high-multiplicity events, obviously originating from cascades of highly converted M1 transitions within rotational bands built on high K states in ^{254}No [3].

Following the success of the RDT experiments at JYFL, the Jurosphere2 array + RITU system was employed in an in-beam gamma-ray study of ^{252}No for which the production cross-section in the ^{206}Pb(^{48}Ca,2n) reaction is only 300 nanobarn [4]. The yrast rotational band of ^{252}No was observed up to I=20 indicating that ^{252}No is less deformed than ^{254}No and showing evidence for quasiparticle alignment. Both the ^{254}No and ^{252}No data reveal that the fission barrier exists at least up to I ~ 20 in these nuclei.

In order to gain experimental knowledge of single-particle states in heavy nuclei the next in-beam recoil-tagging experiment in Jyväskylä was focused on ^{255}Lr and in Argonne on ^{253}No. They were produced via the ^{209}Bi(^{48}Ca,2n) and ^{207}Pb(^{48}Ca,2n) reactions, with cross-sections of about 300 nanobarn and 500 nanobarn, respectively. Strong X-ray peaks in the resulting spectra indicate that the decay along the yrast line of these nuclei proceeds by strongly converting M1 transitions, which calls for electron-spectroscopic methods.

In the present contribution, the results obtained at Jyväskylä will be discussed in more detail. New data from the on-going RDT campaign at JYFL with the new JuroGam array and the GREAT spectrometer combined with RITU will be shown.

References

[1] P. Reiter *et al.*, Phys. Rev. Lett. **83**, 1108 (1999).
[2] M. Leino *et al.*, Euro. Phys. Jour. **A6**, 63 (1999).
[3] P.A. Butler *et al.*, Phys. Rev. Lett. **89**, 202501 (2002).
[4] R.-D. Herzberg *et al.*, Phys. Rev. **C65**, 014303 (2002).

Properties of superheavy nuclei

R. Smolanczuk[1]

[1] Soltan Institute for Nuclear Studies, Poland

smolan@fuw.edu.pl

Alpha-decay and spontaneous-fission of deformed and spherical superheavy nuclei are discussed. Calculations are performed in the framework of a macroscopic-microscopic model. Spontaneous fission is described in a dynamical approach. Half-lives of heaviest nuclear systems are compared with experimental data. Some conclusions and remarks on the possibility of forming and detecting still heavier elements are presented.

Structure of superheavy elements with meson field theory

W. Greiner[1]

[1] Institut für Theoretische Physik, Universität Frankfurt, Germany

greiner@th.physik.uni-franfkurt.de

[Abstract not available at time of printing]

Limits of stability, formation mechanism and structure of shell-stabilzed heavy nuclei

T.L. Khoo[1], P. Reiter[2], A. Afanasjev[1], I. Ahmad[1], A. Heinz[1], T. Lauritsen[1], C.J. Lister[1], D. Seweryniak[1], N. Amzal[3], P.A. Butler[3], M.P. Carpenter[1], A.J. Chewter[3], J.A. Cizewski[4], C.N. Davids[1], S. Frauendorf[5], P.T. Greenlees[6], K. Helariuta[6], R.D. Herzberg[3], G. Jones[3], R.V.F. Janssens[1], R. Julin[6], H. Kankaanpää[6], H. Kettunen[6], F. Kondev[1], P. Kuusiniemi[4], G.A. Lalazissis[7], M. Leino[6], A.A. Sonzogni[1], S. Siem[1], I. Wiedenhöver[1], J. Uusitalo[6]

[1] Argonne National Laboratory, USA
[2] University of Munich, Germany
[3] University of Liverpool, United Kingdom
[4] Rutgers University, USA
[5] University of Notre Dame, USA
[6] University of Jyväskylä, Finland
[7] Aristotle University of Thessaloniki, Greece

khoo@anl.gov

Recent experiments and theoretical calculations have shed new light on heavy nuclei that are stabilized by the shell-correction energy. This abstract describes results from experiments with Gammasphere and the Fragment Mass Analyzer at Argonne [1-2], and compares these results with those from recent self-consistent mean-field models. The experimental data provide information on: (i) the limits of stability as functions of spin and excitation energy; (ii) the fission barrier as a function of spin; (iii) the survival probability against fission of hot nobelium nuclei [from (i and ii)], which is critical for understanding the formation mechanism of superheavy nuclei; (iv) the importance of high partial waves in the synthesis of superheavy nuclei; (v) the moments of inertia of rotational bands in ^{253,254}No; and (vi) a neutron quasiparticle energy from ^{253}No. As an example, the first figure below shows a spectrum of the ground-state band of ^{254}No up to spin 20 and the entry distribution (in spin and excitation energy), which reveals that ^{254}No survives fission up to at least 22 hbar in spin and 8 MeV excitation energy and that the fission barrier above spin 10 hbar is at least 5 MeV. Clearly the entry distribution extends well beyond the blue shaded region, which denotes the stability limits of a rotating liquid drop, thereby graphically illustrating the addtional stability given by the shell-correction energy. Experiments at Jyväskylä, with RITU in combination with various Ge arrays and an electron spectrometer, have also revealed the properties of ^{252}No [3], as well as of ^{254}No.

Calculations have been performed in the framework of non-relativistic and relativistic self-consistent mean field theories (see, for example, [4-7]), as well as with the microscopic-macroscopic approach (by Sobiczewki *et al.*). For the self-consistent mean-field models, the heaviest nuclei provide an especially interesting test since the effective forces have been selected from fits to the bulk properties of "normal" lighter nuclei, where the binding comes predominantly from the liquid-drop term (from the viewpoint of the Strutinsky approach). In brief, the self-consistent models (i) provide good descriptions of the moments of inertia of ^{252,253,254}No, although details of the variation with A and spin are not fully described; (ii) suggest that the fission barrier remains large at high spin [4-5], in agreement with experimental entry distribution measurements; and (iii) reproduce many quasiparticle energies of deformed nuclei within 0.5 MeV, although there are systematic discrepancies of >1 MeV for certain classes of orbitals--results [6] with the NL1 and NL3 Lagrangians are given in the second figure below. Ref. [6] presented the first systematic test of the accuracy of self-consistent mean-field quasiparticle energies, by examining the known quasiparticle states in the transuranic nuclei ^{249}Bk and ^{249,251}Cf. (A similar test has been conducted in [7]). The third figure compares experimental and theoretical kinematic and dynamic moments of

inertia, $J^{(1)}$ and $J^{(2)}$, for ^{252,254}No and for the 7/2$^+$[624] band in ^{253}No. The upper panel shows the results from experiment [1-3] and the lower panel presents results from the Skyrme Hartree-Fock Bogolubov model [7]. The magnitudes and general trends are reproduced by theory, but details, such as the variation with spin and mass, are not in perfect agreement, probably due to some imperfections in the energies of high-*j* single-particle orbitals.

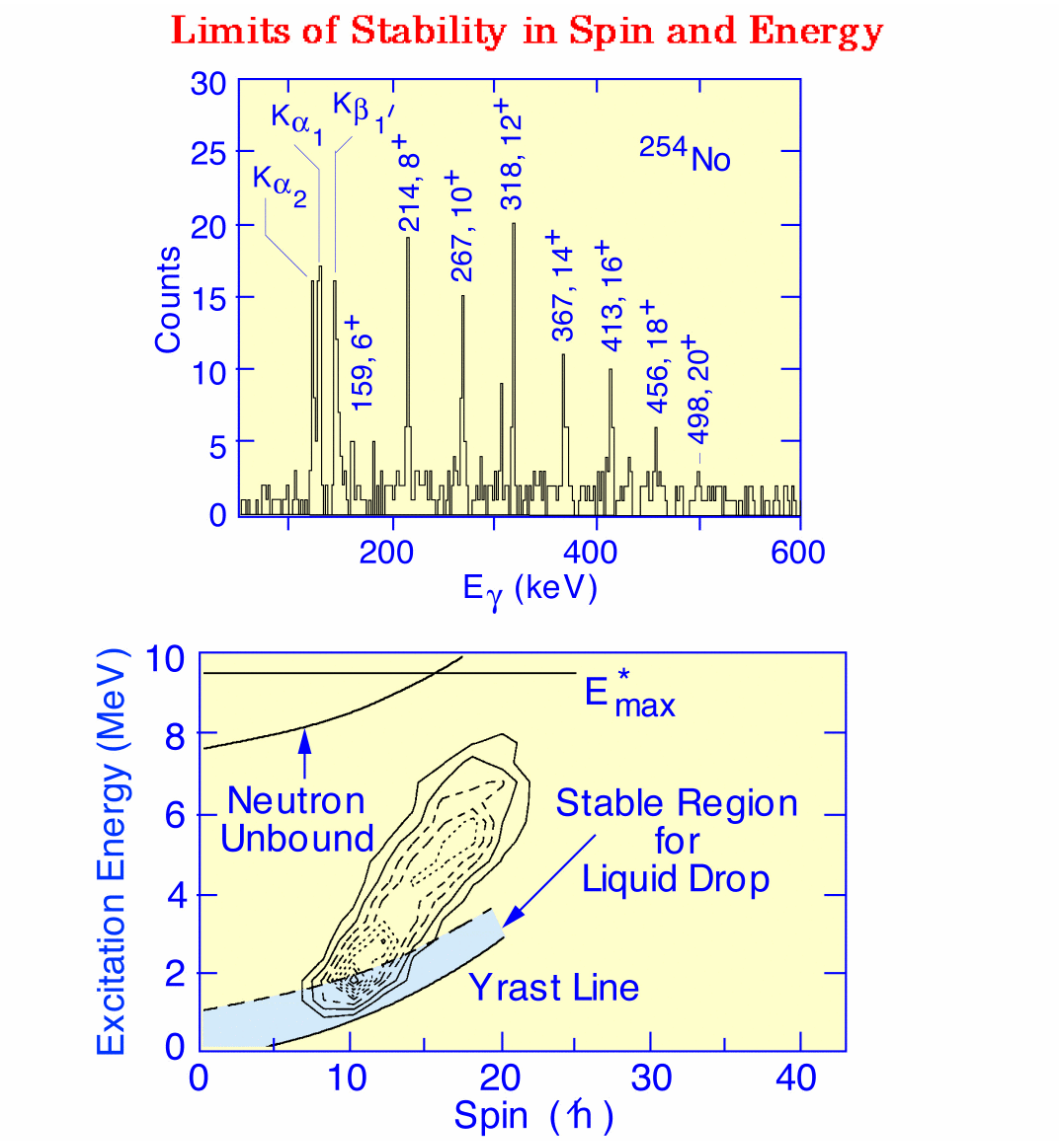

^{254}No is stable up to at least spin 22ħ and
8 MeV energy -- much more robust than expected.
$B_f(\ell) > 5$ MeV $\ell \geq 10\,\hbar$

Gammasphere at ANL Reiter et al. PRL 84, 3542 (2000)

Figure 1.

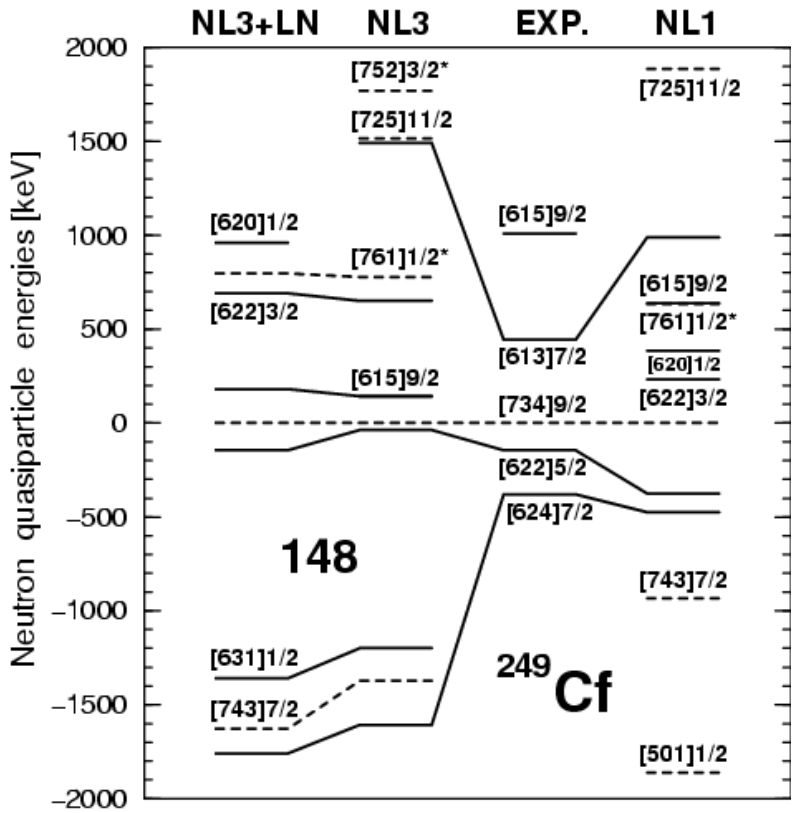

Figure 2.

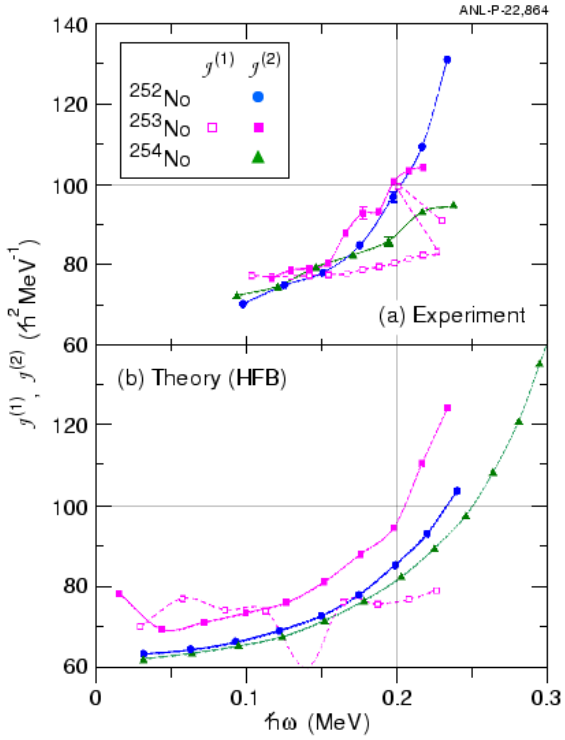

Figure 3.

Acknowledgements

This research is partially supported by the US Dept. of Energy under contract No. W-31-109-ENG-38.

References

[1] P. Reiter *et. al.*, Phys. Rev. Lett. **82**, 509 (1999); *ibid*. **84**, 3542 (2000).
[2] P. Reiter *et. al.*, preprint (2003).
[3] R. Herzberg *et. al.*, Phys. Rev **C61**, 014303 (2002).
[4] L. Egido and L. Robledo, Phys. Rev. Lett. **85**, 1198 (2000).
[5] T. Duguet, P. Bonche and P.-H. Heenen, Nucl. Phys. **A679**, 427 (2001).
[6] A. Afanasjev *et. al.*, Phys. Rev. **C67**, 024309 (2003).
[7] M. Bender *et al.*, Nucl. Phys. **A** (2003), in press; private comm. (2003).

Charge and mass renormalization in no-photon QED

H. Siedentop[1], C. Hainzl[1]

[1] Ludwig-Maximilians-Universitaet Muenchen, Germany

h.s@lmu.de

Starting from a formal Hamiltonian as found in the physics literature - omitting photons - we define a renormalized Hamiltonian through charge and mass renormalization. We show that the restriction to the one-electron subspace is well-defined. Our construction is non-perturbative and does not use a cut-off.

The Hamiltonian is relevant for the description of the Lamb shift in muonic atoms.

Conversion electron measurement for the α decay of ^{257}No

M. Asai[1], K. Tsukada[1], S. Ichikawa[1], Y. Nagame[1], T. Ishii[1], I. Nishinaka[1], K. Akiyama[1], A. Osa[1], M. Sakama[2], Y. Oura[3], K. Sueki[4], M. Shibata[5]

[1] Japan Atomic Energy Research Institute, Japan
[2] University of Tokushima, Japan
[3] Tokyo Metropolitan University, Japan
[4] University of Tsukuba, Japan
[5] Nagoya University, Japan

asai@tandem.tokai.jaeri.go.jp

The stability of superheavy nuclei is one of the most interesting subjects in nuclear physics. This stabilization is caused by nuclear shell effects. Many theoretical studies have predicted the shell structure around the superheavy region, while the experimental information is very scarce. In particular, little is known about the level structure, e.g. level energies of excited states, spin-parities and single-particle configurations of the ground state as well as the excited states, and γ transitions between them. The aim of this study is to establish Nilsson single-particle states in odd-mass Z>100 and N>152 nuclei through experimental spin-parity assignments for the ground state as well as excited states by means of α-γ and α-conversion electron spectroscopy. In this presentation, we report our first results on the α decay of ^{257}No.

The nucleus ^{257}No was produced by the ^{248}Cm(^{13}C,4n) reaction at the JAERI tandem accelerator facility. Reaction products recoiling out of the targets were thermalized in He gas loaded with PbI_2 clusters, and transported into a surface ionization-type thermal ion source of the JAERI on-line isotope separator (ISOL) with a gas-jet transport system [1]. Mass-separated ions were implanted into a Si PIN photodiode detector (9 mm x 9 mm x 0.3 mm^t) around which another three photodiodes were placed to detect α particles and electrons simultaneously. Energy calibration of the detectors was performed using a mass-separated ^{221}Fr source implanted into the same Si detector by this ISOL system before and after the on-line experiment, and also using an ^{241}Am source. Energy resolution of the detectors was 2.1 keV (FWHM) for 59 keV γ rays, and about 3.5 keV for 100 keV electrons. Typical γ and electron spectra of ^{241}Am and ^{221}Fr are shown in Fig. 1.

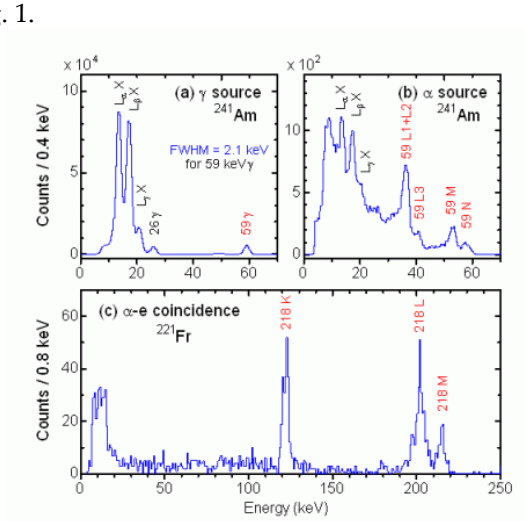

Figure 1. Typical γ and electron spectrameasured by a Si PIN photodiode detector. (a) Gamma-ray spectrum for an ^{241}Am γ source. (b) Gamma and electron spectrum measured using an ^{241}Amα source. (c) Electron spectrum in coincidence with 6126 keV αparticles of ^{221}Fr.

Figures 2(a) and (b) show an α singles spectrum for the mass-257 fraction and an electron spectrum in coincidence with the 7500-8500 keV α particles. As shown in Fig. 2(b), two prominent electron peaks are observed at 50.0 and 97.4 keV, which correspond to the L internal-conversion electrons of the 77.5 and 124.9 keV γ transitions in ^{253}Fm, respectively. The M electron peaks are also observed at 70.4 and 117.6 keV. Taking into account the α-e and e-e coincidence relationships, we have established a newly proposed decay scheme of ^{257}No given in Fig. 3 together with a previously evaluated one [2,3]. It has been revealed that the 8323 keV α transition populates the excited state of ^{253}Fm, not the ground state, and the 8270 keV transition does not exist in the decay scheme; this α peak arises from the coincidence summing effect between the 8222 keV α particles and the 50 keV electrons.

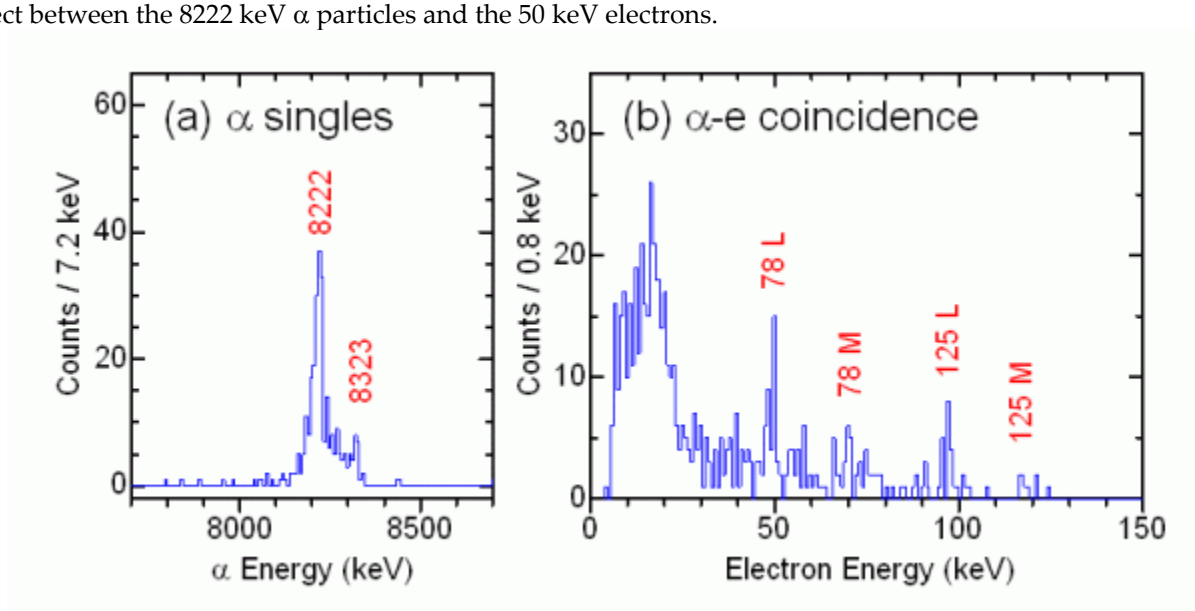

Figure 2. (a) Alpha singles spectrum for ^{257}No measured by a detectorwith a 20% detection efficiency. (b) Electron spectrum in coincidence with 7500-8500 keVα particles of ^{257}No.

Theoretical L internal conversion coefficients (ICCs) of a 125 keV γ transition in Z=100 nuclei (α_{L1}, α_{L2}, α_{L3}) are (0.031, 0.021, 0.015), (0.33, 4.3, 2.3), and (4.0, 0.48, 0.014) for E1, E2, and M1 multipolarities, respectively [4]. The observed electron/α intensity ratio allows us to exclude the E1 assignment for both the 78 and 125 keV transitions owing to small ICCs of E1 transitions. The L3 ICC of E2 transitions is about a half of the L1+L2 ICC, while that of M1 transitions is negligibly small. The observed L electron spectra show no such a large L3 component. Therefore, the M1 multipolarity is assigned to both the 78 and 125 keV transitions. Since the spin-parity of the ground state of ^{253}Fm is $1/2^+$, that of the 125 keV level is either $1/2^+$ or $3/2^+$. The 125 keV level is populated by the allowed α transition with HF=1.3, indicating that the configuration of this level is the same as that of the ground state of ^{257}No. Only the 3/2[622] state could lie at such low energy in ^{253}Fm among the Nilsson single-particle states with a spin $1/2^+$ or $3/2^+$. Thus, we assign the 3/2[622] configuration to the ground state of ^{257}No as well as the 125 keV level in ^{253}Fm. The 24 and 47 keV levels would be the $3/2^+$ and $5/2^+$ members of the 1/2[620] band whose energies are consistent with those in neighboring nuclei.

In conclusion, excited states in ^{253}Fm populated via the α decayof ^{257}No have been established through α-e coincidence spectroscopy. Spin-parities of the ground state of ^{257}No as well as the excited states in ^{253}Fm were determined from the multipolarity of γ transitions and α decay hindrance factors. The 3/2[622] configuration was assigned to the ground state of ^{257}No, which is different from the ground state of other N=155 isotones ^{255}Fm and ^{253}Cf having the 7/2[613] configuration. Next experiment, we will measure α-γ coincidences for the α decay of ^{261}Rf to establish excited states in ^{257}No and assign spin-parities of the

ground state of ^{261}Rf as well as the excited states in ^{257}No based on the present spin-parity assignment for the ground state of ^{257}No.

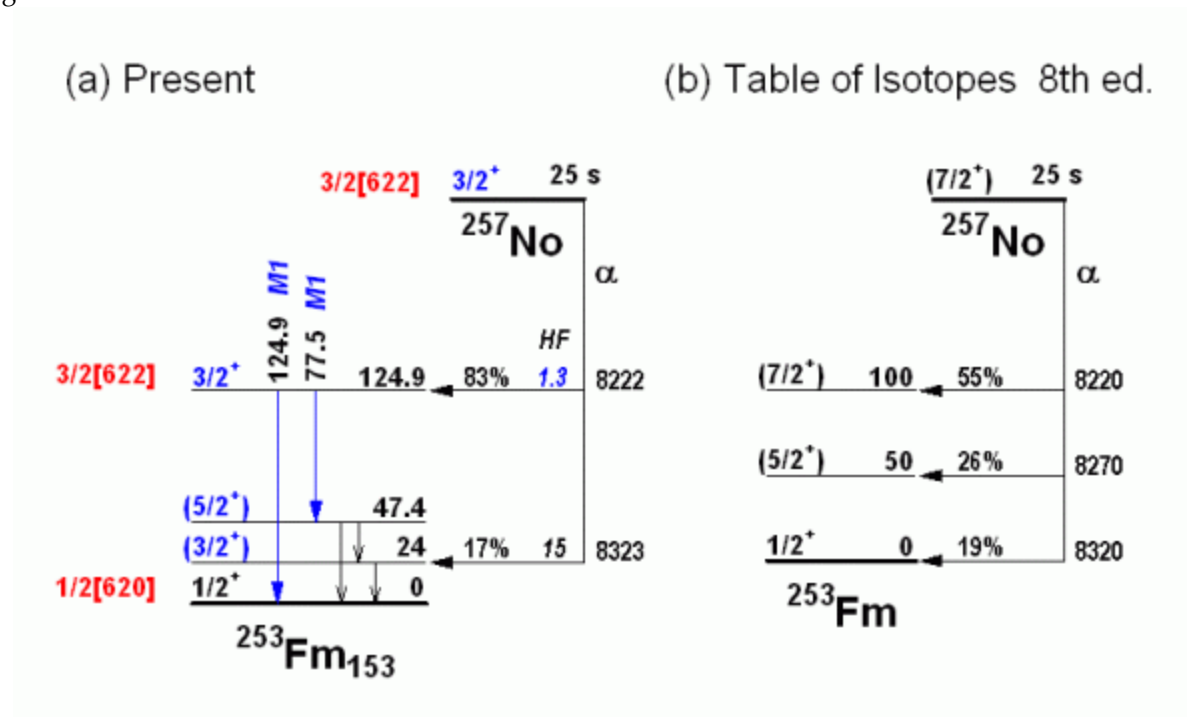

Figure 3. (a) A newly proposed decay scheme of ^{257}No established on the basis of the present experimental result. (b) A previously evaluated one in Refs. [2,3].

References

[1] S. Ichikawa, K. Tsukada, M. Asai, H. Haba, M. Sakama, Y. Kojima, M. Shibata, Y. Nagame, Y. Oura, and K. Kawade, Nucl. Instrum. Methods Phys. Res. B **187**, 548 (2002).

[2] Table of Isotopes, 8th ed., edited by R. B. Firestone and V. S. Shirley (Wiley & Sons Inc., New York, 1996).

[3] P. Eskola, K. Eskola, M. Nurmia, and A. Ghiorso, Phys. Rev. C **2**, 1058 (1970).

[4] F. Roesel, H. M. Fries, K. Alder, and H. C. Pauli, At. Data Nucl. Data Tables **21**, 91 (1978).

Pairing correlations in superheavy nuclei

Z. Patyk[1]

[1] Soltan Institute for Nuclear Studies, Poland

zygmunt.patyk@fuw.edu.pl

In theoretical description of atomic nucleus very important role plays pairing correlations. Direct mass measurements of nuclei carried out at GSI-Darmstadt [1] opens a new possibility to predict the pairing force at the region of heavy and superheavy nuclei. We have tested, in the macroscopic-microscopic approach [2], a sensitivity of the theoretical description of properties of superheavy nuclei as a function of the strength of pairing forces. Basic properties for superheavy nuclei as odd-even nuclear mass staggering, a height of fission barrier, Q_α and a neutron separation energy are discussed. Recently superheavy nuclei are intensively investigated in many laboratories [eg. 3,4].

References

[1] Yu.A. Litvinov *et al.*, to be published; T. Radon et al. Nucl. Phys. **A677**, 75 (2000).
[2] Z. Patyk and A. Sobiczewski, Nucl. Phys. **A533**, 132 (1991).
[3] S. Hofmann and G. Münzenberg, Rev. Mod. Phys. **72**, 733 (2000).
[4] Yu.Ts. Oganessian, Yad. Fiz. 63, 1391 (2000); Phys. At. Nucl. **63**, 1315 (2000).

Investigation of the decay property of extremely low-lying isomer ^{229m}Th

Y. Kasamatsu[1], H. Kikunaga[2], K. Takamiya[3], T. Mitsugashira[4], T. Nakanishi[2], T. Ohtsuki[4], H. Yuki[4], W. Sato[1], H. Yamana[3], Y. Ohkubo[3], H. Kimura[1], S. Shibata[3], Y. Kawase[3], A. Shinohara[1]

[1] Osaka University, Japan
[2] Kanazawa University, Japan
[3] Kyoto University, Japan
[4] Tohoku University, Japan

kasamatu@chem.sci.osaka-u.ac.jp

Introduction

The chemical and physical properties of the isomeric state of ^{229}Th, having the lowest excitation energy, is an interesting subject in both experiment and theory. Helmer and Reich reported that the excitation energy of ^{229m}Th is about 3.5 eV from the result of precise γ-ray spectroscopy for the α-decay of ^{233}U [1]. A simplified level scheme of ^{229}Th is shown in Fig.1. This level corresponds to a 3/2+ [631] Nilsson state while the ground state to a 5/2+ [633] one [2]. The emission of internal conversion electrons is forbidden because the excitation energy is lower than the first ionization energy of thorium atoms. Thus the deexcitation from ^{229m}Th to the ground state is expected to occur through a direct γ-ray transition. Furthermore, if the outer-shell electron of ^{229m}Th can be involved in the decay of ^{229m}Th nucleus, ^{229m}Th may decay via an electron bridge (EB) mechanism [3]. The diagram of EB mechanism is shown in Fig.2. This implies that the half-life of ^{229m}Th is dynamically variable depending on its chemical state. The photons emitted in a direct isomeric transition from this level to the ground state should have about 350 nm wavelength, and the photons involved in the transition via EB process are deduced to correspond to visible rays. However, there has been no direct observation for the transition of ^{229m}Th yet. The successful observation will allow us to research the details of EB mechanism.

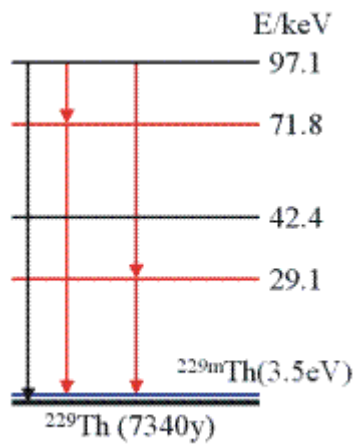

Figure 1. Level scheme of ^{229}Th.

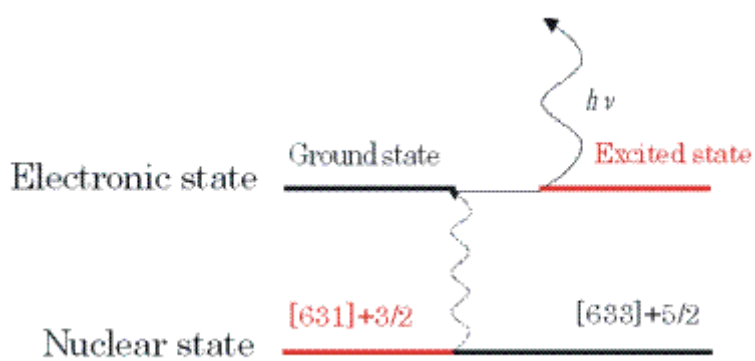

Figure 2. Diagram of Electron Bridge Mechanism.

The ^{233}U sample contains a given amount of ^{229m}Th produced through an α-decay from ^{233}U with a branching ratio of about 1-2 percents. Several kinds of experiments were performed by other groups for the observation of photons emitted from the ^{233}U sample [4,5]. These observations were not successful,

however, owing to the α-particle-induced fluorescence of the materials (nitrogen and quartz, etc.) around the radioactive sample [6].

We introduce a new photon detection system and an α-ray spectroscopic technique to investigate the decay property of ^{229m}Th. The ^{229m}Th samples were prepared by two different methods, chemical separation of decay product from ^{233}U or ^{229}Ac, and direct production by several nuclear reactions. Here preliminary results are reported.

Experimental

The new method of production of ^{229m}Th was performed by novel method using several nuclear reactions: ^{228}Ra(n,γ)^{229}Ra, ^{232}Th(γ,p2n)^{229}Ac, ^{230}Th(γ,n)^{229}Th, ^{232}Th(p,p3n)^{229}Th and ^{230}Th(p,d)^{229}Th. ^{229}Ra decays into ^{229}Ac ($T_{1/2}$=~4m), and ^{229}Ac decays into ^{229}Th ($T_{1/2}$=62.7m). In the decay process from ^{229}Ac, ^{229m}Th is expected to be produced with high probability.

We tried to observe the decay from ^{229m}Th directly by two different methods to investigate the decay mechanism of ^{229m}Th. One is to detect the ultraviolet and visible photons from ^{229m}Th. Although this attempt has not been successful yet, it is essential to investigate the EB mechanism. Photon measurement was performed only for ^{229}Th samples separated from ^{233}U or ^{229}Ac, because the detector was very sensitive to each radiation and thermal phenomenon. The other method is to detect the α particle emitted from ^{229m}Th. We may observe the α rays from ^{229m}Th, since the partial half-life of α-decay in ^{229m}Th is considered to be shorter than that in ^{229}Th as will be mentioned below. The results obtained by the photon measurement can be attributed to the nuclear phenomenon by taking the results for the α-ray measurement into account.

1) Sample preparation

a) α-decay from ^{233}U

The half-life of ^{229m}Th has not been determined experimentally yet, estimated in wide range from about ~10^{-2}s to tens of hours [1,7]. Therefore we developed a rapid ion exchange apparatus so as to make successfully the measurement even when the lifetime was rather short.

The experimental procedure is as follows. First ^{233}U was adsorbed on an anion exchange resin layer in 8M hydrochloric acid solution. Making use of a chemical property that the daughter nuclides of ^{233}U cannot be adsorbed to the resin layer, ^{229}Th grown up during a certain time (Growth Time) was eluted and separated from ^{233}U. It takes only a few minutes for this separation.

Not only the elution peak but all the other range of the elution were also measured to confirm whether the photon emission derived from ^{229m}Th. The ^{229g}Th sample as well as the separated ^{229}Th sample was measured under the almost same conditions to evaluate the effects of fluorescence of thorium atoms and those of radiation from ^{229}Th nuclei.

b) ^{228}Ra(n,γ)^{229}Ra

^{228}Ra was prepared by separating Ra from a ^{232}Th sample in radio-equilibrium. The ^{232}Th sample (thorium nitrate $Th(NO_3)_4$-$5H_2O$) was dissolved in 0.5M Nitric acid. All elements in the decay-chain of ^{232}Th except Ra were precipitated by adding ammonia solution. After centrifuging Ra solution was obtained. Th was completely removed by anion exchange method. Then the ^{228}Ra solution sample was dried up on a quartz boat.

The neutron irradiation was performed in Kyoto University Reactor. ^{228}Ra of about 220kBq was prepared as a target. Neutron flux was 2.8×10^{13} n/s. The duration of irradiation was 60 minutes. After

irradiation the sample was rapidly dissolved in 2M HCl, and Ac was separated by a cation exchange method. We measured the γ-ray energy to ascertain the production of ^{229}Ac. The separated Ac solution sample was divided in half, one was assayed for α-ray measurement. The other was left for 3hours until ^{229}Th was grown fully. Th was isolated by the anion exchange method, and a part of that was assayed for photon measurement and the residual for α-ray measurement.

c) ^{230}Th(γ,n)^{229}Th, ^{232}Th(γ,p2n)^{229}Ac

About 30 μg of 95% ^{230}Th molecular-plated on a 5N aluminum plate was enclosed in a quartz tube for Bremsstrahlung irradiation. About 1.5g of ^{232}Th oxide was also enclosed in a quartz tube and used as a target. The irradiation was carried out using the Electron Linear Accelerator of Tohoku University (Linac). The linac was operated at electron energies of 27 MeV with the beam pulse width of 3 μs the peak current around 100 mA, and the pulse repetition rate of 300 s^{-1}.

After the irradiation, thorium isotopes were chemically separated from the other nuclear reaction products and fission products by the anion exchange and cation exchange method. The thorium isotopes in the effluent were then coprecipitated with samarium trifluoride by adding 30 - 250 μg samarium and hydrofluoric acid solution.

d) ^{232}Th(p,p3n)^{229}Th, ^{230}Th(p,d)^{229}Th

Proton irradiation was carried out with AVF Cyclotron at Research Center for Nuclear Physics in Osaka University. 770 μg of ^{232}Th molecular-plated on a 5N aluminum plate was prepared as a target. Proton beam energy was 34-36 MeV, and the beam current was about 1 μA. The duration of irradiation was 8 hours.

About 5μg of ^{230}Th was used for irradiation. The target was exposed to about 14.8 MeV, 1 μA proton beam for 8 hours. Another target was irradiated for 1 hour in the same beam condition. Immediately after the irradiation, this sample was measured by silicon detector without chemistry to confirm the production of ^{228}Th, Pa and Ac. At this beam energy it is expected that the nuclear reaction producing compound nuclei would be inhibited by the coulomb barrier, only ^{229}Th should be produced.

Pa and fission products produced simultaneously were first removed by an anion exchange separation after the irradiation. After removal of aluminum by precipitation adding NaOH, the Th fraction was separated from Ac and other fractions by a cation exchange method. Acquired sample was coprecipitated with samarium, and assayed for an α-ray measurement.

2) Measurements

a) Photon measurement

Low noise photomultiplier (PM) was used for the photon detection. PM was installed in a PM cooler to lower the thermal noise. Further, the oval reflector was employed, as shown in Fig.3, to focus as many photons emitted from the sample as possible on the photocathode (5mm×8mm) of PM. The output signals from PM was transformed, through only Pre-Amplifier and Discriminator, to MCS-mode data collecting system.

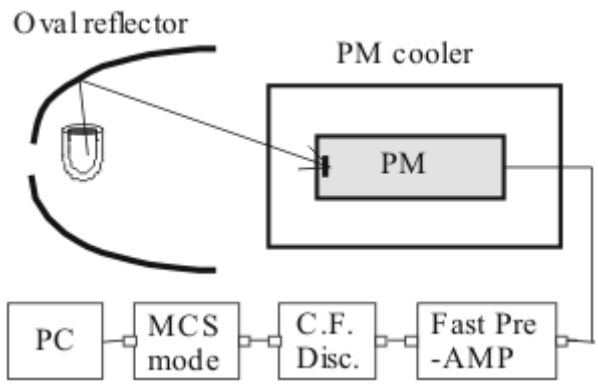

Figure 3. Photon detection system with oval reflector.

The sample measured was usually solution put in a quartz tube (ϕ8mm, 1cm). Several droplets of eluent at elution peak of thorium were collected in it.

b) α-ray measurement

The most favored α-transition from the ground state of ^{229}Th feeds to the 5/2+[633] state at 236.3 keV level of the daughter ^{225}Ra, and only rather weak α-transitions are observed in the higher energy range, as shown in the column for ^{229}Th in Table 1. The transition from ^{229}Th to the 149.96 keV 3/2+[631] level of ^{225}Ra (Eα=4.930 MeV) that is expected to be the most favored α-transition from ^{229m}Th has a branching ratio of only 0.16%. In addition, the α-transition to the parity coupled 3/2+ state at 42.77 keV that is assigned to the rotational band of the ground state of ^{225}Ra (1/2+[631]) is also expected to be another favored α-transition from ^{229m}Th. As a result, the α-particles from ^{229m}Th have higher energies than those from ^{229}Th. This implies that the partial half-life of the α-transition of ^{229m}Th is considerably shorter than that of ^{229}Th, and that the α-particle might be observable when ^{229m}Th is produced by a suitable reaction.

Table 1. Levels of ^{225}Ra and the α-transition ratio from ^{229}Th.

Orbit	Excitation Energy/keV	α-branch		Eα/Mev
		^{229}Th (%)	^{229m}Th	
[631]1/2+	0	weak	favored	5.079
3/2+	42.77	0.24	strong	5.036
5/2+	25.41	6.6	favored	5.053
7/2+	111.60	5.97		4.968
9/2+	100.5	3.17		4.978
[631]3/2+	149.96	0.16	strong	4.93
5/2+	179.75	10.2	weak	4.901
7/2+	243.6	5.0		4.836
[633]5/2+	236.3	56.2	weak	4.845
7/2+	267.9	9.3		4.815
9/2+	321.8	1.9		4.761

The sample for α-spectrometry was prepared by coprecipitating thorium isotope with samarium as fluoride or hydroxide on 0.1 μm or 0.02 μm pore size membrane filter. The precipitate was subjected to α-spectroscopy using a 450 or 900 mm^2 silicon detector.

Results and Discussion

1) Photon measurement

Photon emissions were observed for the solution samples separated from both ^{233}U and ^{229}Ac produced by $^{228}Ra(n,\gamma)^{229}Ra$ reaction. There was no decay component in the time dependence as shown in Fig.4. The eluent sample that is lying out of elution peak position also emitted a few visible or ultraviolet photons. It is difficult to attribute the origin of photon emission to ^{229m}Th nucleus.

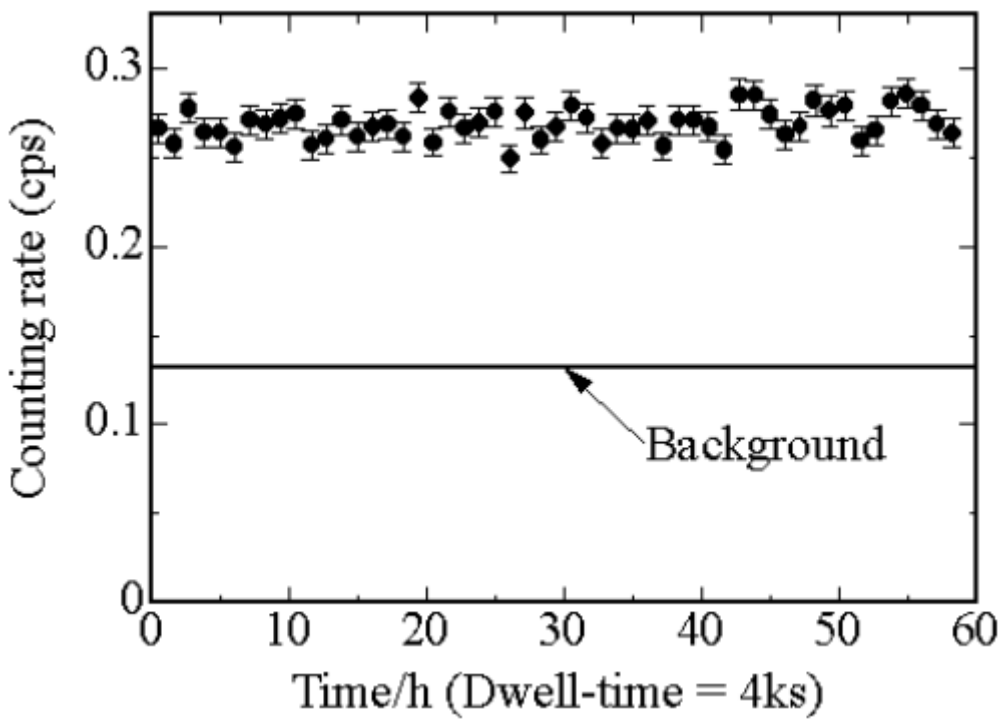

Figure 4. An exmaple of photon measurement result from ^{229}Th solution sample chemically separated from ^{233}U.

Little photon emission was observed from ^{229g}Th sample. The fluorescence of thorium atoms and the other photons derived from α-particle emission of ^{229g}Th do not contribute to the detected photons.

The transition energy of ^{229m}Th may lie out of the energy region of the present detector.

Development of a spectroscope for one-photon counting is under consideration to distinguish the decaying component of a certain wavelength. We are measuring photons with the detector working in higher energy region.

2) α-ray measurement

In the $^{228}Ra(n,\gamma)^{229}Ra$ experiment, α-ray spectrum in the region of interest for ^{229m}Th was obscure because of the disturbance of the tail of α-ray peaks of ^{228}Th. γ-rays from ^{229}Ac (164.5 keV) were measured and the production of ^{229}Ac was ascertained.

In the ^{230}Th(γ,n)^{229}Th and ^{232}Th(γ,p2n)^{229}Ac (see Fig.5) experiments, α-ray peak of ^{229g}Th appeared to be detected in the α-ray spectrum of both experiments. There were some peaks in the energy region of ^{229m}Th, but the contribution from ^{231}Pa disintegrated from ^{231}Th was not negligible for the experiment using ^{230}Th target. The half-life of ^{229m}Th would be too long as compared with the estimation, if the α-decay of ^{229m}Th were observed as well as ^{229g}Th.

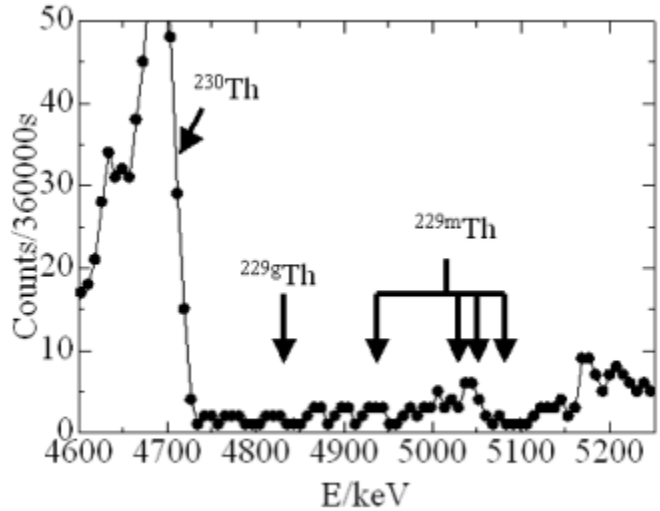

Figure 5. α-ray measurement result of ^{229}Ac sample chemically purified from ^{232}Th(γ,p2n)^{229}Ac reaction products.

In the ^{232}Th(p,p3n)^{229}Th (see Fig.6) and ^{230}Th(p,d)^{229}Th experiments, α-rays from ^{229g}Th were observed. However, these of ^{229m}Th were not measured clearly.This result implies that the half-life may be shorter than a few hours.

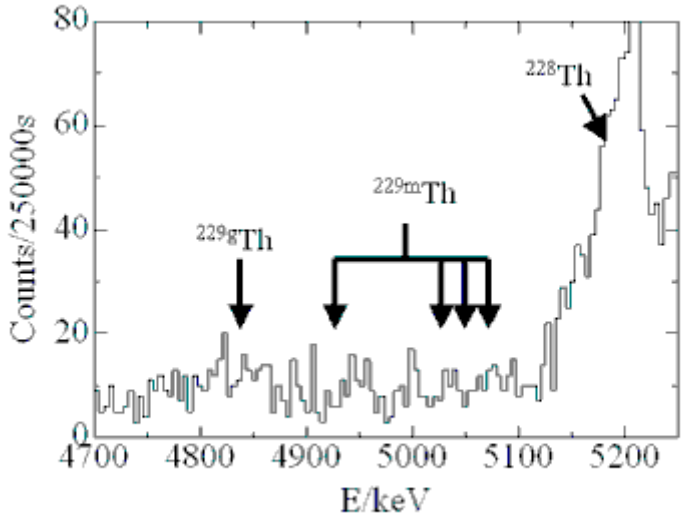

Figure 6. α-ray measurement result of ^{229}Th sample chemically separated from ^{232}Th(p,p3n)^{229}Th reaction products.

Consequently we could not observe the decay of ^{229m}Th or determine the half-life from the present results. Additional experiments and improvement of the detection methods are in progress.

References

[1] R. G. Helmer and C. W. Reich, Phys. Rev. **C49**, 1845(1994).
[2] D. G. Burke, P. E. Garrett, and T. Qu, Phys. Rev. **C42**,499 (1990).
[3] V. F. Strizhov and E. V. Tkalya, Sov. Phys. JETP **72**, 387(1991).
[4] D. S. Richardson *et al*., Phys. Rev. Lett. **80**, 3206 (1998).
[5] R. W. Shaw, J. P. Young, S. P. Cooper and O. F. Webb, Phys. Rev. Lett. **82**, 1109 (1999).
[6] J. P. Young, R. W. Shaw and Oren F. Webb, Inorg. Chem. **38**, 5192 (1999).
[7] A. M. Dykhne and E. V. Tkalya, JETP Lett. **67**, 251 (1998).

Super- and hyperdeformed isomeric states and long-lived superheavy elements

A. Marinov[1], S. Gelber[1], D. Kolb[2], R. Brandt[3], R.V. Gentry[4], A. Pape[5]

[1] The Hebrew University of Jerusalem, Israel
[2] University GH Kassel, Germany
[3] Philipps University Marburg, Germany
[4] Earth Science Associates, USA
[5] IN2P3-CNRS/ULP Strasbourg, France

marinov@vms.huji.ac.il

In recent years long-lived super- and hyperdeformed isomeric states have been discovered [1-4]. It was found that these isomeric states live much longer than the corresponding nuclei in their ground states (see Table 3 in [4]), and in addition, they have unusual radioactive decay properties. Thus, an isomeric state in the second minimum of the potential energy surface (a superdeformed (SD) isomeric state) may decay by relatively high energy and retarded α particles to the ground state, or to the normal deformed states, of the daughter nucleus, and also by low energy and enhanced α particles to the second minimum of the potential in the daughter. In addition it may also decay by very retarded proton radioactivity. An isomeric state in the third minimum of the potential (a hyperdeformed (HD) isomeric state) may decay by relatively high energy and retarded α particles to the second minimum of the potential in the daughter nucleus, or by low energy and enhanced α particles to the third minimum of the daughter. All these new and unusual radioactive decay properties have been found experimentally [1-4].

Based on these results the discovery [5,6] of element 112, back in 1971, produced via secondary reactions in CERN W targets irradiated with 24 GeV protons (see also [7,8]), has consistently been interpreted [4]. The long lifetime of several weeks, as compared to typical lifetimes of less than 1 ms [9], shows that a long-lived isomeric state rather than the normal ground state was produced in the reaction. The deduced fusion cross section in the region of a few mb, as compared to about 1 pb obtained in ordinary heavy ion reactions [9], is due to two effects:

a) The projectile in the secondary reaction experiments is not a normal nucleus in its ground state, but rather a fragment that has been produced by the high energy proton within about $2x10^{-14}$ sec before interacting with another W nucleus in the target. During this short time it is at high excitation energy and quite deformed. Deformations increase the fusion cross section by several orders of magnitude as is well known from the sub-barrier fusion phenomenon [10] (see Fig. 10 in [8] and Fig. 7 in [4].)

b) The production of the compound nucleus in a super- or hyperdeformed isomeric state is much more probable than its production in the normal deformed ground state. The shapes of the compound nucleus in these isomeric states are close to those of the projectile-target combinations in their touching points. Therefore, much less inter-penetration and dissipation are needed in the formation of the compound nuclei in these isomeric states as compared to their production in the ground states (see Fig. 8 in [4]).

The discovery of the long-lived super- and hyperdeformed isomeric states enables one also to consistently interpret the unusually low energy and very enhanced α-particle groups seen in various actinide fractions separated from the same CERN W target. Thus the 5.14, 5.27 and 5.53 MeV α-particle groups, with corresponding half-lives of 3.8 ± 1.0 yr, 625 ± 84 d and 26 ± 7 d, seen in the Bk, Es and Lr-No sources, respectively, have consistently been interpreted, both from the point of view of their low energy and their five to seven orders of magnitude enhanced lifetimes, as possible $II^{min} \rightarrow II^{min}$, $III^{min} \rightarrow III^{min}$ and $III^{min} \rightarrow III^{min}$ transitions in ^{238}Am, ^{247}Es and ^{252}No [4].

Based on the newly observed modes of radioactive decay of the super- and hyperdeformed isomeric states, consistent interpretations have recently been suggested by us for previously unexplained phenomena seen in nature [11,12]. These are the Po halos, the low-energy enhanced 4.5 MeV α-particle group proposed to be due to an isotope of a superheavy element with Z=108, and the giant halos.

Po Halos were observed in mica minerals [13,14] where the concentric halos correspond to the decay chains of ^{210}Po, ^{214}Po and ^{218}Po. Since the lifetimes of these isotopes are short, and halos belonging to their long-lived precursors from the ^{238}U decay chain are absent, their origin is puzzling. It has been suggested [11,12] that their origin might be due to the existence of long-lived super- and hyperdeformed isomeric states in nuclei around ^{210}Po, ^{214}Po and ^{218}Po which undergo β- and γ-decays to the ground states of these isotopes.[1]

The second unexplained phenomenon is the observation [16-19], in several minerals, of a low energy 4.5 MeV α-particle group with an estimated half-life of $(2.5\pm0.5)\times10^8$ yr which, based on chemical behavior, has been suggested to be due to the decay of an isotope of Eka-Os (Z=108; Hs). However, 4.5 MeV is a low energy compared to the predicted 9.5 - 6.7 MeV for β-stable isotopes of Hs [20-22], and $T_{1/2}$ $=2.5\times10^8$ yr is too short by a factor of 10^8, compared to predictions [23,24] from the lifetime versus energy relationship for normal 4.5 MeV α particles from Hs. It was recently shown [11,12], though, that these data can be quantitatively understood as a hyperdeformed to hyperdeformed transition from an isotope with Z=108 and A ≈ 270. The low energy agrees with extrapolations from predictions [25] for $III^{min} \rightarrow III^{min}$ α transitions in the actinide region, and a half-life in the region of 10^9 yr is obtained if one takes into account in the penetrability calculations typical deformation parameters for a hyperdeformed nucleus.

Still another unexplained phenomenon is that of the giant halos [26]. Halos, with radii that fit the known ranges of 10 and 13 MeV α particles, have been seen in mica [26]. Unlike the situation with the Po halos, here it is not absolutely certain that their origin is from such high energy α particles [26-28]. However, if they are, then their existence is puzzling. For nuclei around the β-stability valley, 10 and 13 MeV α particles are respectively predicted [20-22] for Z values around 114 and 126. The estimated [23,24] half-life for 10 MeV α's in Z=114 nuclei is about 1 sec, and for 13 MeV α's in Z=126 nuclei, it is about 10^{-4} sec. It is not clear how halos with such high-energy α particles and such short predicted lifetimes can exist in nature.

Here too an interpretation in terms of hyperdeformed isomeric states has been given [12]. A good candidate for the sequence of events producing the 10 MeV halo is a long-lived HD isomeric state decaying by a 4.8 MeV[2] $III^{min} \rightarrow III^{min}$ α transition, followed by β^+(EC) transitions to a normal state which decays by 10 MeV α particles. As a specific example, one may consider the following scenario where a HD isomeric state in ^{282}114 decays by 4.8 MeV α's to a HD isomeric state in ^{278}112, followed by two β^+(EC) decays to a normal deformed state or to the g.s. of ^{278}110. This latter nucleus is predicted [20-22] to decay by 10 MeV α particles. For deformation parameters which are typical for a HD nucleus, the predicted $T_{1/2}$ value for a 4.8 MeV $III^{min} \rightarrow III^{min}$ α transition from ^{282}114 is 10^8 - 10^{11} yr [12], and the sum of the two Q_β values of above 6 MeV [20-22] makes the transition from the isomeric state in the third minimum to a normal state in one of the daughter nuclei possible.

Similarly, for the 13 MeV halo a possible scenario has been suggested [12] where a HD isomeric state in ^{316}126 decays by a $III^{min} \rightarrow III^{min}$ low-energy α transition of about 5.1 MeV[3] to ^{312}124, followed by two β^+(EC) transitions, leading to the g.s. of ^{312}122. The ^{312}122 nucleus is predicted [20,21] to decay by α particles of around 13 MeV. For a 5.1 MeV HD to HD α transition from ^{316}126, the predicted [12] half-life, using the parameters of Ref. [29] for a HD shape of ^{232}Th, is 3×10^{11} yr. (Larger deformation parameters give shorter lifetimes).

The above analysis suggests that primordial heavy and superheavy nuclei in long-lived isomeric states might exist in nature. A program has been started to search for such nuclei in petzite (Ag_3AuTe_2) and monazite ($(Ce,La,Th)PO_4$) minerals using the accelerator mass spectrometry (AMS) system [30,31] of the Weizmann Koffler Pelletron accelerator in Rehovot. The first mineral was chosen since there is an

indication that induced Po X-rays in such a mineral from Romania has been observed [32]. The second mineral is the same as the one where the giant halos were found [26]. A progress report will be given.

References

[1] A. Marinov, S. Gelberg and D. Kolb, Mod. Phys. Lett. A **11,** 861 (1996).
[2] A. Marinov, S. Gelberg and D. Kolb, Mod. Phys. Lett. A **11,** 949 (1996).
[3] A. Marinov, S. Gelberg and D. Kolb, Int. J. Mod. Phys. E **10,** 185 (2001).
[4] A. Marinov, S. Gelberg, D. Kolb and J. L. Weil, Int. J. Mod. Phys. E **10,** 209 (2001).
[5] A. Marinov, C. J. Batty, A. I. Kilvington, G. W. A. Newton, V. J. Robinson and J. D. Hemingway, Nature 229, 464 (1971).
[6] A. Marinov, C. J. Batty, A. I. Kilvington, J. L. Weil, A. M. Friedman, G. W. A. Newton, V. J. Robinson, J. D. Hemingway and D. S. Mather, Nature **234,** 212 (1971).
[7] A. Marinov, S. Eshhar, J. L.Weil and D. Kolb, Phys. Rev. Lett. **52,** 2209 (1984); **53**, 1120 (1984) (E).
[8] A. Marinov, S. Gelberg and D. Kolb, Int. School-Seminar on Heavy Ion Physics, Eds. Yu. Ts. Oganessian *et al*., Dubna, Russia (1993) Vol. 1, p. 163.
[9] S. Hofmann, V. Ninov, F. P. Hessberger, P. Armbruster *et al.,* Z. Phys. A **354,** 229 (1996).
[10] R. G. Stokstad, Y. Eisen, S. Kaplanis, D. Pelte, U. Smilansky and I. Tserruya, Phys. Rev. Lett. **41,** 465 (1978); Phys. Rev C **21,** 2427 (1980).
[11] A. Marinov, S. Gelberg, D. Kolb, R. Brandt and A. Pape, Phys. At. Nucl. **66**, 1137 (2003); ArXiv:nucl-ex/0210039.
[12] A. Marinov, S. Gelberg, D. Kolb, R. Brandt and A. Pape, to be published in Int. J. Mod. Phys E; ArXiv:nucl-th/0303059.
[13] G. H. Henderson and F. W. Sparks, Proc. Roy. Soc. Lond. A **173,** 238 (1939).
[14] R. V. Gentry, Science **160,** 1228 (1968).
[15] R. V. Gentry, *Creation's Tiny Mystery*, Earth Science Associates, Knoxville, Tennessee (1992).
[16] V. V. Cherdyntsev and V. F. Mikhailov, Geochemistry No. 1, 1 (1963).
[17] R. D. Chery, K. A. Richardson and J. A. S. Adams, Nature **202,** 639 (1964).
[18] V. V. Cherdyntsev, V. L. Zverev, V. M. Kuptsov, and G. L. Kislitsina, Geochemistry No. 4, 355 (1968).
[19] H. Meier, et al., Z. Naturforsch. **25**, 79 (1970).
[20] P. Moller, J. R. Nix and K. -L. Kratz, At. Data Nucl. Data Tables **66**, 131 (1997).
[21] H. Koura, M. Uno, T. Tachibana and M. Yamada, Nucl. Phys. A **674**, 47 (2000); RIKEN-AF-NP-394 (April 2001).
[22] S. Liran, A. Marinov. And N. Zeldes, Phys. Rev. C **62,** 047301 (2000); arXiv:nucl-th/0102055.
[23] V. E. Viola Jr. and G. T. Seaborg, J. Inorg. Nucl. Chem. **28,** 741 (1966).
[24] G. Royer, J. Phys. G: Nucl. Part. Phys. **26,** 1149 (2000).
[25] W. M. Howard and P. Moller, At. Data Nucl. Data Tables **25,** 219 (1980).
[26] R. V. Gentry, Science **169**, 670 (1970).
[27] R. Brandt, Proc. Int. Symp. on Superheavy Elements, ed. M. A. K.Lodhi, Lubbock, Texas (1978) p. 103.
[28] D. Molzahn, R. Brandt, R. Helmbold, H. Jungclas, and P. Vater, Nuclear Tracks **4,** 4 (1980).
[29] S. Cwiok, W. Nazarewicz, J. X.Saladin, W. Plociennik and A. Johnson, Phys. Lett. B **322,** 304 (1994).
[30] M. Paul et al., Nucl. Instr. Meth. B **83,** 275 (1993).
[31] D. Berkovits et al., Nucl. Instr. Meth. B **172**, 372 (2000).
[32] H. Hulubei and Y. Cauchois, Comp. Rend. **224**, 1265 (1947).

[This page was left blank intentionally.]

Nuclear Reaction Theory

[This page was left blank intentionally.]

Theoretical predictions of residue cross-sections for the superheavy elements

Y. Abe[1], B. Bouriquet[1], G. Kosenko[2], C. Shen[3]

[1] Yukawa Institute for Theoretical Physics, Kyoto University, Japan
[2] University of Omsk, Russia
[3] China Institute of Atomic Energy, China

abey@yukawa.kyoto-u.ac.jp

1. Introduction

Productions of the superheavy elements are predicted with the two-step model for fusion of massive systems [1], combined with the theory of the statistical decay of the compound nucleus. As is well known, the fusion of lighter heavy-ion systems is determined by whether the incident system can enter the inner side of the Coulomb barrier or not, but in heavy systems an additional process is indispensable for the formation of the compound nucleus, because there is a conditional saddle point which locates between the position of the Coulomb barrier top and the spherical shape of the compound system. Therefore, the fusion of massive heavy-ion systems which are necessary for the synthesis of superheavy elements (SHE) requires two steps as schematically shown in the first figure; firstly the approaching phase up to the contact of the incident ions after overcoming the Coulomb barrier and secondly the shape evolution phase to the spherical compound nucleus, starting from the pear-shaped composite system made by the projectile and the target of the incident channel. Thus, the product of the sticking and the formation probabilities (P_{stick} and P_{form}), which are obtained by solving dynamics in the two steps, respectively, gives the fusion probability P_{fusion}.

$$P^J_{fusion}(E_{c.m.}) = P^J_{stick}(E_{c.m.}) \times P^J_{form}(E_{c.m.}) \quad (1)$$

where J denotes a total spin of the system and $E_{c.m.}$ a c.m. incident energy. The amalgamated system is expected to be excited internally, that is, the incident kinetic energy is transferred to a thermal energy. The dissipation of the incident kinetic energy may start before the top of the Coulomb barrier, or may start at the moment of touching of the two nuclear matters. If we presume the latter case, the sticking probability is given by a quantum-mechanical barrier penetration factor or simply by a step function at the barrier height, and the formation probability should be calculated by a Langevin equation with the initial momentum being defined by the incident kinetic energy and with a time-dependent temperature which describes a heating-up process. On the other hand, if we presume the former case, the sticking probability should be calculated by a Langevin equation with a frictional force and with a time-dependent temperature, and the formation probability is calculated with a Langevin equation with a constant temperature for shape evolution, if the incident energy is mostly damped at the moment of the contact or of the amalgamation. In view of the results of the Deep-Inelastic Collisions (DIC), it is natural to presume the former. Of course, one would be interested in the enhancement in the sub-barrier energy which is known to originate from coherent couplings with some other channels and to be very important in lighter heavy-ion systems. But, taking into account a strong fusion hindrance which is well known to exist in massive systems, an incoherent treatment, i.e., a treatment of effects of the couplings as a friction would be reasonable.

2. Approaching Phase

We employ a classical treatment for the description of the relative motion of the incident ion system with a frictional force and an associated fluctuation force which is missing in the original classical treatments [2, 3]. The equation is as follows,

$$\begin{cases} m\dfrac{d^2r}{dt^2} = -\dfrac{\partial V}{\partial r} - \dfrac{\partial}{\partial r}\dfrac{\hbar^2 L^2}{2\mu r^2} - C_r(r)\dfrac{dr}{dt} + R_r(t) \\ \dfrac{dL}{dt} = -\dfrac{C_T(r)}{\mu}\left[L - \dfrac{5}{7}L_0\right] + R_T(t) \end{cases} \qquad (2)$$

$$\langle R_i(t) R_j(t') \rangle = 2T(t) \cdot C_i(r(t)) \cdot \delta_{ij} \cdot \delta(t - t')$$

where m is the reduced masse and V is the sum of the Coulomb and the nuclear attrative potentials. $C_i(r)$ is the radial and tangenatial frictions, respectively, where the rolling friction is neglected.L_0 is the incident angular momentum and 5/7 L_0 so called sliding limit. R(t) denotes a Gaussian random force with zero mean value. The last equation is the dissipation-fluctuation theorem assumed and in case i=j=r, r^2 factor is necessary for $C_i(r)$. As for the friction in the approaching phase, there are two models available; one is the surface friction model (SFM) [2] and the other the proximity friction [4]. The former is rather successful in reproducing DIC data except spins of outgoing fragments which appears to require the inclusion of the rolling friction. And the strengths are very different between the radial and tangential frictional forces, which may be unnatural. On the other hand, the latter does not take into account effects of strong couplings to inelastic channels which are important in low energy. Thus, no outstandingly good model for the friction in the approaching phase is available for the moment. Thus, these models were used to calculate sticking probabilities [5]. It turned out that SFM is much stronger than the proximity one, i.e., sticking probabilities calculated by SFM are extremely small, though which one is realistic is not determined yet. At the same time, there is a common feature that the radial momentum has a distribution with a Gaussian shape which would be due to the assumption of the Gaussian random forces associated with the frictional force. The width of the distribution is consistent with the temperature determined by the internal energy transferred from the kinetic energy. The distribution is used for the initial condition for the dynamics of the second phase, i.e., for shape evolution toward the spherical shape. In this sense the model should be called a stochastic two-step model.

3. Shape Evolution

As stated in the Introduction, the amalgamated system locates at the outside of the conditional saddle point or at the outside of the ridgeline. Therefore, in order to obtain the formation probability, we have to solve shape evolution towards the spherical shape under a frictional force and its associated random force. The ratio between the number of trajectories that pass over the ridge line and the total number gives the formation probability, though most of them return back to reseparation due to the conservative potential calculated with the liquid drop model (LDM). An example of LDM energy surface is shown in the second figure for the system with A=272 and Z=112. Shapes are specified in terms of the two-center parameterization (R/R_0,a) with the neck parameter fixed to be 1.0 [6]. The cross in the figure denotes the contact configuration of $^{64}Ni+^{208}Pb$, i.e., the starting point of the evolution.

The dynamics is again described by a Langevin equation, generally multi-dimensional one,

$$\begin{cases} \dfrac{dq_i}{dt} = (m^{-1})_{ij} \cdot p_j \\ \dfrac{dp_i}{dt} = -\dfrac{\partial V^J}{\partial q_i} - \dfrac{1}{2}\dfrac{\partial}{\partial q_i}(m^{-1})_{jk} \cdot p_j \cdot p_k - \gamma_{ij} \cdot (m^{-1})_{jk} \cdot p_k + g_{ij} \cdot R_j(t) \end{cases}$$

$$\langle g_{ik} \cdot g_{jk} \rangle = \gamma_{ij} \cdot T^J \qquad (3)$$

where V^Jdenotes the LDM potential plus the centrifugal force for spin J. The last equation is again the dissipation-fluctuation theorem with a constant temperature T^J for spin J. We calculate the friction tensor by employing so-called one-body model (OBM), i.e., one-body wall-and-window formula [7] with the two-center parameterization of nuclear shapes. For a given initial momentum conjugate with the distance, we calculate many trajectories, some of which pass over the ridgeline. Then, the formation probability is given by the average over the initial momentum distribution obtained in the first step.

4. Residue Cross Sections

Assuming the compound nucleus theory of reactions, residue cross sections of the superheavy elements are given by a product of the fusion probability P_{fusion} and the survival probability P_{surv}as follows,

$$\sigma_{res} = \pi \lambda\!\!\!^{-2} \sum (2J+1) P^J_{fusion}(E_{c.m.}) \cdot P^J_{surv}(E^*) \qquad (4)$$

where $E^* = E_{c.m.} + Q$ with the fusion Q-value. P_{surv}denotes the probability for the compound nucleus to survive against fission and charged particle emission. It is calculated by the new computer program which is constructed, based on the theory of the time-dependent statistical decay [8]. An essential parameter is the shell correction energies for the superheavy elements. Although there are many predictions on them by the structure calculations with various levels of nuclear model [9], but unfortunately they differ with each other. We introduce a single reduction factor 0.4 for P. Moeller et al's predictions, because their predictions mostly appear to be largest compared with others' in the absolute values for nucleides around Z=114. An example of the residue cross section is shown in the last figure for ^{64}Ni+^{208}Pb system leading to Z=112 element after one neutron emission. The result is compared with the available data [10]. Theory reproduces the data remarkably well. Similar results are obtained for ^{70}Zn+^{208}Pb, though the data to be compared are few. Predictions are made on Z=113 and 114 elements.

It should be worth to remind that the model has been already applied to the hot fusion path, i.e., ^{48}Ca+ actinide systems with the same parameters and resulted in a reasonabely good reproduction of the available data [1, 11].

References

[1] C. Shen, G. Kosenko and Y. Abe, Phys. Rev. C66, 061602 (R) (2002); Y. Abe, et al., Prog. Theor. Phys. Suppl. 146, 104 (2002).

[2] D.H.E.Gross and H. Kalinowski, Phys. Rep. 45, 175 (1978).

[3] D. Banger and H. Freiesleben, Nucl. Phys. A340, 205 (1980).

[4] J. Randrup, Ann. Phys. 112,356 (1978).

[5] G. Kosenko, C. Shen and Y. Abe, J. Nucl. Radiochem. Sci◎D3, 19 (2002).
[6] K. Sato et al., Z. Phys. A290, 145 (1979).
[7] J. Blocki et al., Ann. Phys. 113,330 (1978).
[8] B. Bouriquet, D. Boilley and Y. Abe, to be published.
[9] P. Moeller et al., At. Data Nucl. Data Tables 59,185 (1995); S. Liran, A. Marinov and N. Zeldes, Phys. Rev. C62, 047301 (2000); S.Cwiok et al., Nucl. Phys. A611, 211 (1996); M. Bender et al., Eur. Phys. J. A7, 467 (2000).
[10] S. Hofmann et al., Rep. Prog. Phys. 61, 639(1998); K. Morita et al., private communication; LBNL, private comunication.
[11] Y. Abe et al, to be published in Proc. Heavy Ion Physics, Dubna 27 May-1 June, 2002.; Y. Abe et al., Proc. Symp. On Nuclear Clusters, Rauischholzhauzen, Germany, 5-9Aug.2002 ,p.383.; Y. Abe and B. Bouriquet, Acta Physica Polonica B34, 1927(2002); Y. Abe et al., Acta Physica Polonica B34, 2091 (2003).

The physics of nucleus-nucleus fusion

W. Swiatecki[1]

[1] LBNL, USA

wjswiatecki@lbl.gov

Twelve measured cross sections for one-neutron-out reactions with ^{208}Pb and ^{209}Bi targets and projectiles ranging from ^{48}Ca to ^{70}Zn are compared with a theoretical model. The model assumes that the cross section is the product of three factors: a) the cross section for the nuclei to stick, b) the probability for the system to diffuse ("up hill") over the barrier separating it from the compound-nucleus configuration and c) the probability for the compound nucleus to survive fission and the emission of a second neutron. With one parameter adjusted to have the value 1.6 fm (equal to the separation between the nuclear surfaces at which the diffusion process begins) the cross sections, ranging over 6 orders of magnitude, are reproduced adequately. The centroids and widths of the excitation functions are in good agreement with measurements. The model is used to calculate cross sections for even heavier reactions, using the same targets and ^{76}Ge, ^{82}Se and ^{86}Kr as projectiles.

Production of spherical super-heavy nuclei

K.H. Schmidt[1], A. Heinz[2], A.R. Junghans[3]

[1] Gesellschaft für Schwerioneforschung, Germany
[2] Yale University, USA
[3] Forschungszentrum Rossendorf, Germany

Andreas.Heinz@yale.edu

Introduction

Since GSI started its research program on super-heavy elements in the 1970s, an extensive program has continuously been carried out to explore the physics involved in the different processes which are relevant for the synthesis of the heaviest nuclei. Special emphasis was put on those features which are particularly relevant for reaching the next doubly magic spherical shell closure beyond ^{208}Pb. This long-term research program included several aspects, reaching from the amalgamation process of projectile and target nuclei under the influence of the strong repulsive Coulomb force up to the cooling down of the compound nucleus by particle evaporation in competition with a strong fission branch. It was decided to perform the necessary elaborate investigations by studying the synthesis of proton-rich nuclei near the 126-neutron shell, whose formation can be considered as a realistic test case for the production of spherical super-heavy nuclei. The common features are the spherical shape of the nuclear ground state and a large shell effect of more than 5 MeV. The larger liquid-drop component of the fission barrier of a few MeV ensures sizeable formation cross sections, which are a pre-requisite for systematic studies.

Entrance channel

Specific features of the entrance channel arise in the synthesis of spherical super-heavy nuclei, because the projectile-target combinations available on the basis of primordial nuclei require rather mass-symmetric systems, which consequently experience a very strong Coulomb repulsion in the amalgamation phase. The most extensive exploration of entrance-channel effects in fusion of massive systems, extending from ^{90}Zr + ^{90}Zr to ^{110}Mo + ^{110}Mo, is documented in Ref. [1]. These experiments revealed the onset of a considerable reduction of the fusion probability near the potential barrier already for symmetric systems with Z_1*Z_2=1600. This hindrance was related to the "extra-push" phenomenon, postulated by W. Swiatecki. More massive systems showed a stronger fusion hindrance and a more gradual increase of the fusion probability as a function of bombarding energy. The gradual increase of the fusion probability was interpreted as an evidence for strong fluctuations connected with the extra push. The nuclear-structure properties of projectile and target were found to have a decisive influence on this phenomenon: Projectile-target combinations with nuclei close to major shells were less affected. Some new experiments performed in other laboratories shed new light on these results. H. Ikezoe *et al*. have shown that the fusion probability of a deformed projectile or target nuclei can be understood by variations in the orientation of the colliding nuclei [2]. Tip-on-tip configurations lead to less compact contact configurations and experience a stronger extra-push in contrast to side-on-side collisions. In another very important work, Hinde *et al*. completed the series of projectile-target combinations leading to the compound nucleus ^{220}Th studied in [1] by the system ^{16}O + ^{204}Pb [3]. They obtained the surprising result that already the system ^{40}Ar + ^{174}Hf, which was considered previously to fuse in the lower angular-momentum range with high probability, experiences a strong fusion hindrance. On the basis of this new

result, the systematics of fusion probabilities deduced in ref. [1] is to be revised. As a general conclusion, the extra-push phenomenon is found to set in for considerably lighter systems than previously known.

Exit channel

The exit channel in the synthesis of spherical super-heavy nuclei is subject to very specific features, which may differ considerably from those met in the production of deformed super-heavy nuclei. In the de-excitation of slightly excited highly fissile nuclei, nuclear-structure phenomena are expected to govern the competition between particle evaporation and fission due to the influence of shell effects and collective properties on the level density. Therefore, any extrapolation based on the experience in the synthesis of the heaviest nuclei reached up to now is highly doubtful. Again, extended studies on the synthesis of proton-rich nuclei near the 126-neutron shell were chosen as the appropriate tools to explore the features of the exit channel in the production of spherical super-heavy nuclei.

The results of a first experimental program, based on the production of a series of compound nuclei around the 126-neutron shell by heavy-ion fusion reactions, are documented in ref. [1]. It was found that the strong ground-state shell effect of these nuclei does not enhance the survival probability of the fused system against fission, although it is responsible for about half the height of the fission barrier.

In order to avoid the influence of fusion hindrance on these results, the fission competition of these nuclei was studied recently with a different experimental approach. The nuclei of interest were produced as secondary beams. They were excited by electromagnetic interactions to states of low angular momentum at energies only slightly above the fission barrier, and the cross sections for consecutive fission were measured [4]. Even at these low excitation energies no influence of the 126-neutron shell on the fission probability was observed.

A third approach exploited the production of proton-rich nuclei near the 126-neutron shell by bombarding copper, hydrogen and deuterium nuclei with ^{238}U at 1 A GeV [5-7]. In these reactions, a field of nuclides slightly lighter than the projectile are produced with excitation energies extending to several hundred MeV or more. The production of these prefragments is certainly not influenced by nuclear-structure properties. Only in the last steps of the deexcitation process an eventual influence of the 126-neutron shell on the fission competition is expected, which would lead to a structure in the nuclide distribution observed. Since the spallation process produces a large field of nuclei with comparable cross sections, it is well suited to reveal a possible enhancement of the survival probability of nuclei near N=126 in the deexcitation process by the appearance of a ridge which would be superimposed on the broad distribution of nuclide cross sections formed by the spallation process. The results of this approach also agreed with those found in our preceding experiments: The large ground-state shell effect of N=126 nuclei does not lead to a noticeable enhancement of the survival probability against fission in the deexcitation process.

These findings have been traced back to the specific features of the level densities of magic spherical nuclei [4,5]. While the number of intrinsic excitations is influenced by the sequence of single-particle energies, which would strongly enhance particle emission with respect to fission, the spherical nuclear shape only allows for collective excitations of vibrational character. Compared to the large number of rotational levels found at the fission-barrier deformation, this leads to strong enhancement of fission. It seems that these two counteracting structural effects cancel to a great extent in the case of proton-rich N=126 nuclei. As a consequence for the production of spherical super-heavy nuclei, we expect qualitatively a similar effect. Therefore, we expect that the systematics of production cross sections found in the synthesis of deformed super-heavy nuclei cannot be extrapolated for estimating the production cross sections of spherical super-heavy nuclei. Instead, one will probably face a considerably stronger

decrease in the formation cross sections in the transition from the deformed to the spherical super-heavy region.

References

[1] K.-H. Schmidt, W. Morawek, Rep. Prog. Phys. **54**, 949 (1991).

[2] H. Ikezoe, S. Mitsuoka, K. Nishio, K. Satou, I. Nihinaka, INPC 2001, conference proccedings by E. Norman, L. Schroeder, G. Wozniak, AIP 610, p. 604. (2001) and K. Satou, H. Ikezoe, S. Mitsuoka, K. Nishio, S.C. Jeong, Phys. Rev. C **65**, 054602 (2002).

[3] D. J. Hinde, M. Dasgupta, A. Mukherjee, Phys. Rev. Lett. **89**, 282701 (2003).

[4] A. Heinz, K.-H. Schmidt, A. R. Junghans, P. Armbruster, J. Benlliure, C. Boeckstiegel, H.-G. Clerc, A. Grewe, M. de Jong, J. Mueller, M. Pfuetzner, S. Steinhaeuser, B. Voss, Nucl. Phys. **A713**, 3 (2003).

[5] A. R. Junghans, M. de Jong, H.-G. Clerc, A. V. Ignatyuk, G. A Kudyaev, K.-H. Schmidt, Nucl. Phys. **A629**, 635 (1998).

[6] J. Taieb, K.-H. Schmidt, L. Tassan-Got, P. Armbruster, J. Benlliure, M. Bernas, A. Boudard, E. Casarejos, S. Czajkowski, T. Enqvist, R. Legrain, S. Leray, B. Mustapha, M. Pravikoff, F. Rejmund, C: Stephan, C. Volant, W. Wlazlo, Nucl. Phys. A, in press.

[7] E. Casarejos, Ph.D. thesis, 2001, Universidad de Santiago de Compostela, Spain.

Fusion-fission dynamics and perspectives of superheavy element formation

V.I. Zagrebaev[1]

[1] JINR, Russia

valeri.zagrebaev@jinr.ru

The interest in the synthesis of super-heavy nuclei has lately grown due to the new experimental results [1] demonstrating a real possibility of producing and investigating the nuclei in the region of the so-called "island of stability". The new reality demands a more substantial theoretical support of these expensive experiments, which will allow a more reasonable choice of fusing nuclei and collision energies as well as a better estimation of the cross sections and unambiguous identification of evaporation residues (ER). The talk will focus on reaction dynamics of superheavy nucleus formation and decay at beam energies near the Coulomb barrier. The aim will be to review the things we have learned from recent experiments [1,2] on fusion-fission reactions leading to the formation of compound nuclei with Z^3102 and from their extensive theoretical analysis [3-6]. Major attention is paid to the dynamics of formation of very heavy compound nuclei taking place in strong competition with the process of fast fission (quasi-fission). The choice of collective degrees of freedom playing a principal role, finding the multi-dimensional driving potential and the corresponding dynamic equations of motion regulating the whole process are discussed along with a new approach proposed in [3,5] to description of fusion-fission dynamics of heavy nuclear systems based on using the two-center shell model idea. A possibility of deriving the fission barriers of superheavy nuclei directly from performed experiments is of particular interest here. In conclusion the results of detailed theoretical analysis of available experimental data on the "cold" and "hot" fusion-fission reactions will be presented. Perspectives of future experiments will be discussed along with additional theoretical studies in this field needed for deeper understanding of the fusion-fission processes of very heavy nuclear systems.

A whole process of super-heavy nucleus formation can be divided into three reaction stages. At first stage colliding nuclei overcome the Coulomb barrier and approach the point of contact $R_{cont}=R_1+R_2$. Quasi-elastic and deep-inelastic reaction channels dominate at this stage leading to formation of projectile-like and target-like fragments (PLF and TLF) in exit channel. At sub-barrier energies only small part of incoming flux with low partial waves reaches the point of contact. Denote the corresponding probability as $P_{cont}(l,E)$. At the second reaction stage touching nuclei evolve into the configuration of almost spherical compound mono-nucleus. For light or very asymmetric nuclear systems this evolution occurs with a probability close to unity. Two touching heavy nuclei after dynamic deformation and exchange by several nucleons may re-separate into PLF and TLF or may go directly to fission channels without formation of compound nucleus. The later process is usually called quasi-fission. Denote a probability for two touching nuclei to form the compound nucleus as $P_{CN}(l,E)$. At third reaction stage the compound nucleus emits neutrons and γ-rays lowering its excitation energy and forming finally the residual nucleus in its ground state. This process takes place in strong competition with fission (normal fission), and the corresponding survival probability $P_{xn}(l,E^*)$ is usually much less than unity even for low-excited superheavy nucleus.

Thus, the production cross section of a cold residual nucleus B, which is the product of neutron evaporation and γ-emission from an excited compound nucleus C, formed in the fusion process of two heavy nuclei $A_1+A_2\rightarrow C\rightarrow B+xn+N\gamma$ at center-of mass energy E close to the Coulomb barrier in the entrance channel, can be decomposed over partial waves and written as

$$\sigma_{ER}^{xn}(E) \approx \frac{\pi\hbar^2}{2\mu E}\sum_{l=0}^{\infty}(2l+1)P_{cap}(l,E)P_{CN}(A_1+A_2 \rightarrow C;l,E)P_{xn}(C \rightarrow B;l,E^*) \quad .(1)$$

Different theoretical approaches are used for analyzing all the three reaction stages. However, the dynamics of the intermediate stage of the compound nucleus formation is the most vague. Setting here P_{xn}=1 we get the cross section of CN formation σ_{CN}, which can be measured by detection of ERs and fission fragments forming in normal fission (if they are distinguished from quasi-fission fragments and from products of deep inelastic collision). Setting in addition P_{CN}=1 we get the capture cross section σ_{cap}, which can be measured by detection of all fission fragments (if they are distinguished from products of deep inelastic collision). For symmetric fusion reactions σ_{CN} and σ_{cap} cannot be measured experimentally.

Coupling with the excitation of nuclear collective states (surface vibrations and/or rotation of deformed nuclei) and with nucleon transfer channels significantly influences the capture cross section at near-barrier energies. Incoming flux has to overcome in fact the multi-dimensional ridge with the height depending on orientation and/or dynamic deformation. In [3,4] a semi-empirical approach was proposed for calculating the penetration probability of such multi-dimensional potential barriers. The capture cross sections calculated within this approach are shown in Fig. 1 for the three reactions (solid curves). They are compared with theoretical calculations made within a model of one-dimensional barrier penetrability for spherical nuclei (dashed curves). In all three cases a substantial increase in the barrier penetrability is observed in the sub-barrier energy region. Good agreement between the calculated and experimental capture cross sections allows us to believe that we may get rather reliable estimation of the capture cross section for a given projectile-target combination if there are no experimental data or these data cannot be obtained at all (symmetric combinations).

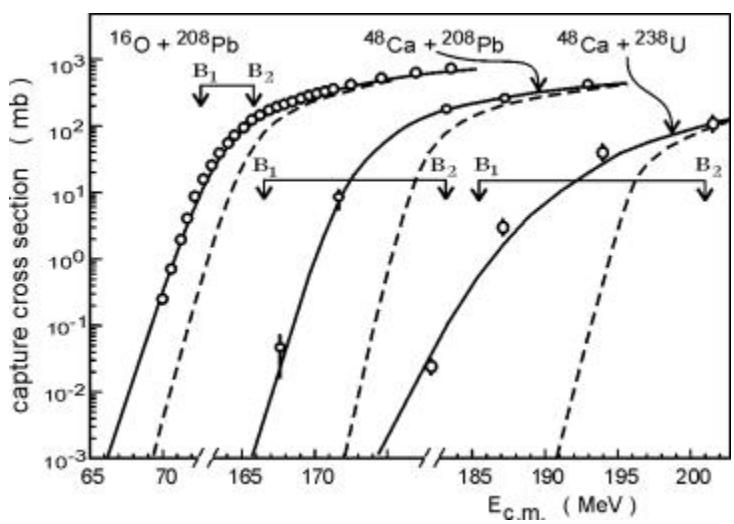

Figure 1. Capture cross sections in the $^{16}O+^{208}Pb$, $^{48}Ca+^{208}Pb$, and $^{48}Ca+^{238}U$ fusion reactions. Dashed curves represent one-dimensional barrier penetration calculations with the Bass barriers. Solid curves show the effect of dynamic deformation of nuclear surfaces (two first reactions) and orientation of statically deformed nuclei ($^{48}Ca+^{238}U$ case).

The processes of the compound nucleus formation and quasi-fission are the least studied stages of heavy ion fusion reaction. To solve the problem we have to answer very principal questions. What are the main degrees of freedom playing most important role at this reaction stage? What is the corresponding driving potential and what are appropriate equations of motion for description of time evolution of nuclear system at this stage? Today there is no consensus for the answers and for the mechanism of the compound nucleus formation itself, and quite different, sometimes opposite in their physics sense,

models are used for its description. In [3,5] a new approach was proposed for description of fusion-fission dynamics based on a simplified semi-empirical version of the two-center shell model idea [7]. It is assumed that on a way from the initial configuration of two touching nuclei to the compound nucleus configuration and on reverse way to the fission channels the nuclear system consists of two cores (Z_1,N_1) and (Z_2,N_2) surrounded with a certain number of common (shared) nucleons ΔA=ACN-A1-A2 moving in the whole volume occupied by the two cores. The processes of compound nucleus formation, fission and quasi-fission take place in the space (Z_1,N_1,β_1;Z_2,N_2,β_2), where β_1 and β_2 are the dynamic deformations of the cores. The compound nucleus is finally formed when two fragments A_1 and A_2 go in its volume, i.e., at $R(A_1)+R(A_2)=RCN$ or at $A_1^{1/3}+A_2^{1/3}=ACN^{1/3}$.

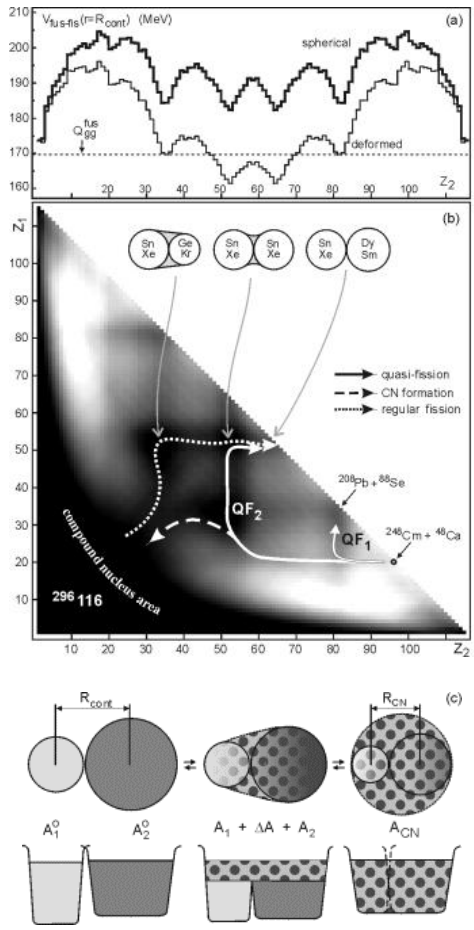

Figure 2. Driving potential $V_{fus\text{-}fis}(Z_1,Z_2)$ of the nuclear system consisting of 116 protons and 180 neutrons. (a) Potential energy of two touching nuclei at $A_1+A_2=A_{CN}$, $\Delta A=0$, i.e., along the diagonal of the lower figure. The thick line corresponds to the case of spherical nuclei, whereas the thin line corresponds to $\beta_1+\beta_2=0.3$. (b) Topographical landscape of the driving potential on the plane (Z_1, Z_2) (zero deformations). The dark regions correspond to the lower potential energies (more compact configurations). (c) Schematic view of the process of compound nucleus formation, fission and quasi-fission in the space of A_1, A_2 and ΔA, i.e., the number of nucleons in the projectile-like nucleus, target-like nucleus, and shared nucleons, here $A_1+A_2+\Delta A=A_{CN}$.

The corresponding driving potential $V_{fus\text{-}fis}(r, Z_1, N_1, \beta_1, Z_2, N_2, \beta_2)$ was derived in [3] and is shown in Fig. 2 as a function of Z_1, Z_2 (minimized over N_1, N_2 and at fixed values of $\beta_1+\beta_2$). There are several advantages of the proposed approach. The driving potential is derived basing on experimental binding

energies of two cores, which means that the "true" shell structure is taken into account. The driving potential is defined in the whole region $R_{CN} < r < \infty$, it is a continuous function of r at $r=R_{cont}$, and it gives the realistic Coulomb barrier at $r=R_B>R_{cont}$. At last, instead of using the variables (A_1,A_2), we may easily recalculate the driving potential as a function of mass asymmetry $(A_1-A_2)/(A_1+A_2)$ and elongation $R_{12} = r_0 (A_1^{1/3}+A_2^{1/3})$ (at $r > R_{cont}$, $R_{12} = r = s+R_1+R_2$, where s is the distance between nuclear surfaces). These variables along with deformation $\beta_1+\beta_2$ are commonly used for description of fission process. The corresponding driving potential is shown in Fig. 3.

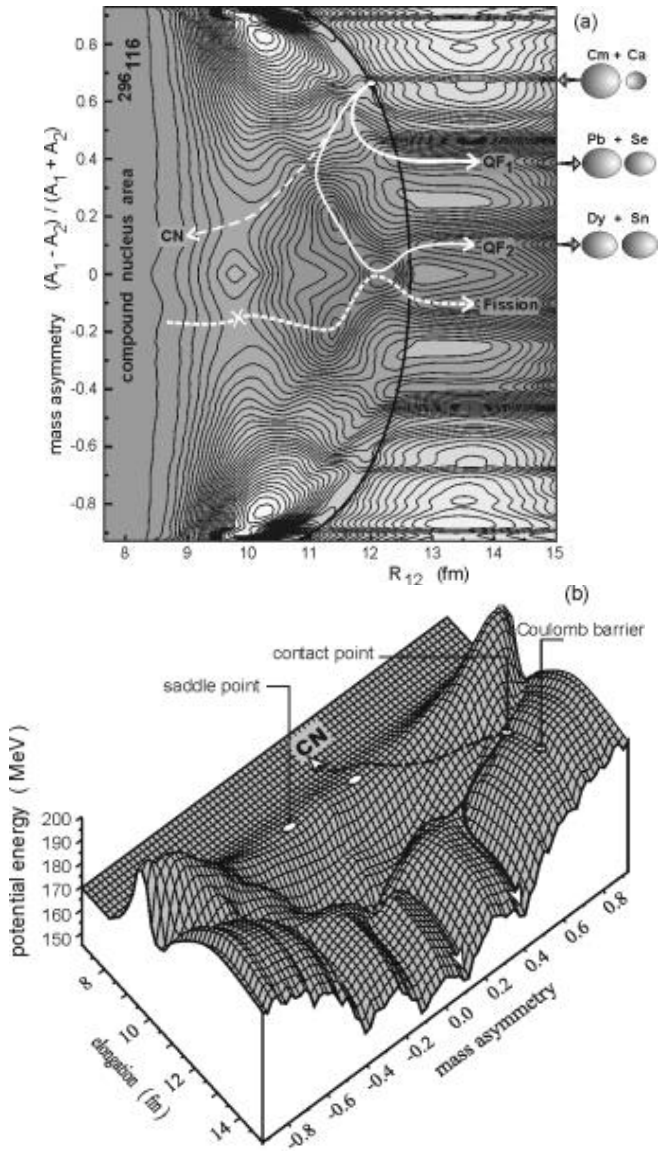

Figure 3. Driving potential $V_{fus\text{-}fis}$ as a function of mass asymmetry and distance between centers of two nuclei with the deformations $\beta_1+\beta_2=0.3$, topographical landscape (a) and three-dimensional plot (b). The black solid curve in (a) shows the contact configurations. The paths QF_1 and QF_2 lead to the asymmetric and near-symmetric quasi-fission channels, the dashed curve shows the most probable way to formation of the compound nucleus, and dotted curve corresponds to the normal (regular) fission. See the conformity with Fig. 2.

As can be seen from Fig. 2 and Fig. 3, the shell structure, clearly revealing itself in the contact of two nuclei (Fig. 2a), is also retained at $\Delta A \neq 0$ ($R_{12} < R_{cont}$), see the deep minima in the regions of $Z_{1,2}$—50 and $Z_{1,2}$—82 in Fig. 2b. Following the fission path (dotted curves in Fig. 2b and Fig. 3) the system overcomes a multi-humped fission barrier, which is well known in fission dynamics. The intermediate minima correspond to the shape isomeric states. From our analysis we may definitely conclude that these isomeric states are nothing else but two-cluster configurations with magic or semi-magic cores (see the inset in Fig. 2b).

As regards the superheavy compound nucleus formation in the fusion reaction $^{48}Ca+^{248}Cm$, one can see that after the contact, the nuclear system may easily decay into the quasi-fission channels (mainly asymmetric: Se+Pb, Kr+Hg and also near-symmetric: Sn+Dy, Te+Gd) - solid arrow lines in Fig. 2b and Fig. 3. Only a small part of the incoming flux reaches a compound nucleus configuration (dashed arrow line). The experimental data on the yield of quasi-fission fragments in collisions of heavy nuclei [2] were found quite understandable in terms of multi-dimensional potential energy surface shown in Fig. 2 and Fig. 3 [6].

Using the driving potential $V_{fus\text{-}fis}(Z_1, N_1, \beta_1, Z_2, N_2, \beta_2)$ we may determine the probability of the compound nucleus formation $P_{CN}(A_1+A_2 \rightarrow C)$, being part of expression (1) for the cross section of the synthesis of super-heavy nuclei. It was by solving the transport equation for the distribution function $F(Z_1, N_1, \beta_1, Z_2, N_2, \beta_2;t)$. The probability of the compound nucleus formation is determined as an integral of the distribution function over the region $R_1+R_2 <= R_{CN}$. Similarly one can define the probabilities of finding the system in different channels of quasi-fission, i.e., the charge and mass distribution of fission fragments measured experimentally. Results of such calculations demonstrate quite reasonable agreement with the corresponding experimental data.

The detailed theoretical analysis of available experimental data on the "cold" and "hot" fusion-fission reactions has been performed and the cross sections of superheavy element formation have been calculated up to Z_{CN}=120 as well as the mass and charge distributions of quasi-fission fragments obtained in these reactions. The corresponding excitation functions for 2n, 3n, and 4n evaporation channels were calculated depending on different theoretical estimations of the neutron separation energies and fission barriers of superheavy nuclei. Optimal beam energies were found for production of the cold evaporation residues of new elements in the "hot" fusion reactions. We found also a possibility of deriving the fission barriers of superheavy nuclei directly from analysis of experimental data on the fusion-fission cross sections and from experimental data on the survival probability of those nuclei in evaporation channels of 3 and 4 neutron emission. In particular, the lower limits that we have obtained for the fission barrier heights of $^{283\text{-}286}112$, $^{288\text{-}292}114$ and $^{292\text{-}296}116$ nuclei are 5.5, 6.7 and 6.4 MeV respectively [6], which are really quite high resulting in relatively high stability of these nuclei.

References

[1] Yu.Ts. Oganessian et al., Nature, **400**, 242 (1999); Yad.Fiz., **63**, 1769 (2000).
[2] M.G. Itkis et al., in Fusion Dynamics at the Extremes, WS, Singapore, 2001, p.93.
[3] V.I. Zagrebaev, Phys.Rev. C **64**, 034606 (2001).
[4] V.I. Zagrebaev et al., Phys.Rev. C **65**, 014607 (2002).
[5] V.I. Zagrebaev, J.Nucl.Radiochem.Sci., Vol. **3**, No. 1, 13 (2002).
[6] M.G. Itkis, Yu.Ts. Oganessian, and V.I. Zagrebaev, Phys.Rev. C **65**, 044602 (2002).
[7] J. Maruhn and W. Greiner, Z. Physik, **251**, 431 (1972).

The cold formation and decay of superheavy nuclei including the orientation degree of freedom

R.K. Gupta[1], M. Balasubramaniam[1], R. Kumar[1], N. Singh[1]

[1] Panjab University, India

gupta_rajk@hotmail.com

Theoretically, cold synthesis of new and superheavy elements (SHE) was proposed by one of us and collaborators [1-3] as back as in 1974-75, where a method was given for selecting out an *optimum* cold target-projectile combination. Cold compound systems were considered to be formed for *all* those target + projectile combinations that lie at the bottom of the *potential energy minima*, referred to as "cold reaction valleys" or reaction partners leading to "cold fusion" [2-6]. This information on cold reaction valleys was optimized [3] by the requirements of smallest interaction barrier, largest interaction radius and non-necked (no saddle) nuclear shapes, identifying the cases of "cold", "warm/ tepid" and "hot" fusion reactions. The theory, called the Quantum Mechanical Fragmentation Theory (QMFT), was advanced as a unified approach both for fission (including the cluster radioactivity (CR)) and heavy ion collisions. The key result behind the cold fusion reaction valleys (or the decay products in fission and CR) is the *shell closure effects* of one or both the reaction partners (or decay products). Also, fission and CR were considered as cold phenomenon on the basis of the QMFT, prior to their being observed experimentally as cold processes in 1980 and 1984, respectively [7].

In this paper, we review this theory via some new calculations based on the use of oriented and radioactive nuclei as beams and/ or targets. The use of neutron-rich radioactive nuclei is essential for overshooting the *center* of island of SHE (the next doubly magic nucleus) and the deformed oriented collisions could be useful since the fusion barrier gets lowered, or, in other words, the excitation energy of the cold compound system gets further reduced. As an example, we choose the recently used highly neutron-rich beam of ^{48}Ca on neutron-rich actinide targets ^{232}Th, ^{238}U, ^{242,244}Pu and ^{248}Cm, forming the compound systems $^{280}110^*$, $^{286}112^*$, $^{290,292}114^*$ and $^{296}116^*$ [8]. Note that the targets used are the deformed nuclei and, for near the Coulomb barrier energies, the compound nucleus excitation energy $E^* \sim 30$-35 MeV, in between the one for cold (10-20 MeV) and hot (40-50 MeV) fusion reactions. The resulting "warm/ tepid" compound systems de-excite by 3n and/ or 4n evaporations (and γ rays), compared to 1n and 2n in cold and 5n in hot fusion reactions, and give rise to new nuclei $^{277}110$, $^{283}112$, $^{287,288,289}114$ and $^{292}116$. These final nuclei are relatively long-lived and decay only via α-particles, giving the α-genetically related nuclei, called an α-decay chain. Then, as a second aim of this paper, we investigate the observed α–decay characteristics of these nuclei within the preformed cluster decay model (PCM) of Gupta and Collaborators [9-11] which is also based on the QMFT.

The QMFT is a dynamical theory of the three cold processes mentioned above, worked out in terms of the mass (charge) asymmetry $\eta=(A_1-A_2)/(A_1+A_2)$ ($\eta_Z=(Z_1-Z_2)/(Z_1+Z_2)$), the relative separation **R**, the deformations β_1^λ, β_2^λ (λ=2) of two nuclei or, in general, the fragments, and the neck parameter ε [12,13]. We extend the QMFT here to include the multipole deformation parameter λ=3 and 4 i.e. octupole and hexadecupole deformations also. In addition, we introduce two orientation angles θ_1 and θ_2 [14], see Fig. 1(a). So far, the time-dependent Schrödinger equation in η is solved for non-oriented collisions and for weakly coupled η and η_Z motions:

$$H\Psi(\eta,t)=i\hbar\frac{\partial}{\partial t}\Psi(\eta,t). \qquad (1)$$

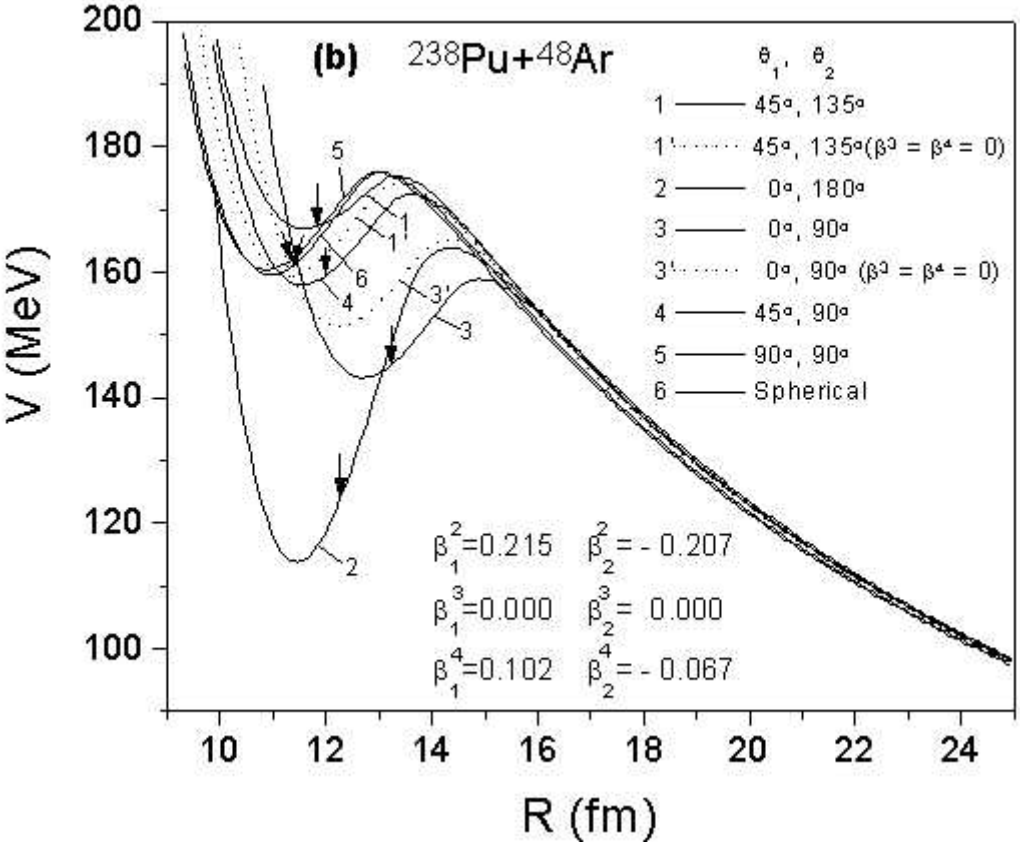

Figure 1. (a) Schematic configuration of two axially symmetric quadrupole deformed, oriented nuclei, in same plane. (b) Scattering potentials for $^{48}Ar+^{238}Pu$ at different orientations. Arrows denote R-values for s_0=1.0 fm.

Here R(t) is treated classically and the quadrupole deformations β_i^2 (i=1,2) and ε are fixed by minimizing the collective potential $V(R,\eta,\eta_Z,\beta_i^2,\varepsilon)$ in the above coordinates. Eq. (1) is solved for a number of heavy systems [13], which shows that for target + projectile combinations coming from *outside* the potential energy minima, a few nucleon to a large mass transfer occurs, whereas the same is zero for a target + projectile referring to potential energy minima. This means that *for cold reaction partners, the two nuclei stick together and form a deformed compound system*. A few nucleon transfer may, however, occur depending on whether a "conditional" saddle exists or not. Since the solution of Eq. (1) is very much computer-time consuming, the following simplifications are exercised based on calculated quantities.

The potentials $V(R,\eta)$ and $V(R,\eta_Z)$, calculated within the Strutinsky method i.e. $V=V_{LDM} + \delta U$, the liquid drop energy plus the shell effects calculated by using the asymmetric two-center shell model (ATCSM), show that the motions in both η and η_Z are much faster than the R-motion. This means that these both potentials are nearly independent of the R-coordinate and hence R can be taken as a time-independent parameter. This reduces the time-dependent Schrödinger equation (1) in η to the stationary Schrödinger equation in η,

$$\left\{-\frac{\hbar^2}{2\sqrt{B_{\eta\eta}}}\frac{\partial}{\partial\eta}\frac{1}{\sqrt{B_{\eta\eta}}}+V_R(\eta)\right\}\Psi_R^{(\nu)}(\eta)=E_R^{(\nu)}\Psi_R^{(\nu)}(\eta) \tag{2}$$

where R is fixed at the post saddle point. This choice of R-value is justified by many good fits to both fission and heavy-ion collision data [7] and by an explicit, analytical solution of time-dependent Schrödinger equation in η_Z coordinate [15]. An interesting result of these calculations is that the yields ($\propto |\Psi(\eta)|^2$ or $|\Psi(\eta_Z)|^2$, respectively, for mass or charge distributions) are nearly insensitive to the detailed structure of the kinetic energy term in the Hamiltonian i.e. the Cranking masses $B_{\eta\eta}$ calculated consistently by using ATCSM. In other words, the static potential $V(\eta)$ or $V(\eta_Z)$ contain all the important information of a fissioning or colliding system. The positions of the minima are due to shell effects. Since these potentials are nearly independent of the choice of R-value, we have calculated them at some critical distance R_c where the two nuclei come in close contact with each other. We do the same here for oriented, neutron-rich radioactive nuclei having higher multipole deformations also.

For oriented nuclei, the potential $V(\eta)$ is the sum of binding energies (taken from Möller et al. [16] for $Z\geq 8$; and from experiments for $Z\leq 7$), the Coulomb and the proximity potential (both taken from [14] and extended to include higher multipole deformations) that depend on deformations as well as on orientations:

$$V(\eta)=\sum_{i=1}^{2}B\left(A_i,Z_i,\beta_i^{\lambda}\right)+E_c(Z_i,\beta_i^{\lambda},\theta_i)+V_P(A_i,\beta_i^{\lambda},\theta_i). \tag{3}$$

In Eq. (3) i=1,2 and λ =2,3,4. For the fixed orientations, the charges Z_1 and Z_2 in (3) are fixed by minimizing this potential in η_Z coordinate (which fixes the deformation coordinates β_i^{λ}). The relative separation distance R, in terms of the minimum surface separation distance s_0, is $R=s_0+R_1(\alpha_1)\cos\psi_1+R_2(\alpha_2)\cos\psi_2$. For a fixed R, s_0 is different for different orientations. Alternatively, for fixed s_0, R is different for different orientations, and we use this latter one in the following.

Fig. 1(b) illustrates for prolate-oblate ^{238}Pu+ ^{48}Ar reaction, the scattering potentials at different orientations (for λ=2,3,4 and λ=2 alone). An interesting result is that the barrier is lowered in each case except for 90^0-90^0 configuration, and that the barrier is lowest for 0^0-90^0 configuration. Note that for prolate-prolate collisions, the barrier is lowest for 0^0-180^0 configuration [14]. Thus, in the following, we neglect the 90^0-90^0 configuration since for fusion it is as un-favorable as the spherical nuclei. Also, note that the inclusion of higher multipole deformations is not always favored (barriers lowered) since for 45^0-135^0 and 45^0-90^0 orientations the barrier gets raised, rather than lowered as in 0^0-90^0, 0^0-180^0 and 90^0-90^0 (see Fig. 1(b) for 45^0-135^0 and 0^0-90^0 cases).

Fig. 2(a) illustrates the fragmentation potentials for various orientations of different target + projectile combinations at a fixed separation s_0=1.0 fm, forming the same compound nucleus $^{286}112^*$ (for 0^0-180^0 s_0=1.5 fm, since in this configuration the nuclei come much closer to each other). Apparently, due to the orientation degree of freedom, the energies of all the potential minima are lowered and the largest effect of the higher multipoles is for 0^0-180^0 which though is not the most favorable orientation for fusion (barrier not lowest) . We concentrate here only on the ^{48}Ca or ^{50}Ca minimum (marked by vertical lines; for some orientations, Ca changes to Ar). We notice that w.r.t. ground state energy (also marked), the Ca and/ or Ar minima have now the excitation energies E^*~15-20 MeV compared to ~ 30 MeV for spherical nuclei. This means that Ca or Ar beam could be used for cold fusion reactions, if the colliding target nuclei are oriented, a result obtained for the first time. Note that ^{50}Ca is also a radioactive nucleus and all orientations and higher multipole deformations are not always favorable for the fusion process.

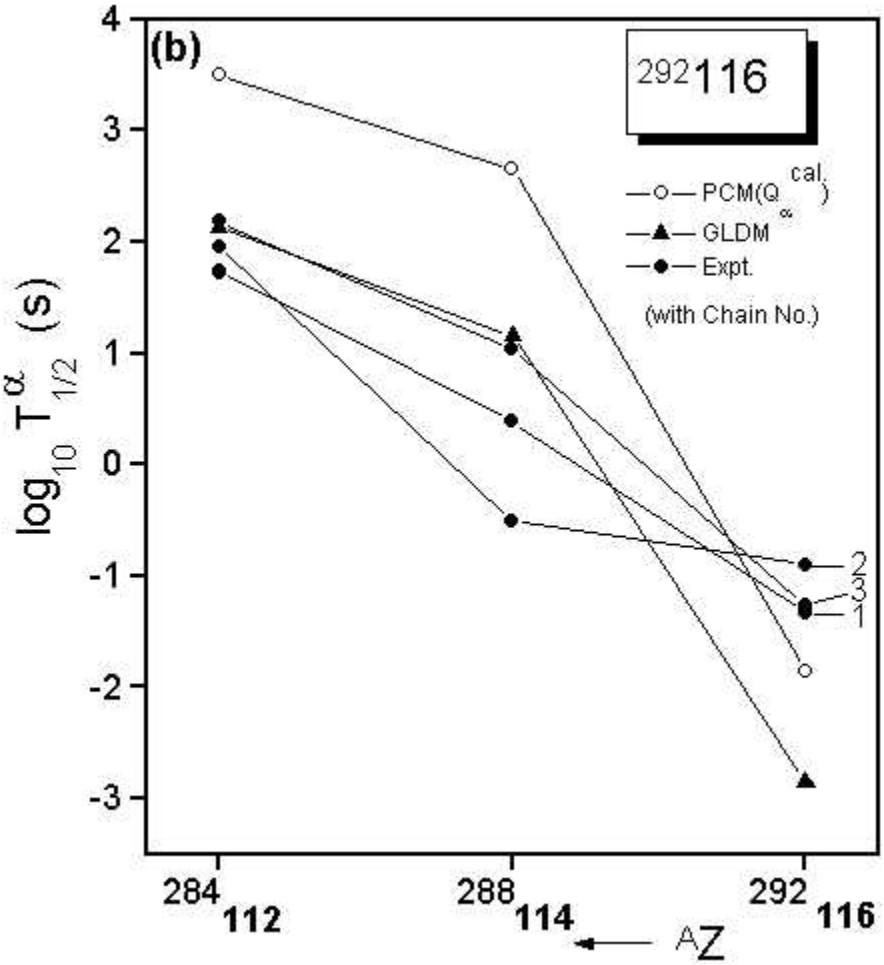

Figure 2. (a) Fragmentation potentials of $^{286}112^{*}$ for various orientations of different target + projectile combinations with λ=2,3,4 and λ=2 alone. For Z≤ 7, β_i^2 are from RMF with TM2 force [17]. (b) Calculated half-lives for α-decay chain of $^{292}116$, compared with experiments and GLDM calculation.

For α-decay studies, the preformed cluster-decay model (PCM) used here is also based on QMFT and hence on the same coordinates as are introduced above. In a PCM, the decay half-life is defined as,

$$T_{1/2} = \frac{\ln 2}{P_0 \nu_0 P} \tag{4}$$

The P_0, the cluster (and daughter) preformation probabilities in the ground state of nucleus referring to η-motion, are the solutions of the stationary Schrödinger equation (2) for the ground-state ν=0, and P, referring to R-motion, is WKB tunneling penetrability. The ν_0 is the barrier assault frequency. For details, see Refs. [9-11].

Fig. 2(b) illustrates our results of calculation for α-decay chain of $^{292}116$ parent [18], compared with the experimental data and another recent calculation [19], denoted GLDM. The numbers 1,2,3 in the figure mean that more than one chain is observed. We notice that the comparisons of $T_{1/2}$ values for the

two models with experiments are within experimental errors, i.e. within less than two orders of magnitude. Both model calculations give similar trends.

Summarizing, we have extended the QMFT for use of oriented collisions and including higher multipole deformations, which result in the reduction of excitation energies of the compound system formed due to different target-projectile combinations. This means that both the "warm" and "hot" fusion reactions could also be reached in "cold fusion", if the target and/or projectile were oriented and have also octu- and hexa-decapole deformations. The QMFT based PCM is also shown to explain the α-decay characteristics of SHE.

References

[1] H.J. Fink, W. Greiner, R.K. Gupta, S. Liran, H.J. Maruhn, W. Scheid and O. Zohni, *Proc. Int. Conf. on Reactions between Complex Nuclei*, Nashville, Tenn., USA, 1974, North-Holland Pub. Co., Vol. 2, p. 21.

[2] A. Sândulescu, R.K. Gupta, W. Scheid and W. Greiner, Phys. Lett. B **60**, 225 (1976).

[3] R.K. Gupta, A. Sândulescu and W. Greiner, Phys. Lett. B **67**, 257 (1977).

[4] R.K. Gupta, C. Pârvulescu, A. Sândulescu and W. Greiner, Z. Physik A **283**, 217 (1977).

[5] R.K. Gupta, A. Sândulescu and W. Greiner, Z. Naturforsch. 32 **a**, 704 (1977).

[6] R.K. Gupta, Sovt. J. Part. Nucl. **8**, 289 (1977).

[7] R.K. Gupta; and R.K. Gupta et al., *Heavy Elements and Related New Phenomena* edited by W. Greiner and R.K. Gupta (World Sc. Publications, 1999) Vols. I & II

[8] Yu.Ts. Oganessian, et al., Nature **400**, 242 (1999); Phys. Rev. C **62**, 041604(R) (2000); Phys. Rev. Lett. **83**, 3154 (1999); Phys. Rev. C **63**, 011301(R) (2000); Nucl. Phys. A **682**, 108c (2001).

[9] S.S. Malik and R.K. Gupta, Phys. Rev. C **39**, 1992 (1989).

[10] S. Kumar and R.K. Gupta, Phys. Rev. C **49**, 1922 (1994).

[11] R.K. Gupta and W. Greiner, Int. J. Mod. Phys. E **3**, 335 (1994, Supp.).

[12] R.K. Gupta, et al., Phys. Rev. Lett. **35**, 353 (1975); J. Maruhn and W. Greiner, *ibid*. **32**, 548 (1974).

[13] R.K. Gupta, Phys. Rev. C **21**, 1278 (1980); S. Yamaji, et. al., J. Phys. G **3**, 1283 (1977).

[14] Malhotra and R.K. Gupta, Phys. Rev. C **31**, 1179 (1985).

[15] D.R. Saroha, R. Aroumougame and R.K. Gupta, Phys. Rev. C **27**, 2720 (1983).

[16] P. Möller, J.R. Nix, W.D. Myers and W.J. Swiatecki, At. Data Nucl. Data Tables, **59**, 185 (1995).

[17] M.S. Mehta, S.K. Patra and R.K. Gupta, Private Communication (2003).

[18] S. Kumar, M. Balasubramaniam, R.K. Gupta, G. Münzenberg and W. Scheid, J. Phys. G: **29**, 625 (2003).

[19] G. Royer and R.A. Gherghescu, Nucl. Phys. A **699** (2002) 479.

Four-dimensional dynamical approach to the multi-modal fission

T. Wada[1], T. Asano, M. Ohta

[1] Konan University, Japan

wada@konan-u.ac.jp

In the low energy fission of heavy nuclei, namely actinides and transactinides, it has been demonstrated that there exist more than one deformation paths for fission process. In mass distribution of fission fragments, mass-asymmetric fission is observed on top of the rather broad symmetric fission distribution. The mass-symmetric component decreases as the excitation energy of the compound nucleus increases, and it is expected that the shell correction is the origin of the asymmetric fission. Sometimes, the shape of the mass distribution shows a drastic change with the change of N (neutron number) and of Z (proton number). In the total kinetic energy (TKE) distribution, several components have been observed and it is expected that TKE reflects the compactness of the scission configuration.

The problem of fission modes has been studied theoretically as well [1, 2]. Because of the importance of the shell correction for the appearance of the multi-modal fission, the nuclear energy surface in a multi-dimensional deformation space has been investigated first to obtain static fission paths. Strutinsky◎fs shell correction method has been used to estimate the shell correction energy. Saddle points are found in the deformation space and the fission paths are defined as valley paths.

Recently, we proposed a dynamical approach to this problem. The multi-dimensional Langevin equation has been applied to the study of fission of highly excited nuclei and succeeded in reproducing the experimental data like pre-scission particle multiplicities and TKE distribution [3]. Importance of the nuclear friction has been stressed in these studies. By including the shell correction energy to the potential energy surface, we proposed to apply this method to the fission of low excitation as well.

By solving the Langevin equation in multi-dimensional deformation space, the compound nucleus finds its way to fission automatically without assuming the valley paths. Langevin trajectories go out of the spherical region through saddle points; each saddle point is selected according to its barrier height automatically. After passing through the saddles, the trajectories go down the nuclear potential energy surface and they reach the scission points. By looking at the shapes at scission points and by tracing the paths, we can easily distinguish the fission modes for each trajectory.

We applied this approach to several systems, like heavy actinides (Fm, Bk) and transactinides (Sg) [4]. We used a three-dimensional deformation space, namely we employed elongation, fragment deformation and mass-asymmetry to describe the nuclear shape. Since we restrict the model space to be three-dimensional, we put a constraint on the deformations of two future fragments; we assume that both fragments have the same deformation. The shell correction energy is calculated with the code TWOCTR [5]. We assume the hydrodynamical inertia mass and the one-body wall-and-window friction. In the study of Sg and Bk, we found a mass-asymmetric fission component together with a mass-symmetric one. We did not find a mass-asymmetric valley in the potential energy surface and concluded that this mass-asymmetric component appears as a result of the multi-dimensional dynamics. In the study of Fm, we found at least three modes: a compact mass-symmetric mode that corresponds to the magic daughter nucleus Sn, a mass-asymmetric component that has the same origin as in the case of Bk and Sg, and an elongated mass-symmetric component. The TKE value obtained in the theoretical study agreed with the experimental systematics well [6]. However, in these studies, we could not reproduce the experimental fractions of the mass-symmetric and mass-asymmetric components.

In the present paper, we extend the model space to four-dimensional one; we use independent deformation for each fragment. In this way, we can take account of the shell correction more precisely, especially for spherical shells that are strongest. We apply this four-dimensional approach for several heavy-actinides and transactinides.

References

[1] V. V. Pashkevich, Nucl. Phys. Prog. **A 169**, 275 (1971).
[2] P. Moller, Proc. Tours Symp. On Nuclear Physics IV, AIP Conf. Proc. **561**, 455 (2001).
[3] T. Wada, Y. Abe and N. Carjan, Phys. Rev. Lett. **70**, 3538 (1993).
[4] T. Ichikawa, T. Asano, T. Wada and M. Ohta, Jour. Nucl. Radio. Sci. **3**, 67 (2002).
[5] A. Iwamoto, S. Yamaji, S. Suekane and K. Harada, Prog. Theor. Phys. **55**, 115 (1976).
[6] Y. L. Zhao et al., Phys. Rev. Lett. **82**, 3408 (1999).

Chemical Experiments

[This page was left blank intentionally.]

Current status and future of transactinide heavy element chemistry

A. Türler[1]

[1] Technische Universität München, Institut für Radiochemie, Walther Meissner Str. 3, D-85748 Garching, Germany

andreas.tuerler@radiochemie.de

1. Introduction

The knowledge and understanding of the chemistry of the superheavy elements, especially of the early transactinides Rf, Db and Sg and their compounds, both experimentally and theoretically, is nowadays quite extensive as documented by a first textbook entitled "The Chemistry of Superheavy Elements" edited by M. Schädel [1]. While rapid chemical separations in aqueous solution were (and are) the method of choice for detailed investigations of Rf and Db, the development of gas-phase chemical separation methods have allowed first chemical studies of increasingly heavier transactinide elements.

The spectacular results obtained at Flerov Laboratory in Dubna using 48Ca ion beams and targets of ^{238}U, ^{242,244}Pu, ^{248}Cm and ^{249}Cf to synthesize isotopes of elements 112 [2], 114 [3,4], 116 [5] and 118 [6] give chemists the perspective to experimentally investigate the chemistry of even the heaviest known elements. Especially since some of the isotopes attributed to elements 108, 110, 112, and 114 seem to have half-lives of the order of seconds to minutes.

2. Status

Since 1999 when the first TAN conference was held in Seeheim, Germany, chemists have made a quantum leap and are now working with nuclides that can be produced with picobarn (10^{-36} cm^2) cross sections only. One of the highlights of TAN'99 was the announcement of the first gas-phase chemical isolation of bohrium (Z=107) as volatile BhO_3Cl using the OLGA technique [7]. The nuclides ^{266}Bh and ^{267}Bh were produced in the reaction ^{249}Bk(^{22}Ne, 4,5n) with maximum cross sections of about 100 pb [8]. Even though the experiment was successful and deserved highest scientific merits, the outlook to apply the same technique to the investigation of even heavier elements was bleak, since the overall efficiency to detect a correlated mother-daughter α-particle decay chain was only about 4%. The experimental chemical investigation and characterization of the next heavier transactinide element hassium has, for some years, constituted a daunting task even though from the very beginning the selection of a volatile compound was absolutely clear. Hassium, as a presumed member of group 8 of the Periodic Table and thus a homologue of Fe, Ru, and Os, should form stable and at the same time very volatile HsO_4 molecules, very similar to OsO_4. However, in order to gain access to hassium (Z=108) the overall efficiency of the experiment had to be improved by at least one order of magnitude. By developing a completely new approach of separation (IVO) [9] and detection (CTS, COLD) [10] and also by introducing the rotating target set-up ARTESIA [11], which allowed the use of much higher beam intensities, the first chemical characterization of Hs become reality [12]. This spectacular progress however is limited to a few selected cases which chemically are extremely favorable. One such case is also element 112 in its elemental state. First experiments made in Dubna [13,14] and recently at GSI [15] seem to indicate a quite spectacular difference in chemical behavior between element 112 and its lighter homolog Hg in the elemental state. Compared to chemical investigations of the early transactinide elements Rf through Hs, where always the highest possible oxidation state was investigated, now with elements 112 through 118,

which are expected to be moderately to highly volatile in the elemental state, the influence of relativistic effects of the valence electrons should become noticeable in direct experimental investigations. These relativistic effects might be responsible for some quite dramatic differences in chemical behavior as this seems to be the case in the adsorption properties of element 112 compared to its lighter homologue Hg [16].

Experiments on the aqueous chemistry of transactinide elements focused mainly on a much deeper understanding of the properties of Rf in solution [17]. A fully **A**utomated **I**on exchange apparatus coupled to a **D**etection system for **A**lpha-particle spectroscopy (AIDA) developed at JAERI, was used to extensively study the behavior of Rf in pure HCl solution [18]. Future experiments with Db using the reaction ^{248}Cm(^{19}F, 5n)^{262}Db are planned [18]. A series of trendsetting experiments were performed by the SISAK collaboration [19]. The nuclide ^{257}Rf was produced in the reaction ^{208}Pb(^{50}Ti, 1n)^{257}Rf, separated in the Berkeley Gas-filled Separator (BGS) and transferred to a gas jet using the Recoil Transfer Chamber (RTC) [20]. The activity delivered by the gas jet was dissolved in nitric acid and Rf was extracted into dibutyl-phosphoric acid in toluene. The decay of Rf nuclides was registered on-line by flow-through liquid scintillation counters. This was the first time a transactinide element was extracted and unequivocally identified by the SISAK system. The use of the BGS provided the necessary reduction of background from interfering by-products of the nuclear reaction. Another approach to extend liquid-phase chemical studies to heavier transactinides is the so-called Multi Column Technique (MCT) [21]. In this continuous on-line chromatography, the solution containing the dissolved transactinide element passes through a series of columns. The transactinide element of interest passes a first column where only its actinide daughter nuclei (and other actinides) are retained. The transactinide element is then retained on a second column. However, its actinide decay daughters pass this column and are retained on a third column from which they are eluted after completion of the experiment and assayed by alpha-particle spectroscopy. This technique is very efficient and allows to access relatively short-lived nuclei. However, a breakthrough even of a small fraction of actinides in the first column can ruin the experiment. Also, all information about the nuclear decay properties of the transactinide element is lost.

Heavy element chemistry is not only dependent on outstanding radiochemists, but also on the necessary infrastructure consisting of powerful heavy ion accelerators and facilities and equipment to produce and handle highly radioactive and also extremely valuable exotic target materials such as ^{248}Cm. In this respect the greatly reduced availability or even the closure of the 88-Inch cyclotron at LBNL without adequate replacement signifies a hard blow to our community. In this respect it is of importance to note that new groups have entered the field of transactinide chemistry, such as the group at JAERI. Remarkable is also the synthesis of the new nuclide ^{259}Db at IMP Lanzhou, China [22] allowing also future transactinide chemistry experiments.

3. Future of transactinide chemistry

The spectacular results obtained at Flerov Laboratory in Dubna in the synthesis of new superheavy elements already have stimulated chemists to experimentally investigate the chemistry of even the heaviest known elements. A first step into this direction certainly are the chemical experiments performed with the spontaneously fissioning nuclide ^{283}112. Nevertheless, it is highly desirable to develop techniques that are sensitive to reveal also isotopes that decay by chains of α-particles in order to independently verify the results obtained by kinematical separator systems.

What are the prerequisites to achieve the ultimate goal of chemically identifying a new, superheavy element? Due to the very low production cross sections of 1 pb or less highest possible beam intensities must become available in the near future. This ultimately calls for a new accelerator capable of delivering a continuous beam of up to $5 \cdot 10^{13}$ ions/s. Evidently, this also calls for improved target irradiation facilities,

since target thicknesses of the order of 1 to 1.5 mg/cm² are useful. Nevertheless, the experiences with ARTESIA clearly demonstrated, that this setup already today allows accepting a 3 to 4 fold higher beam intensity if a DC beam were available instead of a pulsed beam.

Chemical separation procedures need to be improved with respect to sensitivity and speed. Here, gas phase chemical separations will play an important role, since many of the superheavy elements with atomic numbers between 112- 118 may be moderately or even highly volatile in their elemental state. Thus future experiments point to investigations of elements 112 and 114 in their elemental state. However, a particularly difficult problem constitute some Rn isotopes, since their Po daughter nuclides decay with α-decay energies which strongly interfere with the detection of heavy transactinide nuclides. Especially element 112 seems to exhibit a very similar volatility as Rn. A possible solution to this problem, although not yet available, may constitute a dedicated kinematical pre-separator which is coupled to chemical set-ups. A workshop held a GSI in 2002 clearly demonstrated the future need for such an instrument. Possible pathways to gas chemical investigations of element 112 and 114 are outlined in Fig.1. The currently most convenient production reaction of element 114 is the reaction $^{48}Ca+^{244}Pu$.

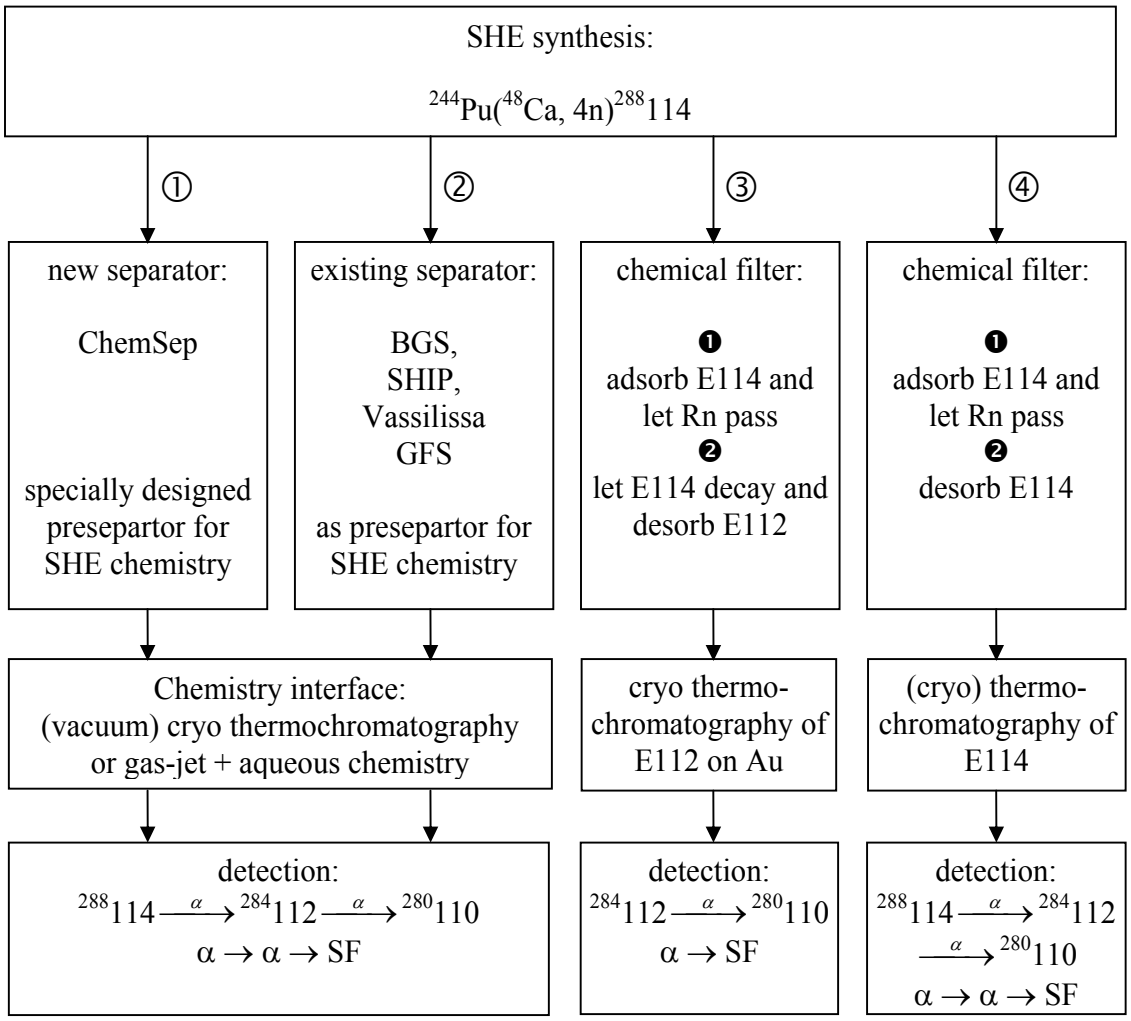

Figure 1. Routes to chemical investigations of SHE providing the unambiguous identification of the investigated nuclides.

Even more challenging than the investigation of elements 112 and 114 is probably the chemical identification of elements 109 through 111, the heavy analogs of Ir, Pt, and Au. Here, no obvious chemical properties or compounds as for instance with group 8 elements are at hand. Again, the use of a kinematic preseparator of nuclear reaction products might considerably facilitate chemical investigations.

The fact that some isotopes of elements 112 and 114 have half-lives of the order of seconds to minutes indicates that there exist similarly long-lived isotopes of elements 113 and 111 that are accessible with current projectile and target combinations. Also here, no chemical separation schemes have been worked out, which would allow an immediate experimental investigation.

To conclude it is fair to say that chemists have made enormous progress in investigating the chemical properties of transactinide elements and certainly the successful hassium experiment will serve as a text book example for years to come. With the synthesis of relatively long-lived superheavy elements with Z=112-118 chemists are facing an extremely challenging but also rewarding future. The possibility to experimentally characterize the complete 7th row of the periodic table has never become more real than starting with today.

References

[1] M. Schädel (Ed.): "The Chemistry of Superheavy Elements", Kluver Academic Publishers, Dordrecht, 2003.
[2] Yu.Ts. Oganessian et al., Eur. Phys. J. A **5**, 63 (1999).
[3] Yu.Ts. Oganessian et al., Nature **400**, 242 (1999).
[4] Yu.Ts. Oganessian et al., Phys. Rev. C **62**, 041604(R) (2000).
[5] Yu.Ts. Oganessian et al., Phys. Rev. C **63**, 011301(R) (2000).
[6] Yu.Ts. Oganessian et al., JINR preprint D7-2002-287 (2002).
[7] R. Eichler et al., Nature **407**, 63 (2000).
[8] P.A. Wilk et al., Phys. Rev. Lett. **85**, 2697 (2000).
[9] Ch.E. Düllmann et al., Nucl. Instrum. Methods A**479**, 631 (2002).
[10] U.W. Kirbach et al., Nucl. Instrum. Methods A**484**, 587(2002).
[11] M. Schädel, Acta Physica Polonica B **34**, 1701 (2002).
[12] Ch.E. Düllmann et al., Nature **418**, 859 (2002).
[13] A.B. Yakushev et al., Radiochim. Acta **89**, 743 (2001).
[14] A.B. Yakushev et al., Radiochim. Acta **91**, 433 (2003).
[15] R. Eichler et al., contribution to this conference.
[16] V. Pershina et al., Chem. Phys. Lett. **365,** 176 (2002).
[17] E. Strub et al., Radiochim. Acta **88**, 265 (2000).
[18] Y. Nagame et al., Czech. J. Phys. **53**, A299 (2003).
[19] J.P. Omtvedt et al., J. Nucl. Radiochem. Sci. **3**, 121 (2002).
[20] U.W. Kirbach et al., LBNL Nuclear Science Division Annual Report 1999.
[21] J.V. Kratz et al., Radiochim. Acta **88**, 273 (2000).
[22] Z.G. Gan et al., Eur. Phys. J. A **10**, 21 (2001).

Gas phase chemistry of bohrium (element 107)

R. Eichler[1], for a PSI-University Bern-LBNL-GSI-FZR-FLNR collaboration[@]

[1] Paul Scherrer Institute, Switzerland

robert.eichler@psi.ch

The transactinide element bohrium (Bh, element 107) was discovered in 1981 at GSI Darmstadt, Germany [1]. The systematic order of elements in the periodic table suggests Bh to be a member of group 7, together with manganese, technetium, and rhenium. Doubts about an unchanged periodicity of chemical properties along the rows of the periodic table rise especially for the heaviest elements. The fields of their highly charged nuclei may lead to strong relativistic effects deviating the order in the electron shell structure [2-4]. Relativistic effects force a stronger attraction of the relativistic electron orbitals with a spherical shape (s and $p_{½}$,) to the nucleus. The resulting shielding of the nuclear charge causes an expansion of the other p-, d-, and f- electron orbitals - the indirect relativistic effect. Therefore, chemical properties as for example ionization potentials, binding energies and geometries of the electron orbitals of the heaviest elements and their compounds may be strongly influenced by relativistic effects. The chemical studies of rutherfordium (Rf, element 104), dubnium (Db, element 105) and seaborgium (Sg, element 106) revealed a typical behavior for members of the transition metal series in the groups 4 to 6 of the periodic table, respectively [5].

Prior to the studies described in the current presentation, two attempts to search for long-lived isotopes of bohrium and to study chemical properties of this element have been conducted in 1984 at JINR in Dubna, Russia in the reaction ^{249}Bk(^{22}Ne,4-5n)^{266,267}Bh [6] and in 1992 at LBNL Berkeley, USA in the reaction ^{254}Es(^{16}O,4-5n)^{265,266}Bh [7]. In both experiments Bh was assumed to form a volatile oxide or oxyhydroxide similar to its homologues in group 7 of the periodic table, Tc and Re. Gas phase chemical separations have been carried out. The cross section limits reached in these experiments were about 0.1 nb in Dubna and about 1 nb in the experiment in Berkeley. Both experiments were not sensitive enough to measure the decay of the Bh-isotopes $^{265-267}$Bh. Meanwhile, neutron-rich isotopes ^{266,267}Bh have been discovered at the LBNL Berkeley [8] in the heavy ion induced nuclear fusion reaction ^{249}Bk(^{22}Ne,4-5n) revealing the enhanced nuclear shell stabilization against spontaneous fission (SF-) and α–decay, which is predicted and experimentally confirmed for deformed nuclei close to ^{270}Hs (Hassium, element 108) [9-13]. The half-life ($T_{½}$) of about 17 s and the predominant α-decay mode (E_{α} = 8.83±0.03 MeV) made ^{267}Bh an ideal nuclide for fast gas chemical experiments. The production cross section of ^{267}Bh at a ^{22}Ne energy of 117±1 MeV was about 60 pb, indicating the necessity of an exceptional sensitive experimental chemical approach. Hence, gas phase chemical model studies with Tc and Re were conducted in preparation of the experimental chemical characterization of the transactinide element [14, 15]. The gas phase separation of the volatile oxychloride species of these elements, presumably MO_3Cl (M=Tc, Re) in a low temperature isothermal gas chromatography, based on the OLGA technique [16], appeared to be most promisingin terms of separation yield, quality, and velocity. The results of these model experiments were used for empirical predictions of the behavior of Bh in the reactive gas system HCl/O_2. The most stable gas phase compounds and their behavior in a gas-solid adsorption separation have been predicted. From thermochemical extrapolations the standard adsorption enthalpy of BhO_3Cl on a fused silica surface, ΔH_{ads} = - 75 ± 12 kJ/mol, was predicted [17]. With a physisorption model adjusted to the experimental results with Tc and Re Pershina and Bastug [18] estimated ΔH_{ads} =-78 ± 5 kJ/mol.

The Bk-target preparation was conducted at LBNL. A HDEHP redox-extraction separation procedure for Pb, Bk, and Cf was carried out using ultra pure chemicals and carefully cleaned tools in an exceptionally clean glove box endeavouring to avoid accidental heavy metal contaminations.

Subsequently, a target of ^{249}Bk (670 μg/cm²) covered by a layer of ^{159}Tb(100 μg/cm²) was prepared by a molecular plating procedure of $^{249}Bk(NO_3)_3$ and $^{159}Tb(NO_3)_3$ on a 2.77mg/cm² Be foil. At the Philips cyclotron of the Paul Scherrer Institute, Switzerland this target was irradiated for about 4 weeks at a beam dose of $3*10^{18}$ $^{22}Ne^{6+}$ at a beam energy of 119±3 MeV in the middle of the target. ^{176}Re was simultaneously produced in the fusion reaction $^{159}Tb(^{22}Ne,5n)$ and served as a yield monitor for the chemical separation of group 7 oxychlorides. The nuclear reaction products, recoiling from the target were thermalized in He gas loaded with carbon aerosol particles. Adsorbing on the particle surface, they are swept to the remotely controlled OLGA III device. HCl and O_2 are admixed. On a quartz wool plug in the reaction oven of the apparatus held at 1000°C the carbon particles are burned. At the same time the nuclear reaction products form compounds, which are evaporated and separated on-line in the isothermal chromatography quartz column. The retention times of the compounds in the column are mainly dependent on their adsorption interaction with the column surface at the isothermal temperature (Table 1, T_{iso}) and on the carrier gas velocity. The experiment ends for the individual molecule with the decay of the nuclide. Thus, only the species with a longer nuclear lifetime than the retention time pass the chromatography set-up and were subsequently attached to CsCl aerosol particles of a second gas-jet to be transported to the detection device - ROMA. There, the CsCl particles were impacted in vacuum on thin polyethylene foils (~30 μg/cm²) mounted on the circumference of a stepwise rotating wheel. Every 10 s the gathered samples are successively moved between a series of 12 pairs of PIPS detectors to measure α - and SF-decay in an event-by-event mode with about 70% detection efficiency. ^{176}Re was measured using a HPGE-γ-detector. About 180000 samples were measured during the entire experiment. The overall yield of the complete separation process, from the thermalization of the recoiling fusion products to the sample preparation in the detection device, was determined for ^{176}Re to be about 16%. During the irradiation three different temperatures were adjusted in the isothermal quartz column. Four correlated decay chains, attributed to the decay of ^{267}Bh, were detected at 180°C. At 150°C 2 decay chains were observed. Finally, at 75°C isothermal temperature, where $^{169}ReO_3Cl$ still passes the isothermal part of the column with about 80% relative yield, no ^{267}Bh was registered (see Table 1).

Table 1. Detected correlated decay chains related to the decay of ^{267}Bh.

T_{iso} [°C]	Beam dose: $^{22}Ne^{6+}$	$E_{\alpha 1}$ [MeV]	t_1 [s]	E_2 [MeV]	Δt_2 [s]	$E_{\alpha 3}$ [MeV]	Δt_3 [s]	Decay assignment	N_R
180	$1.02*10^{18}$	8.84	26.7	8.35	73.4			$^{267}Bh \rightarrow {}^{263}Db$ or ^{259}Lr	1.2
		8.72	2.9	8.40	29.9			$^{267}Bh \rightarrow {}^{263}Db$ or ^{259}Lr	
		8.81	18.4	101/86	16.3			$^{267}Bh \rightarrow {}^{263}Db$ or ^{259}Lr	0.1
		8.91	10.5	8.37	0.8	8.41	14.6	$^{267}Bh \rightarrow {}^{263}Db \rightarrow {}^{259}Lr$	0.001
150	$1.00*10^{18}$	8.81	24.5	82	21.1			$^{267}Bh \rightarrow {}^{263}Db$ or ^{259}Lr	0.1
		8.85	34.4	46	98.9			$^{267}Bh \rightarrow {}^{263}Db$ or ^{259}Lr	
75	$1.00*10^{18}$								

$E_{\alpha 1}$ and $E_{\alpha 3}$ represent the α decay energies of ^{267}Bh and ^{259}Lr, respectively.
E_2 indicates the α (E_2<10 MeV) or SF (E_2>30 MeV) decay energy of the indistinguishable in this experiment decay of ^{263}Db (E_α = 8.35, 8.41 MeV) and ^{259}Lr (E_α = 8.45 MeV).
t_1 is the life-time of ^{267}Bh from the beginning of the measurement.
Δt_2 shows the life-time of ^{263}Db or ^{259}Lr after the ^{267}Bh decay.
Δt_3 represents the life-time of ^{259}Lr after the ^{263}Db decay.
N_R is the number of random correlations.

Based on the detection of 6 atoms we conclude that Bh behaves like a typical member of group 7 in the periodic table. Bh, similarly to Tc and Re, forms a volatile oxychloride compound, presumably

BhO_3Cl. A careful statistical analysis of the experimental data was applied. The number of random correlations (Table 1, N_R) was evaluated. From the number of detected correlated decay chains, the initial number of ^{267}Bh atoms in the measured samples was determined. Assuming the experimental result at 180°C to be 100 %, the relative yields at 150°C and 75°C were calculated (see Fig.1, filled squares). Assuming the same adsorption process as for TcO_3Cl and ReO_3Cl, using a microscopic model of mobile adsorption [19], first thermodynamic data of element Bh - the standard adsorption enthalpy of BhO_3Cl on a quartz surface - was evaluated: $\Delta H_{ads}(BhO_3Cl) = -75^{+9}_{-6}$ kJ/mol [20]. This value is in a very good agreement with the predictions. Using empirical thermochemical methods different macroscopic properties related to Bh and its compounds have been evaluated. In different chemical systems it was shown that ΔH_{ads} is closely related to the macroscopic volatility of the species. Employing a linear correlation between the microscopic data ΔH_{ads} and the macroscopic data sublimation enthalpy (ΔH_{subl}), which was obtained for the adsorption of chlorides and oxychlorides on quartz surfaces in [21], we estimated from our experimental result $\Delta H_{subl}(BhO_3Cl) = 89 \pm 20$ kJ/mol. Consequently, in agreement with the predictions, BhO_3Cl is supposed to be less volatile than TcO_3Cl ($\Delta H_{subl} = 49 \pm 12$ kJ/mol) and ReO_3Cl ($\Delta H_{subl} = 67 \pm 12$ kJ/mol)

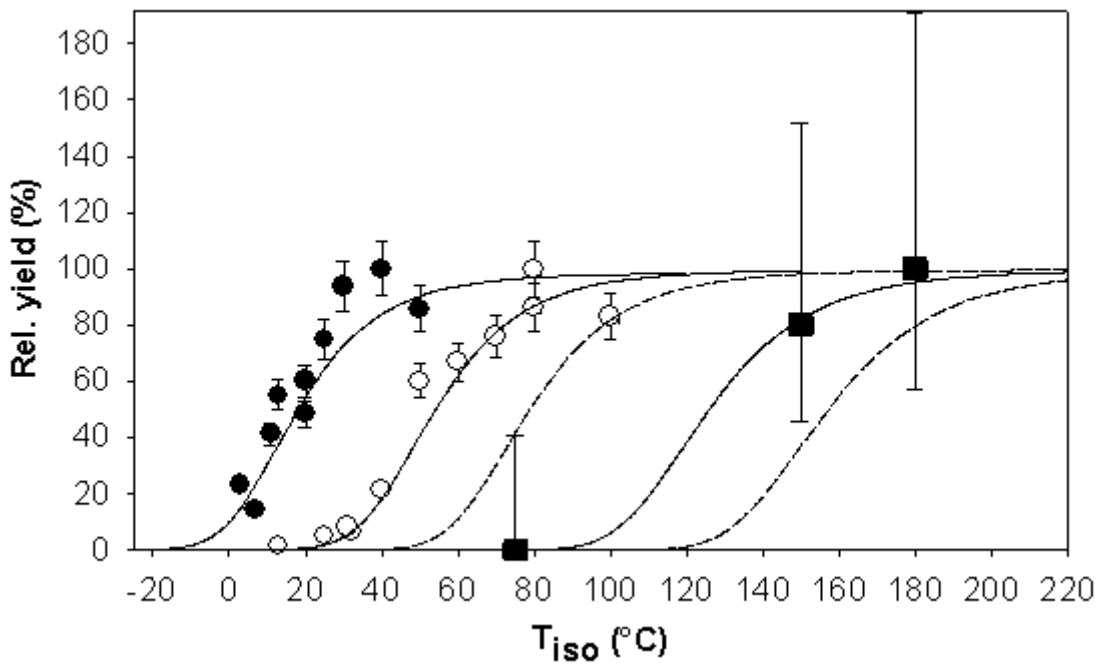

Figure 1. Experimental results of isothermal gas adsorption chromatographic separations in quartz columns. Presented are the relative yields of the compounds $^{108}TcO_3Cl$ (filled black circles), $^{169}ReO_3Cl$ (open circles) and $^{267}BhO_3Cl$ (filled black squares, this work) after separation in a OLGA device as a function of isothermal temperature (T_{iso}). The error bars indicate a 68% confidence interval. The lines represent calculated relative yields applying a microscopic model of the adsorption process based on a Monte Carlo approach, with standard adsorption enthalpies of –51 kJ/mol (TcO_3Cl), –61 kJ/mol (ReO_3Cl), and -75^{+9}_{-6} kJ/mol (BhO_3Cl), respectively.

Acknowledgements

We are indebted to the Office of Science, Office of Basic Energy Research, Division of Chemical Sciences, of the U.S. Department of Energy, for making the ^{249}Bk target material available through the

transplutonium element production program at the Oak Ridge National Laboratory. We thank the staff of the PSI Philips cyclotron for providing intense beams of ^{22}Ne. This work was supported in part by the Office of Science, Office of High Energy and Nuclear Physics, Division of Nuclear Physics, of the U. S. Department of Energy under Contract DE-AC03-76SF00098 and by the Swiss National Science Foundation.

References

[1] Münzenberg, G. et al. Z. Phys. A 300, 107-108 (1981).
[2] Pyykkö, P. Chem. Rev. **88,** 563 (1988).
[3] Pershina, V.G. Chem. Rev. **96,** 1977 (1996).
[4] Schwerdtfeger, P., Seth, M. Relativistic effects of the superheavy elements. In Encyclopaedia of computational chemistry, Vol. 4, 2480 (Wiley, New York, 1998).
[5] Kratz, J.V. Chemical properties of the transactinides. In Heavy Elements and Related New Phenomena. Eds. W. Greiner and K. Gupta (World Scientific, 1999).
[6] Zvara, I. et al. Radiokhimia 26 (1), 76-82 (1984).
[7] Schädel, M. et al. Radiochimica Acta 68, 7-12 (1995).
[8] Wilk, P. A. et al. submitted to Phys. Rev. Lett. **85,** 2697 (2000).
[9] Patyk, Z. et al. Nucl. Phys. **A533,**132 (1991).
[10] Smolanczuk, R. et al. Phys. Rev. C **52,** 1871 (1995).
[11] Lazarev, Yu. A. et al. Phys. Rev. Lett.**73,** 624 (1994).
[12] Türler, A. et al. Phys. Rev. C **57,** 1648 (1998).
[13] Hofmann, S. et al. Z. Phys. **A354,** 229 (1996).
[14] Eichler, R. et al. Radiochim. Acta **87,** 151 (1999).
[15] Eichler, R. et al. Radiochim. Acta **88,** 87 (2000).
[16] Gäggeler, H.W. et al. Nucl.Instr.Meth. **A309,** 201 (1991).
[17] Eichler, R. PSI internal report **TM-18-00-04** (in german) (2000), unpublished.
[18] Pershina, V. et al. J. Chem. Phys. **113,** 1441 (2000).
[19] Zvara, I. Radiochimica Acta **38,** 95 (1985).
[20] Eichler, R. et al. Nature **407,** 63 (2000).
[21] Eichler, B. et al. J. Phys. Chem. **A103,** 9296 (1999).

@: R. Eichler[1,2], W. Brüchle[3], R. Dressler[4], Ch. Düllmann[1,2], B. Eichler[2], H.W. Gäggeler[1,2], K.E. Gregorich[5], D.C. Hoffman[5], S. Hübener[6], D.T. Jost[2], U. Kirbach[5], C.A. Laue[5], V.M. Lavanchy[1], H. Nitsche[5], J. Patin[5] D. Piguet[2], M. Schädel[3], D. Strellis[5], S. Taut[6], L. Tobler[2], Y. Tsyganov[7], A. Türler[1,2], A. Vahle[7], P. Wilk[5], A.B. Yakushev[7]

[1] Departement für Chemie und Biochemie, Universität Bern, 3012 Bern, Switzerland
[2] Labor für Radio- und Umweltchemie, Paul Scherrer Institut, 5232 Villigen, Switzerland
[3] Gesellschaft für Schwerionenforschung, 64291 Darmstadt, Germany
[4] Institut für Kern- und Hadronenphysik, Forschungszentrum Rossendorf, 01314 Dresden, Germany
[5] Lawrence Berkeley National Laboratory, Berkeley, 94720, USA
[6] Institut für Radiochemie, Forschungszentrum Rossendorf, 01314 Dresden, Germany
[7] Flerov Laboratory of Nuclear Reactions, Joint Institute of Nuclear Research, 911621 Dubna, Russia.

Chemical investigations of element 108, hassium (Hs)

Ch.E. Düllmann[1,2]

[1] Lawrence Berkeley National Laboratory, Berkeley, USA
[2] University of California, Berkeley, USA

CEDuellmann@lbl.gov

Introduction

The basic aim of chemistry experiments of transactinide elements (TAN) is to establish their place in the periodic table of the elements, i.e. to determine if their chemical behavior is similar to the one of supposed homologs. In this contribution I will try to give an overview of all chemical experiments on element 108, hassium (Hs) that have been reported to date.

Based on the systematics of the periodic table, Hs is expected to be a member of group 8 and therefore homologous to osmium (Os) and ruthenium (Ru). As a member of the transactinide series, its experimental investigation is complicated by low production cross-sections and short half-lives. It has therefore been successfully investigated only recently. Already in the seventies of the last century, several authors mentioned the tetroxides of the two heavier group 8 elements, Ru and Os, to be very outstanding compounds with respect to their unusually high volatility. A possible HsO_4 was considered suitable for isolating Hs from unwanted by-products of the nuclear production reaction [1-4]. While RuO_4 is rather unstable, OsO_4 is well-known to be a stable compound and is widely used in organic chemistry. Recent theoretical calculations on the electronic structure and properties of Hs [5,6] predict the formation of a stable HsO_4 whose properties should be similar to the ones of OsO_4. This is in agreement with an extrapolation of the trend established in group 8 of the periodic table by Ru and Os [7]. All of the reported experiments on the chemistry of Hs therefore aimed at a formation of this compound.

Hs was discovered in 1984, when Münzenberg et al. reported the observation of a correlated decay-chain from ^{265}Hs formed in the nuclear reaction ^{58}Fe(^{208}Pb; n) [8]. However, its half-life is only 1.55 ms, too short for a successful chemistry experiment. Early chemistry experiments therefore aimed at the production and detection of more neutron-rich Hs isotopes which were expected to be longer-lived. In some experiments, a nuclide with a higher Z was produced which was expected to subsequently decay to an isotope of element 108. In 1996, ^{269}Hs ($T_{1/2}$~10 s) was discovered [9], and it was this relatively long-lived isotope which was used in the recent experiments.

In the following, all experiments on the chemical investigation of Hs are presented in a chronological order.

Early experiments

The first attempts to chemically identify elements 108, which had been discovered only one year earlier, were undertaken in Dubna in 1985. Spontaneously fissioning (SF) isotopes produced in the heavy-ion induced fusion reactions ^{40}Ar+^{235}U (leading to ^{275}110 as the compound nucleus, CN) and SF or α-decaying ^{267}Hs produced in the ^{22}Ne+^{249}Cf reaction (CN ^{271}Hs) were searched for [10,11]. ^{267}Hs was believed to have a half-life on the order of 1 s. The nuclear reaction products were thermalized in a Ar/O_2 gas mixture and continuously swept out of the target chamber through a heated CaO filled column which acted as a filter to separate non-volatile transfer products as e.g. actinides, Ra, Fr, and Po. The volatile species were blown onto the surface of a Pb coated Si detector. At the opposite side an annular lavsan track detector was located for registering fission fragments.

In Berkeley, a set-up called the On-line Separation and Condensation AppaRatus (OSCAR) [12] was used for a search for α-decaying ^{272}Hs which was expected to be the electron capture daughter product of ^{272}Mt produced in the reaction ^{254}Es(^{22}Ne, 4n) [13]. Nuclear reaction products were transported with a KCl gas-jet to the chemistry setup where O_2 was added to the carrier gas. The aerosol particles were caught on a heated quartz wool plug where the transported species were converted to oxides. Non volatile transfer products remained in the reaction area while the volatile oxides were swept out by the gas flow and deposited on a silver disk which was cooled by liquid nitrogen (LN_2). Opposite of the metal disk, an annular Si surface barrier detector was mounted which registered α- and SF decaying nuclides adsorbed on the disk.

In all of these experiments, the decontamination from actinides and other interfering species was excellent. Nevertheless, no events that could be attributed to the decay of Hs were observed and upper limits of 100 pb for the production cross sections of α-decaying nuclides and 50 pb for SF decaying nuclides were established in the Dubna experiments and a limit of 1 nb was reported from the OSCAR experiment. As we know nowadays, the sensitivity of these early experiments was too low to yield positive results. Meanwhile, several isotopes that were unknown at that time were discovered and exhibited decay properties different from the ones assumed (and necessary for a successful experiment).

The IVO-COLD experiment

In 2001, the next attempt to chemically investigate Hs was undertaken by a large collaboration. A schematic of the set-up used is depicted in Figure 1.

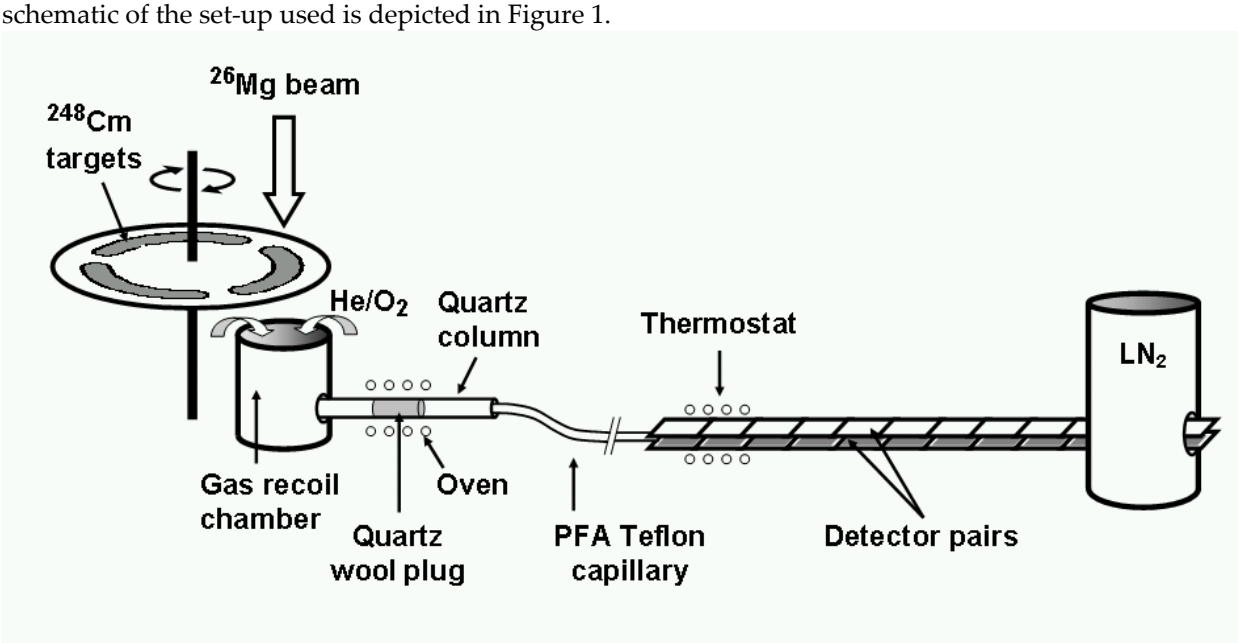

Figure 1. Schematic of the experimental setup in the IVO-COLD experiment. For explanations see text. Adapted from [14].

Relatively long-lived Hs isotopes were produced in the reaction ^{248}Cm(^{26}Mg; 5,4n)^{269,270}Hs. Reaction products recoiling from the target were thermalized in a gas filled volume called the recoil chamber which was flooded with a He/O_2 mixture. The formed radionuclides were transported by the gas flow to a nearby oven kept at 600 °C where formation of the tetroxide took place. Hs was then transported through a PFA Teflon tube to the detection device in the form of HsO_4. This technique was named In-situ Voaltilization and On-line detection (IVO) [15]. The efficiency of IVO to forward formed short-lived Os

isotopes to the detection system was measured to be 60-90% in test experiments. The method of gas phase adsorption thermochromatography [16] was used to measure the deposition temperature of HsO_4 on the surface of a chromatography column. An on-line thermochromatography system has been developed at Berkeley [17] and an improved version called the Cryo-On-Line Detector (COLD) [14,18] has been built at the Paul Scherrer Institute in Switzerland. The chromatography column consisted of 12 pairs of PIN-diodes (Area: 1x3 cm^2 each) forming a narrow rectangular channel with a spacing of 1.6 mm. PIN-diodes are suitable for registering α-particles and fission fragments. By means of a thermostat and a vessel containing LN_2, a temperature gradient from -20 to -170 °C was established along the column. Deposition of HsO_4 was expected at a temperature lying between these two values. The overall efficiency of the IVO-COLD system was 30-50%.

Table 1. Observed correlated decay chains. Given are the energies of the observed events and the time difference between an event and the preceding one. The setup used did not allow for determining the lifetime of the mother events. Fission events are marked with an asterisk. Two asterisks identify SF events where only one fragment was registered. n_R is the probability of a chain to be of random origin not related to the decay of a Hs isotope. Det. indicates the detector unit in which the chain was observed. The last column gives the isotope to which the decay chain was assigned to.

#	E_1 [MeV]	E_2 [MeV]	Δt_2 [s]	E_3 [MeV]	Δt_3 [s]	E_4 [MeV]	Δt_4 [s]	n_R	Det.	Isotope
1	9.16	8.66	25.665	94+93*	0.199			$<8x10^{-6}$	2	^{270}Hs
2	9.18	8.69	4.409	8.50	2.365	8.21	55.567	$<2x10^{-6}$	3	^{269}Hs
3	-	8.72	-	53**	3.124			$<2x10^{-4}$	4	$^{269/270}Hs$
4	8.97	8.64	11.911	94+92*	1.216			$<5x10^{-5}$	4	^{270}Hs
5	9.10	8.68	9.325	94+85*	7.920			$<7x10^{-6}$	3	^{269}Hs
6	8.88	8.90	17.078	8.50	0.846			$<7x10^{-5}$	3	^{269}Hs
7	9.14	-	-	108**	42.615			$<4x10^{-4}$	3	$^{269/270}Hs$

Data was acquired during 64.2 h and a total of 10^{18} particles passed through the target. The obtained α-spectra were very clean and exhibited only α-particle lines of ^{211}At and $^{219,220}Rn$ and their daughters. ^{219}Rn was added to the carrier gas to allow for an on-line calibration of the detectors. The correlation analysis revealed a total of seven correlated decay chains [19] which are given in Table 1. The distribution of Hs and Os in the temperature gradient tube is shown in Figure 2 which contains the merged thermochromatogram of $^{172}OsO_4$ ($T_{1/2}$: 19 s) and the events attributed to the decay of a Hs isotope.

The enthalpy of adsorption ΔH_{ads} of the species on the column surface material (silicon nitride, Si_3N_4) was extracted from the measured deposition distribution by using Monte Carlo simulations of the trajectories of single molecules as they move along the column under real experimental conditions [20] (see Fig. 2, solid lines). The only free parameter is the ΔH_{ads} of the compound on the stationary phase. The half-life of the nuclide is a crucial parameter in this procedure and since it has not yet been measured for ^{270}Hs, the ΔH_{ads} of the compound on the silicon nitride surface was evaluated using only the three decay chains attributed to ^{269}Hs which occurred in detector pair 3. Values of ΔH_{ads}=(-46±2) kJ/mol (68% c.i.) for HsO_4 and (-39±1) kJ/mol for OsO_4 were deduced using a $T_{1/2}$ value of (11^{+15}_{-4}) s [9,21] for ^{269}Hs. This result points to HsO_4 as the transported species. The ΔH_{ads} value of OsO_4 of (-39±1) kJ/mol deduced from this experiment was in good agreement with earlier investigations using quartz surfaces [1,15,17].

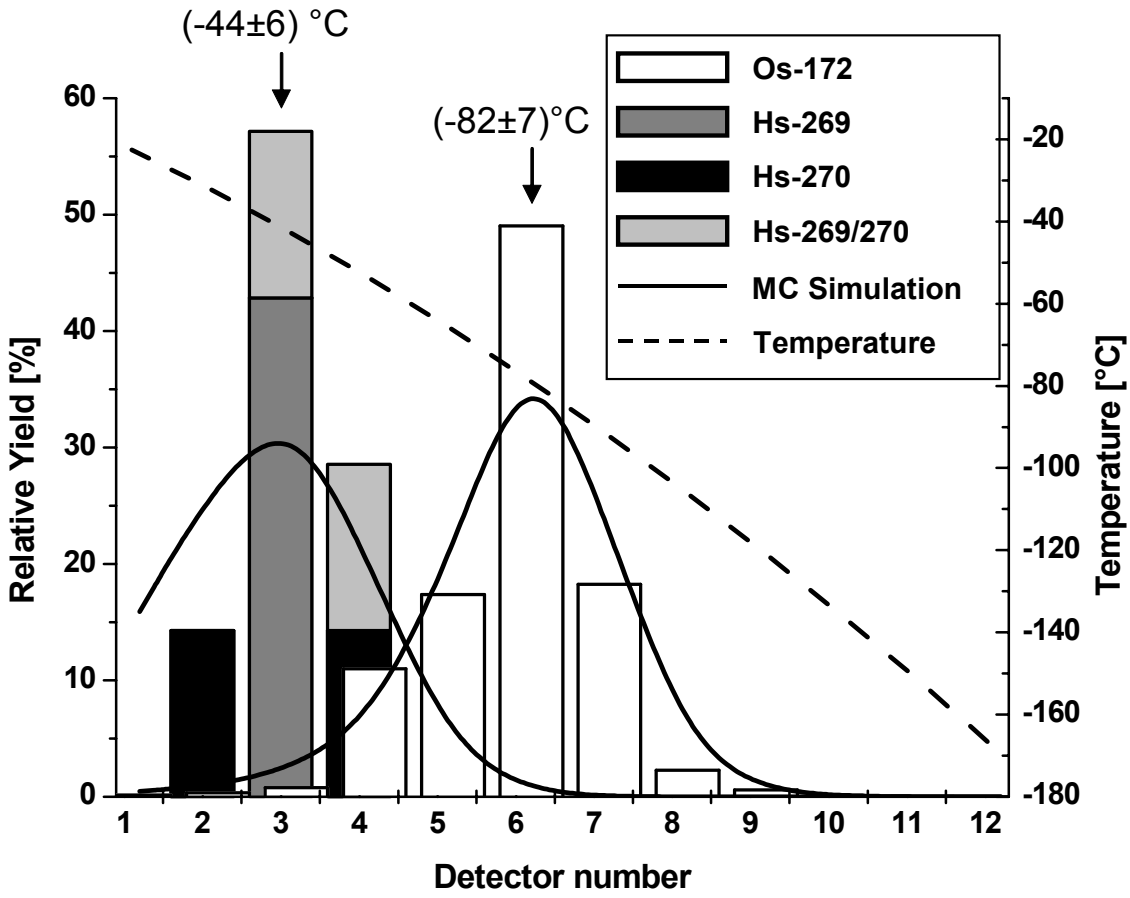

Figure 2. Merged thermochromatogram of HsO_4 and OsO_4 [14]. The deposition temperatures are indicated. Solid lines represent results of a Monte Carlo simulation. The dashed line indicates the temperature gradient. Adapted from [14].

The CALLISTO experiment

The most recent Hs experiment has been performed by a GSI - Univ. Mainz - JAERI collaboration. The setup used was named Continuously working Arrangement for for cLusterLess transport of In-SiTu produced volatile Oxides (CALLISTO) [22] and is depicted in Figure 3. The goal of the experiment was the deposition of the volatile HsO_4 on a reactive substrate. OsO_4 is known to react with hydroxides forming osmates(VIII) of the composititon $[OsO_4(OH)_2]^{2-}$ and test experiments at GSI showed that carrier-free OsO_4 deposits on hydroxide surfaces with high yields [23]. Hs was produced using the same nuclear reaction as the IVO-COLD experiment, i.e. $^{26}Mg(^{248}Cm; 5,4n)^{269,270}Hs$. These isotopes were converted to HsO_4 immediately behind the target and transported to the chemistry device with the gas flow. HsO_4 was deposited on a thin layer of NaOH, presumably due to reduction according to $2\,NaOH + HsO4 \rightarrow Na_2[HsO_4(OH)_2]$, yielding a hassate(VIII) [24]. The detection system consisted of a narrow rectangular channel with the bottom coated with a thin-layer of NaOH. The top consisted of PIN-diodes allowing for registering α-particles and fission fragments in a 2π-geometry. A total of 4 of these detector boxes were available. Three were serially coupled while the fourth one was available for maintenance and coating.

The present status of the data analysis shows that formed HsO_4 was deposited on the first few centimeters of the NaOH covered channel. The preliminary results indicate one correlated α-α-α-decay chain and 5 α-SF chains which were attributed to the decay of a Hs isotope [25]. The distribution of the 6 decay chains in the detection system is similar to the one observed for Os. Thus, it appears likely that Hs reacts with the NaOH surface in a similar way as Os.

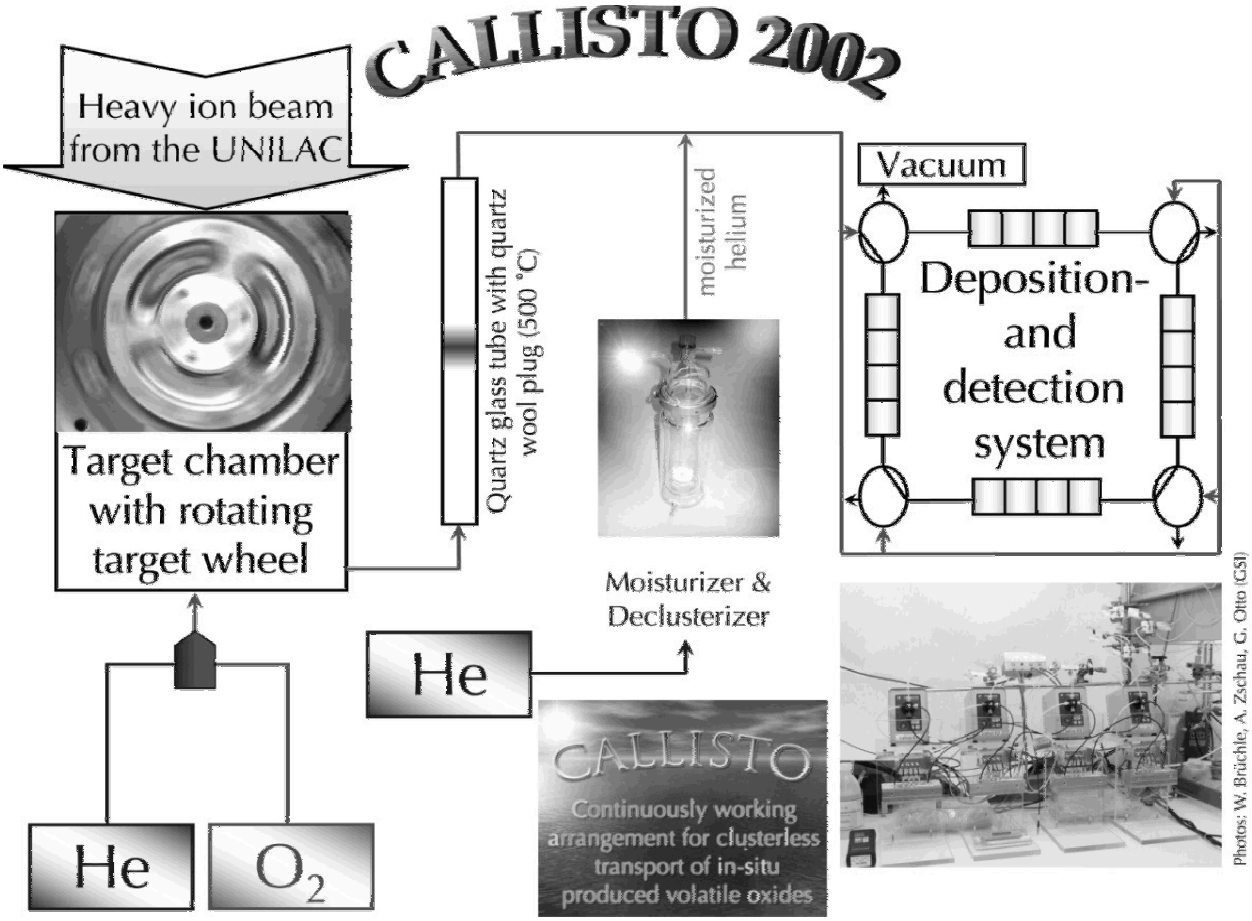

Figure 3. The CALLISTO setup [22]. For details see text. Figure courtesy of A. v. Zweidorf.

Conclusions

Currently, two expriments have successfully investigated the chemical behavior of Hs. In the first study, formation of a volatile oxide, presumably HsO_4 and its deposition on a dielectric surface was studied. It was found that the interaction was slightly stronger for HsO_4 than OsO_4. Nevertheless, the findings justified the classification of Hs into group 8 of the periodic table. In the second experiment, the reaction of HsO_4 with a NaOH surface was investigated and evidence for the formation of a hassate(VIII) was obtained. Therefore, Hs has revealed an analogous behavior to Os also in this system.

Acknowledgment

The author thanks A. v. Zweidorf for the communication of preliminary data from the CALLISTO experiment as well as Figure 3.

References

[1] V.P. Domanov *et al*. Sov. Radiochem. **26**, 731 (1984) ; translated from Radiokhimiya **26**, 770 (1984).
[2] B. Fricke, Structure and Bonding **21**, 92 (1975).
[3] K. Bächmann, Radiochim. Acta **15**, 153 (1971).
[4] F. Zude *et al*. Radiochim. Acta **62**, 61 (1993).
[5] V. Pershina *et al*. J. Chem. Phys. **115**, 792 (2001).
[6] E. Johnson *et al*. J. Chem. Phys. **116**, 1862 (2002).
[7] Ch.E. Düllmann *et al.* J. Phys. Chem. B **106**, 6679 (2002).
[8] G. Münzenberg *et al*. Z. Phys. A **317**, 235 (1984).
[9] S. Hofmann *et al*. Z. Phys. A. **354**, 229 (1996).
[10] V.I. Chepigin *et al*. Abstr. School-Seminar on Heavy Ion Physics 1985, Report P7-86-322, JINR, Dubna (1986) p. 15 (in Russian).
[11] B.L. Zhuikov *et al*. Abstr. School-Seminar on Heavy Ion Physics 1985, Report P7-86-322, JINR, Dubna (1986) p. 26 (in Russian).
[12] R.J. Dougan *et al*. Lawrence Livermore National Laboratory, Nuclear Chstmistry Division, Ann. Rep. FY 87, UCAR 10062/87, p. 4-17 (1987) (unpublished).
[13] E.K. Hulet *et al*. Lawrence Livermore National Laboratory, Nuclear Chstmistry Division, Ann. Rep. FY 87, UCAR 10062/87, p. 4-9 (1987) (unpublished).
[14] Ch.E. Düllmann *et al.* Nature **418**, 859 (2002).
[15] Ch.E. Düllmann *et al.* Nucl. Instrum. Meth. **A479**, 631 (2002).
[16] I. Zvara, Isotopenpraxis **26**, 251 (1990).
[17] U.W. Kirbach *et al*. Nucl. Instrum. Meth. **A484**, 587 (2002).
[18] Ch.E. Düllmann *et al.* Czech. J. Phys. **53 Suppl. A**, A291 (2003).
[19] A. Türler *et al*. Eur. Phys. J. A **17**, 505 (2003).
[20] I. Zvara, Radiochim. Acta **38**, 95 (1985).
[21] S. Hofmann *et al*. Rev. Mod. Phys. **72**, 733 (2000).
[22] A. v. Zweidorf *et al.* Gesellschaft für Schwerionenforschung mbH, Darmstadt, Sci. Rep. 2002, 2003-1, p.176.
[23] A. v. Zweidorf *et al*. Gesellschaft für Schwerionenforschung mbH, Darmstadt, Sci. Rep. 2001, 2002-1, p.181.
[24] A. v. Zweidorf *et al*. Gesellschaft für Schwerionenforschung mbH, Darmstadt, Sci. Rep. 2002, 2003-1, p.175.
[25] A. v. Zweidorf, private communication and to be published.

Chemical properties of element 112

A. Yakushev[1]

[1] Institute for Radiochemistry TU Munich, Germany

yak@rad.chemie.tu-muenchen.de

Introduction

Study of chemical properties of element 112 (E112) are of great interest in itself. In addition, they can provide an independent determination of its atomic number and decay properties. E112 has been obtained directly in the ^{238}U (^{48}Ca; 3n) reaction [1] and also as the daughter of element 114 produced in the ^{242,244}Pu (^{48}Ca; 3(4)n) reaction [2,3]. The isotope ^{283}112 with a 3-min half-life decaying by spontaneous fission (SF) [1] is a very attractive nuclide for a first chemical identification in the super heavy element (SHE) region.According to its predicted ground state electronic structure, E112 belongs to group 12 of the Mendeleev Periodic System (MPS), and is the nearest homologue of Hg. Based on classical extrapolations, E112 should form stronger bonds with surfaces of some metals, than the bonding between E112 atoms in the hypothetic metallic phase [4]. Chemical studies of E112 might reveal strongly pronounced "relativistic effects" that are theoretically predicted. The expected enhanced volatility of E112 makes it an ideal object for the study of its elemental state chemical behavior by gas-phase chemical methods. The strong interaction with suitable metallic surfaces at ambient or even below-ambient temperatures opens up good prospects for using modern semiconductor detectors for on-line detection of volatile SHE on a one-atom-at-a time level. The calculations and prognoses made for E112 predict a weaker interaction with Au and a higher volatility than that of its lighter homologue Hg [5,6]. At the same time, relativistic quantum chemistry predicts increasingly strong “relativistic effects” in the chemistry of super-heavy elements [7,8]. The calculated contraction stabilizes the spherical *s* and $p_{1/2}$ electron orbitals, which more efficiently shield the nuclear charge and thus destabilize the $p_{3/2}$- and *d*- orbitals. This may strongly influence the chemical behavior of the 7*s* and 7*s*7$p_{1/2}$ elements, E112 and E114. They are predicted to approach the behavior of noble gases in volatility and chemical inertness [9]. Therefore, one has to investigate the volatility and adsorption behavior of E112 concurrently with those of Hg and Rn.

The chemical study of element 112 in Dubna

As a first approach in January 2000 [10], performed in Dubna, an international team tried to detect an “Hg-like” behavior of E112, by assuming that it should strongly adsorb on gold surfaces at ambient temperature. The reaction products were transported from a recoil chamber through Teflon capillary 30 m in length by helium. This transportation method was also a very good chromatographic separation – only very volatile species could reach the detector. The detector consists of 8 chambers in series, placed in an assembly of 86 neutron counters. In the each chamber were two detectors (2x2 cm) covered with thin gold layers, the distance between the top and bottom detectors was 1 mm. More than 95% of ^{185}Hg was deposited in the first chamber. During the 10 days of bombardment an integral dose of $6.85 \cdot 10^{17}$ was collected. However, no SF events were registered. Thus, the first experiment did not provide an answer as to the physical and chemical properties of element 112. The second experiment was performed at the FLNR JINR in November/December 2001 [11]. The experimenters had to increase by several times, the beam dose to detect E112 atoms in both, the adsorbed state or the gaseous phase. For this purpose, a special flow-through ionization chamber was designed to register SF-decays in the gaseous phase. Figure 1 shows a basic schematic of the setup. As in the first experiment, a ~2 mg/cm^2, 20 mm in diameter $^{nat}U_3O_8$

target (2), containing 100 μg of ^{nat}Nd was deposited on a 2 μm HAVAR foil. It also served as a vacuum window and was supported by a thick water-cooled Cu grating (3) with a transparency of 80%. The recoils were thermalized in pure helium and transported through a 25 m long PTFE capillary to detectors situated behind a concrete wall, which served as a shield against radiation from the cyclotron. The first detector assembly (6) was a circular chamber with 8 pairs of PIPS detectors with a working area of 18×18 mm^2 each, covered with 30 μg/cm^2 Au. The gap between the "top" and "bottom" detectors was 1 mm (Fig. 2a). The gas exiting the chamber (6) was mixed with appropriate quantities of argon and methane, then passed through an aerosol filter into the ionization chamber (7), see Fig. 2b. Both detection chambers were mounted in an assembly of 126 ^{3}He-filled counters (8), which registered fission neutrons with an efficiency of about 35%. Discriminated pulses from the PIPS detectors and the ionization chamber triggered measurement of fission neutrons. In the latest experiment the beam energy in the middle of the target layer was 234 MeV. After 22.5 days of bombardment, an integral beam dose of $2.8 \cdot 10^{18}$ of ^{48}Ca ions was accumulated.

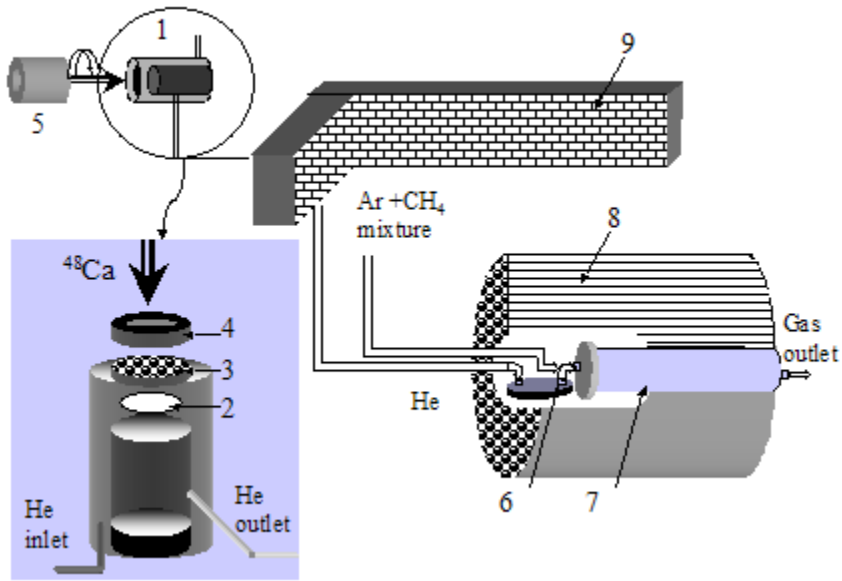

Figure 1. Schematic view of the experimental setup: 1 – recoil chamber; 2 – ^{238}U target; 3 – Cu grating; 4 – Cu collimator; 5 – wobbler device; 6 – circular chamber with 8 pairs of PIPS detectors; 7 – ionization chamber; 8 - assembly of 126 ^{3}He neutron counters; 9 – concrete shielding wall.

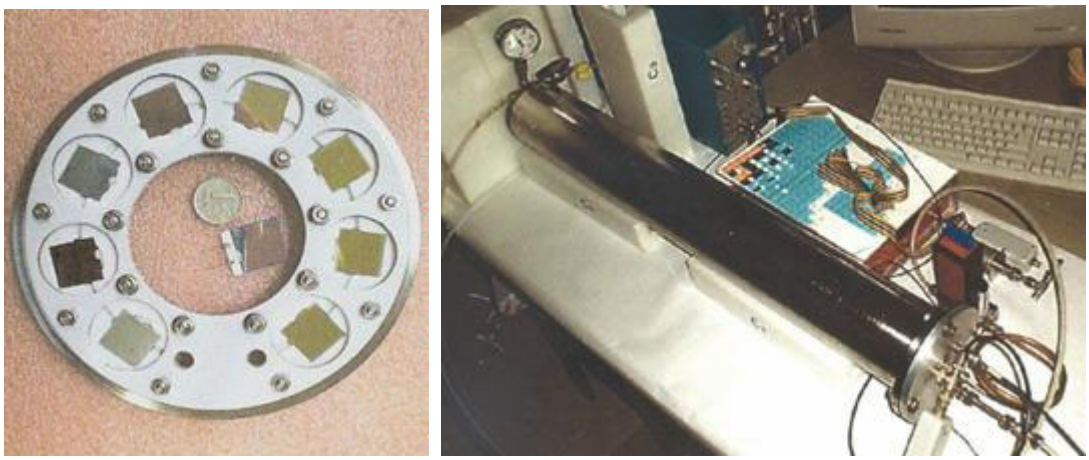

a) b)

Figure 2. View of the open PIPS detector assembly* (a) and ionization chamber (b).
*Only 8 bottom detectors mounted in the PTFE disks are shown.
The top detectors, gas inlet and outlet, as well as covers are removed.

The behavior of Hg and Rn atoms in the PIPS detector assembly was traced by registering the α-decays of ^{185}Hg ($T_{1/2} = 49$ s) and ^{220}Rn ($T_{1/2} = 55$ s), which were produced in the fusion reaction ^{nat}Nd(^{48}Ca;xn) and in transfer reactions ^{238}U+^{48}Ca. More than 95% of ^{185}Hg atoms were adsorbed already in the first pair of PIPS detectors. In contrast to this, only a minute part of ^{220}Rn nuclei decayed within this detector assembly, practically uniformly over all the 8 pairs of PIPS detectors. Under the experimental conditions, no known volatile species of heavy actinides or light transactinides could be formed. Gamma spectra measurements and comparison of long-living α-activities in the recoil chamber and on PIPS detectors yielded a of gaseous element purification factor of $5 \cdot 10^5$. Non-volatile species could reach the detectors only by aerosol transportation. The aerosol filter installed between the PIPS detector assembly and the ionization chamber increased the factor of purification from non-volatile products by 10^4. No signals corresponding to the energy release higher than 12 MeV came from the PIPS detectors, i.e. no SF event were detected. In the ionization chamber 8 spontaneous fission events were registered in coincidence with prompt fission neutrons. During 100 days of background measurements with the ionization chamber before and after the experiment, 4 signals were detected in the fission fragment energy range. From these data, the 95% confidence interval for the events counting rate the is $7^{+7.0}_{-4.4}$. Assuming an overall procedure efficiency of 40% the effective production cross section of ^{283}112 in the reaction ^{238}U + ^{48}Ca was calculated to be $2^{+2.0}_{-1.2}$ pb. Using a model of mobile adsorption, for the description of migration velocity of species in chromatographic column, and a Monte Carlo simulation, the authors evaluated the adsorption enthalpies of Rn to be: $-\Delta H_{ads}$(Rn)≈36 kJ/mol and from the estimated upper limit of the retention time of E112: $-\Delta H_{ads}(112) \leq 60$ kJ/mol. Thus, in the atmosphere of an inert gas, the atoms of E112 showed enhanced volatility and did not form strong metal-metal bonds when hitting the Au surface – E112 behaves more like the noble gas Rn rather than Hg. Such marked difference in the chemical properties of the transactinide E112 and its nearest homologue Hg was demonstrated for the first time. Undoubtedly, the next step is a quantitative comparative study of physical-chemical properties of Hg, Rn and E112. This experiment was performed in Darmstadt in spring of this year.

Comparative study of Hg, Rn and element 112 using COLD cryo-detector

In the third experiment the same technique was used, that was earlier developed for chemical experiments with element 108, hassium [12,13]. The principal distinction from two previous experiments was detection of Hg, Rn and element 112 in the same thermo-gradient detector. It opened the possibility for comparative quantitative study of these elements. The set-up involves a ^{238}U target (medial thickness 1.6 mg cm^{-2}) on a rotation wheel bombarded with up to $1 \cdot 10^{12}$ $^{48}Ca^{7+}$ particles per second, supplied by the UNILAC accelerator at the Gesellschaft für Schwerionenforschung mbH (GSI). The 346 MeV beam delivered by the UNILAC, after passing through a medial 3.7 mg cm^{-2} Be vacuum window and a medial 2.2 mg cm^{-2} backing-foil (Be) resulted in a ^{48}Ca projectile energy of around 222 – 239 MeV inside the ^{238}U target. Products of the heavy ion induced nuclear fusion reaction recoiling backwards out of the target were thermalized in dried 1 l/min He carrier gas. The inner surface of the newly designed recoil chamber was completely covered by a quartz insert to inhibit an adsorption of a potentially metallic E112 on its metal surfaces. Only gaseous products are swept out of the recoil chamber through an open quartz column. Subsequently, they are transported to an oven with a quartz wool filter heated to 850°C. Aerosol particles produced by beam induced sputtering in the target material and from the beam dump are stopped in this filter. Ultimately, separation factors of about 10^7 have been measured for non-volatile species. The volatile products pass this filter and a connected 10 m long PFA-capillary to a Ta-Ti-getter heated up to 1000 °C. Trace amounts of water are removed from the carrier gas by this getter. Subsequently, the remaining gaseous products enter the COLD [14] – cryo on-line detector – thermo chromatography column. COLD establishes a negative temperature gradient from + 35°C to –187°C (see Fig. 3). The new version of this device consists of 32 silicon PIN-photodiodes with 10 x 9.8 mm^2 active area mounted in a row at a distance of 1.6 mm opposite to an Au surface and forming a rectangular gas chromatographic column. α- or SF-decays from atoms adsorbed on the Au surface were detected with 2 π-detection geometry. Au layer was selected as chromatographic surface to distinguish, if possible, between metallic and non-metallic properties of E112. Similar to Hg, the formation of a metal bond with the Au surface is expected for a metallic E112 [15]. Furthermore, chemical inertness of Au to oxidation provides a clean metallic chromatographic surface. The over-all-efficiency detecting a fission fragment generated from a mother isotope adsorbed on the detector array was 77 %. The whole detector set-up is placed into a vacuum tight steel box under low pressure to isolate it thermally and to eliminate the moisture from the surrounding air. The experiment to produce E112 lasted 17.08 days during which a total of around $2.8 \cdot 10^{18}$ ^{48}Ca particles passed through the target. For continuous verification of the IVO-COLD-system one of the three banana shaped segment of the $^{nat}U_3O_8$ target contained 21.7 µg cm^{-2} ^{nat}Nd for producing $^{182-185}Hg$ in the nuclear reaction $^{nat}Nd(^{48}Ca,8n)$. The Hg-isotopes deposited completely on the Au-surface opposite the first five detectors (see Fig. 3). In the reaction of ^{48}Ca on ^{238}U, different Rn-isotopes were produced as transfer products and transported to COLD. $^{219-221}Rn$ and their daughters decays were a second parameter to check the proper functioning of the system, as they were – according to their half-lives – adsorbed on the last 4 detectors of the cold end of the chromatography column (Fig. 3). During the entire experiment 13 fission events above 35 MeV (incorrect energy calibration) were observed. In the background measurement at the GSI – lasting 24 days – 5 fission events above 35 MeV were detected. No indications for actinides and other non volatile transfer reaction products, which could be transported by aerosol particles through the whole setup were observed during the experiment and in the subsequent background measurement. The result shows evidence for the observation of a spontaneous fissioning isotope $^{283}112$, which is extremely volatile in elemental state and accumulates at temperatures below -160°C on the last detectors. The final data analysis is in progress.

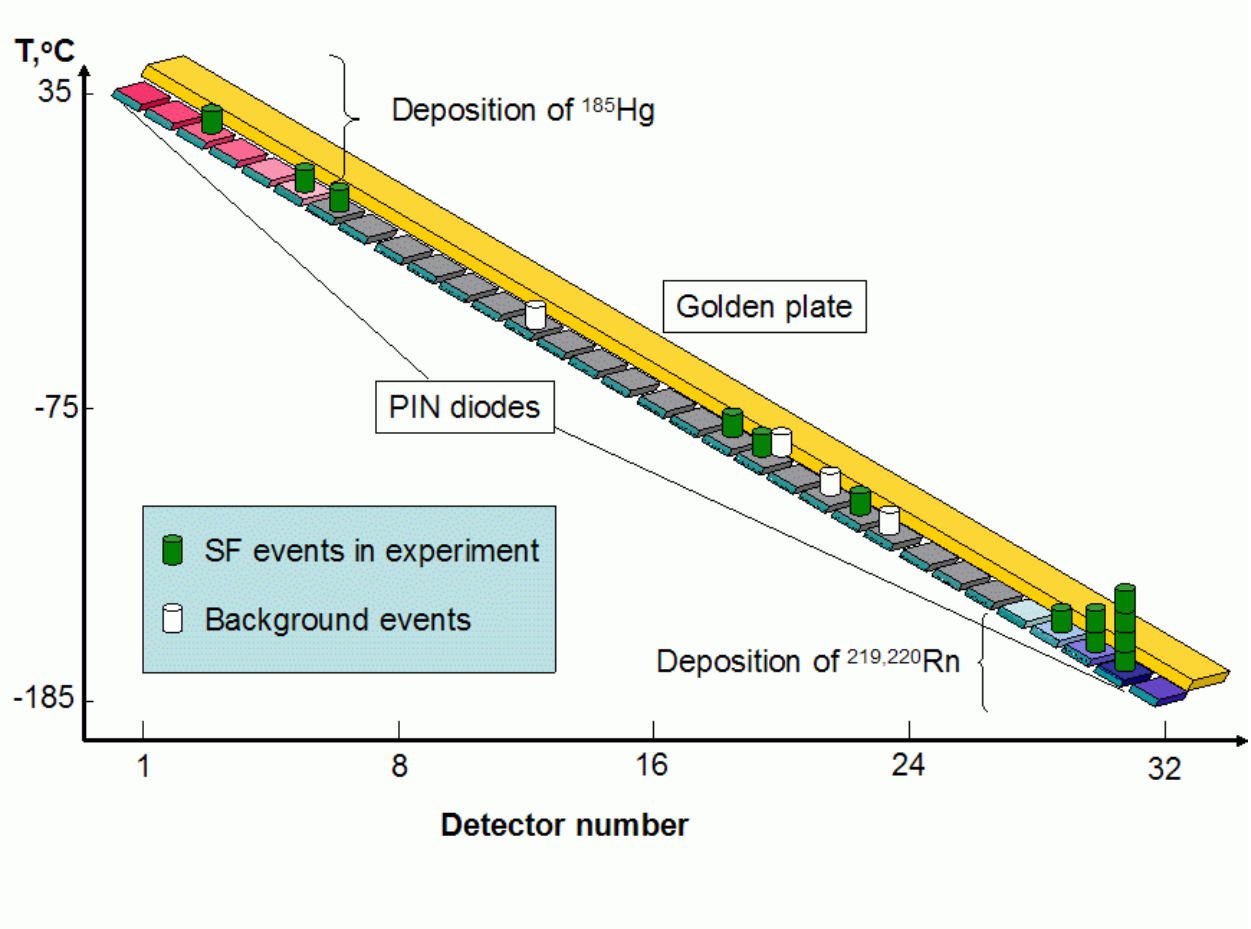

Figure 3. Schematic of the detector and distribution of Hg, Rn and SF events.

References

[1] Oganessian, Yu. Ts.; Yeremin, A. V; Gulbekian, et al., Eur. Phys. J. A 5, 63 (1999).
[2] Oganessian, Yu. Ts.; Yeremin, A. V; Popeko, et al., Nature 400, 242 (1999).
[3] Oganessian, Yu. Ts.; Utyonkov, V. K.; Lobanov, et al., W. Phys. Rev. Lett. 83, 3154 (1999).
[4] Eichler B., Kernenergie 19, 307, (1976).
[5] Eichler B., Rossbach H., Radiochim. Acta 33, 121, (1983).
[6] Eichler, B. PSI Reprint 00-09, PSI Villigen (2000) ISSN 1019 0643.
[7] Pitzer K.J., Chem. Phys. 63, 1032, (1975).
[8] Pyykkö P., Chem. Rev. 88, 563, (1988).
[9] Schwerdtfeger P., Seth M., In Encycl. Of Comp. Chem.; Willey: N.Y., 4, 2480, (1998).
[10] Yakushev A.B., Buklanov G.V., et al., Radiochim. Acta 89, 743, (2001).
[11] Yakushev A.B., Zvara I., Belozerov A.V. et al., Reprint JINR E12-2002-297, Dubna (2002), Radiochim. Acta, in press.
[12] Düllmann Ch.E., Brüchle W., Dressler R. et al., Nature 418, p.859-862 (2002).
[13] Kirbach U. et al., Nucl. Instr. Meth. A484, 587-594 (2002).
[14] Ch. E. Düllmann et al., Nucl. Instr. Meth. A479, 631 (2002).
[15] B. Eichler, PSI Report Nr. 00-09 (2000).

Anion-exchange behavior of rutherfordium and dubnium in pure HF solution

K. Tsukada[1], H. Haba[2], M. Asai[1], K. Akiyama[1], A. Toyoshima[3], I. Nishinaka[1], M. Hirata[1], K. Hashimoto[1], S.I. Ichikawa[1], Y. Nagame[1], K. Yasuda[1], Y. Miyamoto[1], Y. Tani[3], H. Hasegawa[3], W. Sato[3], A. Shinohara[3], S.I. Goto[4], M. Ito[4], J. Saito[4], H. Ishizu[4], H. Kudo[4], Y. Oura[5], K. Sueki[6], H. Nakahara[3], N. Kinoshita[7], H. Kikunaga[7], A. Yokoyama[7], M. Sakama[8], M. Schädel[9], J.V. Kratz[10]

[1] Japan Atomic Energy Research Institute, Japan
[2] RIKEN, Japan
[3] Osaka University, Japan
[4] Niigata University, Japan
[5] Tokyo Metropolitan University, Japan
[6] University of Tsukuba, Japan
[7] Kanazawa University, Japan
[8] University of Tokushima, Japan
[9] Gesellschaft für Schwerionenforschung mbH, Germany
[10] Universität Mainz, Germany

ktsuka@popsvr.tokai.jaeri.go.jp

Many attempts have been made to study the aqueous chemistry of element 104, rutherfordium, and element 105, dubnium [1]. Differences in the complex formation among Rf, Db and their lighter homologues were deduced from some of the experiments, and some yielded conflicting results [1]. Although several experiments for Rf and Db in various HF solutions have been performed [2-5], enough data have not been accumulated to discuss in detail the fluoride complexations and/or relativistic effects. In the present work, we have investigated the chemical behavior of Rf and Db together with their group-4 and group-5 homologues by an anion-exchange chromatography in pure HF solution expected to be a fast and simple reaction mechanism to form anionic complexes.

The isotopes ^{261}Rf, ^{85}Zr, and ^{169}Hf were produced in the ^{248}Cm(^{18}O,5n), ^{nat}Ge(^{18}O,xn), and ^{nat}Gd(^{18}O,xn) reactions, respectively, at the JAERI tandem accceralator [6]. On-line anion-exchange separations for Rf, Zr, and Hf in 3.9-13.9 M HF solutions were performed using the Automated Ion exchange separation apparatus coupled with the Detection system for Alpha spectroscopy (AIDA) [7]. AIDA enables us to perform cyclic discontinuous chromatographic separations in aqueous phase and automatic detections of α-particles within a typical cycle time of 1 - 2 min. The reaction products recoiling out of the target were transported by the He/KCl gas-jet system to AIDA, and were dissolved with 240 μL of 3.9 to 13.9 M HF and fed into an anion-exchange column (MCI GEL CA08Y, 1.6 mm i.d. □~7.0 mm) at a flow rate of 0.74 mL/min. Figure 1 shows typical elution curves of short-lived ^{85}Zr and ^{169}Hf in 14 M HF solution. These elution curves exhibit a good performance of the present anion-exchange separation system, expecting that the chemical equilibrium is established. The effluent was collected on a Ta dish as Fraction 1 and evaporated to dryness with hot He gas and a halogen heat lamp. The products remaining in the column were eluted with 210 μL of 4.0 M HCl. This effluent was collected on another Ta dish and evaporated to dryness as Fraction 2. Each pair of Ta dishes, Fractions 1 and 2, was automatically transferred to the α spectrometry station equipped with the eight 600 mm^2 PIPS detectors. Figure 2 shows typical α particle energy spectra for Fractions 1 and 2. From the activities A_1 and A_2 observed in Fractions 1 and 2, respectively, the percent adsorption (%*ads*) on CA08Y was evaluated by the equation: $\%ads = 100A_2/(A_1 + A_2)$. The %*ads* values of Rf, Hf and Zr in the various concentrations of HF are shown in Figure 3. This result shows a notable difference in the sorption behavior between Rf and its homologues Zr and Hf. The %*ads* values of Zr and Hf are in good agreement with each other and both decrease steeply with an

increase of the HF concentration above 8 M. Although the *%ads* of Rf also decreases with the HF concentration, the values are apparently smaller than those of Zr and Hf, suggesting that the fluoride complexing strength of Rf is weaker than that of Zr and Hf.

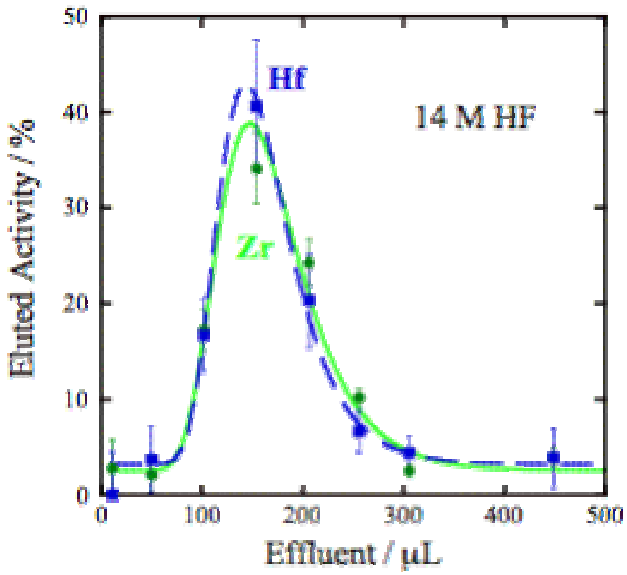

Figure 1. Elution curves for ^{85}Zr and ^{169}Hf in 14 M HF from an anion-exchange column (MCI GEL CA08Y, 1.6 mm i.d. □~7.0 mm) at a flow rate of 0.74 mL/min.

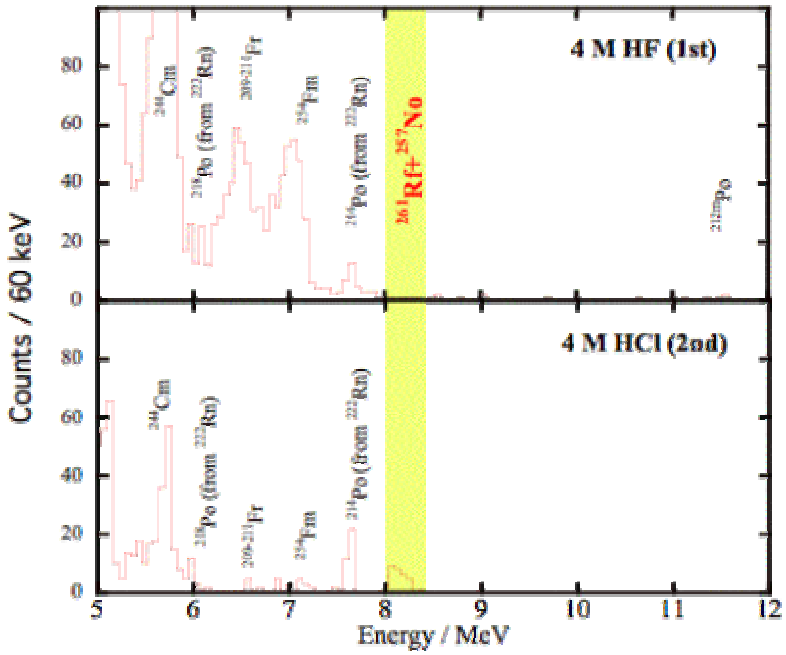

Figure 2. α-particle energy spectra of two eluted fractions: (upper) 4 M HF and (lower) 4.0 M HCl.

On the other hand, we are also interested in a fluoride complexing strength of Db and its group-5 homologues, Nb and Ta, and pseudo-homologue Pa on the anion-exchange resin. The sorption sequence of Ta≥Nb>>Pa in 2-15 M HF solutions was observed in the batch experiment, and the *%ads* value of Db

together with Ta in a 14 M HF solution was investigated. ^{262}Db and ^{169}Ta were produced in the ^{248}Cm(^{19}F, 5*n*) and ^{nat}Gd(^{19}F, *xn*) reactions, respectively, at the JAERI tandem accelerator [6]. 1702 anion-exchange separations were conducted using AIDA with a small column of 1.0 mm i.d. □~ 3.5 mm. It was found that the *%ads* value of Db is smaller than that of Ta, suggesting that the sequence of the fluoride complexing strength is Ta≥Nb>Db≥Pa.

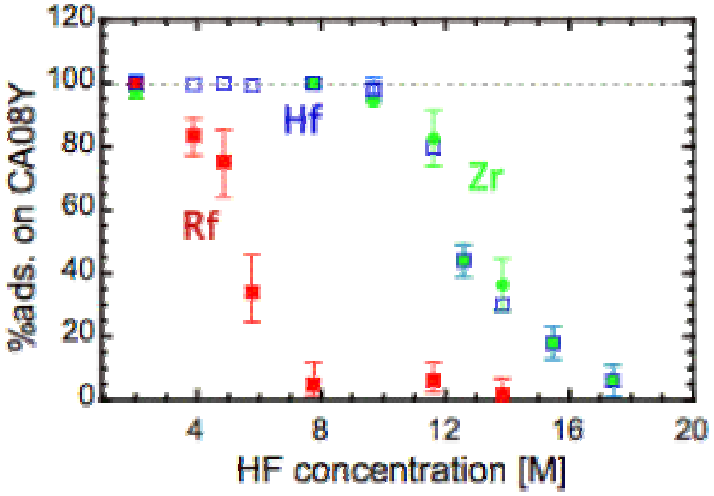

Figure 3. Variation of the percent adsorption (*%ads*) of Zr, Hf, and Rf on CA08Y as a function of the HF concentration.

References

[1] J.V. Kratz, *Chemical Properties of the Transactinide Elements*, Heavy Elements and Related New Phenomena, W. Greiner and R.K. Gupta (Edts.), World Scientific, Singapore, 1999, pp.129-193.

[2] Z. Szeglowski, H. Bruchertseifer, V.P. Domanov, B. Gleisberg, L.J. Guseva, M. Hussonnois, G.S. Tikhomirova, I. Zvara, and Yu.Ts. Oganessian, Radiochim. Acta **51**, 71 (1990).

[3] G. Pfrepper,R. Pfrepper, D. Krauss, A.B. Yakushev, S.N. Timokhin, and I. Zvara, Radiochim. Acta **80**, 7 (1998).

[4] E. Strub *et al.*, Radiochim. Acta **88**, 265 (2000).

[5] W. Paulus *et al.*, Radiochim. Acta **80**, 69 (1999).

[6] Y. Nagame *et al.*, J. Nucl. Radiochem. Sci. **3**, 85 (2002).

[7] K. Tsukada, I. Nishinaka, M. Asai, S. Goto, M. Sakama, H. Haba, S. Ichikawa, Y. Nagame, and M. Schaedel, JAERI-Review **29**, 49 (2002).

Current status of transactinide research with the liquid-liquid extraction system SISAK

J.P. Omtvedt[1], J. Alstad[1], D. Polakova[1], G. Skarnemark[2], L. Stavsetra[1], L. Zheng[1]

[1] University of Oslo, Norway
[2] Chalmers University of Technology, Sweden

j.p.omtvedt@kjemi.uio.no

Introduction

SISAK[a] is a fast, chemical-separation system for liquid-liquid extraction. It was developed to investigate short-lived nuclides recoiling out of an irradiated target and transported in a gas jet. The system is based on small centrifuges with a continuous feed and output [1-3].

During recent years, work has been undertaken to deploy SISAK in studies of the chemical properties of the transactinide elements ($Z \geq 104$) [4-8]. The only suitable detection method found was liquid-scintillation (LS) detection [9]. This was mainly because of the rather high flow rates (0.5-2.0 mL/s) encountered in the SISAK system. Other detection methods usually require either thin, dry samples or very thin liquid films. No suitable method was found to prepare such samples without an unacceptable time delay between separation and detection.

In 2000 the first successful transactinide experiment [5] with SISAK was performed at the Lawrence Berkeley National Laboratory (LBNL) in Berkeley, USA. In this experiment it was proved that it was possible to extract and detect the transactinide ^{257}Rf with SISAK. The ^{257}Rf activity was produced with a 235 MeV $^{50}Ti^{12+}$ beam from the LBNL 88-inch cyclotron hitting a rotating ^{208}Pb target. The recoils from the target were then separated in the Berkeley Gas-filled Separator (BGS) and transferred to the chemistry apparatus in a gas jet. The preseparated recoil products were transferred from the BGS to the gas jet by using a unique Recoil Transfer Chamber (RTC), then recently constructed by Uwe Kirbach.

After the successful transactinide pilot-experiments in 2000 and 2001 with the BGS, work was undertaken in Oslo to develop suitable extraction systems to make detailed investigations of the chemistry of Rf. The first stage of this investigation was detailed checks on the reproducibility of the SISAK system, i.e. how accurate measurements are possible using such an on-line extraction system? As is reported below, this showed that several chemical systems thought to be usable with the SISAK system could not be used due to problems with sorption on or in the construction material of the SISAK centrifuges.

The second stage of the mentioned investigation was to develop the chemical extraction system to be used in future Rf experiments. This work is reported in a separate extended abstract to the TAN'03 conference and will be presented as a poster at the conference (Darina Poláková and co-workers).

In parallel to the work on the chemistry to be used in the SISAK system, work has been performed in Oslo to improve the performance of Liquid Scintillation (LS) detection system and to improve the acquisition and analysis methods. LS counting has high efficiency, but suffers from relatively poor energy resolution (about 300-keV FWHM at 7-MeV α energy) and is sensitive to β-particles and γ-rays. This puts very stringent demands on the detection system, because most of the β- and γ-emitting contaminants are produced with orders of magnitude higher yield than the transactinide under study. Therefore, further improvements to the SISAK detection system have been pursued. This work is also reported in a separate extended abstract and will be presented as a poster at the conference (Liv Stavsetra and co-workers).

The SISAK system as an analytical tool

If the SISAK system is to be used for detailed chemical studies of transactinide elements, then it is paramount to know the precision at which distribution ratios can be measured. The distribution ratio for a given element is its concentration in the organic phase divided by its concentration in the aqueous phase. The most obvious limit to the precision of which such values can be measured is of course the uncertainty due to counting statistic. The largest relative uncertainty will dominate the uncertainty for the distribution ratio. At high distribution ratios, $D > 100$, or low distribution ratios, $D < 1/100$, less than 1% of the activity will be in one of the phases. Therefore, in situations where limited amounts of activity are available, the amount of activity in this phase is practically impossible to determine. In addition to this, and even more significant, one has the practical problem of achieving perfectly clean phases. Thus, if the phase separation is not perfect and traces of the wrong phase are carried with the one with the least amount of activity, serious errors might results. Therefore, distribution ratios between 1/10 and 10 is the safest range to work in when only small amounts of activity are available. This is a typical situation in a transactinide experiment. For experiments with the transactinide's homologues, the activity is available in larger amounts and one can typically extend the range to between 1/100 to 100.

For rutherfordium experiments an extraction system based on extraction from high concentration nitric acid (2-6 M) with dibutyl-phosphoric acid was originally developed [4]. The distribution ratio for Hf was measured at many different installations and at different times with this system. After a while it became clear that the results varied much more than could be attributed to counting statistics. This was worrying, as it either meant there was a very large entrainment of the wrong phase, or some other property of the SISAK system interfered with the measurements. Therefore, a detailed investigation of this effect was initiated at the beginning of 2002. The parameters investigated were: Flow rate and flow-rate ratio of the phases, rotation speed of the centrifuge, temperature of the phases, and sensitivity to reaction rates. The latter might be important because the mixing and separation of the phases are too fast to reach equilibrium conditions, thus variations in closeness to equilibrium might be important. Experiments at the Oslo Cyclotron Laboratory soon showed that neither of these parameters were to blame, but the large variation of the distribution ratios persisted. It became evident that the variations seemed to be a function of the time the system had been in contact with the aqueous phase (> 1 M nitric acid). This indicated interference with the centrifuge construction-material (PolyEtherEtherKetone, PEEK) or tubes (made of PerFluoroAlkoxy, PFA) of the system. This problem is illustrated in Fig. 1, where the distribution ratio is plotted as a function of the sum of activity in the two phases (compared to how much activity enters the centrifuge). As can clearly be seen, there is a large loss of activity. Furthermore, when more activity is retained in the centrifuge, the distribution value increases. This is because mainly the aqueous phase activity is retained, not the activity extracted into the organic phase.

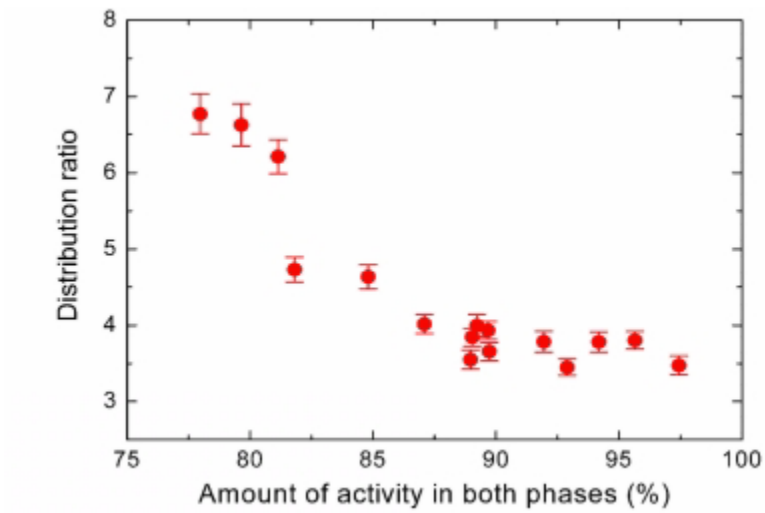

Figure 1. Comparison between the amount of ^{169}Hf activity at the centrifuge outlets and the distribution ratio between activity in the two phases.

First it was suspected that the PFA tubes were at fault, thus they were changed with PEEK tubes. However, this made the problem even worse. Therefore, it could be concluded that the PEEK acted as a sort of chromatography column, retaining at least one of the aqueous phase species. This was a surprising result, as the PEEK construction-material was selected due to its ability to withstand strong acids, among them nitric acid. Unfortunately, there obviously is a significant difference between being resistant and inert. In the case of the nitric acid the PEEK acts much like a sponge.

On basis of these findings, a search for a more suitable system to study the chemistry of rutherfordium was undertaken. In addition, such a system was required to differentiate between Zr and Hf. This is necessary as it is of interest to classify the chemistry of rutherfordium as either Zr- or Hf-like, or to be able to point out certain trends in the extraction of Zr, Hf and Rf. This can not be done if they all extract with more than 90% yield. As reported in one of our other TAN'03 contributions (Poláková and coworkers), such a system has been developed.

The future: SISAK after shutdown of the 88-inch LBNL cyclotron

The BGS coupled to the 88-inch LBNL cyclotron was a very good tool for producing transactinide activity for SISAK. Unfortunately, the cyclotron is being shut down. Hopefully, a similar facility will be established at the Gesellschaft für Schwerionenforschung (GSI) in Darmstadt, Germany. Until then, SISAK has to utilize other methods to remove unwanted activity from the product stream. A general method would be to insert a chemical cleaning-stage in front of the centrifuge used to study the extraction chemistry of a given element. This can be done by adding two additional centrifuges for extraction/back-extraction, as illustrated in Fig. 2. Such systems have been developed for a number of extraction systems, see e.g. [10], but needs to be developed for the TOA/sulphuric acid system described by Poláková and coworkers.

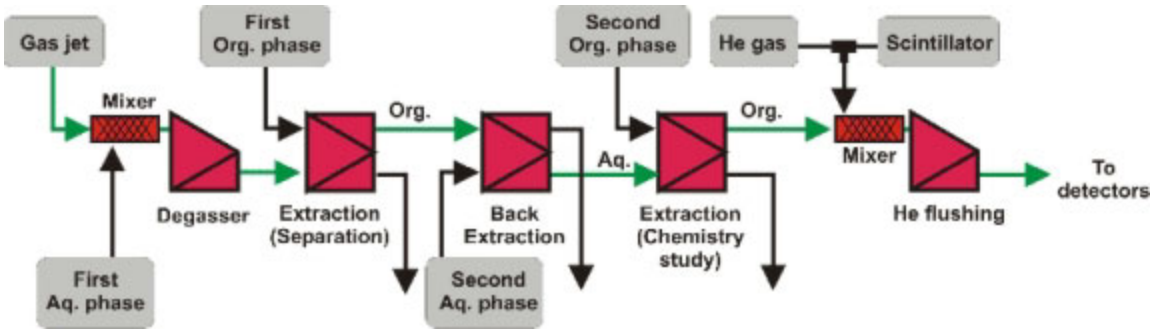

Figure 2. Schematic drawing of a three stage SISAK system which first removes unwanted activity by an extraction/back-extraction section and then have a third extraction stage to study the chemistry of the selected element. The wanted activity follows the green arrows, the black arrows represent feed and waste streams.

An alternative is to exploit gas phase properties of certain elements to suppress unwanted activity in the transport from the target chamber to the chemical apparatus. A good candidate for such separation is element 108, hassium. As has been shown in a recent GSI gas-phase experiments with hassium [11], it is possible to selectively transport Hs by oxidizing it to the tetroxide immediately after they escape the target chamber. Because the tetroxide is volatile, one does not need aerosol particles in the He gas-jet transporting the products to the chemistry apparatus. This reduces the background significantly in the detectors, because most of the unwanted activity will not be volatile and thus remains in the target chamber [12].

By dissolving the HsO_4 in a liquid phase in the SISAK degasser, it should be possible to study the liquid phase properties of Hs. Model experiments using ruthenium and osmium are planed and results will be reported at the TAN'03 conference.

References and notes

a. Short-lived Isotopes Studied by the AKUFVE-technique, where AKUFVE is a Swedish acronym for an arrangement for continuous investigations of distribution ratios in liquid extraction.

[1] H. Persson *et al*. Radiochim. Acta **48**, 177 (1989).

[2] G. Skarnemark *et al.* Phys. Script. Sweden **34**, 597 (1986).

[3] G. Skarnemark *et al.* Nucl. Instr. and Meth. **171**, 323 (1980).

[4] J.P. Omtvedt *et al.* J. Alloys and Comp. **271-273**, 303 (1998).

[5] J.P. Omtvedt *et al*. J. Nucl. Radiochem. Sci. **3**, 121 (2002).

[6] B. Wierczinski *et al.* J. Radioanal. Nucl. Chem. **236**, 193 (1998).

[7] B. Wierczinski *et al.* Radiochim. Acta **69**, 77 (1995).

[8] K. Eberhardt *et al.* The 4th international conference on nuclear and radiochemistry, NRC4, September 8-13, 1996. St. Malo, France.

[9] B. Wierczinski *et al.* Nucl. Instr. Meth. **A370**, 532 (1996).

[10] M. Johansson, Radiochemical Separation Systems adapted for Studying Transactinide Chemistry with SISAK, PhD thesis at Department of Chemistry, 2001, University of Oslo.

[11] C.E. Düllmann *et al.* 2001 GSI Scientific Report, Germany (2002).

[12] C.E. Düllmann *et al.* 1999 Annual Report, Paul Scherrer Institut, Villigen, Switzerland (2000).

X-ray absorption fine structure spectroscopy of Zr and Hf in HCl solution for chemical characterization of Rf

H. Haba[1], K. Akiyama[2], K. Tsukada[2], M. Asai[2], A. Toyoshima[2], T. Yaita[2], M. Hirata[2], K. Sueki[3], Y. Nagame[2]

[1] RIKEN, Japan
[2] Japan Atomic Energy Research Institute, Japan
[3] Tsukuba University, Japan

haba@riken.go.jp

Introduction

Chemical behavior of the first transactinide element, rutherfordium (Rf), in hydrochloric acid solutions has been investigated by ion-exchange and solvent extraction methods together with the group-4 homologues Zr and Hf [1–5]. On the other hand, relativistic molecular density-functional calculations of electronic structure have been performed for hydrated, hydrolyzed, and chloride complexes of Rf, Zr, and Hf [6]. Although chloride complexation and hydrolysis of Rf have been considered in Refs. [1–6], no structural data of Zr and Hf in HCl solutions, which are essential to discuss the experimental results and to perform the theoretical calculations, are available. The Extended X-ray Absorption Fine Structure (EXAFS) measurements can provide information on the local environment around the central atom such as the atomic number and the number of neighboring atoms and their distance from the central atom. In the present work, we have measured EXAFS spectra of Zr complexes systematically in 1.0–11.5 M HCl. A change in the complex structure with HCl concentration is discussed together with our anion-exchange result of Zr [5].

Experimental procedures

Commercially available $ZrCl_4$ powder was dissolved with 1.0, 3.0, 5.0, 8.0, 9.0, 10.0, and 11.5 M HCl solutions to obtain 0.01 M concentration of Zr. EXAFS spectra were collected on the BL27B beam line using a Si (111) monochromater at the High Energy Accelerator Research Organization Photon Factory (KEK-PF). Measurements were performed in the fluorescence mode using a 7-element Ge detector at the Zr *K* edge. Curve-fitting amplitudes and phases were calculated by the FEFF8 code [7].

Results and discussion

Fourier transformed *K*-edge EXAFS spectra of the Zr complexes in 1.0, 3.0, 5.0, 8.0, 9.0, 10.0, and 11.5 M HCl solutions, which represent radial distribution functions of the atoms surrounding the Zr atom, are shown by solid curves in Fig. 1 together with the simulations by the FEFF8 code [7] by dotted curves. The FT peaks for shells Zr=O, Zr-O, Zr-Cl, and Zr---Zr are indicated by vertical dashed lines. The structural parameters, the number of neighboring atoms (*N*) and the distance to the neighboring atom (*R*) for shells Zr-O, Zr-Cl, Zr=O, Zr---Zr, and Zr---O, are summarized in Table 1. Accuracy of the *R* and *N* values was estimated to be about ◎}0.02 Å and ◎}0.5, respectively. Note that the spectra shown in Fig. 1 are not corrected for the EXAFS phase shifts, *f¢*, so that each FT peak position does not correspond to the real distance *R* in Table 1.

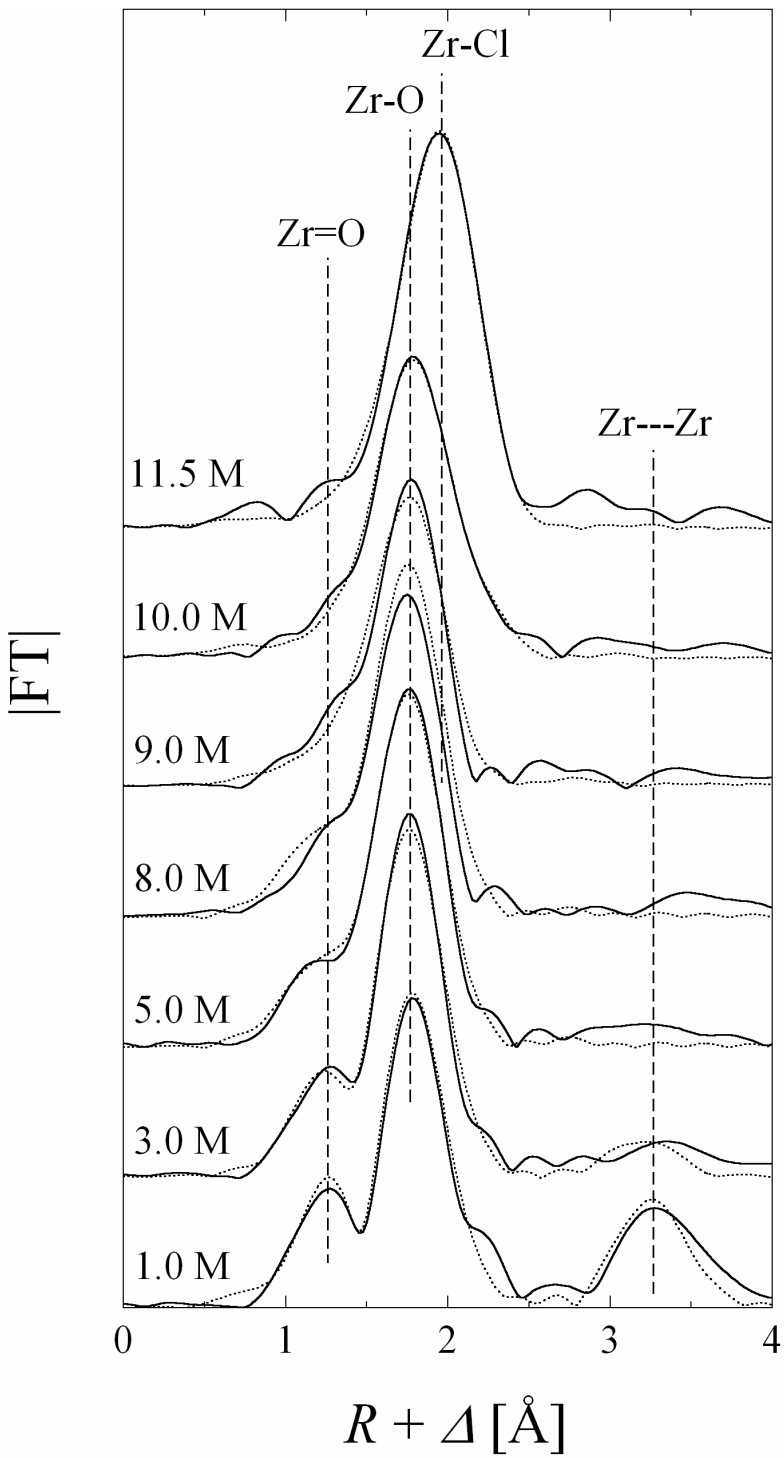

Figure 1. Fourier transformed *K*-edge EXAFS spectra of the Zr complexes in 1.0, 3.0, 5.0, 8.0, 9.0, 10.0, and 11.5 M HCl (solid curves) and the simulations by the FEFF8 code [7] (dotted curves).

Table 1. Structural parameters, the number of neighboring atoms (*N*) and the distance to the neighboring atom (*R*).

[HCl]	Zr-O		Zr-Cl		Zr=O		Zr---Zr		Zr---O	
(M)	*N*	*R* (Å)	*N*	*R* (Å)	*N*	*R* (Å)	*N*	*R* (Å)	*N*	*R* (Å)
1.0	6	2.21	-	-	1	1.63	1	3.58	4	4.95
3.0	6	2.20	-	-	0.5	1.63	0.5	3.58	-	-
5.0	6	2.21	-	-	0.8	1.65	-	-	-	-
8.0	6	2.22	-	-	-	-	-	-	-	-
9.0	7	2.23	-	-	-	-	-	-	-	-
10.0	4	2.21	3	2.43	-	-	-	-	-	-
11.5	-	-	6	2.43	-	-	-	-	-	-

In Fig. 1, the intense Zr-O peaks for Zr-OH_2 and/or Zr-OH^- bonds are seen at HCl concentrations of [HCl]=1–10 M. As listed in Table 1, the *R* values for the Zr-O shell are 2.20–2.23 Å and the *N* are 6–7. Above 10 M, the coordinated H_2O and/or OH^- are replaced with Cl^- with an increase of [HCl], and the Zr-Cl shell with *R*=2.43 Å appears. This change in the complex structure is reasonably consistent with that of the distribution coefficient (K_d) of Zr on the anion-exchange resin, CA08Y [5]. In the range of 1–7 M, the K_d values of Zr are almost constant, 2–4 mL g^{-1}, while at the higher [HCl], the K_d values increase steeply up to 10^4 mL g^{-1}, forming the anionic hexachloride zirconium, $ZrCl_6^{2-}$, at 11.5 M.

It is also interesting to note that the Zr=O peak with *R*=1.63–1.65 Å is shown in Fig. 1 at 1–5 M, though the Zr=O structure has not been reported in this system. Furthermore, the Zr---Zr peak, which indicates the formation of a dimer complex of Zr, is observed at the lower [HCl] of 1 and 3 M: presumably $[(ZrO)(H_2O)_4]_2(OH)_2$.

Previously, we investigated the anion-exchange behavior of Rf together with Zr and Hf in 4.0–11.5 M HCl [5]. It was found that the adsorption trend of Rf is very similar to that of Zr and Hf, indicating that Rf is typically the member of the group-4 elements. The adsorption order is Rf > Zr > Hf, which reflects a difference in the chloride complexing strength. Recently, we have conducted the EXAFS measurements for Hf in 1.0–11.5 M HCl. In the conference, the Hf result will be compared with that of Zr, and the chloride complexation and hydrolysis of Rf as well as Zr and Hf will be discussed by referring to the ion-exchange and solvent extraction results [1–5].

References

[1] E. K. Hulet, R. W. Lougheed, J. F. Wild, J. H. Landrum, J. M. Nitschke, and A. Ghiorso, J. Inorg. Nucl. Chem. **42**, 79 (1980).

[2] K. R. Czerwinski *et al.* Radiochim. Acta **64**, 23 (1994).

[3] K. R. Czerwinski *et al.* Radiochim. Acta **64**, 29 (1994).

[4] R. Günther *et al.* Radiochim. Acta **80**, 121 (1998).

[5] H. Haba *et al.* J. Nucl. Radiochem. Sci. **3**, 143 (2002).

[6] V. Pershina, D. Trubert, C. Le Naour, and J. V. Kratz, Radiochim. Acta **90**, 869 (2002).

[7] A. L. Ankudinov, B. Ravel, J. J. Rehr, and S. D. Conradson, Phys. Rev. B **58**, 7565 (1998).

First results of the CALLISTO-experiment: evidence for the formation of a hassate(VIII)

A. von Zweidorf[1], R. Angert[1], W. Brüchle[1], S. Bürger[2], K. Eberhardt[2], R. Eichler[3], H. Hummrich[2], E. Jäger[1], R. Jera[2], H.O. Kling[2], J.V. Kratz[2], U. Krille[2], B. Kuczewski[2], G. Langrock[2], G. Lehr[2], M. Mendel[2], A. Nähler[2], A. Peil[2], V. Pershina[1], U. Rieth[2], M. Schädel[1], B. Schausten[1], E. Schimpf[1], H.J. Schött[1], E. Stiel[1], P. Thörle[2], N. Trautmann[2], K. Tsukada[4], N. Wiehl[2], G. Wirth[1]

[1] GSI, Germany
[2] Institut fuer Kernchemie Universitaet Mainz, Germany
[3] University of Bern, Switzerland
[4] JAERI, Japan

w.bruechle@gsi.de

Hassium, element 108, was produced in the fusion reaction $^{26}Mg + ^{248}Cm$ at the UNILAC accelerator of GSI [1]. A rotating target wheel with an average target thickness of 467μg/cm^2 ^{248}Cm was used, partly together with a ^{152}Gd segment. After stopping in a He/O_2- mixture the recoils were oxidized, presumably to HsO_4, and were transported to the apparatus CALLISTO (Continuously Working Arrangement for Clusterless Transport of In-situ Produced Volatile Oxides), Fig.1. Nuclear reaction products could react with a NaOH surface under controlled humidity (2g H_2O/Kg gas); the nuclear decays of adsorbed species were detected with 16 PIPS-detectors (10x10mm^2 each), Fig. 2. In the detection array, a stainless steel plate, coated with 1 M ethanolic NaOH (on the average 20 μmol NaOH), is facing 4 detectors at a distance of 1mm. The volatile oxides are allowed to react with the thin alcaline layer, forming non-volatile products which are deposited. The deposition material was replaced every 60 minutes because the deposition efficiency decreases with time [1]. A possible explanation may be, that the alcaline surface is partially neutralized by CO_2, which is an impurity of the used gases and may be formed by a reaction of the carbon beam dump with the oxygen of the jet gas, too. Every 60 minutes, the 4 computer-controlled valves of the deposition and detection system switched one of the detector-arrays out of the gas flow. In this "service mode" the reactive surface can be renewed without interrupting the experiment. Thus a continuously measuring arrangement of 12 detectors was established. After 2 weeks of beam-time and an integral of 2.82×10^{18} beam particles, 5 correlated α-SF chains and one α-α-α-chain (Fig. 3,4) could be detected and attributed to the decay of Hs and / or Sg daughter. Due to pile-up from the high α-activity of Os, produced from the reaction $^{26}Mg + ^{152}Gd$ in the first part of the experiment, it was not possible to attribute 19 α-α-chains with appropriate energies and decay times to the decay of Hs; most of them were estimated to be random coincidences.

In analogy to OsO_4, HsO_4 presumably was deposited as $Na_2[HsO_4(OH)_2]$, a hassate(VIII). A comparison of Hs to the Os-behavior (measured simultaneously) will be given.

References

[1] A. v. Zweidorf et al. GSI Scientific Report 2002, p. 175-177

Figure 1. Diagram of CALLISTO.

Figure 2. Photograph of a detector array.

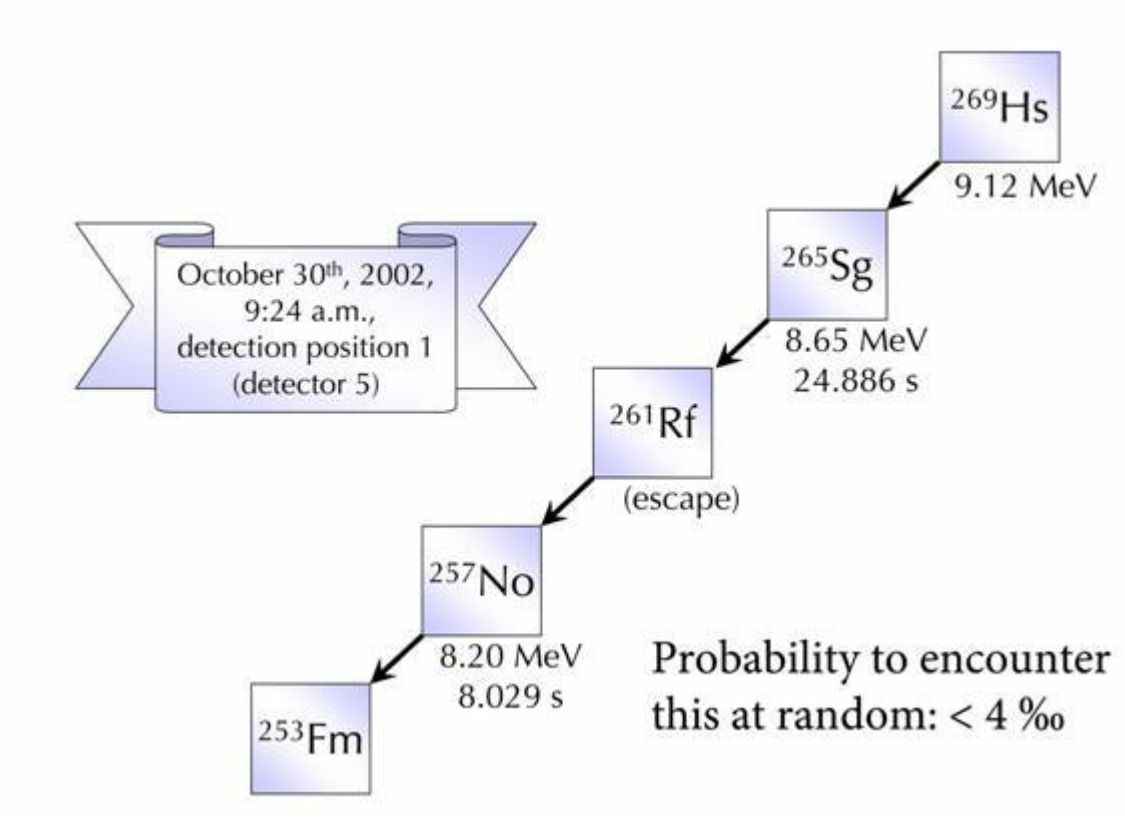

Figure 3. α-α-α-chain.

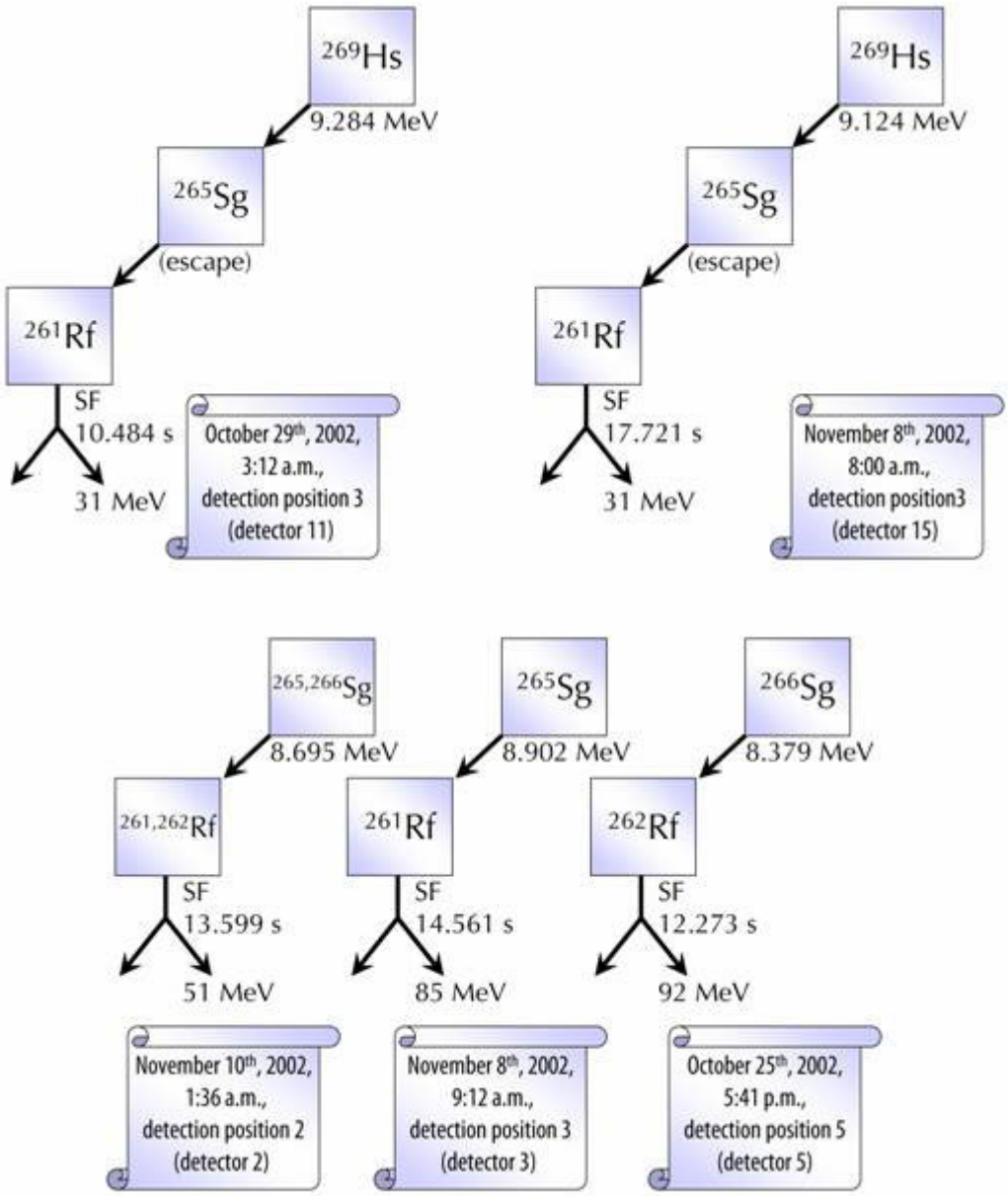

Figure 4. 5 α-SF –chains.

Gas phase studies of volatile group 4 metal complexes using the BGS - test experiments with Zr and Hf

Ch.E. Düllmann[1,2], G.K. Pang[1], C.M. Folden III[1,2], K.E. Gregorich[1], D.C. Hoffman[1,2], H. Nitsche[1,2], R. Sudowe[1,2], P.M. Zielinski[1,2]

[1] Lawrence Berkeley National Laboratory, Berkeley, USA
[2] University of California, Berkeley, USA

CEDuellmann@lbl.gov

Introduction

The chemical investigation of the transactinide elements (TAN, Z≥104), the heaviest elements known today, is an interesting topic of recent nuclear chemistry research. The strong electrical field of the highly charged nucleus accelerates the innermost electrons to relativistic velocities thus causing contraction of spherical (s, $p_{1/2}$) orbitals and expansion of the others ($p_{3/2}$, d, and f), which directly affects the chemical behavior of these elements. Deviations from trends established in the periodic table might therefore occur due to these so-called relativistic effects [1,2].

The heaviest elements which have been chemically investigated so far are the lighter TAN up to hassium (Hs, Z=108) [3,4] and element 112 [5,6,7]. More detailed studies have only been performed for the first two TAN, rutherfordium (Rf, Z=104) and dubnium (Db, Z=105). For Rf and Db, deviations from trends in chemical properties established by the lighter homologs have been observed in a few chemical systems [8,9], while for Sg, Bh and Hs such effects have not been reported so far. One important fact one has to bear in mind when assessing these results is the still rather scarce knowledge of the chemistry of elements heavier than Db which is mainly due to decreasing production cross sections and nuclear half-lives with increasing Z.

Gas chemical methods proved especially suitable to investigate TAN. Volatile inorganic compounds (e.g., halides or oxides) were investigated, and their adsorption behavior on different surfaces (usually quartz) was determined. For recent reviews see e.g., Refs. [10-12]. For several reasons, such as low production cross-sections, short half-lives, but also technical challenges, more sophisticated chemical studies have not been possible. One restriction in present TAN research is the plasma behind the target caused by the intense heavy ion beam. Any "weak" molecule (e.g., organic ligands) is immediately destroyed, thus limiting the possibilities of synthesizing chemical compounds directly behind the target to a few "simple" and robust inorganic compounds. It would be highly desirable to expand the knowledge on the chemical behavior of the TAN to classes of compounds that have not been investigated so far, e.g., volatile complexes or organometallic compounds. The use of a physical pre-separator, e.g., the Berkeley Gas-filled Separator (BGS) [13,14] allows separating the beam from the desired TAN isotopes, thus making such studies possible. The BGS is currently the only device worldwide that is used as a pre-separator for chemistry experiments and its power was recently demonstrated in liquid-liquid extraction experiments with Rf [15] but also in extraction studies with short-lived isotopes of lighter homologs [16]. With the beam separated in the BGS, less robust molecules can be introduced directly into the gas volume where nuclei recoiling from the BGS are thermalized. Therefore, it appears possible to form volatile organometallic compounds or metal complexes of TAN in-situ in the so called recoil-transfer-chamber (RTC) [17]. Theses species can then be rapidly transported to a chromatography setup and detection system.

Volatile β-diketonate metal complexes

A compound class that appears suitable for such studies are the β-diketonates, i.e., coordination compounds of a metal with ligands of the general structure shown below:

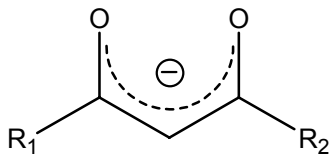

The β-diketonate anions are well known to act as bidentate ligands forming neutral complexes some of which can be transferred to the gas phase without decomposition. It has been experimentally observed that the introduction of fluorine (F) atoms to the system significantly enhances the volatility [18,19]. Therefore the trend in volatility (or sublimation enthalpy, ΔH_{sub}) for 2,4-pentanedionates (acetylacetonates, acac; R_1=R_2=CH_3), 1,1,1,-trifluoro-2,4-pentanedionates (1,1,1-trifluoroacetylacetonates, tfa; R_1=CF_3; R_2=CH_3) and 1,1,1,5,5,5-hexafluoro-2,4-pentanedionates (1,1,1,5,5,5-hexafluoroacetylacetonates, hfa; R_1=R_2=CF_3) is generally given as:

$$\Delta H_{sub}[M(acac)_n] > \Delta H_{sub}[M(tfa)_n] > \Delta H_{sub}[M(hfa)_n].$$

Recently, Ono et al. studied the behavior of ^{252}Cf fission products that were combined with another β-diketone anion, 2,2,6,6-tetramethyl-3,5-heptanedione (dipivaloylmethane dpm; R_1=R_2=$C(CH_3)_3$) in isothermal gas chromatography experiments and observed the selective formation of volatile Ru and Rh compounds [20]. Greulich and co-workers reported on the successful separation of nine lanthanide elements and yttrium in the form of hfa complexes using gas chromatography [21]. The fractional sublimation of ^{86}Zr and ^{87m}Y as fluorinated β-diketonate complexes as an example of the separation of radioisotopes is also reported [19]. In studies of β-diketonates of Sc, Yb, and Hf using carrier-free isotopes produced simultaneously in heavy-ion induced fusion reactions, Fedoseev and coworkers demonstrated that single molecules of Hf-hfa complexes deposited at temperatures below 100°C in a temperature gradient tube [22]. However, no separation of the three elements could be achieved. This may also be the case for different nuclides formed in nuclear reactions. However, by employing a physical pre-separator this should no longer be a problem, since transfer products are strongly suppressed by the BGS. We therefore envisaged to use the hfa system for first studies of a volatile metal complex.

Experimental / Results

Our studies are directed towards an experiment with the lightest TAN, Rf, since ^{257}Rf ($T_{½}$=4.7 s) can be produced at a relatively high rate of 1-2 atoms/s at the BGS [15]. A natural first step towards an experiment with a transactinide is the investigation of its lighter homologs, i.e., Zr and Hf for group 4.

Production of short-lived Zr and Hf isotopes using a heavy ion cocktail

To rule out the role of differing experimental conditions in the measurement of chemical properties, it is desirable to investigate isotopes of several homologs simultaneously. Due to their different magnetic rigidities, BGS cannot forward them to the chemistry setup simultaneously. The next best approach is to switch quickly between short-lived isotopes of these elements without having to open the chemistry setup. This can be achieved when they can be produced in heavy-ion induced fusion reactions employing

beams of similar A/q and E/A which can be generated simultaneously in the cyclotron. This technique is referred to as a heavy-ion cocktail and already employed at the 88 inch cyclotron [23]. In first experiments, short-lived Zr and Hf isotopes were produced by using a cocktail of $^{18}O^{4+}$ and $^{50}Ti^{11+}$ with E/A~4.5 MeV/n and their magnetic rigidities (Bρ) in dilute He were measured. Three different Sn targets ($^{116,120,124}Sn$) and a ^{nat}Ge target were mounted on a target ladder installed at the irradiation position of the BGS allowing for quick switching from Zr to Hf production.

Formation and observation of volatile hfa compounds of Hf

A schematic of the experimental setup is shown in the following Figure:

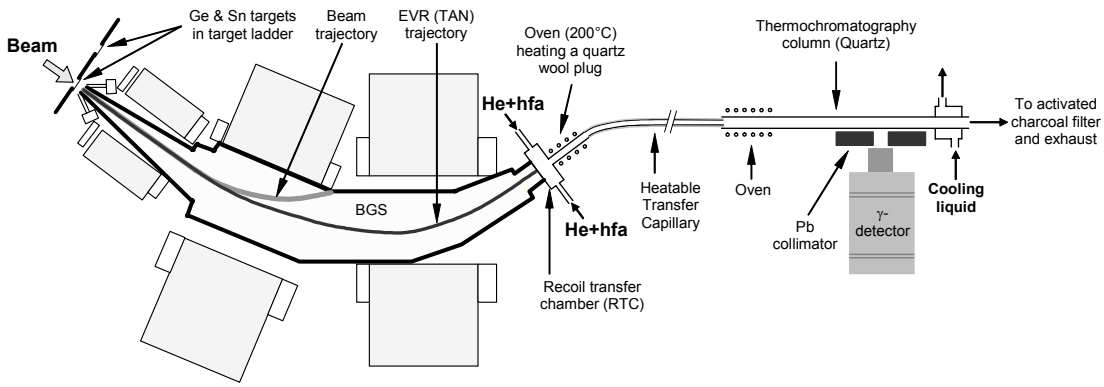

The beam delivered by the 88 inch cyclotron induces nuclear reactions in the target at the irradiation position. The beam is deflected using the BGS and does not reach its exit. The evaporation residues (EVR) enter the RTC through a thin Mylar window and are thermalized in the RTC. hfa-enriched He is introduced into the RTC and it transports the EVRs to a nearby oven kept at an elevated temperature. In first experiments, the formation of a volatile compound of Hf was observed when hfa was present in the carrier gas, while no Hf was transported out of the RTC in a pure He gas flow. In irradiations of $^{120,124}Sn$ with ^{50}Ti, ^{165}Hf ($T_{1/2}$: 76 s) and $^{168-170}Hf$, respectively, were observed in an activated charcoal catcher mounted at the exit of the RTC.

Outlook

The next on-line experiments will aim at a thermochromatographic (TC) [24] investigation of the formed compounds. Since hfa complexes are known to be relatively stable [18,19], it should be possible to transport them through a capillary kept at an elevated temperature to an on-line TC apparatus. This apparatus consists of an open quartz column along which a longitudinal negative temperature gradient is established. The distribution of the radionuclides along the gradient will be measured with a γ-detector. Using a lead collimator allows for achieving a spatial resolution of one centimeter. These experiments are under way. Parallel to the on-line studies, complementary experiments with macroamounts of Zr and Hf as well as off-line TC studies using long-lived radionuclides are being performed. First results will be reported at the conference.

Conclusion

With the planned synthesis of a new class of compounds of TAN, namely volatile coordination complexes, a more thorough investigation of their chemical properties becomes possible. These results

are complementary to those gained in past gas chemical studies as well as those in aqueous phase and will help elucidating the influence of relativistic effects in the chemistry of the heaviest elements. The validity of the periodic table in the region of the heaviest elements is still a fundamental question that cannot be fully answered at the moment, and predictions concerning even heavier elements are controversial. Future studies could then also include heavier TAN since the basic experimental system appears to be relatively easily adaptable to other similar chemical systems.

Acknowledgments

Fruitful discussions with W.W. Lukens are gratefully acknowledged. We thank the staff of the 88-inch cyclotron and the ion source team for the production of the O/Ti-cocktail beam. This work was supported by the Swiss National Science Foundation and the Office of Science, Office of High Energy and Nuclear Physics, of the U.S. Department of Energy.

References

[1] K.S. Pitzer, J. Chem. Phys. **63**, 1032 (1975).
[2] V.G. Pershina, Chem. Rev. **96**, 1977 (1996).
[3] Ch.E. Düllmann *et al.* Nature **418**, 859 (2002).
[4] A. von Zweidorf *et al.* Gesellschaft für Schwerionenforschung mbH, Sci. Rep. 2002: Darmstadt, 2003-1, ISSN 0174-0814, p. 175; and contribution to this conference.
[5] A.B. Yakushev *et al.* Radiochim. Acta **89**, 743 (2001).
[6] A.B. Yakushev *et al.* Radiochim. Acta **91**, 433 (2003).
[7] S. Soverna *et al.* contribution to this conference.
[8] A. Türler, J. Alloys Comp. **271-273**, 287 (1998).
[9] J.V. Kratz *et al.* Radiochim. Acta **48**, 121 (1989).
[10] A. Türler, Radiochim. Acta **72**, 7 (1996).
[11] H.W. Gäggeler, Proc. *Robert A. Welch Foundation, 41st Conference on Chemical Research, The Transactinide Elements;* The Robert A. Welch Foundation: Houston, 1997; p. 43.
[12] M. Schädel, J. Nucl. Radiochem. Sci. **3**, 113 (2002).
[13] V. Ninov *et al.* ENAM98, edited by B. M. Sherrill, D. J. Morrissey, and C. N. Davids (AIP, Woodbury, 1999) p. 704.
[14] K.E. Gregorich *et al.* J. Nucl. Radiochem. Sci **1**, 1 (2000).
[15] J.P. Omtvedt *et al.* J. Nucl. Radiochem. Sci. **3**, 121 (2002).
[16] R. Sudowe *et al.* contribution to this conference.
[17] U.W. Kirbach *et al.* Nucl. Instrum. Meth. **A484**, 587 (2002).
[18] R.E. Sievers *et al.* Inorg. Chem. **2**, 693 (1963).
[19] R.E. Sievers *et al.* Science **201**, 217 (1978).
[20] S. Ono *et al.* J. Radioanal. Nucl. Chem. **255**, 571 (2003).
[21] N. Greulich *et al.* Fres. Z. Anal. Chem. **323**, 839 (1986).
[22] E.V. Fedoseev *et al.* J. Radioanal. Nucl. Chem., Lett. **119**, 347 (1987).
[23] D. Leitner *et al.* LBNL-Report 51451 and Proc. *15th Int. Workshop on ECR Ion Sources*, ECRIS02, Jyväskylä, Finland, June 12-14, 2002, p.183.
[24] I. Zvara, Isotopenpraxis **26**, 251 (1990).

Simultaneous measurement of volatility of Zr, Hf and Rf

T. Kaneko[1], K. Tsukada[2], K. Akiyama[2], M. Asai[2], H. Haba[3], A. Toyoshima[4], S. Ono[1], T. Hirai[1], S. Goto[1], S. Ichikawa[2], Y. Nagame[2], H. Kudo[1]

[1] Niigata University, Japan
[2] JAERI, Japan
[3] RIKEN, Japan
[4] Osaka University, Japan

hkudo@sc.niigata-u.ac.jp

Rutherfordium belongs to the group-4 elements as Zr and Hf. It is well known that the chemical properties of Zr and Hf very resemble with each other and halides of these elements are volatile. From the relativistic calculations $RfCl_4$ is predicted to be more volatile than $ZrCl_4$ or $HfCl_4$ [1-3], whereas from the extrapolation, exactly the opposite trend is expected [4,5]. In this special case, the predictions about the relative volatility of $RfCl_4$ compared to $ZrCl_4$ and $HfCl_4$ can be directly tested experimentally in a gas phase.

Türler et al. investigated the volatility of the Hf- and Rf- chlorides with OLGA II [6,7]. They showed that the volatility of the chlorides of the group-4 is very similar among them. Later, HEVI system was developed by Kadkhodayan *et al*. [8] and the volatility of the Zr, Hf and Rf chlorides was investigated. The result shows that the order of volatility is $RfCl_4 > ZrCl_4 > HfCl_4$ [9]. However, each chloride was studied in a separate experiment, so that chemical conditions may have been different among the experiments. And the reported correlation is not consistent that expected from the sublimation enthalpies of Zr and Hf. Türler *et al*. [10] investigated the volatility of the Hf- and Rf- chlorides again, and they showed $RfCl_4 > HfCl_4$ in volatility but did not discuss about Zr chloride.

In the present work, in order to clarify the above mentioned ambiguity, the investigation for volatility of Zr, Hf and Rf chlorides was performed under the identical conditions.

The isothermal chromatographic apparatus consists of a reaction chamber, an isothermal column, and a re-clustering chamber. Each section is made by quartz and connected in a series. The isothermal column is a spiral tube with the 2000 mm long and 3 mm inner diameter. The reaction chamber and the isothermal column were heated independently up to a maximum temperature of 1200° C by electric furnaces.

In order to investigate the isothermal gas chromatographic behavior of Zr, Hf and Rf in the same condition, an irradiation for the production of Zr, Hf and Rf isotopes were performed at the same time at the JAERI 20-MV Tandem accelerator. A target chamber and an irradiation setup are shown in Fig. 1. ^{85}Zr was produced by the ^{nat}Ge(^{18}O, xn) reaction. ^{167,169}Hf were produced by the $^{152\ enriched}$Gd(^{18}O, xn) reaction and ^{261}Rf was produced by the ^{248}Cm(^{18}O, 5n) reaction.

Produced activity is transported from the target chamber to the gas chemistry apparatus via He/KCl gas-jet transport system. The activity-laden aerosols were transported by the helium through a 2.2 mm i.d. stainless steel tube to the gas chromatography apparatus. The stainless steel capillary was employed in order to eliminate any exchange of oxygen through the capillary walls. The concentration of residual oxygen was monitored with the oxygen monitor and was less than 30 ppm for experiment. Domanov *et al*. observed that in gas chromatography experiments the transportation of Zr and Hf chlorides could not be affected by oxygen in this order of amounts [11]. As a chlorinating agent, a mixture of chlorine gas and carbon tetrachloride vapor was used. Chemical reaction took place in the reaction room at 1000° C. The chemically separated species were attached to new KCl aerosol, and transported for α measurement to the detection system MANON [12], which is a rotating wheel detection system with a 80 cmϕ wheel, 80 collection positions, and six pairs of Si PIN photodiodes. The activity-laden aerosols were deposited on a

polyethylene terephthalate foil of 120 μg/cm² in thickness and 20 mm in diameter. Each sample was collected for 30 s and measured for 180 s.

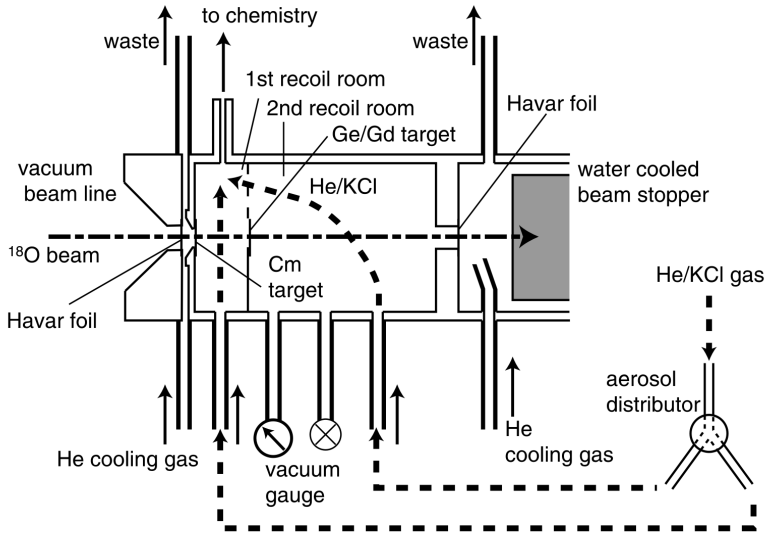

Figure 1. Schematic of the target chamber utilized for simultaneous production of Zr, Hf and Rf isotopes.

The obtained α spectrum is depicted in Fig. 2. The spectrum is dominated by α-lines from the contaminants ^{211}Bi and ^{211m,212m}Po which also form volatile chlorides. Due to the much effort to prevent Pb contamination, the level of background α-particles from them was reduced compared with those by Kadkhodayan *et al* [9]. The α-particle group of 8.00-8.40 MeV was assigned to ^{261}Rf ($T_{1/2}$=78 s) and its daughter ^{257}No ($T_{1/2}$=26 s).

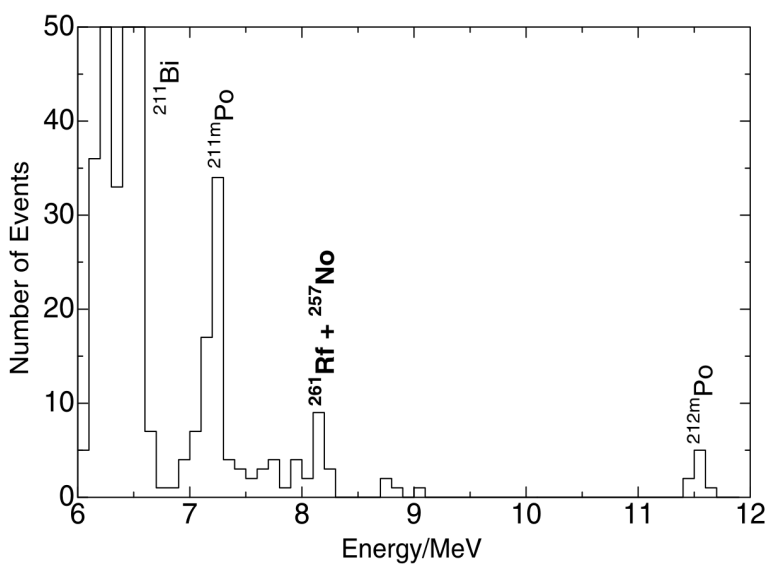

Figure 2. α spectrum after chemical separation.

In Fig. 3 the measured yields of the 8.00-8.50 MeV α-particle group, that of the 454 keV (^{85}Zr) and of 493 keV (^{169}Hf) are shown as a function of the temperature of the isothermal column. At the isothermal temperature of 300° C, a part of Zr, Hf and Rf chlorides were transported to the outlet of the isothermal column. The yield of Zr, Hf and Rf chlorides increased rapidly with the increase of the isothermal temperature, and reached the maximum around 350° C. This rapid change of yield with column temperature is characteristic of the simple adsorption-desorption transport mechanism [13]. Furthermore, since oxygen concentration was kept at less than 30 ppm in the system, it was not considered that the oxychlorides would be concerned with chromatographic transportation [11]. Therefore, it was concluded that the volatile compounds of these three elements would be the tetrachlorides and that they would behave very similar to each other.

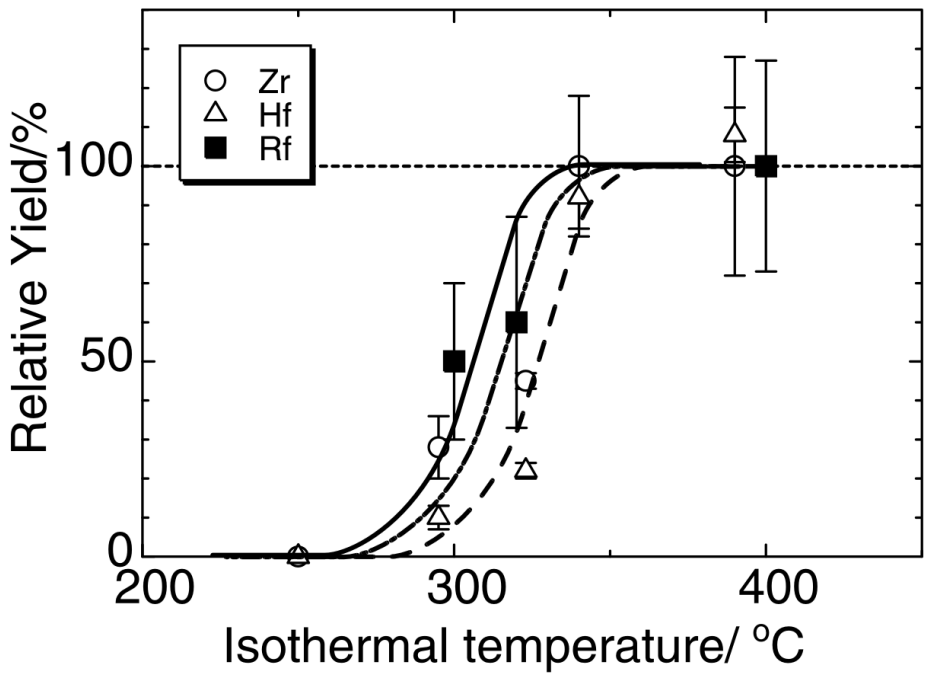

Figure 3. Relative yield curves for ^{85}Zr-, ^{167}Hf- and ^{261}Rf-chlorides. The lines are calculated yield curves from a Monte Carlo simulation.

It should be mentioned that after prolonged gas chemistry experiments in the present work, the quartz surface of the chromatography column is partially coated with a thin layer of KCl, which means that of the chromatography was performed on KCl rather than on SiO_2. As a volatility measurement is strongly dependent on the column surface, we cannot directly compare the present results to those of others. However, relative comparison among the elements is supposed to be reasonable. In this work, Zr and Hf were examined simultaneously, and it was found that the volatility of their chlorides was similar with each other. This result agrees with to the expectations from macro scale chemistry. Since Rf chlorides behaved similarly with Zr and Hf on this surface, it is expected that Rf chlorides would have similar volatility. An adsorption enthalpy was calculated using a Monte Carlo simulation based on a microscopic model [14-16] and the following adsorption entalpies for the group-4 chlorides were obtained for partially KCl coated quartz surfaces: Zr: -118 ± 6 kJ/mol, Hf: -116 ± 6 kJ/mol and Rf: -112 ± 10 kJ/mol. $ZrCl_4$ and $HfCl_4$ were found to have very similar adsorption enthalpies. This tendency is consistent with the results for NaCl surface [17,18].

References

[1] V. S. Nefedov *et al*. Radioanal. Nucl. Chem. Articles, , 103 (1990).
[2] V. Pershina, and B. Fricke, J. Phys. Chem. **98**, 6468 (1994).
[3] M. V. Ryzhkov, V. A. Gubanov, and I. Zvara, Radiochim. Acta **57**, 11 (1992).
[4] A. Türler *et al*. PSI Annual Report 1994, Annex IIIA, 77 (1995).
[5] A. Türler *et al*. PSI Annual Report 1994, Annex IIIA, 76 (1995).
[6] H.W. Gäggeler *et al*. Nucl. Instr. Meth. **A309**, 201 (1991).
[7] A. Türler *et al*. J. Radioanal. Nucl. Chem. Art. **160**, 327 (1992).
[8] B. Kadkhodayan *et al*. Nucl. Instr. Meth. **A317**, 254 (1992).
[9] B. Kadkhodayan *et al*. Radiochim. Acta **72**, 169 (1996).
[10] A. Türler *et al*. J. Alloys. Comp. **271-273**, 287 (1998).
[11] V. P. Domanov and K. U. Zin, Sov. Radiochem. **31**, 160 (1989).
[12] M. Asai *et al*. Radiochim. Acta, , 733 (2001).
[13] A. Vahle *et al*. Radiochim. Acta **84**, 43 (1999).
[14] I. Zvara, Radiochim. Acta **38**, 95 (1985).
[15] A. Türler, Radiochim. Acta **72**, 7 (1996).
[16] D. C. Hoffman *et al*., PSI Progress Report 1991, Annex III, 68 (1992).
[17] J. Rudolph and K. Bächman. J. Chromatogr. **178**, 459 (1979).
[18] J. Rudolph and K. Bächman. J. Chromatogr. **187**, 319 (1980).

Electrochemistry at the tracer scale - an approach to aqueous superheavy element chemistry

H. Hummrich[1], U. Rieth[1], J.V. Kratz[1], G. Lehr[1], M. Mendel[1], P. Thörle[1]

[1] Institut für Kernchemie, Johannes Gutenberg-Universität Mainz, Germany

JVKratz@mail.kernchemie.uni-mainz.de

Due to the recent successful gas-phase experiments with hassium [1, 2] and element 112 [3] the focus of aqueous heavy element chemistry shifted also in that region of the periodic table. Theoretical predictions by Fricke et al. [4] suggest, that the superheavy elements 112-118 have a noble metal character. These predicted properties led to an electrochemical approach for first aqueous studies of the superheavy elements. The electrochemical deposition of tracer amounts on a metal surface usually does not lead to a complete coverage of the electrode. Such sub-monolayer electrodepositions cannot be described by the Nernst equation and may take place at more negative (overpotential deposition, opd) or at more positive potentials (underpotential deposition, upd), depending on the properties of tracer and electrode material. Using macroscopic thermodynamic models, Eichler et al. proposed a modified Nernst equation to describe the electrodeposition of tracer amounts on a given electrode material [5]. They calculated potentials for the deposition of 50% of the tracer ion on a foreign electrode material. In an earlier work, $E_{50\%}$-values of the elements 112-116 were predicted on the basis of relativistic Dirac-Slater calculations [6]. Pd- and Pt-systems have the highest $E_{50\%}$-values and should be preferable electrode materials for electrodeposition experiments. To design an electrochemical deposition experiment for super-heavy elements, we have to investigate how the predicted $E_{50\%}$-values correspond to experimental upd-potentials for the homologs of the elements 112-116 and if a spontaneous deposition of the tracer is possible. Furthermore, we have to figure out what kind of electrode pretreatment is necessary to achieve a clean surface and - due to the very short half-lives of the superheavy isotopes - how a quantitative electrochemical deposition can be performed in a very short period of time. In the first batch experiments with the lighter homologs of the superheavies, we kept our focus on lead (homolog of 114) and polonium (homolog of 116) because carrier free trace amounts of those elements were easy to obtain. ^{212}Pb was obtained via electrostatic gas phase collection of the decay products from a ^{220}Rn emanating source (^{228}Th co-precipitated with Zr-Stearate), whereas ^{210}Po was extracted from irradiated bismuth by ion-exchange chromatography. Already the first experiments, especially with lead, showed, that the spontanous electrodeposition is a relatively slow, diffusion controlled process. Therefore, we continued the work on two different paths. The lead experiments were now performed under a controlled potential using standard electrochemistry equipment. The polonium studies, on the other hand, continued to look into the involved parameters for the spontanous deposition. Reproducible results in electrochemical experiments can only be achieved by using electrodes with very clean surfaces. To get such electrodes, a first procedure was established, where the electrodes (metal foils) are cleaned by heating under an argon/hydrogen (95:5) atmosphere at about 700K to remove oxides from the surface. Using a 0.1M HCl solution of ^{210}Po, a series of experiments on the spontanous electrodeposition of Po has been performed. During these studies a range of parameters was varied. The experiments used Cu, Ag and Ni in form of 6x6mm foils as electrode materials. These foils were introduced into a small electrochemical cell with a volume of only 200µl [7].To get information about the influence of the solvent and its dielectric properties on the deposition process, mixtures of ^{210}Po in 0.1M HCl with organic solvents (acetone, dioxane) were used. To assure a maximum ion motion towards the electrode, the cell was heated to 340K and treated with ultrasound. In these experiments, relatively long reaction times of 5min and 1min were chosen. The determination of the amount of deposited Po was performed by α-spectroscopy.

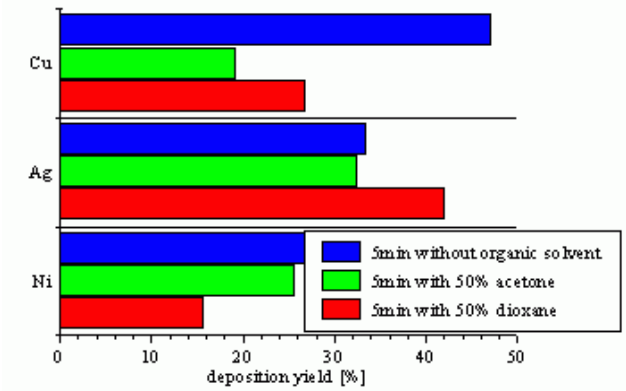

Fig.1: Deposition yields of Po-210 from 0.1M HCl on Cu, Ag and Ni

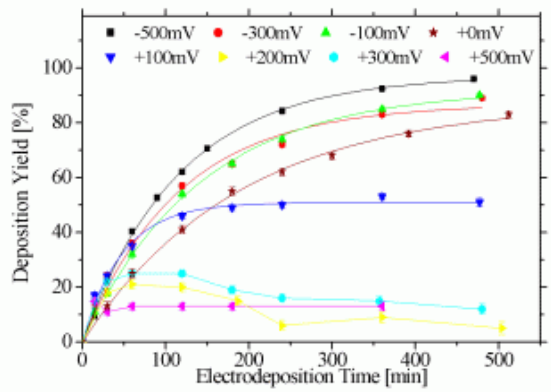

Fig.2: Electrodeposition of Pb on a Pt-electrode in 0.1M HCl vs. time at different potentials

The measured deposition yields (figure) did not show any clear trend with respect to the variation of the reaction time and the change in solvent characteristics. This result can only be attributed to variations in the properties of the electrode surface. Thus, the used cleaning process might still be not sufficient to get reproducible results. As an alternative cleaning process, an electrochemical treatment will be used, where the electrode is cleaned by a quick electrolysis process. After that, it will be stored in a solution of the electrolyte used in the later experiments. This process should prevent the surface from being exposed to air and therefore from being contaminated with oxygen and aerosol particles. Hevesy and Paneth defined the "critical potential" E_{crit} as the potential, at which electrodeposition of a radiotracer on a metal electrode first occurs [8]. Obviously, measured E_{crit}-values should be similar to the predicted $E_{50\%}$-values. To determine the critical potential of the Pb-upd on Pt electrodes, we used a potentiostatic three-electrode-system with a Ag/AgCl (3M KCl) reference electrode, a Pt working electrode, and a Pt counter electrode. The area of the working electrode was 2cm², the total volume of the 0,1M HCl electrolyte solution was 20ml. For agitation, we applied a constant nitrogen flow. Prior to the experiment, the working electrode was electrochemically cleaned. To determine the deposition yield of ^{212}Pb vs. the electrodeposition time without disturbing the system, we measured the decrease of the activity in the solution by γ-spectrometry. The experiment was repeated at different electrode potentials. According to Joliot [9], the electrodeposition rate of a radiotracer is described by

$$dN_{dep}/dt=DF_E/\delta V*(kN_{tot}-N_{dep}). \quad (1)$$

After integration, a relation between the deposition yield N_{dep}/N_{tot} and the reaction time is obtained

$$N_{dep}/N_{tot}=k-k*\exp(-DF_E/\delta V). \quad (2)$$

Here, N_{dep} is the amount of atoms deposited, N_{tot} is the total amount, D is the diffusion coefficient, F_E is the electrode surface, δ is the Nernst diffusion layer and V the volume of the solution. The term k represents the maximum deposition yield that can be reached for the given potential E. In the experiment, we obtain a relation between the deposition yield and the electrodeposition time (Fig.2). After fitting with equation 2, we get the maximum deposition yield k for each potential E (Fig.3). The critical potential E_{crit} for the deposition of Pb on Pt from 0.1M HCl is about +190mV. This value corresponds roughly to the critical potential of +255mV for the deposition of Pb on Pt in 1N HNO_3 measured by Ziv et al. [10]. The predicted $E_{50\%}$-value of +10mV [5] is somewhat lower than the measured E_{crit}-value, but the difference gets smaller if compared with the potential at which the maximum deposition yield is 50% (approx. +100mV).

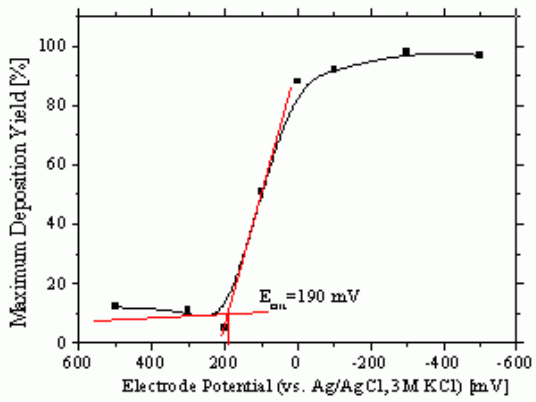

Fig.3: E_{onset} for the Pb-upd on Pt-electrodes in 0.1M HCl

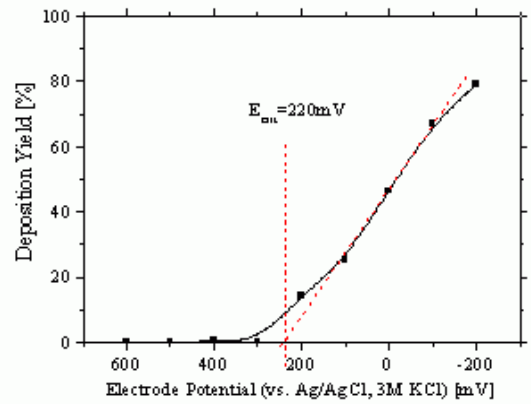

Fig.4: E_{onset} for the Pb-upd on Pd-electrodes in 0.1M $HClO_4$

According to equation (1), the electrodeposition rate dN_{dep}/dt increases with F_E/V. As a consequence, we reduced the dimensions of the electrolytic cell to a total volume of 150µl and an electrode surface of 0.36cm². The deposition rate also depends on the thickness of the Nernst diffusion layer. To keep it low, we agitated the solution with a magnetic stirrer. As reference electrode, we used a micro-Ag/AgCl-electrode. In this experiment, we used Pd as electrode material, and the electrolyte was 0.1M $HClO_4$. Compared to the "macro-expriment" described above, the electrodeposition rate increased - as calculated - by a factor of 24. After 10 minutes, the deposition yield is near to its maximum possible value. After the deposition, the electrode was removed while under current, washed with water and measured on a γ-detector. No activity was lost during the washing process. Fig.4 shows, that no activity is deposited until the critical potential of about +220 mV is reached. From this point on the deposition yield increases with the applied potential. The critical potential we determined in the Pb/Pd-system is similar to that in the Pb/Pt - system. However, a remarkable difference between the two systems is, that the deposited activity can be easily removed from Pt-electrodes by mineral acids, but not from Pd-electrodes. In future experiments, we will further improve the electrolytic cell dimenstion to obtain reaction times in the range of seconds. For online experiments at the Mainz TRIGA reactor and at GSI, an automated apparatus using a tape technique to provide the electrode material is planned. This device will combine the electrode cleaning step, the electrochemistry step, and the detection system.

References

[1] Ch. E. Düllmann et al., Nature **418**, 859 (2002).
[2] A. von Zweidorf et al., GSI Scientific Report 2002, 175 (2003), see also A. von Zweidorf et al., contribution to this Conference.
[3] S. Soverna et al., contribution to this Conference.
[4] B. Fricke, Structure and Bonding **21**, 89 (1975).
[5] B. Eichler, J.V. Kratz, Radiochimica Acta **88**, 475 (2000).
[6] B. Eichler, H. Rossbach, GSI-tr-89-17 (1989).
[7] U. Rieth et al., Annual Report 2001, IKMz 2002 - 1, A12 (2002).
[8] G. v.Hevesy, F. Paneth, Monatshefte **36**, 45 (1915).
[9] F. Joliot, J. Chim. Phys. **27**, 119 (1930).
[10] D.M. Ziv, G.M. Sukhodolov, V.F. Fateev, L.I. Lastochin, Radiochemistry **8**, 182 (1966).

Ion exchange and extraction chromatographic studies with homologs of seaborgium (element 106) in HNO_3-HF medium

P. Mohapatra[1], R. Tripathi[1], J.V. Kratz[2], A. Kronenberg[2], B.S. Tomar[1], A.V.R. Reddy[1], G. Pfrepper[3]

[1] BARC, India
[2] Institut für Kernchemie, Universität Mainz, Germany
[3] Germany

mpatra@magnum.barc.ernet.in

The experiments to understand the chemical behaviour of transactinides such as Rutherfordium (Element 104) and Seaborgium (Element 106) are of considerable interest from basic chemistry point of view. ^{261}Rf and ^{265}Sg have been produced by heavy ion reactions using intense beams of O-18 and Ne-22 on ^{248}Cm target, respectively [1]. Due to their short half lives ($t_{1/2}$ of ^{261}Rf and ^{265}Sg are about 78 s and 34 s, respectively) and limited availability of accelerator beam time for such exotic experiments, it is relevant to develop separation methods using their homologs such as Zr, Hf, (for Rf), Mo and W (for Sg) and pseudo-homologs viz. Th (for Rf) and U (for Sg) for utilization as a guide line for the actual experiment.

Rapid radiochemical separation methods involving Multi-Column Technique (MCT) have been used for the studies on the chemical properties of trans-actinides involving experiments in HNO_3 + HF medium using anion exchangers such as DOWEX 1x8. However, the K_d values of homologs like Mo and W were found to be too high when DOWEX 1x8 resin was used suggesting the need for weaker anion exchangers. The present work is an attempt in that direction where several other anion exchangers with different functional groups have been used along with an extraction chromatographic material made from Aliquat 336, a liquid anion exchanger, in chloroform.

As reported earlier, the contrasting K_d values obtained at 0.01 M HF and 0.1 M HNO_3 are made use of in a proposed scheme for the studies on the chemistry of Sg [2]. Table 1 lists the K_d values for Mo and W with three different anion exchange resins viz. DOWEX 1x8 (with – methyl group), HS 36 (with – ethyl group) and HB 36-I/92 (with – n-butyl group). The batch distribution data are obtained in the 0.1 M nitric acid as well as HCl in the presence of 0.01 M HF. As shown in the following table, the K_d values are significantly larger for the HCl medium as compared to the HNO_3 medium. This can be ascribed to two reasons, first, the chloro complexes are more easily formed than nitrate complex and second, the nitrate ion acts as a better counter anion. As shown in Table 1, the K_d values at 0.1M HNO_3 + 0.01M HF show a decreasing trend of Dowex 1x8 > HS 36 > HB 36-I/92 for Mo, while an opposite trend is observed for W. On the other hand, at 0.1M HCl + 0.01M HF, the trend for both Mo and W is Dowex 1x8 > HS 36 < HB 36-I/92. The results of the ARCA experiments carried out on-line with the accelerator produced ^{170}W have indicated reasonable agreement with those from the batch studies mentioned above.

Table 1. Effect of resin type on the Kd values of Mo and W

Conditions	Mo			W		
	DOWEX 1x8	HS 36	HB 36-I/92	DOWEX 1x8	HS 36	HB 36-I/92
0.1M HNO_3 + 0.01M HF	89	15	5.7	5.0	13	16
0.1M HCl + 0.01M HF	181	40	732	96	46	70

In spite of using three different functionalized ion-exchangers, it was not possible to obtain an experimental condition for which the K_d values of Mo and W fall in the range of 10-50. An extraction chromatographic material was prepared using Aliquat 336 (tri-caproyl methyl ammonium chloride) in chloroform sorbed onto chromosorb W. Figure 1 shows the results obtained with the extraction chromatographic studies carried out at varying concentration of HF at a fixed concentration (0.1M) of nitric acid using Mo and W tracers. It is interesting to note that the sorption of Mo and W onto the extraction chromatographic resin material is significantly high at lower HF concentration. It is attributed to the presence of anionic oxo complexes like MoO_4^{2-} and WO_4^{2-}. The decrease in the K_d values with increasing HF concentration in the case of Mo and W could be explained on the basis of the formation of neutral complexes such as MoO_2F_2 and WO_2F_2. On further increasing the HF concentration, the K_d values of W showed an upward trend while no such trend was seen with Mo. This is explained on the basis that though both the hexavalent Mo and W form anionic fluoride complexes, it is more favorably and readily formed for the latter [2]. The V-shape curve for W was observed earlier when DOWEX 1x8 was used as the ion exchanger [3]. The interesting aspect observed during these studies was that the K_d values are such that (Mo: 45 and W : 18 at the aqueous phase composition of 0.1M HNO_3 + 0.01M HF) experiments with ^{265}Sg can be carried out conveniently. These are much lower than the values obtained with DOWEX 1x8 suggesting that the Aliquat 336 loaded chromatographic material can be an ideal choice for the chemical studies involving ^{265}Sg.

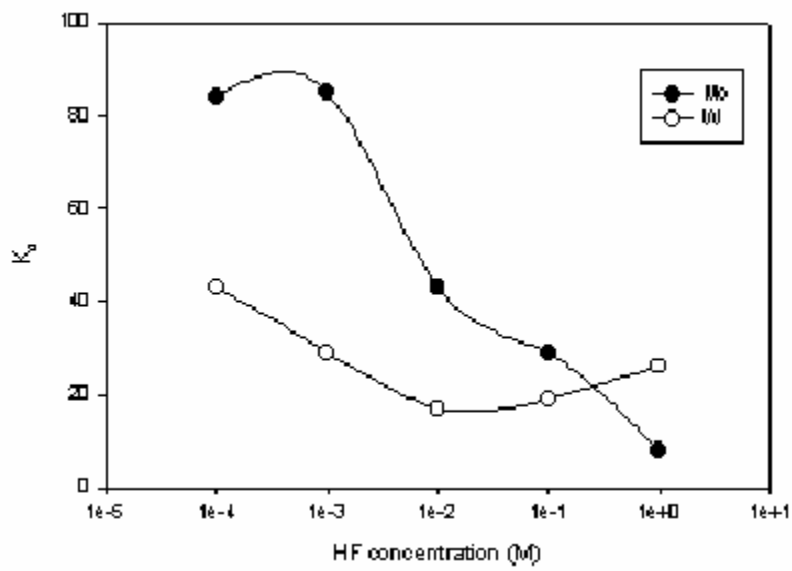

Figure 1. Distribution of Mo and W as a function of HF concentration at 0.1 M HNO_3. Resin: Aliquat 336 sorbed on chromosorb.

References

[1] J.V. Kratz; 'Chemical Properties of the Transactinide Elements', in "Heavy Elements and Related New Phenomena" Vol. 1, R. Greiner and R.K. Gupta (Eds), World Scientific (1999).

[2] M. Schaedel *et al.* Radiochim. Acta **77**, 149 (1997).

[3] P.K. Mohapatra, A. Kronenberg, J. V. Kratz, G. Pfrepper and R. Pfrepper, (Manuscript under preparation)

A liquid-liquid extraction system suitable for studying the chemistry of rutherfordium with SISAK

D. Poláková[1], G. Skarnemark[2], J. Alstad[1], L. Stavsetra[1], L. Zheng[1], J.P. Omtvedt[1]

[1] University of Oslo, Norway
[2] Chalmers University of Technology, Sweden

darina.polakova@kjemi.uio.no

Introduction

A general presentation of the on-line liquid-liquid extraction system SISAK is given in another presentation to the TAN'03 conference (J.P. Omtvedt and coworkers). The presentation given here describes a system suitable for the investigation of the chemistry of rutherfordium. This work is in progress, and *the results presented are preliminary*.

In 2000 and 2001 a pilot SISAK chemistry-experiment with the transactinide rutherfordium was performed at the Lawrence Berkeley National Laboratory (LBNL) in Berkeley, USA. In this experiment it was proved that it was possible to extract and detect the ~4 s transactinide ^{257}Rf with SISAK [1].

The ^{257}Rf activity was produced with a 235 MeV $^{50}Ti^{12+}$ beam from the LBNL 88-inch cyclotron hitting a rotating ^{208}Pb target. The recoils from the target were separated in the Berkeley Gas-filled Separator (BGS). After this, the recoils were transferred from the BGS focal plane into a gas jet by using a then newly constructed Recoil Transfer Chamber (RTC). The activity is transported to the SISAK system with a gas jet. First, in the degasser step, the activity is transferred from gas phase to an aqueous phase, then the activity is extracted with a suitable extraction agent into the organic phase. By carefully selecting the conditions and extraction agents, properties like valence state, charge state, the number and type of ligands can be investigated. The extracted rutherfordium (in the organic phase) is then mixed with a scintillator cocktail and pumped through Liquid Scintillation (LS) detectors. The amount of rutherfordium remaining in the aqueous state can currently not be measured, but must be calculated from measurements of how much activity is entering the SISAK system. An overview of the complete setup is shown in Fig. 1.

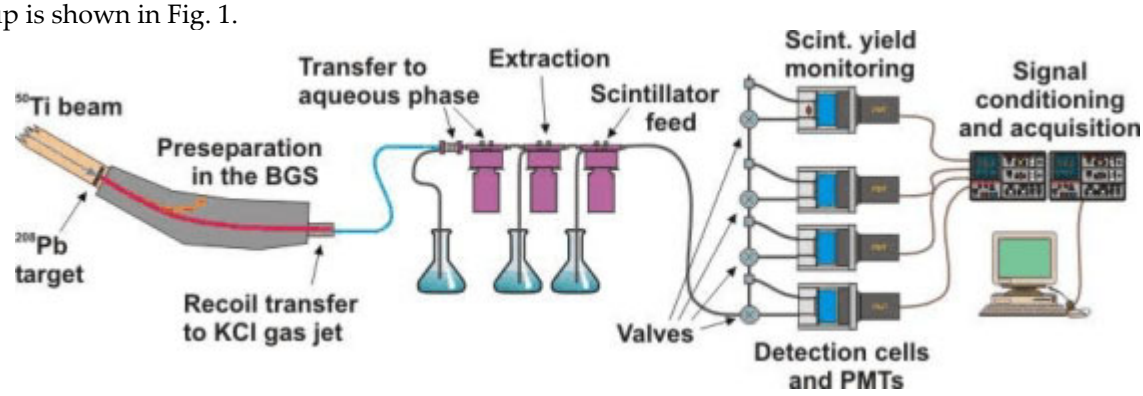

Figure 1. Overview of the complete SISAK setup for transactinide experiments.

As reported in one of our other TAN'03 contributions (J.P. Omtvedt and coworkers), the chemistry system (extraction with dibutyl-phosphate from nitric acid) used in the 2000 and 2001 experiments was not found suitable for detailed chemistry studies of Rf. Therefore the still on-going work reported here was initiated to find a suitable system for investigation of the liquid-phase chemistry of Rf with SISAK.

Search for a suitable extraction systems for Rf experiments

A chemical system, i.e. the concentration and flow rates of the reagents, and the solvents used, must meet a number of criteria to be suitable for a SISAK type of chemical investigation of transactinides:

1. Good separation of Zr and Hf. This is because it is of interest to be able to classify the behaviour of rutherfordium as either Zr or Hf like.
2. No adverse effects (like adsorption) between the chemicals used and the construction material of the SISAK equipment.
3. The complexation and extraction rates must be fast. The contact time between the two liquid phases is between 0.5 and 0.1 s. Therefore the reaction rate must be fast enough to at least approach equilibrium.
4. No (or only small) interference with the liquid scintillation used to detect the α activity can be allowed. Otherwise the detection will be very uncertain or even impossible.

In works by Yagodin and coworkers [2-4], a liquid-liquid extraction system based on extraction of carrier amounts from dilute H_2SO_4 with trioctylamine (TOA) was reported. A good separation between Zr and Hf is achieved. Thus, this seemed like a good starting point for an extraction system to investigate the chemical properties of rutherfordium. A schematic diagram of how this extraction system is setup with SISAK is shown in Fig. 2. Results from our initial tests with carrier free amounts with such a system are shown in Fig. 3.

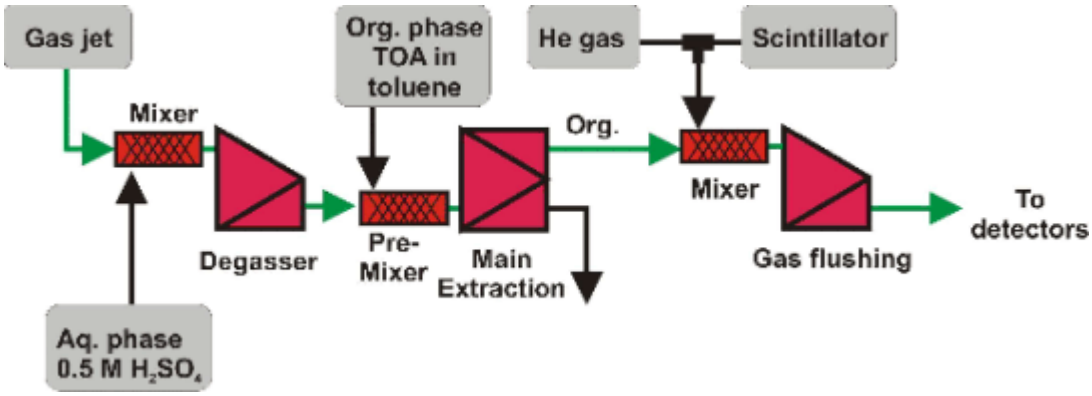

Figure 2. SISAK setup for extraction of carrier free amounts of Zr, Hf and Rf with TOA from sulphuric acid.

The data for Fig. 3 was obtained from on-line experiments at the Oslo Cyclotron Laboratory (OCL). A ~200 nA 45 MeV $^{3}He^{2+}$ beam was used on a combined Sr/Yb target (no isotopic enrichment for either element). The reaction products recoil out of the target and are caught on KCl-aerosol particles in a helium gas-jet. The gas-jet transports the activity in a few seconds to a chemistry lab through a 20 m capillary. Thus, we obtain 14 s ^{87m}Zr and 3.25 m ^{169}Hf activity for on-line SISAK experiments. The advantage of this approach, compared to using off-line produced activity dissolved directly in one of the liquid phases, is that the conditions are nearly identical to those encountered in rutherfordium experiments.

As can be seen from the right-hand panel in Fig. 3, the separation factor between the distribution ratio for Zr and Hf is on average 5.7. This is high enough to satisfy condition no. 1 in the list above. Experiments to optimize this separation with respect to reagent concentrations are under way and the results will be reported at the TAN'03 conference.

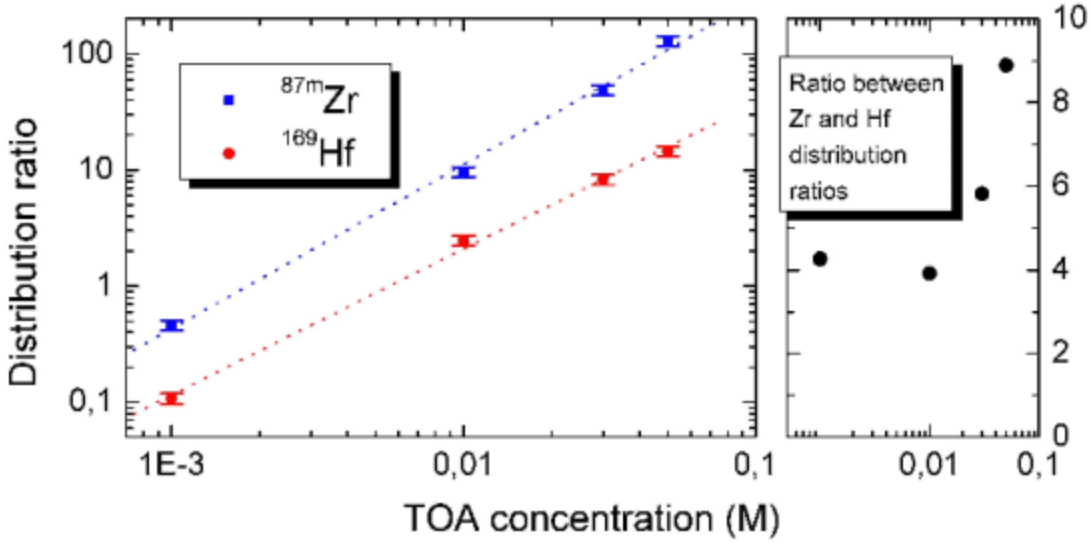

Figure 3. On-line extraction curves for Zr and Hf using 0.5 M H_2SO_4 aqueous phase and various TOA concentrations in toluene as organic phase.

In extended tests of this chemistry we found no adsorption or other unwanted effects between the chemicals used and the SISAK equipment. Thereby, condition no. 2 above is meet. By comparing batch extractions performed at equilibrium conditions and on-line extraction, the difference was found to be small. This indicates that condition no. 3 is also meet, a slow system would not have approached the equilibrium distribution-ratio. Finally, the quenching after contacting the organic phase with the sulphuric-acid aqueous phase was found small enough to not be of any major concern. Thus, the extraction system described here looks very promising as a system for future chemical studies of rutherfordium. More details and results will be presented at the TAN'03 conference.

References

[1] J.P. Omtvedt *et al.* J. Nucl. Radiochem. Sci. **3**, 121 (2002).

[2] G.A. Yagodin, A.M. Chekmarev, and L.M. Vladimirova. Russ. J. Inorg. Chem. **14**, 838 (1969).

[3] G.A. Yagodin, O.A. Sinegribova, and A.M. Chekmarev. In: Proc. Int. Solvent Extraction Conf., 1971, The Haque.

[4] G.A. Yagodin *et al.* Russ. J. Inorg. Chem. **27**, 448 (1982).

Evidence for a very noble element 112

S. Soverna[1], R. Eichler[1], H.W. Gäggeler[1], F. Haenssler[1], Z. Qin[1], B. Eichler[2], R. Dressler[2], D. Piguet[2], W. Brüchle[3], E. Jäger[3], H.-.J. Schött[3], M. Schädel[3], B. Schausten[3], E. Schimpf[3], K. Eberhardt[4], J.V. Kratz[4], P. Törle[4], N. Trautmann[4], A. von Zweidorf[4], A. Türler[5], P. Wilk[5], A.B. Yakushev[5], C.E. Düllmann[6], C.M. Folden III[6], K.E. Gregorich[6]

[1] Universität Bern, Switzerland
[2] Paul Scherrer Institut, Switzerland
[3] Gesellschaft für Schwerionenforschung mbH, Germany
[4] Institut für Kernchemie, Germany
[5] Technische Universität München, Germany
[6] Lawrence Berkeley National Laboratory, USA

soverna@iac.unibe.ch

In recent years, chemical properties have been investigated for transactinide elements up to hassium (Hs, element 108). It could be shown, that hassium forms a very volatile tetroxide [1] and that this tetroxide adsorbs strongly on a sodium hydroxide surface [2]. Both investigations confirm for hassium a typical behavior of a group 8 element in the transition element series of the periodic table.

Due to relativistic effects in the electron shells, increasing deviations of the periodicity of chemical properties along the rows of the periodic table are expected to occur for the heaviest elements. In this context element 112 is exceptional. From the systematics of the periodic table element 112 is expected to be a member of group 12. Hence, it should behave like a volatile metal similar to mercury. However, due to its closed shell $[Rn]5f^{14}6d^{10}7s^2$ electronic structure and the mentioned relativistic effects, the relativistic stabilization of the $7s^2$ electron orbital could be so strong that element 112 might behave like a noble gas, similar to radon [3,4].

Indeed from two experiments performed at Dubna [5,6] it was concluded that element 112 does not behave like mercury. Products from the reaction $^{48}Ca + ^{238}U$ that form a long-lived spontaneously-fissioning isotope of element 112 ($^{283}112$, $T_{1/2} = 3$ min) [7-9] were continuously transported with a carrier gas to a counting device consisting of gold covered PIPS detectors followed by a gas-ionization chamber. Hg-isotopes produced in fusion reactions of ^{48}Ca with the $^{nat.}Nd$ admixture in the target, were quantitatively adsorbed on the noble metal covered detectors, while element 112 was detected in the adjacent gas ionization chamber. Hence, this experiment yielded evidence that element 112 does not adsorb on gold at room temperature, and seems therefore to behave like a very inert metal or even like a noble gas.

In the studies of hassium tetroxide performed by our collaboration the IVO (In-situ Volatilization and On-line counting) device [10] was used. This technique permits *in-situ* thermochromtographic measurements of deposition temperatures of very volatile species on inert surfaces. Based on the expected inertness of element 112 we decided to apply a modified IVO technique for its chemical investigation. Products of the heavy ion induced nuclear fusion reaction recoiling out of the target were thermalized in dried 1 l/min helium carrier gas. The inner surface of the recoil chamber was completely covered by a quartz insert to prevent adsorption of volatile metallic reaction products. Gaseous products were swept out of the recoil chamber through an open quartz column to an oven with a quartz wool filter heated up to 850°C. Aerosol particles produced accidentally by e.g. beam particle induced sputtering processes in the beam dump were stopped in this filter. Separation factors of about 10^7 have been determined for lanthanides (model elements for heavy actinides) in test experiments with ytterbium, produced in the reaction $^{142}Nd(^{20}Ne;6n)^{156}Yb$. Volatile products that passed this filter were transported through a 10 m long PFA-capillary to a Ta/Ti-getter kept at 1000°C. The getter served as trap for trace

amounts of water and oxygen. It was experimentally verified that the transport of carrier free amounts of mercury and radon occurred with almost no loss trough the PFA or quartz capillary tubes at room temperature and through the Ta/Ti-getter. Finally, the gaseous products were injected into the modified detector COLD (Cryo On-Line Detector) [1]. This device consists of an array of 32 silicon PIN-photodiodes (10 x 9.8 mm^2 active area) mounted in a Teflon coated copper channel at a distance of 1.6 mm opposite to a gold covered surface, forming a rectangular gas chromatographic column. The gold surface was produced by vapor deposition of gold on a copper frame. A negative temperature gradient from + 35°C to – 187°C (see Fig. 1, black line) was established along this chromatographic channel using a thermostat heating and a liquid nitrogen cooling. The whole detector set-up was placed in a vacuum tight steel box kept at 900 mbar to isolate it thermally against ambient air.

Event-by-event spectroscopy in a 2π-detection geometry provided the identification of nuclides that were deposited on the gold surface. Calibration of the PIN-photodiodes was performed by α-decaying ^{219}Rn emanating from a ^{227}Ac source and its daughters ^{215}Po and ^{211}Bi. The determined energy resolution was 40-70 keV except for a few detectors that suffered from a reduced resolution of only 100-180 keV. This new set-up was tested on-line with short-lived Hg-isotopes produced in nuclear fusion reactions of ^{20}Ne and ytterbium (enriched in ^{168}Yb) at the PHILIPS cyclotron at the Paul Scherrer Institute and with ^{219}Rn emanating from a ^{227}Ac source. The efficiency of detecting a fission fragment was 77 %. With $^{186-190}$Hg and ^{219}Rn an overall process efficiency of about 60 % and a transport time of less than 25 s was determined [11].

In February/March 2003 three banana shaped segments of a ^{238}U target (average thickness 1.6 mg cm^{-2}), prepared on 2.33 mg cm^{-2} thick Be foils, were mounted in the rotating target assembly ARTESIA [12] and were bombarded by 1.9 x 10^{12} $^{48}Ca^{7+}$ s^{-1} at a Gesellschaft für Schwerionenforschung mbH/UNILAC energy of 346 MeV. After passing the 3.7 mg cm^{-2} Be vacuum window and the target backing-foil the ^{48}Ca projectile energy was degraded to 239 MeV. The energy inside the ^{238}U target was then 222 – 239 MeV. During 16.8 days 2.8 x 10^{18} ^{48}Ca particles were accumulated on the target. One of the three banana shaped segments of the U_3O_8 target contained 21.7 µg cm^{-2} ^{nat}Nd in order to produce α-decaying Hg-isotopes, mainly in the reaction ^{142}Nd(^{48}Ca,4-6n)$^{184-186}$Hg. Since Rn-isotopes were produced in nuclear transfer reactions [13] it was possible to compare the chemical properties of element 112 with both mercury and radon during the entire experiment. The volatile reaction products were transported to the COLD detector with 1 l/min helium. The Hg-isotopes were completely deposited on the gold surface opposite the first nine detectors. About 65 % of ^{220}Rn were adsorbed in the low temperature part of the COLD detector (see Fig. 1).

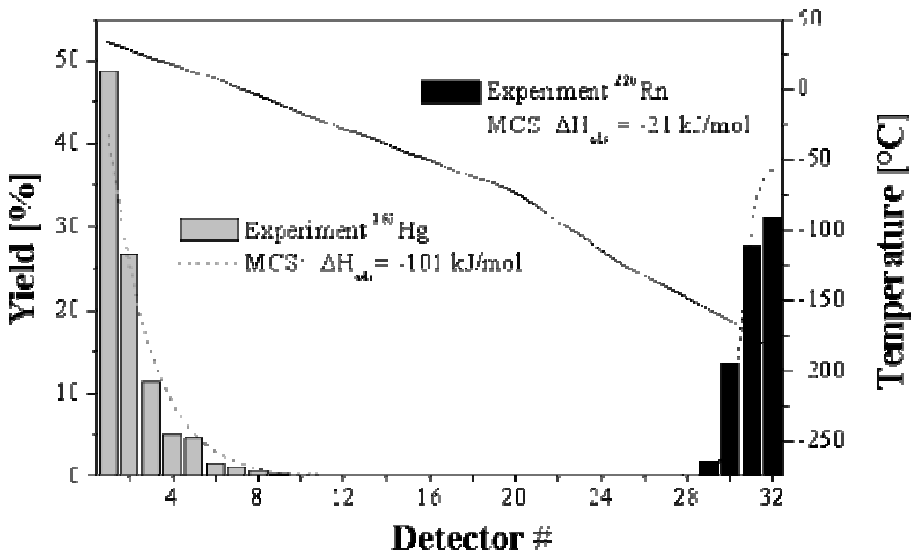

Figure 1. Thermochromatograms of ^{185}Hg (grey bars, left-hand scale) and ^{220}Rn (black bars, left-hand scale) on COLD at a helium carrier gas flow of 1 l/min.Also shown are Monte Carlo simulations of the observed depositions (grey and black dashed lines, left hand scale). The temperature gradient is indicated (black line, right-hand scale).

The spontaneous, diffusion controlled deposition of mercury on gold agrees well with literature values (ΔH_{ads} = -101±2 kJ/mol) [14]. For radon the deposition distribution is reproduced assuming an adsorption enthalpy of ΔH_{ads} = -21±1 kJ/mol. This value is somewhat lower compared to a literature value ΔH_{ads} = -29±3 kJ/mol for radon on gold as measured under molecular flow conditions [15]. We can therefore not exclude that at these very low temperatures the gold surface is covered by a thin ice layer. Indeed, in earlier thermochromatographic experiments of radon on ice surfaces an adsorption enthalpy of ΔH_{ads} = -20±2 kJ/mol was found [16]. Moreover, a careful analysis of the resolution of the α-spectra yielded evidence for an ice formation at temperatures below about -90°C (detector #21). This corresponds to a dew point of water at a partial pressure in the helium carrier gas of 0.2 ppm.

During the experiment 12 fission-like events (with energies above 40 MeV) were detected (Fig. 2). A background measurement performed after the run clearly indicated a non-zero background with scattered events along the entire array at a count-rate of approximately 0.0055 events/detector and day.

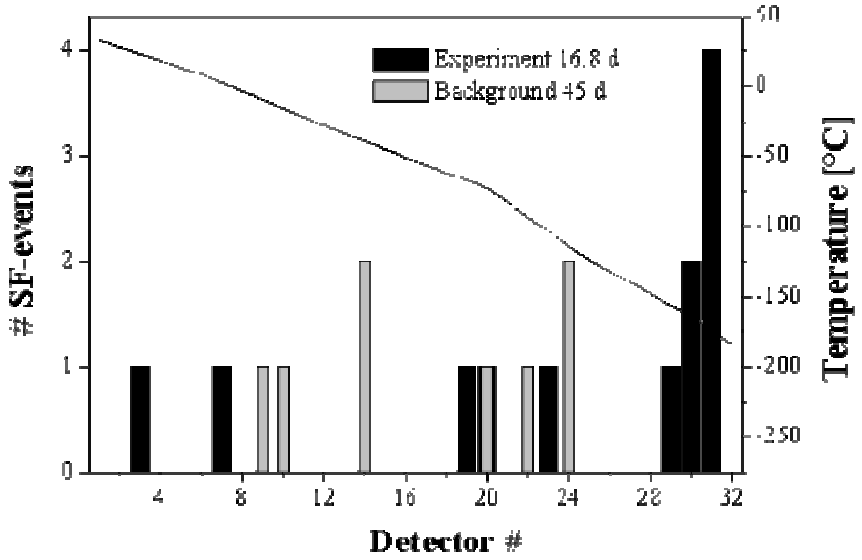

Figure 2. Observed events (with energies > 40 MeV) throughout the $^{48}Ca + ^{238}U$ experiment (black bars, left-hand scale) and during the background measurement performed immediately after the run (grey bars, left-hand scale). The temperature gradient is indicated (black line, right-hand scale).

The assignment of the measured SF events to the decay of $^{283}112$ is only convincing if no actinides are found along the detector array. Therefore, a very careful analysis of the α-spectra was performed. First, the quartz wool filter kept at 850°C was leached with concentrated nitric acid. From the solution a sample was prepared to measure off-line α- and SF-events. Pronounced peaks of $^{226\text{-}228}Th$, $^{224\text{-}226}Ac$, and $^{221\text{-}228}Ra$ were observed but no SF-decays detected during a counting time of 30 days (Fig. 3).

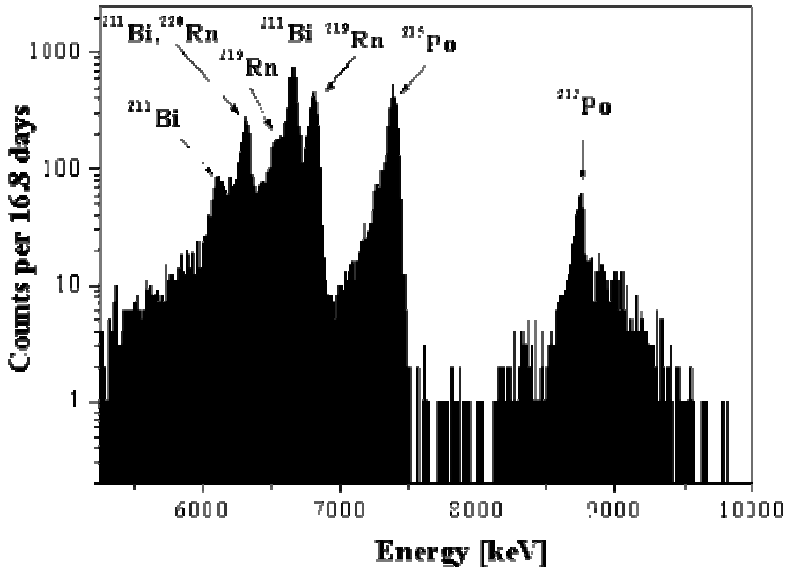

Figure 3. α-spectra of detector # 21 in the energy-range between 5.3 MeV and 10 MeV.

In addition, a thorough analysis of the recorded 32 α-spectra did not indicate any α-peak that might be assigned to a heavy actinide nuclide. Moreover, it is extremely unlikely, that any isotope of radon has a SF-branch. Hence, we assign most of the measured SF events to an isotope of element 112, presumably ^{283}112.

In the detectors 29, 30 and 31 a total of 7 events were measured during the experiment at an expected background of 0.28 events. This deposition peak almost coincides with the deposition peak of radon. Already this preliminary data from the ongoing data analysis of the experiment allow us to conclude, that our experiment yielded strong evidence for a very noble element 112. The final results will be presented in our contribution.

Acknowledgements

We would like to thank the crews of the Gesellschaft für Schwerionenforschung mbH UNILAC and of the Paul Scherrer Institut Philips Cyclotron for providing stable and intense beams of ^{48}Ca and ^{20}Ne. We are indebted to the staff of the Laboratory for Micro- and Nanotechnology at Paul Scherrer Institute for adapting the PIN-diodes for the COLD. These studies were supported in part by the Swiss National Science Foundation.

References

[1] Ch. E. Düllmann et al., Nature, 418, 862 (2002).
[2] A. von Zweidorf et al., GSI Scientific. Rep. 2002, 175 (unpublished).
[3] K. S. Pitzer, J. Chem. Phys. 63, 1032 (1975).
[4] P. Schwertfeger and M. Seth, in Enyclopedia of Computational Chemistry, Vol. 4 (Wiley, New York, 1998), p. 2480.
[5] A. B. Yakushev et al., Radiochim. Acta 89, 743 (2001).
[6] A. B. Yakushev et al., Radiochim. Acta 91, 433 (2003).
[7] Yu. Ts. Oganessian et al., Nature, 400, 242 (1999).
[8] Yu. Ts. Oganessian et al., Eur. Phys. J. A 5, 63 (1999).
[9] Yu. Ts. Oganessian et al., Eur. Phys. J. A, submitted.
[10] Ch. E. Düllmann et al., Nucl. Instr. Meth. A479, 631 (2002).
[11] S. Soverna et al., Ann. Rep. Univ. Bern & PSI 2002, 3 (unpublished).
[12] M. Schädel, Acta Physica Polonica B 34, 1701 (2003).
[13] H. W. Gäggeler et al., Phys. Rev. C33, 1983 (1986).
[14] J. P. Niklaus et al., Ann. Rep. Univ. Bern & PSI 2002, 8 (unpublished).
[15] R. Eichler and M. Schädel, J. Phys. Chem. B106, 5412 (2002).
[16] B. Eichler, H. P. Zimmermann and H. W. Gäggeler, J. Phys. Chem. A104, 3126 (2000).

Investigation of alpha-electron coincidences in data from liquid scintillation detection

L. Stavsetra[1], J. Alstad[1], H. Nitsche[2], D.C. Hoffman[2], J.P. Omtvedt[1]

[1] University of Oslo, Norway
[2] LBNL, USA

liv.stavsetra@kjemi.uio.no

Introduction

SISAK[a] is a fast, chemical-separation system for liquid-liquid extraction. The system is described in another contribution to TAN'03 and in e.g. references [1, 2].

During recent years, work has been undertaken to deploy SISAK in studies of the chemical properties of the transactinide elements (Z ≥ 104) [1, 3-6]. The only suitable detection method found was liquid-scintillation (LS) detection [7], mainly because of the rather high flow rates (0.5-2.0 mL/s) encountered in the SISAK system. Other detection methods usually require either thin, dry samples or very thin liquid films. No suitable method was found to prepare such samples without an unacceptable time delay between separation and detection.

In December 2000 the first successful transactinide experiment [3] with SISAK was performed at the Lawrence Berkeley National Laboratory (LBNL) in Berkeley, USA. This experiment proved that it was possible to extract and detect the transactinide ^{257}Rf with SISAK. ^{257}Rf has a half-life of about 4 s , and the cross section is about 12 nb [8]. The activity is delivered to the chemistry apparatus with a gas-jet transport system. With the SISAK system the gas-jet activity is continuously dissolved in an aqueous phase, then mixed with an organic phase containing a suitable extraction agent, separated and added to a liquid scintillation cocktail for α detection. The whole operation is on-line and continuous and SISAK is probably the fastest system for transactinide studies in the *liquid* phase available today. The on-line LS detection system used for SISAK experiments was developed in Mainz by Wierczinski [7] and co-workers and has continuously been improved [1,3,9]. The search for improvements continue and as a part of this a study of conversion electrons in coincidence with α particles was initiated and is reported here.

The effect of conversion electrons on α-liquid scintillation spectra

If an α decay is populating an exited level in the daughter nucleus and this level deexcites by emission of a conversion electron, the resulting α spectrum can become seriously distorted. This is because the light emitted from the scintillator due to an electron is about 8-12 times as high as from an α particle (due to the differences in the LET (Linear Energy Transfer) between the respective particles and the medium they interact with) [10]. Thus, a 50 keV electron will cause emission of light pulses equivalent to about 0.5 MeV of α energy. The result is that α spectra obtained from sources with coincident or near coincident conversion electrons will have distorted α peaks.

In measurement of transactinides the production rate is rarely high enough to obtain α spectra with prominent α peaks. Instead one usually relies on observing correlated chains of α particles with the correct energy and time sequence. However, when LS detection is used, α - electron coincidences might change the observed α energy so much that it falls outside the energy window. This together with the fact that many transitions in the transactinides are highly converted, can lead to a serious loss of observed events. E.g. in the ^{257}Rf SISAK experiments the correlated daughter to ^{257}Rf is ^{253}No. The decay of ^{253}No feeds a level at 300 keV in ^{249}Fm. From systematics one expects a conversion coefficient of about 0.05,

which means that about 1 out of 20 ^{253}No α decays will be correlated with an electron of around 150 keV (the K electrons are bound by 150 keV for Fm atoms), see Fig. 1. Thus, about 5% of the α particles from ^{253}No will be observed with more than 1 MeV of extra energy, which is outside the energy window used.

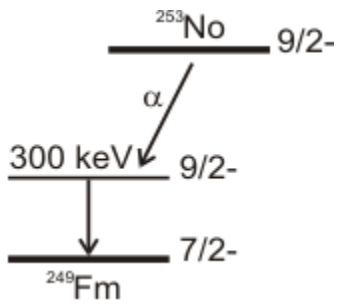

Figure 1. Simplified decay scheme of ^{253}No, showing the converted transition in ^{249}Fm (α_{Total}=0.05).

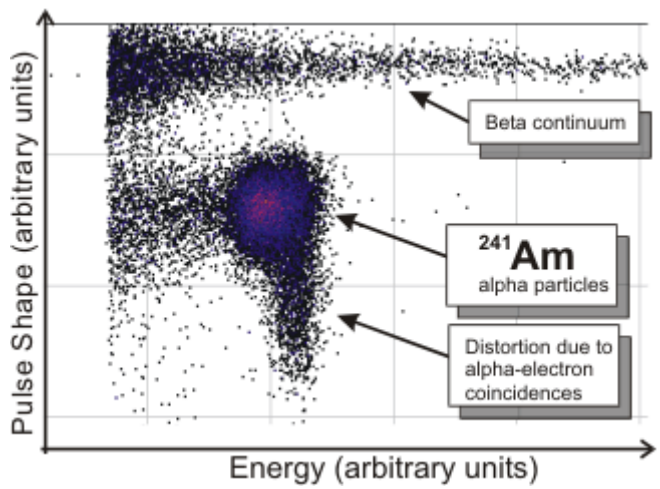

Figure 2. Measured pulse shape vs. energy plot of ^{241}Am α particles.
The half life for the intermediate level in ^{241}Np is 67 ns.

The aim of this work is to find a method to spot such α-electron coincidences and correct the observed energy to coincide with the energy observed for a pure α. Since the SISAK system already employs pulse-shape analysis to discriminate between α's and β's [10], it was natural to investigate if α-electron coincidences would change the pulse shape signal (basically a measurement of the length of the falling edge of the light pulses from the scintillator). As can be seen from Fig. 2, this seems to be the case: Energy vs. pulse shape is plotted in a contour plot for data obtained from ^{241}Am. The long tail of the α peak can be attributed to α-electron coincidences. The shape of the tail can be understood by taking into account the half life of the intermediate level. For ^{241}Am this half life is equal to 67 ns [11], as shown in Fig. 3. For another americium isotope with a similar type of decay, but with a shorter half life of only 1.4 ns [12] (Fig. 3) we can see that the pulse shape is much less effected, see Fig. 4.

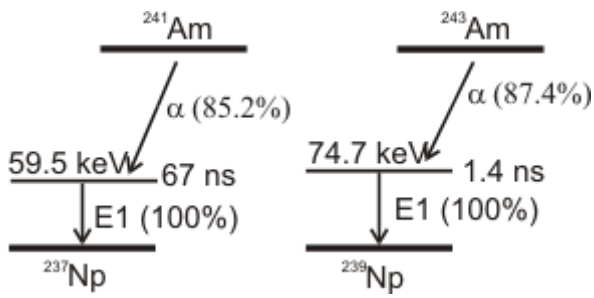

Figure 3. Simplified decay scheme of ^{241}Am and ^{243}Am.

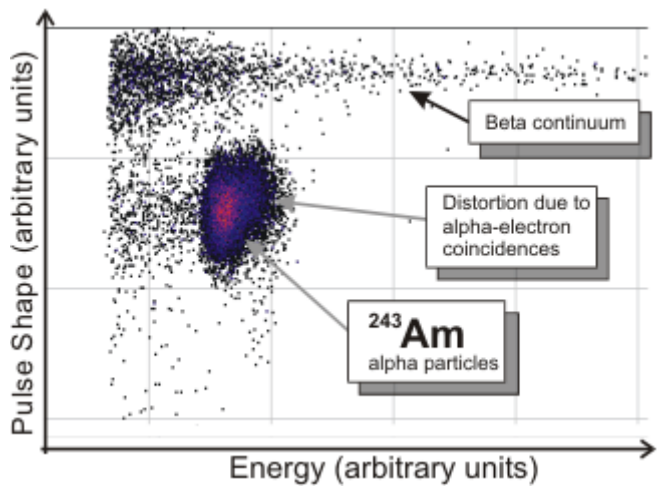

Figure 4. Measured pulse shape vs. energy plot of ^{243}Am α particles.
The half life for the intermediate level in ^{239}Np is 1.4 ns.

Digital Acquisition

From this data it can clearly be seen that the α-electron coincidences will change the LS data, both with respect to energy and pulse shape. It is also clear that the analog electronics used to obtain the data in Fig. 2 and 4 is not precise enough to distinguish between pure α events and α-electron coincidences. Therefore, experiments are under way in which a digital-acquisition system is used to sample each pulse from the scintillator and not only measure its width as the analog electronics do. With the pulses available a much more sophisticated analysis of the pulse shape can be performed, and hopefully this will enable both a better determination of the type of signal (β, α, or α-electron), but also correction for the additional energy added by the extra excitation of the scintillator causes by the electron.

Work with the digital acquisition system is under way and results will be presented at the TAN'03 conference.

Acknowledgements

The Heavy Element Group at LBNL are thanked for their hospitality during Liv Stavsetra's stay at LBNL, where among other things, the Am activity used for the work reported here generously were made available. This project was financed by a grant from the Norwegian Research Council, project number 134882/432.

References and Notes

a. Short-lived Isotopes Studied by the AKUFVE-technique, where AKUFVE is a Swedish acronym for an arrangement for continuous investigations of distribution ratios in liquid extraction.

[1] J.P. Omtvedt, et al., Review of the SISAK system in transactinide research. recent developments and future prospects. Journal of Alloys and Compounds, 1998. **271-273**: p. 303.

[2] G. Skarnemark, et al., Nuclear studies with the fast on-line chemical seperation system SISAK. Physica Scripta Sweden., 1986. **34**(6A): p. 597.

[3] J.P. Omtvedt, et al., SISAK Liquid-Liquid Extraction Experiments with Preseparated 257Rf. Journal of Nuclear and Radiochemical Sciences, 2002. **3**(1): p. 121.

[4] B. Wierczinski, et al., Application of fast solvent extraction processes to studies of exotic nuclides. Journal of Radioanalytical and Nuclear Chemistry, 1998. **236**(1-2): p. 193.

[5] B. Wierczinski, et al., Fast on-line solvent extraction with the SISAK-3 centrifuge system as a test of chemical studies of the elements 105 and 106. Radiochimica Acta, 1995. **69**(2): p. 77.

[6] K. Eberhardt, et al. Studies of the chemical properties of transactinide elements using the fast on-line centrifuge system SISAK 3. in The 4th international conference on nuclear and radiochemistry, NRC4. September 8-13, 1996. St. Malo, France.

[7] B. Wierczinski, et al., Liquid-scintillation spectroscopy of alpha-particle emitters and detection of spontaneous fission events for on-line studies of actinide and transactinide elements. Nuclear Instruments and Methods in Physics Research A, 1996. **370**: p. 532.

[8] F.P. Hessberger, et al., Spontaneous fission and alpha-decay properties of neutron deficient isotopes $^{257\text{-}253}$104 and ^{258}106. Zeitschrift fuer Physik A, 1997. **359**(4): p. 415.

[9] L. Stavsetra and J.P. Omtvedt, Detection Of Transactinides With alpha-liquid Scintillation. Accepted for pulication in Radiocarbon, 2003.

[10] W.J. McDowell and B.L. McDowell, Liquid scintillation alpha spectrometry. 1994, Boca Raton, Florida: CRC Press Inc.

[11] Y.A. Akovali, Nuclear Data Sheets Update for A=243, in Nuclear Data Sheets, J.K. Tuli and M.J. Martin, Editors. 1992, Academic Press, Inc. p. 897.

[12] Y.A. Akovali, Nuclear Data Sheets A=241 Update, in Nuclear Data Sheets, J.K. Tuli and M.J. Martin, Editors. 1994, Academic Press, Inc. p. 191.

Suitability of extraction systems with macrocyclic ligands for the study of rutherfordium

R. Sudowe[1], C.E. Düllmann[1], C.M. Folden III[1], K.E. Gregorich[1], D.C. Hoffman[1], P.M. Zielinski[1], H. Nitsche[1]

[1] Lawrence Berkeley National Laboratory, USA

RSudowe@lbl.gov

Introduction

For the first time, the fast, automated liquid-liquid extraction system SISAK was recently successfully used to study the chemical behavior of element 104, rutherfordium [1]. This was made possible by coupling the SISAK system to the Berkeley Gas-filled Separator (BGS). The BGS was used to achieve a physical pre-separation of the desired species from the beam and unwanted reaction products. This pre-separation reduced the background due to the scattered beam and other reaction products substantially and allowed for the detection of rutherfordium atoms without any interference of undesirable activity. The lack of interfering reaction products has several advantages for the design of chemistry experiments with transactinides. In addition to simplifying the detection and data analysis it allows the use of a different class of extraction systems in future SISAK and other chemistry experiments.

The first goal of experiments to study the chemical behavior of transactinide elements is to establish the position of these elements in the periodic table. Then, the properties of the transactinides are systematically compared with those of their lighter homologues and pseudo-homologues to gain further insight into the periodicities within a group of the periodic table and evidence for the influence of relativistic effects. Differences in extraction behavior can be used to differentiate between the individual elements of a group.

In the past, it was necessary to select extraction systems that removed all interfering reaction products and left only the element of interest. Consequently, a very high decontamination factor between the element of interest and interfering activity had to be favored over a high selectivity between the different homologues within the group being studied.

Due to the success of the experiments with pre-separated activity, selectivity between the members of the same group of the periodic table can now be favored over efficient separation from elements belonging to other groups when designing extraction systems for future experiments [2]. This affects the usefulness of extraction systems for the study of transactinide elements and changes their selection criteria. In addition it also gives access to other classes of extraction systems that previously have not been considered when developing solution chemistry experiments.

These additional extraction systems need to be studied regarding their suitability for future experiments with transactinide elements. After the success of the first experiments with pre-separated rutherfordium isotopes, it was decided to start searching for different extraction systems that could be used to study the chemistry of element 104. The extraction systems need not only to be evaluated for their usefulness for future SISAK experiments, but for other automated systems and manual extraction experiments as well.

Macrocyclic ligands and their application

Several highly selective extractants are currently under investigation in our group, especially systems with macrocyclic ligands.

A macrocyclic ligand can be defined as a compound comprising a ring of at least nine atoms including at least three donor atoms oriented so as to bind to a metal atom. These ligands are a special type of polydentate ligands in which the ligating atoms are constrained in a large ring encircling the metal ion. Examples for such ligands are polyethers in which the ether oxygen atom, separated by two methylene groups each, lie in a nearly planar arrangement about the central metal atom and the remainder of the molecule lies in a "crown" arrangement. All of the oxygen atoms "point" inward toward the metal atom, and these macrocycles form stable complexes with alkali- and other metals [3]. Examples of crown ethers that show promise for experiments with group 4 elements, dibenzo-18-crown-6 (1) and dicyclohexano-24-crown-8 (2), are shown below. Other examples of such macrocyclic ligands include thiacrowns and calixarenes.

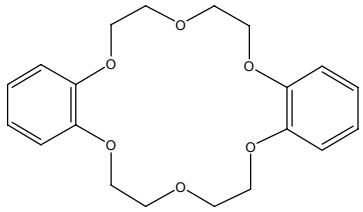

1

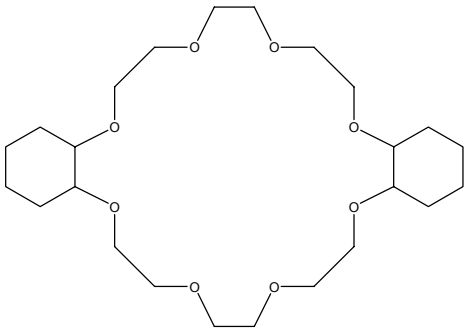

2

The high stability of the complexes of certain metals with macrocyclic ligands and accordingly the high selectivity of such ligands is generally attributed to a size effect. It depends on how closely the metal ion fits into the gap in the center of the ligand. But the differences in metal ion affinities in the gas phase compared to in solution suggest that solvent effects play an important role as well.

The high selectivity of extraction systems with macrocyclic ligands is used in a multitude of applications in analytical and technical chemistry. The coordination chemistry of macrocyclic ligands and alkali and earth alkali metals has been studied in depth [4], and these ligands are most commonly applied for the separation of these metal ions. In addition, these extractants show also promise for the separation of other transition and main group metals [5].

Reaction kinetics is another factor in evaluating the suitability of an extraction system for chemistry with transactinide elements. This factor may even be more important than a high selectivity between the members of a group of the periodic table.

Unfortunately, the size of the organic molecules used as extractants can have a large effect on the kinetics of the reactions. While the time necessary to complete a reaction can be a secondary concern for many applications, it is of great importance for the study of the transactinide elements. Due to the short half-life of the elements studied it is necessary to choose chemical systems that reach equilibrium as fast as possible. This severely restricts the choice of extraction systems with macrocyclic ligands that can be used for the study of rutherfordium or other transactinide elements. The kinetics of any extraction system that shows promise needs to be studied very thoroughly.

The use of different crown ethers, e.g., dicyclohexano-18-crown-6 and dibenzo-18-crown-6, for the separation of zirconium and hafnium has been reported previously in the literature [6,7]. None of these studies were conducted under conditions that can be applied to the study of rutherfordium.

The usefulness of these extractants in experiments with substantially shorter contact and reaction times needs to be studied. In addition the suitability of other systems needs to be also tested.

Experimental

In this work the extraction of the lighter homologues and pseudo-homologues of rutherfordium with different macrocyclic ligands from mineral acid solutions was studied using tracer activities with short and medium half-lives.

Offline experiments were performed using ^{88}Zr ($T_{1/2}$=83.4 d) and ^{175}Hf ($T_{1/2}$=70.0 d) as tracer activities. In addition, on-line experiments were performed at the 88-inch cyclotron at LBNL. Short-lived isotopes of Zr and Hf were produced by bombarding a ^{nat}Gd and a ^{124}Sn target with an $^{18}O^{4+}$ and a $^{50}Ti^{11+}$ beam, respectively. The zirconium and hafnium isotopes produced were separated from the beam and interfering reaction products using the BGS. After traveling through the BGS, the products passed through a thin Mylar window into the Recoil Transfer Chamber (RTC) [8]. Inside the RTC, the recoils were stopped in helium and transported to the chemistry setup using a potassium chloride aerosol gas jet.

The aerosols containing the activity were deposited on platinum foils and dissolved in mineral acid of appropriate concentration to conduct the extraction experiments.

The extraction of zirconium and hafnium with different macrocyclic ligands was studied from dilute and concentrated mineral acids, mainly hydrochloric acid. The distribution ratios for the elements were determined as a function of acid and ligand concentration.

The extraction experiments were performed on a time scale relevant for experiments with transactinide elements (< 2 minutes). The kinetics of the reaction was studied by varying the contact time during mixing and the time allowed for phase separation. In addition, the influence of different solvents on the extraction was studied.

The results of these experiments will be presented.

Acknowledgement

This work was supported by the Director, Office of Science, Office of High Energy and Nuclear Physics, Division of Nuclear Physics, and the Office of Basic Energy Science, Chemical Science Division, U.S. Department of Energy under Contract No. DE-AC03-76SF00098.

The authors would like to thank C. S. Gong, S. E. Herbison, L. M. Farina, J. M. Schwantes and R. E. Wilson for their invaluable help with the online chemistry experiments at the 88-inch cyclotron.

References

[1] J.P. Omtvedt *et al.* J. Nucl. Radiochem. Sci. **3**, 121 (2002).
[2] R. Sudowe, K. E. Gregorich, D. C. Hoffman, J. P. Omtvedt, L. A. Omtvedt, L. Stavsetra, H. Nitsche, Ernest Orlando Lawrence Berkeley National Laboratory, LBNL-49957 (2002).
[3] J. Huheey, E. A. Keitner, R. L. Keitner, Harper Collins College Publishers (1993) 525.
[4] J. W. Steed, Coordin. Chem. Rev. **215**, 171 (2001).
[5] A. T. Yordanov, D. M. Roundhill, Coordin. Chem. Rev. **170**, 93 (1998).
[6] N. V. Deorkar, S. M. Khopkar, Anal. Chim. Acta **245**, 27 (1991).
[7] Y. K. Agrawal, S. Sudhakar, Sep. Purif. Technol. **27**, 111 (2002).
[8] U. W. Kirbach et al., Nucl. Inst. Meth. **A484**, 587 (2002).

Development of a selective separation method for element 107 – bohrium – based on fast liquid-liquid extractions

B. Wierczinski[1], K.J. Volkers[1]

[1] Interfaculty Reactor Institute, Netherlands

B.Wierczinski@iri.tudelft.nl

Abstract

Liquid-liquid extraction has been used to develop a fast separation procedure of the homologues of element 107 (bohrium, Bh) from other reaction products, which can simultaneously be produced in the heavy ion reactions used for transactinide production. Alpha-hydroxyisobutyric acid has been used as complexing agent in the aqueous phasesolution. The organic phasesolution consisted of trioctylamine in Shellsol T. A quantitative extraction of technetium and rhenium has been observed in the pH range from 1.5 to 5.5, with a good separation from most other studied elements, except for iodine, which has been extracted up to 50 % and niobium, which only can be separated from the group VII elements at high pH-values.

Introduction

Knowledge about the chemical properties of transactinide elements allows to determine their position within the periodic table of the elements. If they behave similar to their lighter homologues they can simply be placed under the corresponding group. If their chemical behavior is influenced by relativistic effects, positioning within the table of elements may be more difficult.

Transactinide elements are studied using different chemical separation methods including column separation, gas chromatography and liquid-liquid extraction. Usually only a few atoms of these elements are produced during an accelerator experiment and the half-lives of these elements are in the range of seconds to minutes. Therefore the separation method used has to be very fast, highly selective for the element of interest, very efficient and also the detection method should be capable to measure single atoms with high accuracy and efficiency.

The SISAK (*S*hort-lived *I*sotopes studied by the *AK*UFVE technique) [1] uses fast rotating centrifuges to perform continuous liquid-liquid extractions. In the past, this system has been coupled with an on-line alpha-liquid scintillation system to be able to continuously measure alpha-decaying transactinides.

Presently new developments are taking place to futher improve the performance of the SISAK system: to overcome problems with high overall activity and resulting detection difficulties a pre-separation of the produced transactinide with a gas-filled separator is investigated. First experiments have shown promising results [2]. Secondly, the design of a so-called 'micro-SISAK' system is going on, which should reduce the total amount of aqueous and organic solutions used for the separation [3] and also will allow operation of the system at lower flow-rates. In this case, detection of the extracted nuclides using semi-conductor detectors is also investigated.

However, liquid-liquid extraction still remains the main principle on which the separation is based. Such a liquid-liquid extraction procedure is usually investigated by performing experiments with the lighter homologues of the transactinide of interest as well as some neighbouring elements. In the case of bohrium (element 107), technetium and rhenium are used as homologues and are separated from group 4, 5 and 6 elements, as well as some di- and tri-valent metals and one actinide element.

Experimental

Radionuclides

Table 1 shows the radionuclides used for developing the extraction procedure. If they were not commercially available, production procedures were developed to obtain non-carrier-added radionuclides. These production procedures were usually based on neutron irradiation of certain compounds at the HOR research reactor of the Interfaculty Reactor Institute in Delft, The Netherlands. Ideally, (n,p)- and (n,alpha)- reactions were used to produce the short-lived nuclides. Examples are the production of non-carrier-added ^{64}Cu and ^{58}Co. Other nuclides were produced by beta-decay of the corresponding mother nuclide: ^{95}Nb and ^{105}Rh were produced in this way. Before the radionuclides were used for the extraction experiments, they were chemically separated from their original matrix or mother nuclides.

Table 1. Radionuclides used to develop an extraction procedure for bohrium and their half-lives.

Radionuclide	$t_{1/2}$
^{99m}Tc	6.02 h
^{186}Re	3.78 d
^{188}Re	16.98 h
^{95}Nb	31.15 d
^{105}Rh	1.47 d
^{103}Ru	39.35 d
^{239}Np	2.36 d
^{131}I	8.04 d
^{65}Zn	244 d
^{64}Cu	12.71 h
^{58}Co	70.78 d

Extractions

The aqueous solution consisted of 1 M alpha-hydroxyisobutyric acid, 0.01 M potassium bromate to ensure the +VII oxidation state of the elements, and 0.22 M dodecanol to improve the phase separation. The pH-value was varied using either hydrochloric acid or ammonia. The organic solution consisted of 2 % vol trioctylamine (TOA) in Shellsol T. Liquid-liquid extractions were performed in polyethylene tubes: the tubes were sealed at one end and 0.5 ml of the two phases including the nuclide of interest were added in the tube. After sealing the other end of the tube it was shaken 1 minute using a Vortex apparatus. The phases were separated by centrifugation and an aliquot was removed from both phases

and measured using Ge(Li) semiconductor detector. Extractions were carried out three times and the average value is given for the extraction yield.

Results and Discussion

Figure 1 shows the results obtained for extraction of the above mentioned nuclides: Tc and Re are extracted quantitatively into the organic phase throughout the whole pH range from 1.6 to 5.0. Niobium as a homologue of element 105 is extracted in high yields at lower pH values, but the yield decreases for higher pH values until it is extracted less than 5 % at pH values around 5. This result is in agreement with earlier experiments [4]. Iodine is extracted with a yield of about 50 % throughout the whole pH range. Cobaltd, copper, neptunium and zinc are not extracted at all. The extraction yields of rhodium and ruthenium increase slightly at higher pH values and reach a maximum yield of about 17 % and 30 % and pH values 5.5 and 4.5, respectively.

First results obtained with molybdednum show negligible extraction yields and are not yet included into figure 1.

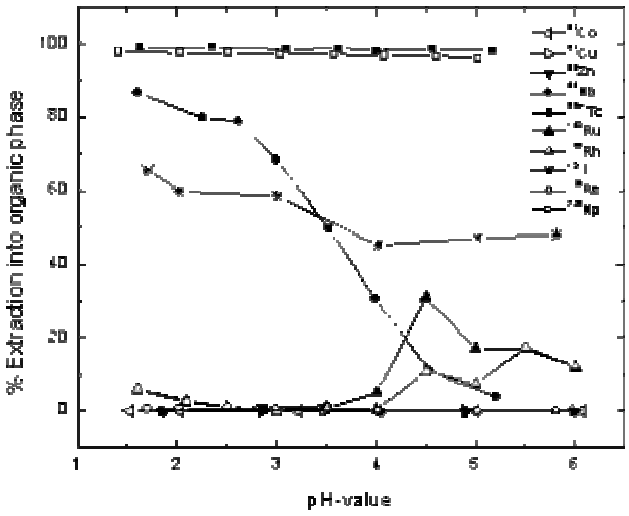

Figure 1. Extraction yields for different nuclides. Organic phase: 2 % Vol trioctylamine in Shellsol, aqueous phase: 1 M alpha-hydroxyisobutyric acid, 0.01 M potassium bromate, 0.22 M dodecanol.

The results suggest that this extraction system using alpha-hydroxyisobutyric acid may be used at pH values above 5 for a quantitative separation of element 107 and its homologues from other reaction products.

Future work

Not only molybdenum but also tungsten isotopes will be used in future experiments to ensure the selective separation of group 6 from group 7 elements. Addition of a small amount of H_2O_2 to the aqueous phase should result in a decreased extraction yield of niobium and will also be investigated. Furthermore, on-line experiments with even shorter lived isotopes are necessary to ensure that the extraction kinetics is indeed fast enough for future continuous separations using the SISAK system.

Also, if on-line alpha-liquid-scintillation counting will be used as detection method for the transactinide element, the organic phase should consist of an aromatic solvent, such as toluene. Although earlier experiments suggest that the above mentioned extractions are in general possible with aromatic solvents [5], some experiments have to be carried out to ensure identical extraction yields as when using Shellsol.

References

[1] H. Persson, G. Skarnemark, M. Skålberg, J. Alstad, J.O. Liljenzin, G. Bauer, F. Haberberger, N. Kaffrell, J. Rogowski, and N. Trautmann, Radiochim. Acta **48**, 177 (1989).

[2] J. P. Omtvedt *et al.* J. Nucl. Radiochem. Sci. **3**, 121 (2002).

[3] K. Eberhardt, personal communication (2003).

[4] B. Wierczinski *et al.* Radiochim. Acta **69**, 77 (1995).

[5] B. Wierczinski *et al.* Nucl. Instrum. Meth. **A370**, 532 (1996).

The new isotopes of element 107: Bh-266 and Bh-267 and the chemistry of bohrium

P.A. Wilk[1], J.L. Adams[2], W. Brüchle[3], R. Dressler[4], C.E. Düllmann[2], B. Eichler[4], R. Eichler[5], H.W. Gäggeler[5], K.E. Gregorich[2], D.C. Hoffman[2], S. Hübener[6], D.T. Jost[4], U.W. Kirbach[2], M.R. Lane[2], C.A. Laue[7], V.M. Lavanchy[5], D.M. Lee[2], H. Nitsche[2], J.B. Patin[7], D. Piguet[4], M. Schädel[3], D.A. Shaughnessy[7], D.A. Strellis[2], S. Taut[6], L. Tobler[4], Y.S. Tsyganov[8], A. Türler[1], A. Vahle[6], A.B. Yakushev[1]

[1] Technische Universität München, Germany
[2] Lawrence Berkeley National Laboratory, USA
[3] Gesellschaft für Schwerionenforschung mbH, Germany
[4] Paul Scherrer Institut, Switzerland
[5] Universität Bern, Switzerland
[6] Forschungszentrum Rossendorf, Germany
[7] Lawrence Livermore National Laboratory, USA
[8] Joint Institute for Nuclear Research, Russia

pwilk-radiochem@hahnium.com

The early history of bohrium

Bohrium was first identified in 1981 by Münzenberg *et al.* as the isotope ^{262}Bh^{m} produced in the ^{209}Bi(^{54}Cr,*n*) reaction [1] using the velocity filter "Separator for Heavy Ion Production" (SHIP) at the Gesellschaft für Schwerionenfourschung (GSI), Darmstadt, Germany. Earlier performed experiments initially claimed synthesis of element 107 via the ^{54}Cr(^{209}Bi,2*n*) reaction, based on observation of the spontaneous fission activity from the decay of ^{261}Bh. However, in subsequent experiments spontaneous fission activity was not detected, and ^{261}Bh was unambiguously identified by correlation with its α-decay daughter ^{259}Ha. [2]. To date, no spontaneous fission activity has been observed that can be attributed to spontaneous fission of any bohrium isotopes and a low upper limit on the spontaneous fission branch was set. The properties of the isotopes of bohrium known previous to this work are: ^{261}Bh ($T_{½}$=11.8 ms; E_{α}=10.40, 10.10, 10.03 MeV [2]), ^{262}Bh ($T_{½}$=102 ms; E_{α}=10.06, 9.91, 9.74 MeV [2]), ^{262}Bh^{m} ($T_{½}$=8 ms; E_{α}=10.37, 10.24 [2]), and ^{264}Bh ($T_{½}$=440 ms; E_{α}=9.62, 9.48 MeV [3]).

The isotopes 266 and 267

Experiments were undertaken to try to produce and identify the new neutron-rich isotopes of bohrium, ^{266}Bh and ^{267}Bh. These isotopes were predicted to have significantly longer half-lives than previously known bohrium isotopes, possibly long enough to enable the first studies of bohrium chemical properties in subsequent experiments. Previous attempts to identify these isotopes by chromatographic separation have failed [4, 5]. Based on predicted Q-values for electron capture and α-decay, ^{266}Bh and ^{267}Bh should decay predominantly by α-emission and possibly by spontaneous fission (SF). The α-particle energies and half-lives for these isotopes are expected to be in the range of 8.7–9.3 MeV [6] and 1-20 seconds [7]. The previously reported decay characteristics of their Ha and Lr daughter nuclei, are: ^{262}Ha ($T_{½}$=34 s; E_{α}=8.45, 8.53, 8.67 MeV [8]), ^{263}Ha ($T_{½}$=27 s; E_{α}=8.35 MeV [9]), ^{258}Lr ($T_{½}$=3.9 s [10]; E_{α}=8.60, 8.62, 8.57, 8.65 MeV [8]), and ^{259}Lr ($T_{½}$=6.34 s; E_{α}=8.45 MeV [10]). Kratz *et al*. [9] report an α-particle energy of 8.35 MeV for ^{263}Ha, but other measurements [11] indicate that ^{263}Ha might also decay by emission of 8.41-MeV α-particles.

Using these predictions as a guide, ^{267}Bh and ^{266}Bh were produced in bombardments of a ^{249}Bk target with 117-MeV and 123-MeV ^{22}Ne ions. Identification was made by observation of correlated α-particle

decays between the bohrium isotopes and their daughters by using our rotating wheel (MG) system. A parent-daughter stepping mode was used to provide detection of α-α correlations with a greatly reduced background [12]. After the end of bombardment and careful analysis of the data, it was found that four atoms of ^{267}Bh were produced during the experiment. ^{267}Bh was produced with a cross-section of ~70 pb and was found to decay with a 17 (+14/-6) s half-life by emission of α particles with an average energy of 8.83±0.03 MeV. One atom of ^{266}Bh was observed, decaying within one second by emission of a 9.29-MeV α particle [13].

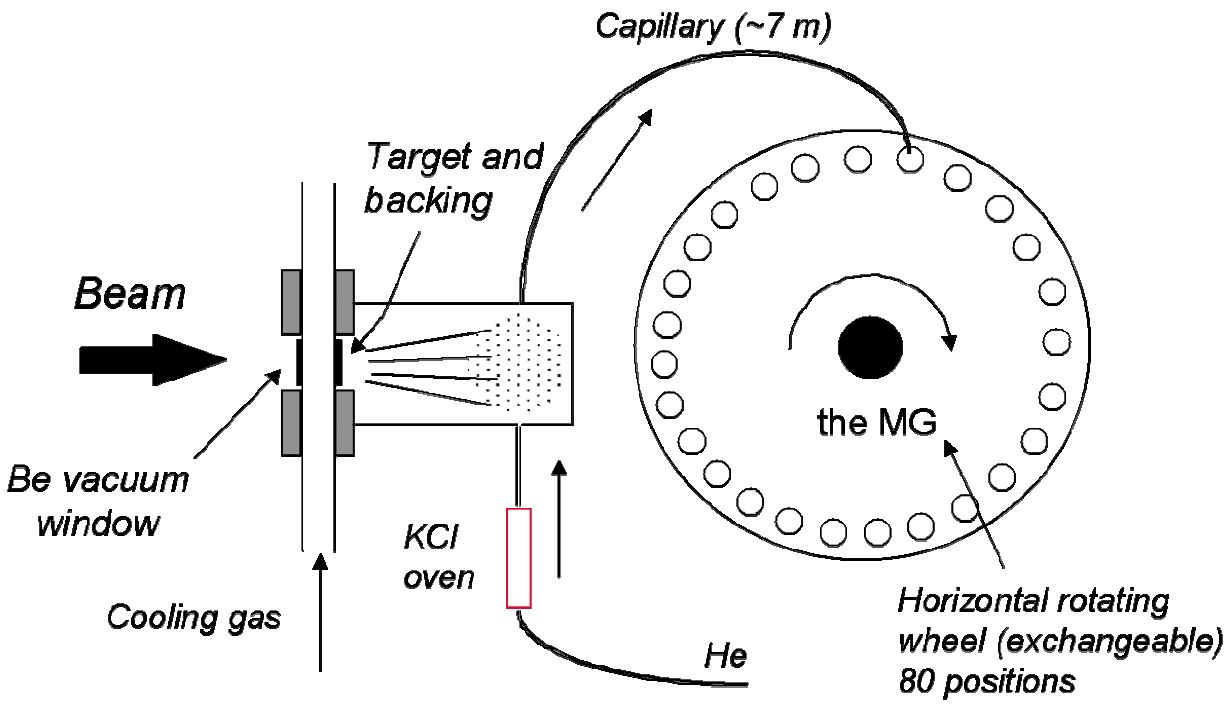

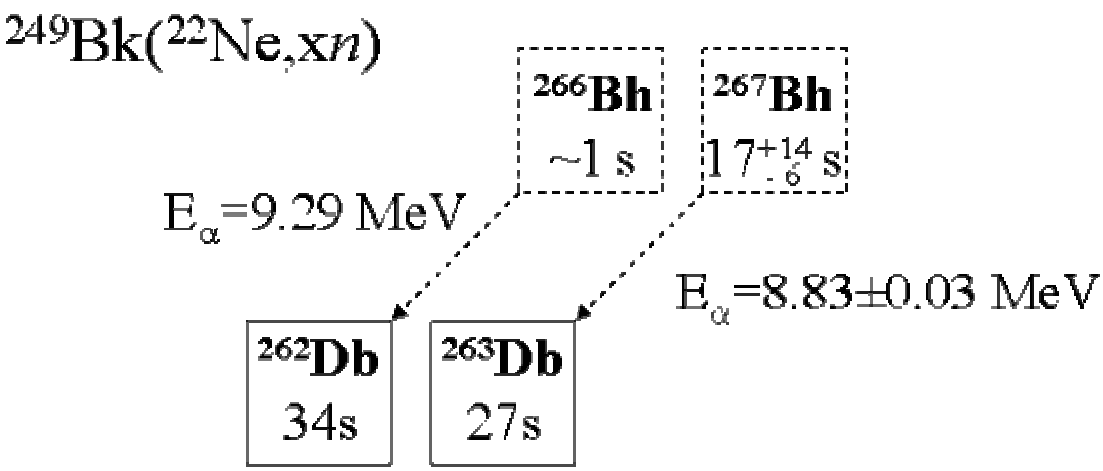

The chemistry of bohrium

The arrangement of the chemical elements in the periodic table indicates similarities of chemical properties, which reflect the elements' electronic structure. For the heaviest elements, however,

deviations in the periodicity of chemical properties are expected due to relativistic effects. Bohrium is expected to be a group seven element and should form oxychloride species in the gas phase in an analogous fashion to rhenium and technetium. During test experiments with rhenium and technetium [14, 15] only one chemical species, assumed to be [Re/Tc]O_3Cl, was seen with the thermochromatography apparatus.

Pershina *et al.* predict that the electronic structure of BhO_3Cl should be very similar to TcO_3Cl and ReO_3Cl. The calculated energy gap (ΔE) and ionization potential (IP) increase from Tc to Bh for the MO_3Cl species. The 7+ oxidation state should also increase in stability down the group following the increasing ΔE. The Bh species is also more covalent than the other two species which they attribute to relativistic effects seen in the component atomic orbital [16, 17]. These effects also influence dipole moments and dipole polarizabilities, which should dominate intermolecular or molecule-surface interactions. These interactions are the basis for volatility that they expect should decrease down the group, i.e. that BhO_3Cl should be less volatile than ReO_3Cl which should be less volatile than TcO_3Cl.

Using the same reaction as for the previous experiment, a volatility experiment to study bohrium chemistry was performed at the Paul Scherrer Institute (PSI), Switzerland. The behavior of Bh was investigated at 180, 150, and 75°C. Two α-SF chains, two α-α chains, and one α-α-α decay chain, all attributed to the decay of ^{267}Bh, were observed at 180°C. At 150°C two α-SF chains were observed, and at 75°C no events were observed. Random correlations should not significantly contribute to the number of α-SF or α-α-α chains seen, but approximately one of the α-α correlations seen are expected to be due to random correlations. The unambiguous identification of Bh after chemical separation allows us to conclude that like its lighter homologues, Bh forms a volatile oxychloride compound, presumably BhO_3Cl, and behaves like a typical group seven element [18]. We found that this compound is less volatile than the oxychlorides of the lighter elements of group VII, thus confirming predictions based on its periodic position.

Assuming the Bh compound to be BhO_3Cl and applying a microscopic model of the adsorption-desorption process [19] and using the Monte Carlo code developed by Türler to fit the measured volatility curves, the evaluated standard adsorption enthalpy (ΔH_{ads}) of BhO_3Cl on the quartz surface was determined to be-75(+9/-6) kJ/mol. The adsorption enthalpies for TcO_3Cl and ReO_3Cl are -51±3 and -61±3 kJ/mol respectively [15]. After the quartz column, BhO_3Cl was transported to ROMA on CsCl aerosols. Unlike ReO_3Cl, TcO_3Cl is so volatile that it can not be transported with CsCl, which again indicates Bh is more like Re than Tc.

Conclusion

Bohrium has been placed decisively on the periodic table and periodic extrapolations confirmed. This first chemistry experiment with bohrium would have been impossible without an adequate candidate isotope of bohrium. These experiments were also reliant on the theoretical predictions of the chemical properties of bohrium and the theoretical predictions of the production and decay properties of the anticipated heavier isotopes of bohrium. These experimental data that we have generated, can now be re-applied to the theory to further fine-tune and increase our understanding of the fundamental processes at work [20,21]. In addition, the target material was provided by Office of Science, Office of Basic Energy Research, Division of Chemical Sciences, of the U.S. Department of Energy, through the transplutonium element production program at the Oak Ridge National Laboratory. The culmination of this collaboration, by the successful determination of the chemistry of bohrium, was only possible by the joint efforts of all the members from many different organizations.

References

[1] G. Münzenberg, S. Hofmann, F. P. Heßberger, W. Reisdorf, K. H. Schmidt, J. H. R. Schneider, P. Armbruster, Z. Phys. A **300**, 107 (1981).

[2] G. Münzenberg, P. Armbruster, S. Hofmann, F. P. Heßberger, H. Folger, J. G. Keller, V. Ninov, K. Poppensieker, A. B. Quint, W. Reisdorf, K. H. Schmidt, J. H. R. Schneider, H. J. Schött, K. Sümmerer, I. Zychor, M. E. Leino, D. Ackermann, U. Gollerthan, E. Hanelt, W. Morawek, D. Vermeulen, Y. Fujita, T. Schwab, Z. Phys. A **333**, 163 (1989).

[3] S. Hofmann, V. Ninov, F. P. Heßberger, P. Armbruster, H. Folger, G. Münzenberg, H. J. Schött, A. G. Popeko, A. V. Yeremin, A. N. Andreyev, S. Saro, R. Janik, M. Leino, Zeitschrift für Physic A **350**, 281 (1995).

[4] I. Zvara, V. P. Domanov, Z. Khyubener, M. R. Shalavskii, S. N. Timokhin, B. L. Zhuikov, B. Aikhler, G. V. Buklanov. Soviet Radiochemistry **26**, 72 (1984); translated from Radiokhimiya **26**, 76 (1984), in russian.

[5] M. Schädel, Radiochimica Acta **70/71**, 207 (1995).

[6] R. Smolańczuk, J. Skalski, and A. Sobiczewski, Physical Review C **52**, 1871 (1995).

[7] Y. Hatsukawa, H. Nakahara, D. C. Hoffman, Physical Review C **42**, 674 (1990).

[8] A. Ghiorso, M. Nurmia, K. Eskola, P. Eskola, Physical Review C **4**, 1850 (1971).

[9] J. V. Kratz, M. K. Gober, H. P. Zimmermann, M. Schädel, W. Brüchle, E. Schimpf, K. E. Gregorich, A. Türler, N. J. Hannink, K. R. Czerwinski, B. Kadkhodayan, D. M. Lee, M. J. Nurmia, D. C. Hoffman, H. Gäggeler, D. Jost, J. Kovacs, U. W. Scherer, A. Weber, Phys. Rev. C **45**, 1064 (1992).

[10] K. E. Gregorich, H. L. Hall, R. A. Henderson, J. D. Lebya, K. R. Czerwinski, S. A. Kreek, B. A. Kadkhodayan, M. J. Nurmia, D. M. Lee, D. C. Hoffman, Physical Review C **45**, 1058-1063 (1992).

[11] H. W. Gäggeler, *et al.*, Paul Scherrer Institut Condensed Matter Research and Material Sciences Progress Report 1993, Annex IIIA Annual Report, Villigen, Switzerland, 92 (1994).

[12] K. E. Gregorich, M. R. Lane, M. F. Mohar, D. M. Lee, C. D. Kacher, E. R. Sylwester, and D. C. Hoffman. Phys. Rev. Lett. 72, 1423-6 (1994).

[13] P. A. Wilk, K. E. Gregorich, A. Türler, C. A. Laue, R. Eichler, V. Ninov, J. L. Adams, U. W. Kirbach, M. R. Lane, D. M. Lee, J. B. Patin, D. A. Shaughnessy, D. A. Strellis, H. Nitsche, and D. C. Hoffman, Physical Review Letters **85**, 2697 (2000).

[14] R. Eichler, B. Eichler, H. W. Gäggler, D. T. Jost, R. Dressler, A. Türler, Radiochimica Acta **87**, 151 (1999).

[15] R. Eichler, B. Eichler, H. W. Gäggleler, D. T. Jost, D. Piguet, A. Türler, Radiochimica Acta **88**, 87 (2000).

[16] V. Pershina, T. Bastug, Journal of Chemical Physics **113**, 1441 (2000).

[17] E. Johnson, B. Fricke, T. Jacob, C. Z. Dong, S. Fritzche, V. Pershina, Journal of Chemical Physics **116**, 5 (2002).

[18] R. Eichler, W. Brüchle, Ch. Düllmann, R. Dressler, B. Eichler, H.W. Gäggeler, K.E. Gregorich, T. Häfeli, U. Kirbach, D.C. Hoffman, S. Hübener, D.T. Jost, V.M. Lavanchy, C.A. Laue, H. Nitsche, J. Patin, D. Piguet, M. Schädel, D. Strellis, S. Taut, L. Tobler, Y. Tsyganov, A. Türler, A.Vahle, P.A. Wilk, A.B. Yakushev, P. Zimmermann, Nature **407**, 63 (2000).

[19] I. Zvara, Radiochimica Acta 38, 95 (1982).

[20] M. S. Mehta, B. K. Raj, S. K. Patra, R. K. Gupta, Physical Review C **66**, 044317 (2002).

[21] S. Liran, A. Marinov, N. Zeldes, Physical Review C **66**, 024303 (2002).

[This page was left blank intentionally.]

Nuclear Reaction Experiments

[This page was left blank intentionally.]

The current status and future of transactinide heavy element production

Yu.Ts. Oganessian[1]

[1] Joint Institute for Nuclear Research, Russia

oganessian@flnr.jinr.ru

[Abstract not available at time of printing]

Reaction studies and the synthesis of superheavy elements at GSI

D. Ackermann[1,2]

[1] Johannes Gutenberg Universität Mainz, Germany
[2] GSI, Germany

d.ackermann@gsi.de

Introduction

The search for superheavy elements, predicted close to the double magic nucleus ^{298}114 [1] was a substantial motivation for the construction of the UNILAC and the velocity filter SHIP [2] at GSI in Darmstadt. Following the concept of "cold" fusion of lead or bismuth targets with medium heavy projectiles like ^{40}Ar or ^{50}Ti, first applied successfully by Oganessian et al [3], the SHIP group succeeded to produce and identify about 25 new isotopes with atomic numbers from Z=98 up to Z=112. Mutual interaction of experimental results and theoretical calculations led to a better understanding of their stability, while measured excitation functions allowed for a reliable empirical extrapolation of optimum bombarding energies and cross sections for 1n de-excitation channels. Continuous technical development pushed the sensitivity of the set-up down to a cross section value of about 1 pb. To proceed towards higher Z an extensive development program is being followed at present. Recently the synthesis of isotopes of the elements 114 and 116 has been reported at Dubna. The unambiguous assignment of those events, however, is not yet possible. A recent review on the discovery of the heaviest elements [4] gives a complete overview over the recent achievements in the field. There can also be found a detailed description of the experimental set-up at GSI.

Recent results on the synthesis of heavy elements with Z=110-112

The elements with Z=107-112 have been synthesized and unambiguously identified at SHIP. The elements 107-109 have already been named and have been entered as Bohrium (Bh, Z=107), Hassium (Hs, Z=108) and Meitnerium (Mt, Z=109) in the periodic table of elements. The properties found for the elements 110, 111 and 112 are presented in this section. In an experiment in November 1994 four α-decay chains were observed, which were attributed to the isotope with the mass number 269 of the new element 110 [5]. The production cross section was $\sigma=3.5(^{+2.7}_{-1.8})$pb. In a directly following experiment in November/December 1994 the ER production by the reaction ^{64}Ni + ^{208}Pb was investigated at E^*=(8-13)MeV. Nine α-decay chains observed in this experiment could be attributed to ^{271}110. A maximum cross section of $\sigma=15(^{+9}_{-6})$pb was measured at E^*=12.1MeV. In an experiment in October 2000 we observed in the reaction ^{64}Ni + ^{207}Pb eight decay chains of correlated ER-α-fission events which we attribute to the decay of the new isotope ^{270}110. Also the daughter and grand daughter products ^{266}Hs and ^{262}Sg have not been observed before [6]. On the basis of these encouraging results for the synthesis of element 110 in the reactions ^{62,64}Ni + ^{208}Pb the production of an isotope of element 111 by the reaction ^{64}Ni + ^{209}Bi was undertaken in December 1994. A total of three decay chains attributed to ^{272}111 was observed with a maximum cross section of $\sigma=3.5(^{+4.6}_{-2.3})$pb [7]. In the series of experiments performed in October 2000 we also confirmed the synthesis of ^{272}111 observing additional three decay chains of this isotope. In early 1996 using the projectile target combination ^{70}Zn + ^{208}Pb two decay chains which had been attributed to ^{277}112 were reported [7]. It was found later that one of the decay chains was spuriously generated [8]. In a recent

experiment in May 2000 a second decay chain of $^{277}112$ was recorded. It is shown together with the first chain from 1996 in Figure 1.

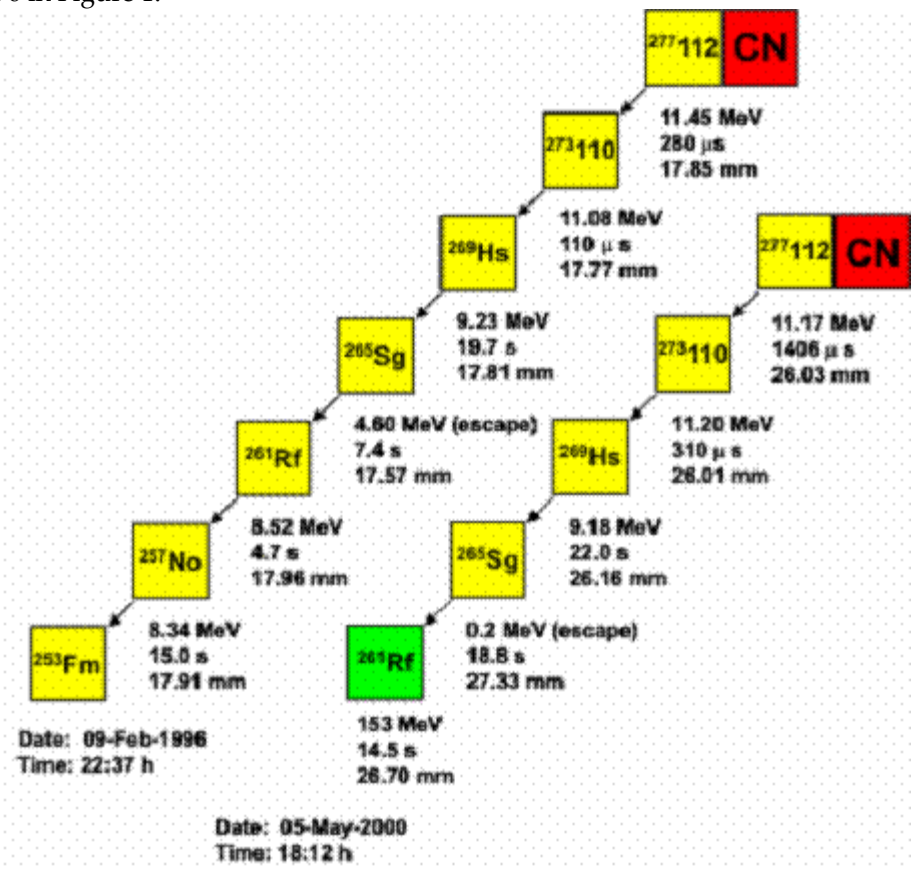

Figure 1. The two decay chains observed for $^{277}112$ in 1996 and 2000.

For this isotope a maximum cross section of $\sigma=0.5(^{+1.1}_{-0.4})$pb has been observed [8]. The chain observed in the second measurement ends with the fission of ^{261}Rf in difference to the first chain which ran all the way down to. Both decay modes of ^{261}Rf have been observed also in an experiment on the chemistry of Hs where this isotope was produced in the decay chain of ^{269}Hs [9] confirming our findings.

Reaction mechanism studies

The steep decrease with increasing Z of production cross section observed for reactions with Pb and Bi-targets and for previous reactions on actinide targets has been contrasted by recent observations made in Dubna. There decay chains have been seen in bombardments of ^{244}Pu and ^{248}Cm with ^{48}Ca projectiles, which were interpreted as the decay of $^{288}114$ [10] and $^{292}116$ [11] with a more less constant production cross section of about 1pb. According to recent self-consistent calculations [12] these nuclei are close to the region where a stabilisation due to shell effects can be expected. However, it was up to now not possible to detect an increasing production cross section for heavy ER's with magic proton or neutron numbers [13,14,15]. For medium to heavy masses it has been shown that nuclear structure and nuclear deformation are important ingredients for the formation of the compound system [16,17]. We have started a program to examine the reaction mechanism in the vicinity of the closed proton shell at Z=82 and N=126 using the partial wave (spin) distribution σ_ℓ [18]. It has been shown that one can extract from the spin distribution information on the barrier structure for heavy ion collisions [19]. Moreover, it yields

information on the single partial wave cross sections and can reveal effects at high angular momentum, which might hint at a stabilisation due to shell effects as shown schematically in Figure 2.

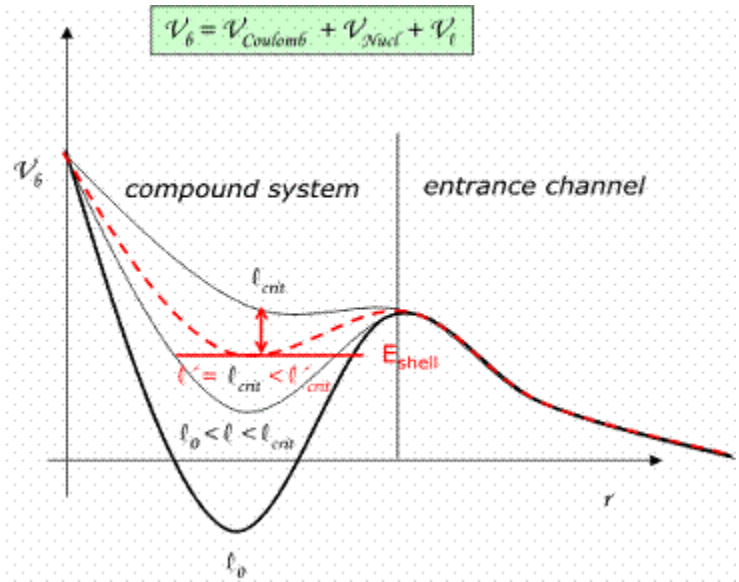

Figure 2. Cartoon illustrating the effect of a shell correction energy E_{shell} on the critical angular momentum for fusion l_{crit}.

Technical development at SHIP

The three areas presently under technical investigation at SHIP are beam development, target development and background reduction. To access a region of lower cross section the number of interactions and, therefore, the number of projectiles has to be increased. The UNILAC at GSI delivers the beam with a duty cycle of about 28%. Apart from raising the beam current, the use of an accelerator with 100% duty cycle (DC) would already provide a factor of 3.5 in higher beam intensity. The ongoing progress in the development of high frequency (28GHz) ECR ion sources promises an increase in beam intensity of another factor of 2-10. The increased beam current, together with a higher Z of the projectiles in some cases, asks for measures to protect the Pb and Bi targets, both having a low melting point. A first step is to spread the beam as homogeneous as possible over a maximum area. With the target wheel presently in use we have already reached the limit for the presently available beam intensities. The introduction of ion optical elements like octupole magnets in the UNILAC beam-line will help to approach the desired optimum of a rectangular beam profile, illuminating the target as uniformly as possible. Besides those "passive" measures also an "active" target cooling is now under development. A set-up providing a gas jet blown onto the spot where the beam hits the target is currently being developed. Chemical compounds of Pb or Bi with higher melting temperatures are also under investigation. We have obtained first promising results with PbS foils sandwiched between two thin layers of carbon. The higher projectile rate required for a successful investigation of reactions with lower cross section will have as a consequence an increase of background per time unit. To improve the background suppression we test the use of foils to stop scattered beam particles which pass SHIP with low kinetic energy. The high energy particles can be suppressed more effectively by in increased deflection in the last magnetic dipole of SHIP.

Acknowledgments

The recent experiments were performed together with H.-G. Burkhard, F.P. Heßberger, S. Hofmann, B. Kindler, G. Münzenberg, B. Lommel, H.-J. Schött, P. Kuusiniemi (GSI Darmstadt), A.G. Popeko, A.V. Yeremin (FLNR-JINR Dubna), S. Antalic, P. Cagarda, R. Janik, Š. Šaro (University of Bratislava), J. Uusitalo and M. Leino (University of Jyväskylä).

References

[1] Meldner, H., Arkiv f. fysik **36**, 593-598 (1967).

[2] Münzenberg, G., Faust, W., Hofmann, S., Armbruster, P., Güttner, K., and Ewald, H., Nucl. Instrum. Meth. **161**, 65-82 (1979).

[3] Oganessian, Yu.Ts., Lecture Notes in Physics **Vol. 33**, edited by H.L. Harney, P. Braun-Munzinger, and C.K. Gelbke, Berlin, Heidelberg, New York: Springer, 1974, pp. 221-252.

[4] Hofmann, S., and Münzenberg, G., Rev. Mod. Phys. **72**, 733 (2000).

[5] Hofmann, S., Ninov, V., Heßberger, F.P., Armbruster, P., Folger, H., Münzenberg, G., Schött, H.-J., Popeko, A.G., Yeremin, A.V., Andreyev, A.N., Šaro, S., Janik, R., and Leino, M., Z. Phys. A **350**, 277-280 (1995).

[6] Hofmann, S., Heßberger, F.P., Ackermann, D., Antalic, S., Cagarda, P., Ćwiok, S., Kindler, B., Kojouharova, J., Lommel, B., Mann, R., Münzenberg, G., Popeko, A.G., Šaro, S., Schött, H.-J., and Yeremin, A.V., Eur. Phys. J. A **10**, 5-100 (2001).

[7] Hofmann, S., Ninov, V., Heßberger, F.P., Armbruster, P., Folger, H., Münzenberg, G., Schött, H.-J., Popeko, A.G., Yeremin, A.N., Šaro, S., Janik, R., and Leino, M., Z. Phys. **A354**, 229-230 (1996).

[8] Hofmann, S., Heßberger, F.P., Ackermann, D., Münzenberg, G., Antalic, S., Cagarda, P., Kindler, B., Kojouharova, J., Leino, M., Lommel, B., Mann, R., Popeko, A.G., Reshitko, S., Šaro, S., Uusitalo, J., and Yeremin, A.V., Eur. Phys. J. A **10**, 5-100 (2001).

[9] Düllmann, Ch.E., Brüchle, W., Dressler, R., Eberhardt, K., Eichler, B., Eichler, B., Gäggeler, H.W., Ginter, T.N., Glaus, F., Gregorich, K.E., Hoffmann, D.C., Jäger, E., Jost, D.T., Kirbach, U.W., Lee, D.M., Nitsche, H., Patin, J.B., Pershina, V., Piguet, D., Qin, Z., Schädel, M., Schausten, B., Schimpf, E., Schött, H.-J., Soverna, S., Sudowe, R., Thörle, P., Timokhin, S.N., Trautmann, N., Türler, A., Vahle, A., Wirth, G., Yakushev, A.B., and Zielinski, P.M., Nature **418**, 859-862 (2002).

[10] Oganessian, Yu.Ts., Utyonkov, V.K., Lobanov, Yu.V., Abdullin, F.Sh., Polyakov, A.N., Shirokovsky, Yu.S., Tysganov, Yu.S., Gulbekian, G.G., Bogomolov, S.L., Gikal, B.N., Mezentsev, A.N., Iliev, S., Subbotin, V.G., Suhkov, A.M., Ivanov, O.V., Buklanov, G.V., Subotic, K., and Itkis, M.G., Phys. Rev. **C62**, 041604(R) (2000).

[11] Oganessian, Yu.Ts., Utyonkov, V.K., Lobanov, Yu.V., Abdullin, F.Sh., Polyakov, A.N., Shirokovsky, Yu.S., Tysganov, Yu.S., Gulbekian, G.G., Bogomolov, S.L., Gikal, B.N., Mezentsev, A.N., Iliev, S., Subbotin, V.G., Suhkov, A.M., Ivanov, O.V., Buklanov, G.V., Subotic, K., and Itkis, M.G., Phys. Rev. **C63**, 011301(R) (2001).

[12] Bender, M., Nazarewicz, W., Reinhard, P.-G., Phys. Lett. B **515**, 42-48 (2001).

[13] Vermeulen, D., Clerc, H.G., Sahm, C.C., Schmidt, J.G. Keller, K.-H., Münzenberg, G., and Reisdorf, W. Z. Phys. **A318**, 157-69 (1984).

[14] Junghans, A. R., de Jong, M., Clerc, H.-G., Ignatyuk, A.V., Kudyaev, G. A, Schmidt, K.-H. Nucl. Phys. **A629**, 635-655 (1998).

[15] Heinz, A., Schmidt, K.-H., Junghans, A.R., Armbruster, P., Benlliure, J., Böckstiegel, C., Clerc, H.-G., Grewe, A., de Jong, M., Müller, J., Pfützner, M., Steinhäuser, S., and Voss, B. submitted to Nucl. Phys. A.

[16] Dasgupta, M., Hinde, D.J., Rowley, N., and Stefanini, A.M., Ann. Rev. Nucl. Part. Sci. **48**, 401- (1998).
[17] Morton, C.R., Berriman, A.C., Butt, R.D., Dasgupta, M., Godley, A., Hinde, D. J., and Newton, J. O., Phys. Rev. **C62**, 024607 (2000).
[18] Ackermann, D., proceedings 284. WE-Heraeus-Seminar Symposium on Nuclear Clusters: from Light Exotic to Superheavy Nuclei, Rauischholzhausen, Germany, August 5-9 2002, to be published in Heavy Ion Physics, Budapest, Hungary, and by EP Systema Bt., Debrecen, Hungary.
[19] Ackermann, D., Acta Phys. Pol. B **26**, 517(1995).

Status and future of transactinide reaction experiments at RIKEN

K. Morita[1]

[1] Cyclotron Center, RIKEN, Japan

morita@rarfaxp.riken.go.jp

[Abstract not available at time of printing]

Sub-barrier fusion in the ^{48}Ca + ^{208}Pb reaction

W.D. Loveland[1], J.B. Patin[2], D. Peterson[1], K.E. Gregorich[2], N. Myers[1], P. Miranda[1], T.N. Ginter[2], K. Aleklett[3]

[1] Oregon State University, USA
[2] Lawrence Berkeley National Laboratory, USA
[3] Uppsala University, Sweden

lovelanw@ucs.orst.edu

The study of the heaviest elements offers one an opportunity to study nuclear structure and nuclear dynamics under the influence of large Coulomb forces. Many years ago, Oganessian recognized the special importance of the doubly magic ^{208}Pb in the synthesis of the heaviest elements [1]. He showed the low excitation energies of the compound nuclei in reactions with ^{208}Pb or ^{209}Bi targets (so-called "cold fusion") (Figure 1) could be utilized to produce heavy nuclei via reactions like ^{208}Pb(X,n) or ^{209}Bi(X,n).

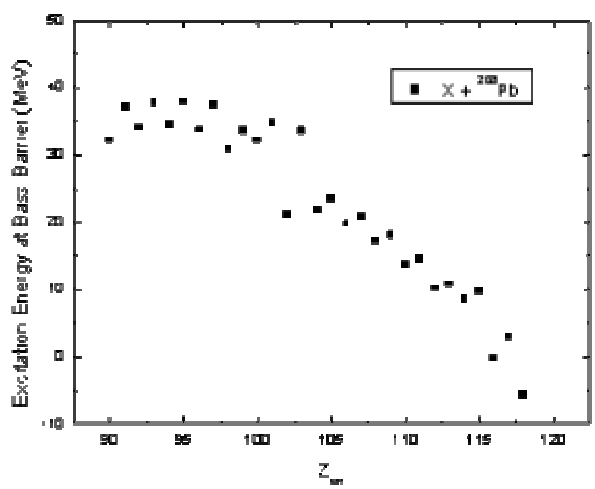

Figure 1. Excitation energies at the Bass barrier for reactions with ^{208}Pb targets.

Using this cold fusion approach, elements 107-112 were successfully synthesized at GSI [2]. The cross sections for these reactions decreased sharply with increasing Z. Attempts to produce element 113 using the cold fusion reaction ^{209}Bi(^{70}Zn,n) were not successful [2] with an upper limit cross section of 0.6 pb. Attempts to produce element 118 using the ^{208}Pb(^{86}Kr,n) reaction were also unsuccessful [3] with an upper limit cross section of ~ 0.2 pb. These findings have generally been taken to indicate the need for significant technical advances before further element synthesis with cold fusion reactions is feasible.

The reaction of the two doubly magic nuclei, ^{48}Ca and ^{208}Pb is one of the most interesting and experimentally challenging cold fusion reactions. The optimal excitation energy for a "1n" reaction is about 13 MeV. As seen in Figure 1, this requires a reaction that occurs significantly below the fusion barrier for the ^{48}Ca + ^{208}Pb system. We report an experimental study of the cold fusion reaction ^{208}Pb(^{48}Ca,n) and a search for the occurrence of the radiative capture reaction ^{208}Pb(^{48}Ca,γ). This study was

undertaken to better understand the capture and fusion probabilities in cold fusion reactions involving n-rich projectiles that might be of interest in the synthesis of heavy nuclei.

The reaction of ^{48}Ca with ^{208}Pb has been extensively studied [4-17,27] , especially the ^{208}Pb(^{48}Ca,2n) reaction. Some of these experimental studies have used this reaction to do nuclear spectroscopy of the transfermium nuclei [10,13-15] but most studies have dealt with measuring cross sections for this reaction. Extensive measurements also exist for the related reaction of ^{48}Ca with ^{206}Pb [18]. For the ^{208}Pb(^{48}Ca,n) reaction, cross sections of <27, 260 ± 30and 180 ± 53 nb have been reported for projectile energies of 208, 212, and 216 MeV, respectively.[7] To the best of our knowledge, no previous measurements of the radiative capture cross section have been made for this system

The reaction of ^{48}Ca with ^{208}Pb was studied at the 88-Inch Cyclotron of the Lawrence Berkeley National Laboratory, using the Berkeley Gas-filled Separator (BGS) [19]. The experimental apparatus was a modified, improved version of the apparatus used in [19], including improved detectors and data acquisition system, continuous monitoring of the separator gas purity, and better monitoring of the ^{48}Ca beam intensity and energy. A $^{48}Ca^{10+}$ beam was accelerated to various energies at typical beam currents of ~ 200 particle nanoamperes. The beam went through the 0.040 mg/cm^2 carbon entrance window of the separator and struck a ^{208}Pb target placed 0.5 cm downstream from the window. The targets were 460 mg/cm^2 thick (sandwiched between 35 mg/cm^2 C on the upstream side and <9 mg/cm^2 C on the downstream side). Nine of them were mounted on a wheel that rotated at 300 rpm. Beam energies at the center of the target were determined using the range-energy data of Hubert et al.[20] The beam intensity was monitored by two silicon detectors (mounted at ± 27° with respect to the incident beam) that detected elastically scattered beam particles from the target. Attenuating screens were installed in front of these detectors to reduce the number of particles reaching them (and any subsequent radiation damage to the detector.) The run lasted 60 hours.

The EVRs (E ~ 40 MeV) were separated spatially in flight from beam particles and transfer reaction products by their differing magnetic rigidities in the gas-filled separator. The separator was filled with helium gas at a pressure of 0.8 torr. For all the measurements, the magnetic field of the separator was set to 2.107 Tm, a setting that produced an optimum distribution of the EVRs on the focal plane detector for the ^{208}Pb(^{48}Ca, 2n)^{254}No reaction. (Using the semi-empirical relationships in [5] would give a predicted value of the optimum Br of 2.099 Tm). The efficiency of the separator for transport of recoils from the target to the focal plane detector was measured to be 57% for the reaction of 200 MeV ^{48}Ca with ^{176}Yb, assuming a cross section for this reaction of ~ 790 mb. (This latter value was extrapolated from the measured data of Sahm, et al. [21]). Monte Carlo simulations of the ion optics of the BGS [3] are consistent with this value (51%). We measured a transport efficiency of 45% for the reaction of 215 MeV ^{48}Ca + ^{208}Pb $\rightarrow$ ^{254}No + 2n. (This efficiency is based on a cross section for the ^{208}Pb^{48}Ca, 2n) reaction of 3.4 mb. [7] This value of the efficiency was used in all calculations.

In the focal place region of the separator, the EVRs passed through a 10 cm x 10 cm parallel plate avalanche counter (PPAC) [22] that recorded the time, DE, and x,y position of the particles. This PPAC has an approximate thickness equivalent to 0.6 mg/cm^2 of carbon. The time-of-flight of the EVRs between the PPAC and the focal plane detector was measured. The PPAC was used to distinguish (97.5 - 99.5% efficiency) between particles hitting the focal plane detector that were beam-related and events due to the decay of implanted atoms.

After passing through the PPAC, the recoils were implanted in a 32 strip, 300 mm thick passivated ion implanted silicon detector at the focal plane that had an active area of 116 mm x 58 mm. The strips were position sensitive in the vertical (58 mm) direction. The position resolution along each strip was measured to be 0.70 mm for recoil-a correlations in the ^{208}Pb(^{48}Ca,3n) reaction. The energy response of each strip of the focal plane detector was calibrated using implanted recoils. An average energy resolution of ~ 40 keV for 5-9 MeV a-particles was measured for this detector.

In searching for the cold radiative capture channel $^{208}Pb(^{48}Ca,\gamma)$, one must be cautious not to confuse the decay of 2.91s ^{256}No (E_α=8.448, 8.402 MeV) with the decay of 2.3 s ^{252}No (E_α=8.42, 8.37 MeV). (^{252}No can be produced by the $^{208}Pb(^{48}Ca,4n)$ reaction or by the $^{206}Pb(^{48}Ca,2n)$ reaction from any ^{206}Pb impurities in the ^{208}Pb target). These channels can be resolved by either looking at EVR-α-α correlations for the ^{252}No decay which leads to 36s ^{248}Fm (E_α=7.87,7.83 MeV) rather than the 25.4 hr ^{252}Fm (from the ^{256}No) or by looking for the more prevalent spontaneous fission branch of the ^{252}No (SF 26.9%) vs an SF branch of 0.53% for ^{256}No. In addition, the $^{208}Pb(^{48}Ca,4n)$ reaction is energetically forbidden for projectile energies less than 223 MeV.

In studying the product of the $(^{48}Ca,n)$ reaction, ^{255}No, one must be careful to disentangle the decay of ^{255}No ($t_{1/2}$=3.1 min, E_α 7927, 8007, 8077, 8121 keV), ^{254}No ($t_{1/2}$=55s, E_α=8093 keV) and ^{253}No($t_{1/2}$=1.7 min, E_α=8010 keV). We used two approaches to this decay curve resolution. At the higher energies, we used the 7927 line to calculate the cross section after resolving its decay curve while at the lower energies, we resolved the complex decay curves.

For center of target projectile energies of 204, 206.5, 207.8, 209.1, and 211.6 MeV with associated particle doses of 2.50 x 10^{16}, 2.40 x 10^{16}, 1.90x10^{16}, 3.50x10^{16}, and 4.90x10^{16}ions, no events corresponding to the production of ^{256}No were observed. This corresponds to one-event upper limit cross sections of 134, 139, 176, 95 and 68 pb, respectively.

Heavy ion radiative capture has been observed previously [23] and was the basis for an unsuccessful attempt to synthesize element 116 using the $^{208}Pb(^{82}Se,\gamma)$ reaction [2]. Two mechanisms for a possible cold radiative capture reaction of the type $^{208}Pb(^{48}Ca,\gamma)$ are fusion of the projectile and target nuclei in which the giant dipole resonance (GDR) of the compound system is excited and decays by the emission of GDR photons or production of a completely fused system whose (E*,J) are within one neutron binding energy of the yrast line, leading to a γ-ray cascade down to the ground state without particle emission. The latter possibility for the ^{208}Pb + ^{48}Ca reaction seems less likely given the data of Reiter et al.[15]who showed the entry distributions in the (E*,J) plane for the $^{208}Pb(^{48}Ca,2n)$ reaction at a similar energy (~ 215 MeV) are sharply tilted relative to the yrast line, suggesting that the initial compound system states do not fulfill the condition of being within one neutron binding energy of the yrast line.

The giant dipole resonance in ^{256}No should be around E* ~ 12-13 MeV, according to the systematic rule that the resonance position is given by 79 $A^{-1/3}$ [24] with a width of 4-6 MeV, which is similar to the range of excitation energies studied (E*=12-18 MeV) (neglecting the splitting of the GDR in the deformed ^{256}No). Thus, from an energetic point of view, decay by GDR photons was possible.

We can make some crude estimates to see if the observed upper limits for the radiative capture reaction are reasonable. If we write for the radiative capture cross section, $\sigma_{x,\gamma}$

$$\sigma_{x,\gamma}=\sigma_C \cdot P_{CN} \cdot W_\gamma$$

where σ_C is the capture cross section, P_{CN} the probability of going from the capture configuration to the completely fused configuration and W_γ is the probability of de-excitation by emission of GDR photons, we can make some order of magnitude estimates for the quantities involved to see if the failure to observe radiative capture is reasonable. The capture cross sections have been measured to be ~ 5 mb for the energy range in question [9], W_γ has been estimated to be 5 x 10^{-5} [23] and thus to get the observed upper limit cross section of 100 pb, we would need P_{CN} to be < 4 x 10^{-3}. Use of the semi-empirical estimates of P_{CN} in ref [25] for this case would give P_{CN} to be ~ 2 x 10^{-3} in agreement with the observed upper limit. Thus, because the centroid of the GDR resonance was 5-10 MeV below the Bass barrier for the reaction in question, our ability to observe cold radiative capture was reduced.

In Figure 2, we show the measured excitation function for the $^{208}Pb(^{48}Ca,n)^{255}No$ reaction along with a previous measurement. At projectile energies of 211.6 and 215.2 MeV (E*=18.6 and 21.7 MeV) , we are unable to resolve the decays of ^{255}No and ^{254}No with the entire decay curve being consistent with being

due to ^{254}No. . The peak cross section for the 1n channel is ~100 nb at a projectile energy of 209.1 MeV (E*=16.1 MeV). The capture cross section at this projectile energy is ~9 mb [9]. If we write the evaporation residue production cross section, σ_{EVR}, as

$$\sigma_{EVR}=\sigma_C \cdot P_{CN} \cdot W_{SUR}$$

then the product of P_{CN} and W_{SUR} is 1.1 x 10^{-5}. This estimate is interesting because it is a low value. Two possible ways of looking at this are as follows. If we take the estimates [26] of W_{SUR} ($=\Gamma_n/\Gamma_{total}$)=10^{-2} for ^{256}No excited to 16.1 MeV, then P_{CN} is 10^{-3} which is an unexpectedly large fusion hindrance for this reaction where Z_1Z_2=1640. On the other hand, if we use the semi-empirical systematics of Armbruster [25] for P_{CN}, we would estimate P_{CN} for this reaction to be 6 x 10^{-3} and a value of W_{SUR}=1.9 x 10^{-3} would result. We are attempting to resolve this ambiguity.

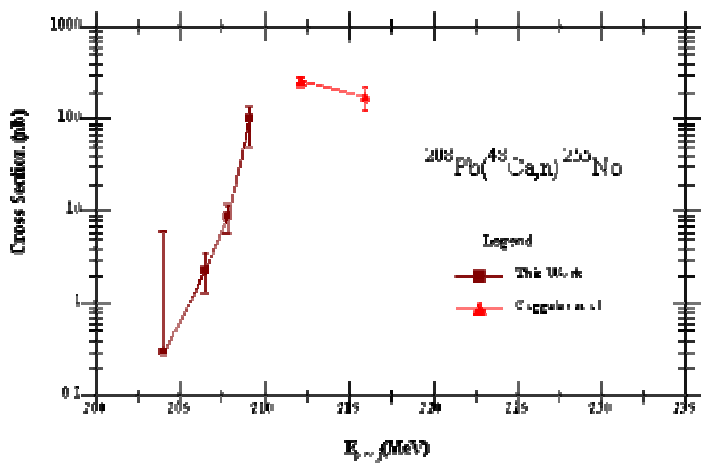

Figure 2. Measured cross sections for the ^{208}Pb(^{48}Ca,n) reaction.

References

[1] Y.T, Oganessian, A.S. Iljinov, A.G. Demin, and S.P.Tretyakova, Nucl. Phys. A239, 353 (1978).
[2] S. Hofmann and G. Münzenberg, Rev. Mod. Phys. 72,733 (2000).
[3] K.E. Gregorich, et al., Eur. Phys. J. A (submitted for publication).
[4] J.M. Nitschke, R.E. Leber, M.J. Nurmia and A. Ghiorso, Nucl. Phys. A313, 236 (1979).
[5] A. Ghiorso, S. Yashita, M.E. Leino, L. Frank, J. Kalnins, P.Armbruster, J.-P. Dufour, and P.K. Lemmertz, Nucl. Instru. Meth. A269,192 (1988).
[6] A. Türler, et al., Z. Phys.A331, 363(1988).
[7] H.W. Gäggeler, et al., Nucl. Phys. A502,561c (1989).
[8] Y. A. Lazarev, Y.V. Lobanov, R.N. Sagaidak, V.K. Utyonkov, M.Hussonnois, Y.P. Kharitonov, I.V. Shirokovsky, S.P. Tretyakova, and Y.T.Oganessian, Phys. Scr. 39, 422 (1989).
[9] A.J. Pacheco, et al., Phys. Rev.C45, 2861, (1992).

[10] P. Reitner, et al., AIP Conference Proceedings, Vol. 481, Nuclear Structure 98, (C. Baktash, ed.) (AIP, Woodbury, 1999).
[11] M.G. Itkis, et al., AIP Conference Proceedings, Vol 455, ENAM98, (B.M. Sherrill, D,J, Morrissey, and C.N. Davids, eds.) (AIP,Woodbury, 1998).
[12] M.G. Itkis, et al., Nuovo Cimento, 111A, 783(1998).
[13] P. Reiter, et al., Phys. Rev. Lett. 82, 509 (1999).
[14] M. Leino, et al., Eur. Phys. J A6, 63 (1999).
[15] P. Reiter, et al., Phys. Rev. Lett. 84, 3542(2000).
[16] M.G. Itkis, Y.T. Oganessian, and V.I. Zagrebaev, Phys. Rev. C65, 044602 (2002).
[17] M.G. Itkis, et al., J. Nucl. Radiochem. Sci. 3, 57 (2002).
[18] Y.T. Oganessian, et al., Proc. 4th Intl. Conf. Dynamical Aspects of Nuclear Fission, (World, Singapore, 2000) pp334-348.
[19] V. Ninov and K. E. Gregorich, ENAM98, edited by B.M. Sherrill, D.J. Morrissey, and C.N. Davids (AIP, Woodbury, 1999), p. 704.
[20] F.Hubert, R. Bimbot, and H. Gauvin, At. Data Nucl. Data Tables 46, 1 (1990).
[21] C.C. Sahm, et al., Nucl. Phys. A441, 316 (1985).
[22] D. Swan, J. Yurkon, and D.J. Morrissey, Nucl. Instru. Meth. Phys. Res. A 348, 314 (1994).
[23] A. Sandorfi, in Treatise on Heavy-Ion Science, Vol 2, D.A. Bromley. ed (Plenum, New York, 1984).
[24] A. Bohr and B.R. Mottelson, Nuclear Structure, Vol II (Benjamin, Reading, 1975) p.476.
[25] P. Armbruster, Rep. Prog. Phys. 62, 465 (1999).
[26] A.N. Andreyev, et al., in Heavy Ion Fusion: Exploring the Variety of Nuclear Properties (World, Singapore, 1994) p. 260.
[27] Y.T. Oganessian, et al., Phys. Rev. C64, 054606 (2001).

Production and study of super-heavy nuclei at GANIL

J. Péter[1], A. Drouart[2], C. Stodel[3]

[1] FULIS, Laboratoire de Physique Corpusculaire, France
[2] FULIS, SPhN - DAPNIA, France
[3] FULIS, GANIL, France

jpeter@in2p3.fr

In recent years, experiments on the production of super-heavy nuclei have been undertaken at Ganil, taking advantage of the powerful velocity filter LISE3 and the high intensity ECR ion sources. Some modifications were made to the velocity filter: - slits, a beam profiler and a Faraday cup were installed between its two identical halves –higher voltage power supplies were installed in order to accommodate experiments in reverse kinematics. A specific reaction chamber was built with large wheels (diameter: 60cm) rotating at 2000 RPM for targets and stripper foils, as well as smaller targets, oscillating stripper foils and elastic scattering target control. The detection chamber contains two MCP's for time-of-flight, two interchangeable implantation x-y Si detectors preceded by a Tunnel of 8 Si detectors and followed by a veto detector. The response, background and efficiency were checked with known reactions and decay chains (Sg isotopes): a background rejection factor of 2×10^{10} and an efficiency > 65 % were obtained.

Recently, a thin ionization chamber has been used in inverse kinematics reactions with a ^{208}Pb beam. The much larger kinetic energy pulse and the TOF provides a mass value. In addition, the IC signal allows us to get a nuclear charge value. Both values are rough but provide additional information on the implanted product. Indeed the identification of transfer products (actinides) through their alpha-chain is ambiguous when their half-life is so short that the alpha signal cannot be distinguished from the implantation signal. The charge signal make it possible to identify them. For a super-heavy nucleus, this direct information on the implanted residue strengthens much its identification via its decay chain. Work is in progress to extend this method to the case of usual kinematics with one single mylar foil: scintillation in a gas provides a signal proportional to the nuclear charge.

Results of planned experiments will be shown and discussed.

Status and future of the RIA project viz. transactinide elements

D.J. Morrissey[1]

[1] Michigan State University, USA

morrissey@nscl.msu.edu

Introduction

The Rare Isotope Accelerator (RIA) is an innovative, large-scale facility that will define the state-of-the-art for the production and use of exotic nuclei. The RIA facility will employ the best features of both projectile-fragmentation (in-flight techniques) and target-fragmentation (ISOL techniques) to provide the widest possible range of exotic nuclei to the nuclear physics community. The project to develop RIA consists of conceptual design as well as research and development studies in many laboratories across the United States. Significant contributions have been made by a very large number of people that, unfortunately, cannot be adequately covered in the present short presentation. In this contribution I will present a brief overview of the RIA facility with an emphasis on the new capabilities for neutron-rich secondary beams.

RIA accelerator

All of the older designs (before the mid-1990's) for the next generation exotic beam facility in the US were based (solely) on the ISOL concept of target fragmentation by light-ion beams (e.g., Nolen [1]). Three important facts emerged during the initial consideration of possible facilities: (A) very sensitive techniques were developed to study nuclear structure with low-intensity fast beams, (B) the limitations from ion-source chemistry on the range of shortest-lived and most exotic nuclei available from ISOL systems were not generally resolved, and most importantly, (C) the IGISOL concept [2], used to thermalize and collection low-energy reaction products, was extended to fast projectile fragments [3,4]. Thus, the scope of the RIA project was increased significantly so that the facility operation would encompass both in-flight and ISOL separation. The optimum production method will be used to produce each secondary beam rather than obtaining those secondary beams available from one or the other technique. This new approach requires the primary or driver accelerator to provide very intense beams of light ions to next-generation ISOL targets as well as intense beams of all heavier stable nuclei to projectile fragment separators. Low energy, target-fragment ions will be extracted from the ISOL targets and accelerated to low energies in the usual way. The high energy, projectile fragments will be delivered to a high-energy experimental arena as well as to a new low energy "ion source" based on new concept of buffer-gas thermalization and reacceleration of projectile fragments. Thus, there will be three different target areas for the primary beam: a set of high power ISOL targets feeding an isobar separator system feeding the low energy accelerator complex, a high intensity projectile fragmentation target with a high resolution fragment separator feeding the high energy complex, and another high intensity projectile fragmentation target with a high acceptance fragment separator connected through a gaseous-ion collector to the low energy complex. The resulting exotic nuclei will be available at four separate experimental regions (ion-source energy, below Coulomb barrier, near Coulomb barrier, and high energy) in order to service a large and diverse user community.

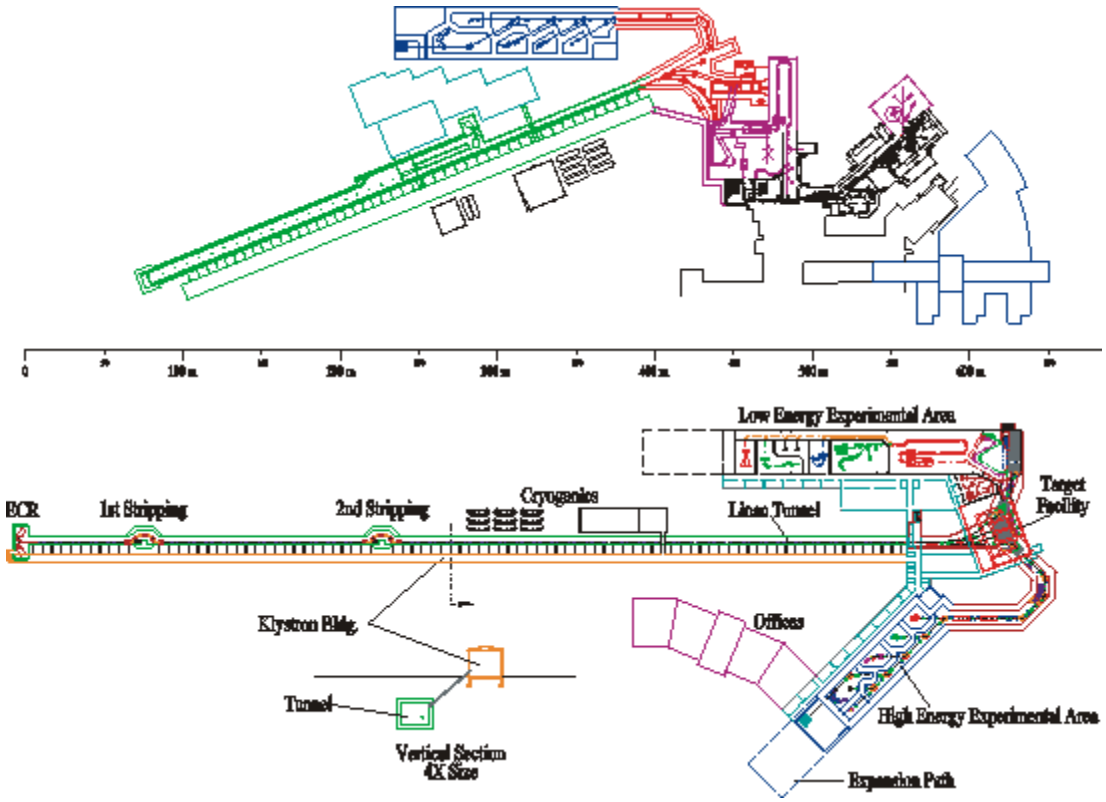

Figure 1. A comparison of the complete RIA facility at the Argonne site (above) and at the Michigan State site (below) at the time of the DoE cost analysis. Both designs contain the same capabilities and experimental areas.

The Nuclear Science Advisory Committee (NSAC) has given RIA the highest priority rating for new construction and has been put forward to the DoE Office of Science as ready for detailed design studies. Preliminary designs for the complete RIA facility have been prepared by the NSCL at Michigan State University and by Argonne National Lab. The schematic layouts of these facilities can be compared in Figure 1. Both layouts are dominated by the layout of the primary linear accelerator that provides beams with E/A ~500 MeV at 400kW up to A~40 and uranium with E/A~400 MeV at 150kW. One difference between the two proposed designs is that the existing ATLAS accelerator is incorporated into the Argonne layout whereas the MSU is a "green field" layout. The technical details of the ion sources, accelerator, target systems, fragment separators, and gas-catchers are being studied in a variety of laboratories around the US. A subcommittee of NSAC has reviewed an independent, bottoms-up cost analysis at the end of 2000. Another DoE panel chaired by Satoshi Otsaki just reviewed the progress on the R&D work in August of this year. An interesting aspect of the RIA accelerator proposed by Ken Shepard and collaborators at Argonne is to have the linac simultaneously accelerate an isotope in multiple charge states to provide very high intensities of the heaviest stable elements. The initial requirements for the experimental facilities and equipment have been prepared by the community [5,6] and have been incorporated into the designs.

Neutron-rich beam production

The neutron-rich beams that will be needed to try new synthetic routes to the heaviest elements will come from either traditional ISOL system or the new ion-collector system. At this point it is too early to

tell which technique will be the most useful but the demands of heavy-element research for the highest beam currents favor the ISOL approach. In the well-known ISOL light primary beams such as protons, deuterons, or ^{3}He beams hit thick production targets closely coupled to ion sources. The raw beams from the RIA ion sources are pre-separated and a small number of beams with nearby masses can be simultaneously delivered to a transport network that includes two high-resolution separators. The monoisotopic beams are then transported to either the low-energy experimental area or to the first stage of the post-accelerator. At present ISOL beam production is carried out with primary beam powers on the order of a few tens of kilowatts. The highest-power ISOL facility (20 kW) presently operational is the ISAC facility at TRIUMF in Canada. Concerted and very specific ISOL R&D work has been carried out for many years in Europe at the ISOLDE facility and elsewhere so that a lot of expertise exists in that community. The biggest challenge for ISOL at RIA is to build target systems that can make use of the order of the extremely high beam power. New ideas have been suggested such as converter systems that accept high-energy deuterons to release high-energy neutrons that go on to induce fission. Substantial R&D is required in order to answer key questions about how traditional and new targets can be build and operated in the ½ megawatt domain. Scaling the beam intensities from the present conditions has been used to obtain the yield predictions for the RIA secondary beams.

Fragment separators have developed significantly over the past decade, see for example [7], so that both of the devices planned for RIA will be next-generation superconducting fragment separators that go well beyond the best present day machines. For comparison, the resolving power and a figure of merit for the A1200 (now retired) and A1900 (recently completed) separators at the NSCL can be compared to the specifications of RIA separators in Table 1.

Table 1. Comparison of ion-optical properties of projectile fragment separators based on superconducting magnets. The resolving power is the dispersion divided by the product of the beam spots size and the magnification in the same coordinate (x). The dimensionless "figure of merit" used to categorize the separators is the product of the relative solid angle ($d\Omega/4\pi$), the momentum acceptance ($\Delta p/p$), and the resolving power.

	$\Delta p/p$ (%)	$d\Omega$ (msr)	$B\rho$ (Tm)	Resolving Power	Figure of Merit
NSCL A1200	+/-1.5	0.8	5.4	2400	0.5
NSCL A1900	+/-2.5	8	6	2900	10.2
RIA High Res.	+/-3	10	8	3000	14.3
RIA High Accpt.	+/-9	10	8	1000	14.3

The new approach for the production of thermalized exotic ions for nuclear structure studies has been pioneered at Argonne and at RIKEN based on ion stopping work at GSI [8]. Moderate [4] and fast [3] nuclear reaction products are stopped in large high-purity helium gas cells and extracted as singly-charged ions through the application of drift fields and gas flow. One of the important ingredients of the new concept is the incorporation of an energy-focusing ion-optical device that can compensate for the large momentum distribution of the projectile fragments. Such devices consist of a dispersive magnetic dipole stage and slowing-down of the fragments in specially shaped energy degraders [8]. The feasibility of momentum compensation, also called range bunching, has been recently demonstrated at the GSI-FRS and recently at Michigan State using pressures near one bar [9]. These results and further calculations have shown that the longitudinal range straggling of typical projectile fragments can be brought down to the level of the intrinsic straggling width of an equivalent monoenergetic beam which is, none the less, on the order of one-half meter of helium gas at one bar. The purity of the buffer gas leading to unwanted ion-molecule reactions has large effects on the efficiency of IGISOL systems as has been shown by the

Leuven group [10]. These neutralization and the many possible effects from the ionization plasma in the buffer gas still has to be fully understood for efficient operation of large-scale gas cells. However, it has been reported that the system operating at Argonne has an efficiency of close to 45% and extraction times below 10 milliseconds [4]. Any upper limit on the rate at which ions can be implanted and efficiently extracted from a large gas cell has yet to be experimentally determined. The total production yields from all of the various techniques have been analyzed by Jiang et al. [11] and various tables and figures are available to check the feasibility of experiments at RIA.

One of the interesting aspects of the study of nuclear reactions induced by radioactive beams is the possibility of using n-rich radioactive projectiles to synthesize new, neutron-rich heavy nuclei. It has been shown by Loveland [12] that new areas in the atomic physics and chemistry of the transactinide elements could be developed using intense n-rich radioactive beams. Various authors have suggested that there will be significant enhancements to the fusion cross sections for n-rich projectiles due to the lowering of the fusion barrier, the excitation of the soft dipole mode and the lowering of the reaction Q values for the more n-rich projectiles. The survival probability of the evaporation residues (EVRs) is also expected to increase due to their reduced fissionability and the lowered excitation energy. There is further speculatation that the use of these projectiles might lead to the successful synthesis of new or superheavy nuclei. Takigawa et al., [13] predict an enhancement of 10^5 in the fusion cross section for the $^{46}K + ^{238}U$ reaction compared to the $^{41}K + ^{238}U$ reaction and an increase of a factor of two in the survival probabilities for the EVRs. Experience from the synthesis of new heavy nuclei by non-radioactive n-rich projectiles shows that an increase of one unit in isospin of the projectile increases the heavy element production cross sections by a factor of 5 [14] so that even small changes in the isospin of the compound nucleus are important.

References

[1] J.A. Nolen, *ENAM98, Exotic Nuclei and Atomic Masses*, AIP Conference Proceedings **455** (American Institute of Physics, New York 1998) 952-959.

[2] P. Dendooven, et al., Nucl. Instrum. Meth. **B126** (1997) 182-189.

[3] M. Wada, et al., RIKEN Review No. 31 (December, 1999), p.56, unpublished, and Nucl. Instrum. Meth. **B204** (2003) 570-581.

[4] G. Savard, et al., Proc. APAC2000 Conf. Hyperfine Int. **132** (2001) 223, and Nucl. Instrum. Meth. **B204** (2003) 582-586.

[5] I.Y. Lee, Editor, *Proceedings of the Workshop on the Experimental Equipment for an Advanced ISOL Facility*, LBNL-42138, (1998), http://srfsrv.jlab.org/ISOL/ExpEquipWkShop.pdf

[6] M.R. Thoennessen, Editor, *Scientific Opportunities with Fast Fragmentation Beams from RIA* NSCL, Michigan State University, (2000), http://www.nscl.msu.edu/research/ria/whitepaper.pdf

[7] D.J. Morrissey and B.M. Sherrill, Phil. Trans. R. Soc. Lond. **A356** (1998) 1985-2006.

[8] H. Weick, et al., Nucl. Instrum. Meth. **B164-5** (2000) 168-179, and C. Schneidenberger, et al., Nucl. Instrum. Meth. **B204** (2003) 119-123.

[9] L. Weissman, et al., Nucl. Instrum. Meth., (2003), submitted for publication, and P.A. Lofy, Ph.D. dissertation, Michigan State University (2003).

[10] Y. Kudryavtsev, Rev. Sci. Instrum. **69** (1998) 738-740.

[11] C.L. Jiang, et al., Nucl. Instrum. Meth. **A492** (2002) 57-73.

[12] W. Loveland, *Proc. 3rd Int'l Conf. on Radioactive Nuclear Beams*, (Editions Frontieres, Gif-sur-Yvette, 1993), 526-536.

[13] N. Takigawa, H. Sagawa, and T. Shinozuka, Nucl. Phys. **A538** (1992) 221c.

[14] G. Munzenberg, Phil. Trans. R. Soc. London, **A356** (1998) 2083.

The RIA project and heavy element physics

J.A. Nolen[1]

[1] Physics Division, Argonne National Laboratory

nolen@anl.gov

An overview of the U.S. Rare Isotope Accelerator (RIA) Project is given in a companion paper by D.J. Morrissey at this conference. In this paper some specific capabilities of the proposed facility for research on the production and studies of heavy elements will be discussed. First, baseline count rate predictions for sample radioactive beams will be given, and then examples of possible enhancements of these capabilities will be presented.

In recent years there has been much discussion and speculation about the role of radioactive beams in research related to super-heavy elements. This paper will explore the capability of RIA to deliver precise and intense radioactive beams of neutron-rich fission products at Coulomb barrier energies for fusion reactions. The best mechanism for the production of such beams is the 2-step, neutron-generator configuration of the standard ISOL technique. The RIA driver will provide beams of protons, deuterons, or other light ions in the energy regime of 1 GeV with beam powers up to 400 kW. Providing the most intense reaccelerated beams for heavy element research using this method will require optimization of each step in the process. With reasonable assumptions about target, ion source, and post acceleration developments fission fragments near the peaks of the distributions, such as ^{132}Sn and ^{140}Xe, should be available with on-target intensities of 10^{10} to 10^{11} ions per second. The details of the various necessary efficiencies and developments necessary to reach these intensities will be discussed. Possible extensions of the method to intensities above 10^{11}/s will also be considered.

Using radioactive ^{132}Sn on stable targets, compared with stable beams on ^{208}Pb targets, the corresponding compound nuclei have 8 more neutrons at element 118 and 12 more at element 120, for example. Hence, the possibilities of increased production cross sections and longer half-lives of the more neutron-rich isotopes may overcome the 10-100 times weaker beam intensities. New instruments, such as the MASHA spectrograph currently being commissioned in Dubna, may be well suited to studies with radioactive beams such as the ones mentioned above. The post-accelerator RIA will also be able to provide intense CW beams of stable ions for measurements complementary to those with radioactive beams.

Research supported by the U. S. Department of Energy under contract W-31-109-ENG-38.

Synthesis and mass determination of heavy and superheavy nuclei at separator VASSILISSA

A.V. Yeremin[1], Y.T. Oganessian[1], A.G. Popeko[1], O.N. Malyshev[1], A.V. Belozerov[1], V.I. Chepigin[1], M.G. Itkis[1], A.P. Kabachenko[1], R.N. Sagaidak[1], A.V. Shutov[1], A.I. Svirikhin[1], S. Hofmann[2], S. Saro[3]

[1] Joint Institute for Nuclear Research, Russia
[2] Gesellschaft fuer Schwerionenforschung, Germany
[3] Comenius University, Slovak Republic

eremin@sunvas.jinr.ru

One of the criteria of the quality and reliability of the experimental results in the field of the synthesis of superheavy elements (atomic number $Z \geqslant 110$) is the reproducibility of the obtained data. Because the cross section values for the synthesis of elements with $Z \geqslant 110$ are at the level of picobarns and even lower it results in possible detection of one nucleus per few weeks using the presently available techniques. Another limiting point in attempts to reproduce presently obtained results is the problem of exact reproduction of the beam energy at the half - thickness of the target. The deviation of the beam energy of 1 % (typically 2 - 3 MeV) could lead to the reduction factor of 2 - 3 and to make the recurring ineffective. Until now only few experiments could be mentioned as successful repetition of previously obtained results. First are the experiments at the velocity filter SHIP aimed to the conformation of the synthesis of the isotopes ^{272}111 and ^{277}112 made earlier with the use of the same experimental set-up [1]. And second are the experiments performed at RIKEN with gas filled separator GARIS successfully repeated SHIP group experiments on the synthesis of the isotope ^{271}110 [2].

The study of the decay properties and formation cross sections of the isotopes of elements 110, 112 and 114 was performed employing high intensity ^{48}Ca beams and ^{232}Th, ^{238}U, ^{242}Pu targets [3,4,5] and the electrostatic separator VASSILISSA [6] during the years 1998 - 1999. At beam energies corresponding to the calculated cross section maxima of the 3n evaporation channels the isotopes ^{277}110, ^{283}112 and ^{287}114 were produced and identified (see also [7]).

Aiming at the continuation of the experiments on the synthesis and study of decay properties of superheavy nuclei with the use of accelerated ^{48}Ca beams and at the increasing the identification ability of the experiments the separator VASSILISSA was upgraded. For that purpose a new dipole magnet, having a deflection angle of 37 degrees, was installed behind the separator VASSILISSA replacing the old 8° magnet. The new magnet provides an additional suppression of unwanted reaction products and a possibility to have the mass resolution at the level of 1.5 -2 % for heavy nuclei with masses of about 300 amu.

The VASSILISSA separator with the new dipole magnet was tested with a number of heavy ion induced complete fusion reactions [8,9]. The evaporation residues produced in reactions of ^{40}Ar bombarding ions with ^{164}Dy and ^{208}Pb targets and of ^{44,48}Ca ions with ^{174}Yb, ^{198}Pt, ^{204,206,208}Pb targets were used in the analysis. Using ER - α and ER - SF correlation analysis for detected ER's TOF and strip number (that corresponds to the certain value of $B\rho$) were evaluated. Together with known value of magnetic field B of magnetic analyzer it was possible to evaluate A/Q values and for known A the charge distributions for investigated nuclei can be extracted. The results obtained for A/Q distributions of the ^{217}Th and ^{254}No ER's are shown in the following figure.

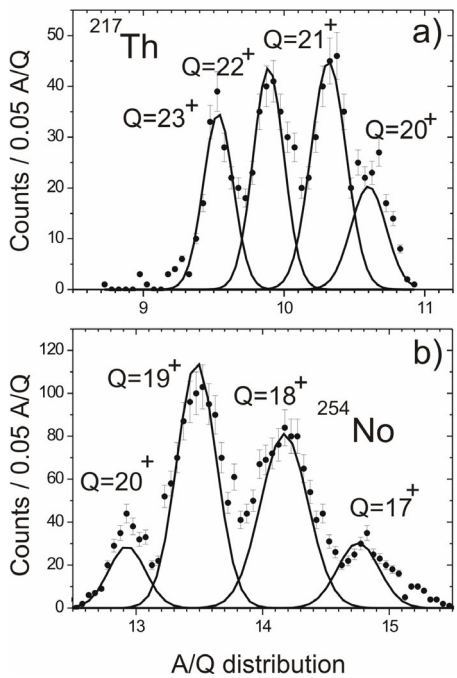

The first planned experiment in the field of superheavy elements with the use of upgraded separator was aimed to the synthesis of the isotope $^{283}112$. It was the first experiment with ^{48}Ca beams in 1998, focused to the synthesis of heaviest elements, and it became the basis for all other search experiments for synthesis elements with Z=114 - 118. An additional reason was the fact that the non-observation of any events in the reaction $^{48}Ca + ^{238}U \rightarrow ^{283}112^*$ studied with the BGS separator at Berkeley at the beam energy $E_{1/2}$=231 MeV in the half - thickness of the target was reported in [10].

Enriched ^{238}U (99.999 %) material was used for the preparation of the targets. The projectile energy was varied by extracting the beam from an appropriate radius of the cyclotron. The beam energy was determined by measuring the energy of the ions scattered at 30^0 in a thin (200 μg/cm^2) Au foil and with a time-of-flight technique. Beam energy values measured by both methods coincide within an interval of ± 1 MeV (± 0.5 %). An accuracy of the determination of the beam energy absolute value was tested using a magnetic spectrometer MSP144 and was about 0.5 % at the level of 243 MeV. The measured energy spread of the scattered ions was 1 % (FWHM).

At a beam intensity of $4 \cdot 10^{12}$ ions·s^{-1}, the total counting rate of all events at the focal plane detectors was 5 - 10 s^{-1}. The counting rate at a single strip in a position interval of 1.0 mm amounted to the following values; for the α - like signals (in the absence of signals from the TOF detectors) with an energy higher than 5.5 MeV - less than 0.075 h^{-1}; for the α - like signals with an energy of 0.5 - 5 MeV (signals corresponding to escaped α particles) - about 0.2 h^{-1}; for recoil - like (ER - like) signals (with a TOF signal) with an energy higher than 5 MeV and time of flight corresponding to heavy ER's (70 - 90 ns) - less than 0.1 h^{-1}.

After preparatory experiments, irradiation of the U target started at the beam energy $E_{1/2}$ =230 - 231 MeV in the middle of the target, which is close to that used in the previous experiment [3]. During a period of 29 days a beam dose of $5.91 \cdot 10^{18}$ projectiles was collected. No SF events were detected during this irradiation. In addition, possible decay chains of the ER $\rightarrow$ $\alpha \rightarrow \alpha 1 \rightarrow \alpha 2$ type were searched for within time intervals 5 μs < t < 1000 s and 8 MeV < E_α < 13 MeV. Signals from α decay could be missed only in the case when an α particle escaped through the open front side of the detector array (30 % probability) or when the lifetime was shorter than 2 μs and the decay occurred in the dead time of the

data acquisition system. The windows for the relative positions were twice as much as the resolution at FWHM. No such decay chains were found for the irradiation at the beam energy $E_{1/2}$ =230 - 231 MeV. The upper cross-section limit obtained at this energy is 2.25 pb at a probability level of 68 %.

Then the energy of bombarding ions was increased up to $E_{1/2}$=234 MeV, resulting in the excitation energy of the compound nucleus ^{286}112 E*=35 MeV. During a period of 15 days a beam dose of $4.68 \cdot 10^{18}$ projectiles was collected. Two events from spontaneous fission were detected in this irradiation at the higher beam energy. Both SF events were characterized by a coincident event of higher energy signals (52 and 130 MeV) in the stop detector and lower energy signals (13 and 40 MeV) in the backward detectors. Correlation analysis of the possible decay chains of the ER $\rightarrow \alpha \ldots \rightarrow$ SF type with the upper limit of the time intervals t of up to 10,000 s resulted in two ER - SF correlations. The position difference determined from the ER and SF signals was 0.6 mm for the first event and 0.8 mm for the second one. Time intervals ΔT=180.5 sec and 1459.5 sec., respectively, were measured. The probability that the first correlation is a chance event is 0.005, for the second SF-event the corresponding probability is 0.038.

We attempted to identify SF activities observed in the ^{48}Ca + ^{238}U reaction using mass determination with the 37° dipole magnet. Using ER - SF correlations, positions of the implanted ER's and corresponding TOF's were extracted. The most probable atomic mass values for the most probable charge states were found by solving a system of equations for A/Q values by the maximum likelihood method. For the first event a corresponding ratio A/Q=16.0 and for the second one A/Q=16.679. The values A=288.0 (Q=18) and A=283.5 (Q=17) for the first and second events were obtained. We estimated the accuracy of mass measurements to be about 2 %. Mean value of the masses for two detected nuclei amount <A> 285.7 ± 5.7. Cutting down the upper limit by the mass of compound nucleus A_{CN}=286, mass interval from A=280 to A=286 could be obtained. This result indicates, first of all, that the observed nuclides belongs to the region of superheavy nuclei and their masses are close to the expected masses of the evaporation products of the reaction ^{48}Ca + ^{238}U. Due to the relatively low excitation energy of compound nucleus E_{CN}* ≈ 35 MeV the evaporation of charge particles (protons or α particles) is strongly prohibited, more probable that the events measured in this work belongs to the isotope ^{283}112 produced via a 3n evaporation channel in the reaction ^{48}Ca + ^{238}U $\rightarrow$ ^{286}112*.

The mean value of the two measured time intervals together with four previously measured events [3,4] results in a half-life $T_{1/2}$ =307^{+212}_{-89} s which coincides well within error bars with reported earlier values [3,4]. The cross-section evaluated for the production of two fission events at a beam energy of 234 MeV in the half-thickness of the target is 3^{+4}_{-2} pb that coincides well in error intervals with reported earlier values obtained with the separator VASSILISSA [3] (5^{+6}_{-3} pb) and in the experiment aimed at the determination of chemical properties of element 112 performed at Dubna in 2001 [11], were 8 SF events were detected, that corresponded to the cross-section $2^{+0.9}_{-0.7}$ pb. In February - March 2003 the experiment aimed to the determination of chemical properties of element 112, synthesized in the reaction ^{48}Ca + ^{238}U, was performed at GSI Darmstadt [12]. Few SF events were detected that corresponded to the cross-section in the range of 1 – 5 pb and is in good agreement with results, obtained with VASSILISSA separator and chemical experiment at Dubna.

The deviation of the beam energy value at which the events were obtained during this experiment and the reported 5 years ago value [3] could be explained by the fact that an accuracy of the absolute values of beam energy measurements 5 years ago was not tested and deviations could be at the level of 1 - 1.5 %, i.e. 2.5 - 3.5 MeV, and/or by the fact that in the past experiment 1.6 mg/cm^2 Al backing foils were used for the target support (about 25 MeV energy losses for ^{48}Ca beam with an energy of about 5 A·MeV) whereas now 0.74 mg/cm^2 Ti backing foils were used (about 10 MeV of energy losses).

The obtained results of mass measurements of heavy ER's allow one to exclude transfer products and incomplete fusion products and to assign the two observed SF events to the complete fusion of ^{48}Ca + ^{238}U with a high probability. The non-observation of α decay, the improbable evaporation of protons or α particles from the compound nucleus and the relatively low excitation energy of 35 MeV let us assign the

fission events measured in this work to the isotope $^{283}112$ produced via the 3n evaporation channel in the reaction $^{48}Ca + ^{238}U \rightarrow ^{286}112^*$.

The non-observation of any events in the reaction $^{48}Ca + ^{238}U \rightarrow ^{286}112^*$ at the beam energy $E_{1/2}$ =231 MeV [8] can be explained by the fact that the beam energy was too low and corresponded to the left side of the excitation function, in which a decrease in the cross section value is very sharp.

Acknowledgments

This work was performed partially under the financial support of the Russian Foundation for Basic Research, contract N 02-02-16116 and JINR – BMBF (Germany), JINR - Polish, JINR - Slovak Cooperation Programs.

References

[1] S. Hofmann, F.P. Hessberger, D. Ackermann, G. Muenzenberg, S. Antalic, P. Cagarda, B. Kindler, J. Kojouharova, M. Leino, B. Lommel, R. Mann, A.G. Popeko, S. Reshitko, S. Saro, J. Uusitalo, A.V. Yeremin, Eur. Phys. J. A14, 147 (2002)

[2] K. Morita, K. Morimoto, D. Kaji, A. Yoneda, A. Yoshida, T. Suda, E. Ideguchi, T. Obnishi, Y.L. Zhao, H. Xu, T. Zheng, H. Haba, H. Kudo, K. Sueki, A. Ozawa, F. Tokanai, H. Koura, A.V. Yeremin, R. Kanumgo, K. Katori, I. Tanihata, RIKEN Accel. Prog. Rep. 35 (2002)

[3] Yu.Ts. Oganessian, A.V. Yeremin, G.G. Gulbekian S.L. Bogomolov, V.I. Chepigin, B.N. Gikal, V.A. Gorshkov, M.G. Itkis, A.P. Kabachenko, V.B. Kutner, A.Yu. Lavrentev, O.N. Malyshev, A.G. Popeko, J. Rohac, R.N. Sagaidak, S. Hofmann, G. Muenzenberg, M. Veselsky, S. Saro, N. Iwasa, K. Morita, Eur. Phys. J. A5, 63 (1999)

[4] Yu.Ts. Oganessian, A.V. Yeremin, A.G. Popeko, S.L. Bogomolov, G.V. Buklanov, M.L. Chelnokov, V.I. Chepigin, B.N. Gikal, V.A. Gorshkov, G.G. Gulbekian, M.G. Itkis, A.P. Kabachenko, A.Yu. Lavrentev, O.N. Malyshev, J. Rohac, R.N. Sagaidak, S. Hofmann, S. Saro, G. Giardina, K. Morita, Nature 400, 242 (1999)

[5] Yu.Ts. Oganessian, A.V. Yeremin, A.V. Belozerov, M.L. Chelnokov, V.I. Chepigin, V.A. Gorshkov, A.P. Kabachenko, S.P. Korotkov, O.N. Malyshev, A.G. Popeko, J. Rohac, R.N. Sagaidak. S. Hofmann, G. Muenzenberg, M. Veselsky, S. Saro, N. Iwasa, K. Morita, G. Giardina. in: Proc. of the Int. Workshop on "Fusion Dynamics at the Extremes", Dubna, Russia, 25--27 May, 2000, Editors Yu.Ts. Oganessian, V.I. Zagrebaev (World Scientific, Singapore, 2001) 81.

[6] A.V. Yeremin, D.D. Bogdanov, V.I. Chepigin, V.A. Gorshkov, A.P. Kabachenko, O.N. Malyshev, A.G. Popeko, R.N. Sagaidak, G.M. Ter-Akopian, A.Yu. Lavrentjev, Nucl. Instr. Meth. B126, 329 (1997)

[7] A.V. Yeremin, A.V. Belozerov, M.L. Chelnokov, V.I. Chepigin, V.A. Gorshkov, A.P. Kabachenko, O.N. Malyshev, Yu.Ts. Oganessian, A.G. Popeko, R.N. Sagaidak, A.I. Svirikhin, S. Hofmann, G. Berek, I. Brida, S. Saro, in: Proc. of VII Int. School-Seminar on Heavy Ion Physics, 27 May - 1 June, 2002, Dubna, Russia; To be published in Yad. Fiz. (Phys. At. Nuclei) 66 (2003)

[8] A.V. Belozerov, M.L. Chelnokov, V.I. Chepigin, T.P. Drobina, V.A. Gorshkov, A.P. Kabachenko, O.N. Malyshev, I.M. Merkin, Yu.Ts. Oganessian, A.G. Popeko, R.N. Sagaidak, A.I. Svirikhin, A.V. Yeremin, G. Berek, I. Brida, S. Saro, Eur. Phys. J. A16, 447 (2003)

[9] O.N. Malyshev, A.V. Yeremin, A.G. Popeko, A.V. Belozerov, M.L. Chelnokov, V.I. Chepigin, V.A. Gorshkov, S. Hofmann, M.G. Itkis, A.P. Kabachenko, Yu.Ts. Oganessian, R.N. Sagaidak, S. Saro, A.V. Shutov, A.I. Svirikhin, Submitted to Nucl. Instr. Meth. A.

[10] W. Loveland, K.E. Gregorich, J.B. Patin, D. Peterson, C. Rouki, P.M. Zelinski, K. Aleklett, Phys. Rev. C66, 044617 (2002)

[11] A.B. Yakushev, I. Zvara, Yu.Ts. Oganessian, A.V. Belozerov, S.N. Dmitriev, B. Eichler, S. Huebener, E.A. Sokol, A. Tuerler, A.V. Yeremin, G.V. Buklanov, M.L. Chelnokov, V.I. Chepigin, V.A. Gorshkov, A.V. Gulyaev, V.Ya. Lebedev, O.N. Malyshev, A.G. Popeko, S. Soverna, Z. Szeglowski, S.N. Timokhin, S.P. Tretyakova, V.M. Vasko, M.G. Itkis, Preprint JINR E12-2002-297, Dubna 2002. Submitted to Radiochimica Acta

[12] H. Gaeggeler, In: Proc. of VIII Int. Conf. "Nucleus - Nucleus Collisions", June 17 - 21, 2003, Moscow, Russia; To be published in Nuclear Physics.

Spectroscopy of the transfermium nuclei ^{251}Md

A. Chatillon[1]

[1] CEA Saclay, France

chatillo@hep.saclay.cea.fr

The study of very heavy nuclei beyond the Fermium isotopes has attracted a strong interest in recent years. Due to the strong Coulomb repulsion, these nuclei are only stabilized by shell effects. After the first successful studies of even-even nuclei where collective properties have been deduced, the spectroscopy of odd-A isotopes is the next step needed to understand the single-particle properties in this mass region. Due to the relatively high cross section, the nucleus ^{251}Md is the best odd-Z candidate.

In order to study the nucleus ^{251}Md (Z=101), three experiments have recently been performed at the university of Jyväskylä: by prompt electron spectroscopy using the electron detector SACRED, by prompt gamma spectroscopy with the new JUROGAM array, and by alpha, electron and gamma spectroscopy after the alpha decay of ^{255}Lr using the GREAT detector. The first results of these experiments will be presented.

Experimental study on photofission of ^{242}Pu, ^{238}U, ^{235}U and ^{232}Th in giant dipole resonance region

T.D. Thiep[1], N.V. Do[1], N.N. Son[1], T.T. An[1]

[1] Institute of Physics, Hanoi, Vietnam, Vietnam

tthn@netnam.org.vn

Photofission represents a powerful tool for investigating the double humped fission barrier of actinide, especially for studies on shape isomer, formed by photonuclear reactions. In general, photofission seems to be favourable for investegation of the nuclear structure as in the case electromagnetic interaction is well - known and the theoretical consideration is simplified. Due to the missing Coulomb barrier compound states of low excitation energy are easily populated. The main advantage, however, is spin selectivety of the electromagnetic interaction leads to the favoured excitation of the few specific fission channels compared with particle induced reactions. The giant electric dipole resonance dominates the photoabsorption cross - section in most important energy range (i.e in giant dipole resonance region).

In photofission the mass and charge distributions and the isomeric ratios of fission fragments are ones of the most interesting observables as their parameters can be related to the dynamics of the fission process. For the reasons, we have concentrated our investigations in these characteristies.

In our investigations for photon sources we used electron accelerators of microtron type. Microtrons are high intense photon sources therefore they are suitable for the studies of photonuclear reactions where the reaction cross-sections are small. The targets after irradiation were measured by direct gamma spectroscopic technique without any chemical separation.

Target preparation, irradiation and measurement: We have carried out photofission of Pu242, U235, U238 and Th242. Our first studies were photofissions of Pu242 and U235 started in 1982 at the Joint Institute for Nuclear Research, Dubna, Russia by using microtron MT - 22 (its maximum bremsstrahlung energy can be varied stepwise from 10 to 22 MeV). By that time the data on photofission of Pu242 have not been published, so our results can be considered as first ones.

The target of 3 (+ or -) 0.3 mg of dioxide Plutonium enriched to 94.7% Pu242 was prepared on a 70 micro metters thick aluminium disc of 55 mm diameter. The active layer had a diameter of 20mm. For photofission of U235, the target of 30mg dioxide uranium enriched to 97% U235 was used in the experiment. The plutonium was irradiated for 5 and 6 hours with 18.1 and 20.7MeV bremsstrahlungs respectively. The U235 target was irradiation for 5 hours with 18.1MeV bremsstrahlung. In order to avoid thermal neutron induced fission of U235 the target was packed by Cd envelope of 0.5mm thickness and fast neutron induced fission is less than 0.2% can be negled. For both the Pu242 and U235 targets the catcherfoil technique was used for collecting fission fragments. The catcherfoil which consisted of 0.1mm thick very pure aluminium foil (purity of 99.99%) was placed at a distance of 1mm from the Pu242 and U235 targets and then was measured with high energy resolution semiconductor detector.

The photofissions of Th232 and U238 were performed with 15 MeV bremsstrahlung produced by microtron MT-17 of the National Institute of Physics, Hanoi by 4 hours irradiations. The target of U238 was an amount of 18mg U3O8 enriched to 99.6% U238 prepared on a 0.5mm thick high pure aluminium disk of 20mm in diameter and the target of Th231 was a pure Th sample having diameter of 20mm, thickness of 0.5mm and density of 15mg/cm2 wrapped in a thin layer of lapsan on 1mm thick pure aluminium disk. The targets after irradiations were measured with direct gamma spectroscopic technique without any chemical separation.

For measuring gamma spectra of photofission fragments two spectrscopic systems were used. At the National Institute of Physics, Hanoi, the targets were measured by a spectroscopic system consisted of 62 cm3 coaxial HPGe detector ORTEC with a resolution of 2.1 KeV at 1332 KeV gamma ray of Co60, a spectroscopic amplifier CANBERRA mode 2001 and a 4096 channel analyzer mode ND-66B, Nucl. Dat. Inc. coupled with a PDP 11/23 computer for data processing. At the Joint Institute for Nuclear Research, Dubna the measuring system consisted of a 45 cm3 Ge(Li) detector, a NOKIA spectroscopic amplifier, a 4096 channel analyzer NOKIA, model LP-4096 was used.

Mass distributions: The relative comulative yields for the fission fragments were determined from successive measurements of gamma fission spectra from the catcherfoils and the target. The relative total yields for a given mass chain were obtained from the relative yields by making correction with the expression for charge distribution. The absolute product yields were obtained by normalization to 200% the area under the total mass distribution.

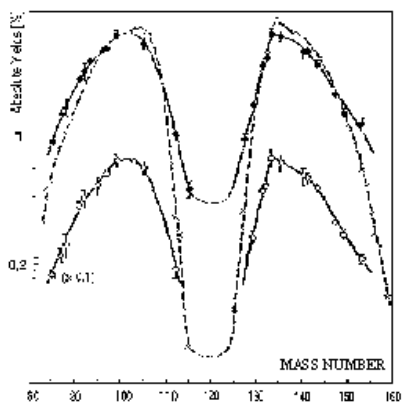

Fig.1. Mass distribution for photofission of Pu^{242} with 20.7 (•) and 18.1 MeV (o) bremstrahlungs, (x) Fission of Pu^{241} with thermal neutrons.

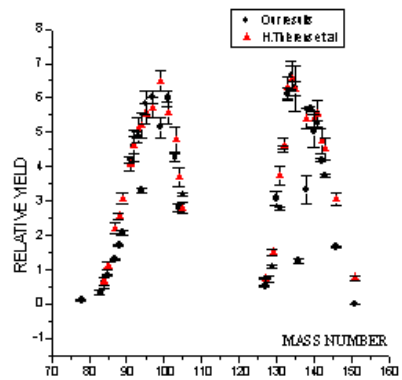

Fig.2. Mass distribution for photofission of U^{238} with 15 MeV bremstrahlung.

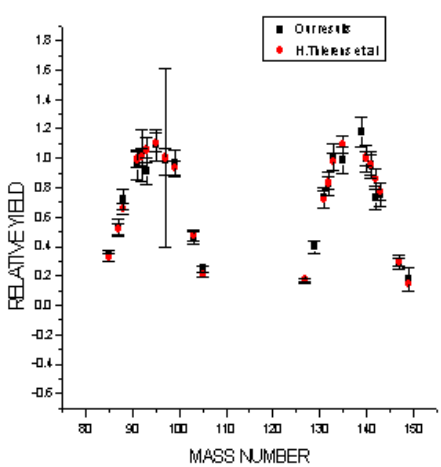

Fig.3. Mass distribution for photofission of U^{235} with 18 MeV bremstrahlung

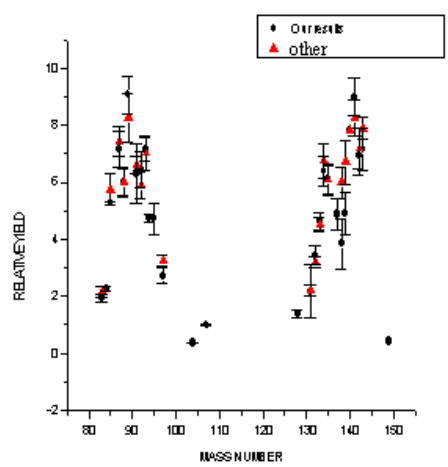

Fig.4. Mass distribution for photofission of Th^{232} with 15 MeV bremstrahlung radiation

Our experimental results are shown in fig.1, 2, 3 and 4. We have obtained for the Pu242 photofission 25 mass chain. We can see in fig.1 a weak fine structure in mass region 133-135 due to the close neutron shell N=82. For the case of U235 photofission 34 product yields were obtained. For U238 the comulative yields for 44 mass chains have been determined. A fine structure in the mass regions 133 - 135 and 140 - 142 was observed and our results are compared to those of De Frenne et al. For Th232 38 comulative mass yields have been established. Our results are compared to that obtained by other groups and fine structure is exhibited.

Charge distribution: We have studied the charge distribution for the photofission of U238 with 15 MeV bremsstrahlung. Most of experimental data on photofission charge distribution were obtained from independent yields which were determined using chemical separation or by direct gamma spectroscopic method. In practice there are very small number of mass chain where it has been possible to determine the independent yields of more than one isobar. The data on independent yields for any photofission system available in the literature are very scarce. In the case of U238 photofission the Zp values lie too far from the beta - stability line. So that in a given mass chain, the isotopes produced with the highest probability have very half - lives, making the measurements of these gamma spectra very difficult. We compromise by assuming that information about charge distribution can be obtained from comulative yields for products lying far enough away from the line of beta - stability. The charge distributions for mass chains 95, 97, 99, 128, 130, 131, 132, 134, 135, 138, 140 and 141 were investigated. We deduced from comulative (or independent) yields the most probable charges Zp for 7 other mass chains based on two methods namely the unchanged charge distribution and the emperical relation.

Fission fragment isomeric yield ratios As it is known in fission the independent isomeric ratios are measure of the primary fission fragment angular momentum. Isomeric yield ratio can be determined if the isomeric pair are screened product, i.e, if the product can be formed only directly in fission process. Up to now the studies on the independent isomeric yield ratios in the photofission of U238 are very limited. In our investigation we succeeded in determining the isomeric yield ratios for the following pairs Sb128m - Sb128m, I132m - I132g and Xe135m - Xe135g.

Beside the above mentioned studies we have also developed the statiscal model to predict independent yields and pairing effects which are in good agreement with experemental data. Recently we have applied successfuly the multimodal fission model to analyze the mass distribution in fission at low excitation energies.

At the presents time we are investigating spontaneous fission and photofission of transactinide element 96Cm. The results will be published in near future.

This report has been completed with the financial support of the Vietnam National Program in Natural Science, project N: 430201. The authors would like to express their sincere thanks for this precious assistance.

Synthesis of new heavy nuclei using RNBs

W.D. Loveland[1], M. Cloughesy[1]

[1] Oregon State University, USA

lovelanw@ucs.orst.edu

In proposing new radioactive beam facilities, such as the RIA facility, the issue arises as to the potential for synthesizing new heavy nuclei using radioactive nuclear beams (RNBs). While it is tempting to write several interesting possibilities, we believe that one must make quantitative estimates of the realistic probability of such studies. Accordingly, we have quantitatively evaluated the possibilities of synthesizing heavy nuclei using the proposed RIA facility.

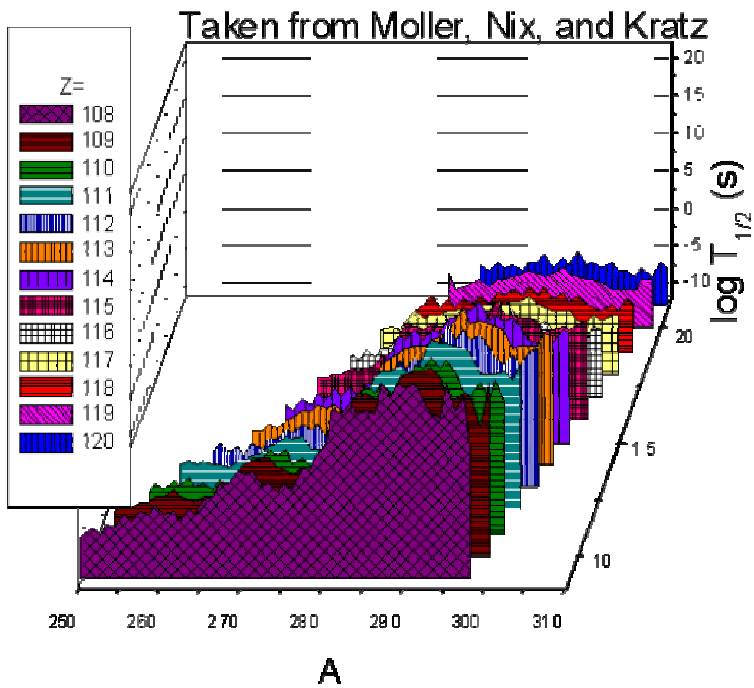

Figure 1. Variation of calculated [1] half-lives of heavy nuclei with Z and A.

We begin by noting the potential value of n-rich beams in synthesizing heavy nuclei (Figure 1). In Figure 1, we show a plot of the calculated half-lives [1] of the heavy nuclei sorted by Z and A. Note that in addition to the expected increases in half-life at the magic numbers N=162 and N=184, one sees a general overall increase in half-life with increasing neutron number. This increase amounts to an increase of orders of magnitude in half-life, that could qualitatively change the character of the studies of the atomic physics and chemistry of these elements. We would also expect that the lowered fusion barriers for the n-rich projectiles might lead to lower excitation energies and greater survival probabilities.

What we have done to examine the possibilities of synthesis of new nuclei using the RIA facility is to do a brute force calculation. We have taken the RIA beam list [2] that gives the identity and intensity of all the expected RNBs that have suitable energies (<15 A MeV) and considered all possible combinations of these projectile nuclei with all "stable" target nuclei (including radioactive actinide nuclei) with appropriate target thicknesses (~0.5 mg/cm^2). All reactions are assumed to take place at a projectile energy equivalent to the Bass barrier [3]. The fusion probability is calculated using a semi-empirical

formalism developed by Armbruster[4] that considers fusion hindrance and assumes fusion to be primarily an s-wave process. Γ_n/Γ_f values used to evaluate the survival probabilities are taken from our semi-empirical systematics of Γ_n/Γ_f [5]. For the most promising cases, the fusion probability was re-calculated using the HIVAP computer code [6]. The yield of each projectile-target combination was evaluated in atoms/day.

This formalism was checked by calculating the cross sections of the formation reactions used to synthesize elements 104-112 and comparing them to the observed cross sections. The results (Figure 2) show an agreement between predicted and observed cross sections within an order of magnitude for cross sections ranging over seven orders of magnitude.

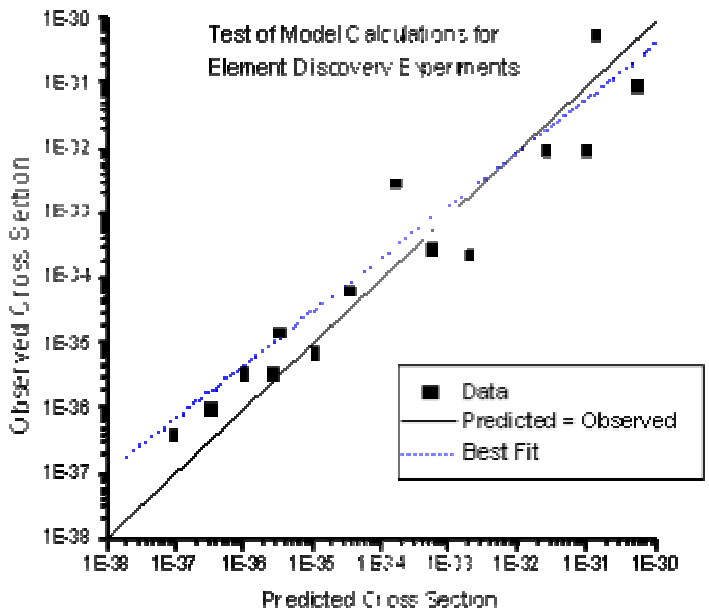

Figure 2. Comparison of observed and calculated formation cross sections for elements 104-112.

The RIA facility appears to offer significant opportunities for the study of the atomic physics and chemistry of the heaviest elements (Figure 3). It appears possible to synthesize significant numbers of very n-rich isotopes of elements 104-108 (Rf-Hs). Because these nuclei have very long half-lives, qualitatively different studies of these nuclei should be possible. These hot fusion reactions typically involve radioactive nuclei that are not far from stability. This is due to the higher fluxes of these nuclei compared to the more exotic projectiles.

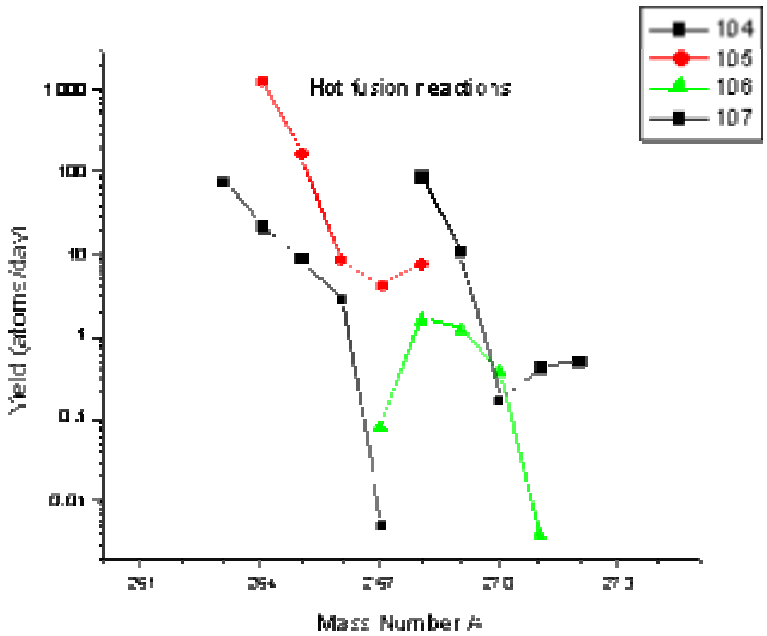

Figure 3. Production rates of n-rich isotopes of elements 104-108 using the RIA facility.

The situation regarding the synthesis of new heavy elements is mixed (Figure 4). While it is possible to make new elements using radioactive beams, the use of stable beams gives higher production rates. (In the stable beam calculations, we have assumed 0.3 pWa beam currents.)

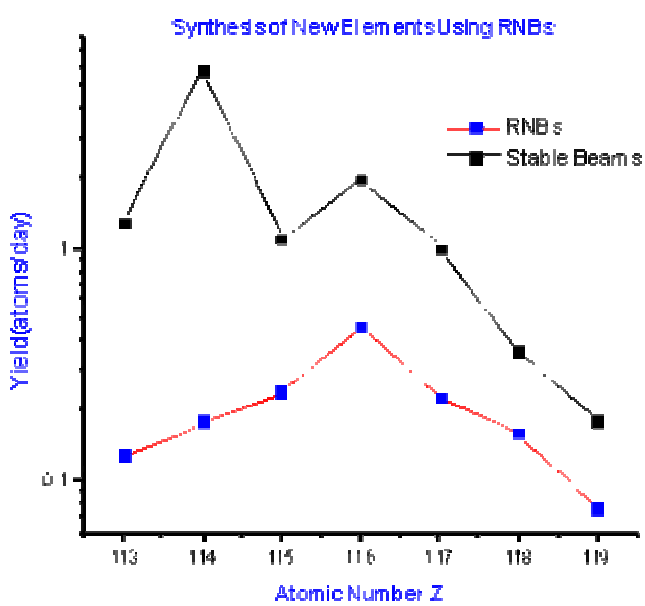

Figure 4. Production rates of new elements using radioactive beams from RIA and stable beams.

The radioactive projectiles lead to more n-rich nuclei than the stable projectiles (Figure 5) which may be important for the study of the nuclear structure of the heaviest elements. One might inquire why the

conventional cold fusion reactions do not play a more important role in these simulations. The product of the cross section and available flux is not sufficient to give suitable production rates.

It should be noted that these estimates of production rates do not include any fusion enhancement effects, other than the lowering of the fusion barriers (and excitation energy) with the n-rich projectiles. This is based upon the experimental studies of fusion with n-rich radioactive beams [9,10].

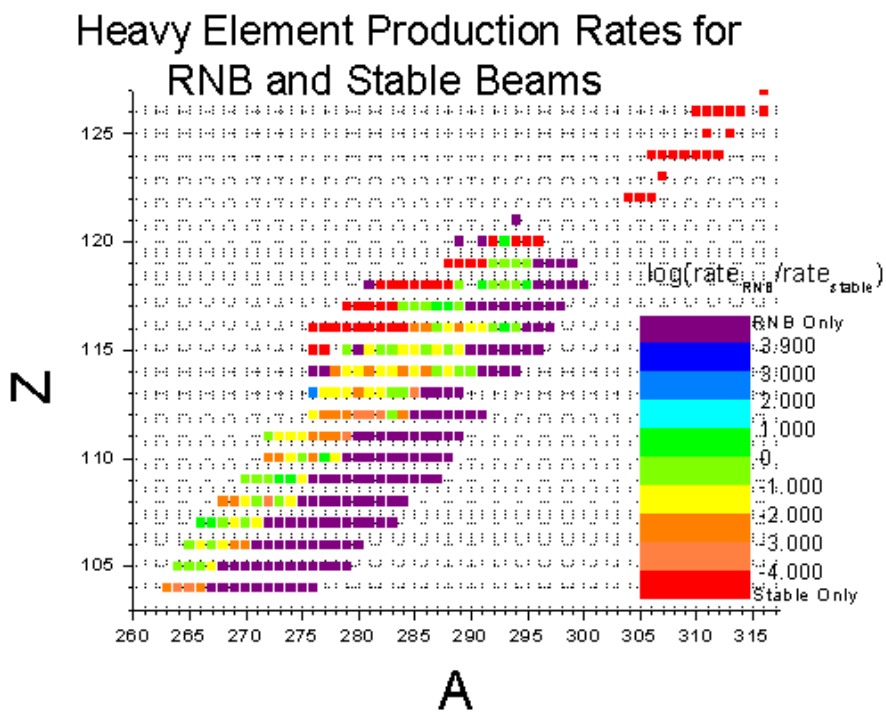

Figure 5. Comparison of production of heavy nuclei with RIA beams and stable beams.

References

[1] P. Moller, J.R. Nix and K.L. Kratz, At. Data and Nucl. Data Tables **66**, 298 (1997).

[2] http://www.phy.anl.gov/ria/ria_yields/reaccelerated.html.

[3] R. Bass, Nuclear Reactions with Heavy Ions, (Springer-Verlag, New York, 1980), pp283-351.

[4] P.Armbruster, Ann. Rev. Nucl. Sci. **35**, 135 (1985).

[5] W. Loveland *et al.* to be published.

[6] W. Reisdorf, Z. Phys. **A300**, 227 (1981).

[7] K.E. Zyromski *et al.* Phys. Rev. **C55**, R562 (1997).

[8] C. Signorini, Nucl. Phys. **A616**, 262c (1997).

Novel isomer spectroscopy and quasiparticle configurations in ^{254}No

G.D. Jones[1] for the Anglo-Finnish-French S.H.E. collaboration

[1] University of Liverpool, United Kingdom

jx@ns.ph.liv.ac.uk

The recently installed GREAT [1] focal plane detector system (with triggerless data acquisition) has been coupled to the gas filled recoil spectrometer RITU at the University of Jyväskylä, Finland, for a study of long-lived isomer decays. The ^{172}Yb(^{48}Ca,4n)^{216}Th reaction at a beam energy of 217 MeV has been used as a 'proof of principle' experiment to verify some new techniques which have been proposed [2] for focal plane isomer spectroscopy. The basic method is a variation on the recoil decay tagging (RDT) technique, by which position-time correlations are performed for recoils, isomer-delayed summed electron conversion transitions and alpha decays at the same position of a multi-pixel, double-sided strip detector. The nucleus ^{216}Th has a long-lived isomeric state [3] with $T_{1/2}$ much greater than 1μs, (which is the approximate transit time of recoils through RITU), followed by an alpha decay of ~25ms ; ideal for the present application. The production cross section is also an order of magnitude larger than that for super heavy elements. The summed electron conversion pulse has been observed in coincidence with γ-rays produced from unconverted transitions in the isomer decay path. The cross section ratio of isomer to prompt decays has been obtained by comparison with RDT events where a summed electron conversion pulse was not present in the position- time correlations. The ^{208}Pb (^{48}Ca,2n)^{254}No reaction has been studied at 219 Mev beam energy, in a similar manner, to obtain, for the first time, the excitation energy and decay path of a long-lived isomer [4] in ^{254}No, which was inferred about 30 years ago. In view of the inherent difficulties, at the present time, associated with the elucidation of single quasiparticle (qp) configurations in odd mass nuclei in this region, the structure of isomeric states may be crucial to our understanding of single particle orbitals in the spherical shell model. An isomer's qp configuration, populating intruder orbitals in the deformed mean field, allows one to deduce their origins from the expected doubly magic, spherical shell model states around A=300. The possible qp configurations of this isomeric state will be discussed.

References

[1] R.D. Page *et al.* Nucl. Instrum. Meth. **B204**, 634 (2003).
[2] G.D. Jones, Nucl. Instrum. Meth. **A488**, 471 (2002).
[3] K. Hauschild *et al.* Phys. Rev. Lett. **87**, 072501 (2001).
[4] A. Ghiorso, K. Eskola, P. Eskola, and M. Nurmia, Phys Rev **C7**, 2032 (1973).

Investigation of the 5n and α4n channels in the ^{20}Ne on ^{244}Pu reaction

R. Dressler[1], B. Eichler[1], D. Piguet[1], R. Eichler[1,2], H.W. Gäggeler[1,2], F. Haenssler[2], S. Soverna[2], M. Schädel[3], E. Schimpf[3], K. Eberhardt[4], P. Thörle[4], N. Trautmann[4]

[1] Paul Scherrer Insitut, CH-5232 Villigen PSI, Switzerland
[2] Departement für Chemie und Biochemie, Universität Bern, Freiestrasse 3, CH-3012 Bern, Switzerland
[3] Gesellschaft für Schwerionenforschung mbH, Planckstrasse 1, D-64291 Darmstadt, Germany
[4] Institut für Kernchemie, Universität Mainz, Fritz-Strassmann-Weg 2, D-55128 Mainz, Germany

rugard.dressler@psi.ch

The isotope ^{259}Rf was firstly investigated by Flerov et al. [1] in the 5n channel of the reaction ^{22}Ne on ^{242}Pu. Two years later Zvara et al. [2] published first ever chemistry experiments with the element Rf (Z=104) based on the products of the same nuclear reaction. These experiments were several times repeated and controversially discussed by different authors in the next two decades (for a nearly complete compilation of these discussions see [3]). Flerov et al. showed in [1] in addition to the excitation function of ^{259}Rf the low energy part of the excitation function of ^{256}No, which is produced in the α4n channel of the reaction ^{22}Ne on ^{242}Pu.

Later, only a few experiments were made to investigate nuclear reactions based on Pu and Ne [4, 5]. In our experiments we will continue the investigation of xn and αxn reactions in the region of Rf and No, which was started already in [5]. The intention is to study formation and decay properties of ^{259}Rf and ^{256}No in the reactions ^{244}Pu(^{20}Ne, 5n) and ^{244}Pu(^{20}Ne, α4n), respectively.

^{259}Rf has a half-life of (3.2±0.6) s and decays with (92±2)% probability by emission of α-particles of 8.77 MeV and 8.87 MeV [6]. ^{256}No with a half-life of (2.91±0.05) s decays also via emission of α-particles of 8.448 MeV and 8.402 MeV [6] with a (99.47±0.06)% branching ratio. For both nuclides a spontaneous fission decay mode was reported.

A Pu target (enriched 98.6% in ^{244}Pu) with a thickness of about 0.5 mg/cm^2 is in preparation at the University of Mainz via molecular plating of its nitrate on a Be-backing of 12 μm thickness.

In a first experiment at the PSI Phillips cyclotron this target will be bombarded with ^{20}Ne^{6+}, at a beam energy of 113 MeV.

The recoiling reaction products are swept out of the recoil chamber using a He-carbon-gas-jet and transported to the PSI Tape System [7] within 3 s. The aerosols are collected by impaction in vacuum on the magnetic tape during 2 s and subsequently the samples are moved in front of 8 consecutive α-PIPS-detectors (450 mm^2 active area). For the event-by-event recording the data acquisition system described in [8, 9] will be used.

In Figure 1 the excitation function given in [1] is compared with model calculations using the HIVAP code [10, 11]. Under the described experimental conditions about 15 events of ^{259}Rf at a cross-section of 0.6 nb will be expected within an 8 day irradiation at beam intensities of about 1.2 eμA. The use of the PSI Tape System inhibits the accumulation of long-lived spontaneously fissioning nuclides, such as ^{256}Fm, which are produced in transfer channels of the nuclear reaction. But the outcome of the experiment also depends very much on the purity of the target material, since by-products (e.g. $^{211-214}$Po) from nuclear reactions with heavy metal impurities in the target may disturb the unambiguous identification of ^{259}Rf and ^{256}No. In that case a fast chemical separation as described in [12] will be necessary.

The results of this first experiment, which is conducted in August 2003, will be presented.

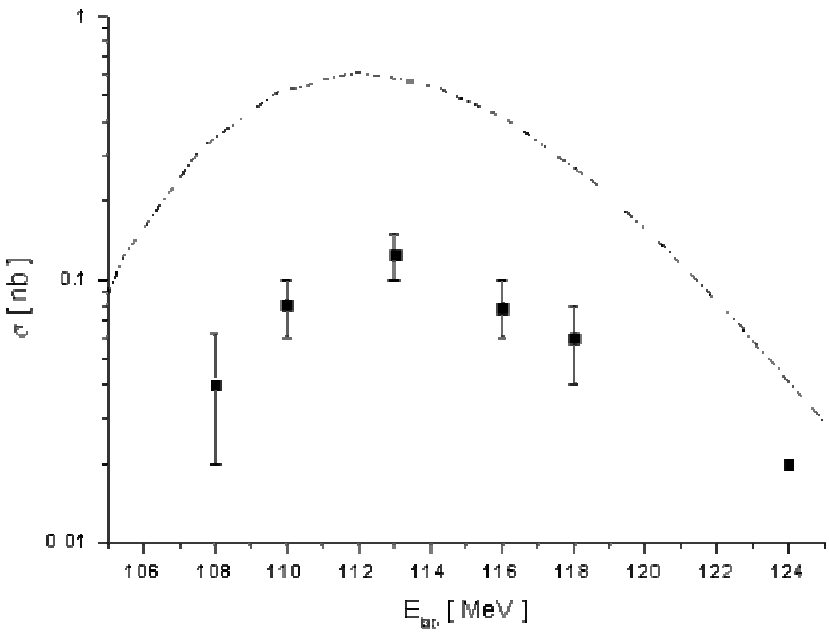

Figure 1. The cross section of ^{259}Rf in the reaction ^{242}Pu(^{22}Ne, 5n). Symbols: experimental data from [1]; dotted line: model calculations using HIVAP for the reaction ^{244}Pu(^{20}Ne, 5n).

References

[1] G.N. Flerov *et al.* Phys. Lett. **13**, 73 (1964).
[2] I. Zvara *et al.* Sov. Atom. Energy **21**, 709 (1966).
[3] E.K. Hyde *et al.* Radiochim. Acta **42**, 57 (1987).
[4] Yu.A. Lazarev *et al.* Phys. Rev. **C62**, 064307 (2000).
[5] R. Dressler, PhD Thesis, Univ. Bern, Switzerland (1999).
[6] A. Artana-Cohen, Nuclear Data Sheets **88,** 275 (1999).
[7] D.T. Jost, D. Vermeulen, IEEE Trans Nucl. Sci. **NS-36**, 1630 (1992).
[8] R. Dressler, PSI Scientific Report 2002, Volume I 68 (2003).
[9] S. Ritt, P.A. Amaudruz, "A versatile and compact data acquisition system MIDAS", (http:\\midas.psi.ch).
[10] W. Reisdorf, M. Schädel, Z. Phys. **A343,** 47 (1992).
[11] R. Dressler, PSI Scientific Report 1998, Volume I 131 (1999).
[12] A. Türler *et al.* J. Alloys and Compounds **271,** 287 (1998).

The search for ^{271}Mt via the reaction ^{238}U + ^{37}Cl

P.M. Zielinski[1,2], K.E. Gregorich[1], Ch.E. Düllmann[1,2], C.M. Folden III[1,2], P.K. Gupta[1,2], D.C. Hoffman[1,2], W. Loveland[3], H. Mahmud[1], D. Peterson[3], M. Schädel[4], J.M. Schwantes[1,2], R. Sudowe[1,2], H. Nitsche[1,2]

[1] Lawrence Berkeley National Laboratory, Berkeley, USA
[2] University of California, Berkeley, USA
[3] Oregon State University, USA
[4] GSI, Germany

PMZielinski@lbl.gov

Introduction

Theoretical calculations show that, in the region of the heaviest elements, liquid drop fission barriers tend to decrease to zero. Therefore, the occurrence of nuclear shells is of special importance for the stability of nuclei [1,2]. Experimentally, the influence of deformed sub-shells at Z=108 and N=162 have been confirmed, with the 300-fold increase in half-life of ^{269}Hs$_{161}$ compared to ^{267}Hs$_{159}$ [3] and our recent discovery of ^{270}Hs$_{162}$ with collaborators in Europe [4]. Production of ^{271}Mt$_{162}$ would allow further examination of the N=162 sub-shell. There are many valid reasons to produce ^{271}Mt:

This reaction type (^{238}U + medium mass projectile) provides access to many nuclides near the deformed sub-shells. The 88-inch cyclotron can provide high intensity beams of projectiles with A~40 and we have calculated BGS efficiencies in a range of 30% for this reaction type. This type of reaction may have important implication with respect to the chemical study of nuclides with Z > 108.

The cross section for the production of a compound nucleus is influenced by shell effects. The projectile N=20 shell results in lower E* when fusing at the Coulomb Barrier (^{37}Cl$_{20}$), and the doubly-magic deformed shell of ^{270}Hs helps with the Γ_n/Γ_f exit channel, especially at the point where the fourth neutron is evaporated [5].

Alpha-decay systematics can be estimated by comparison with ^{270}Hs and ^{272}110, indicating a half-life of ^{271}Mt ~2 seconds. Both ^{270}Hs and ^{272}110 are dominated by α-decay even though as even even nuclei they are unhindered, and are predicted to have a half-lives of 5s and 1,400μs, respectively. Comparing the ^{271}Mt alpha-decay energy provides us with quantitative information on the strength of the shells as shown in the figure below [1]. We expect ^{271}Mt to decay primarily by α-decay, which would produce ^{267}Bh and ^{263}Db. Production of these nuclides would provide more information on their (α and sf) branching ratios.

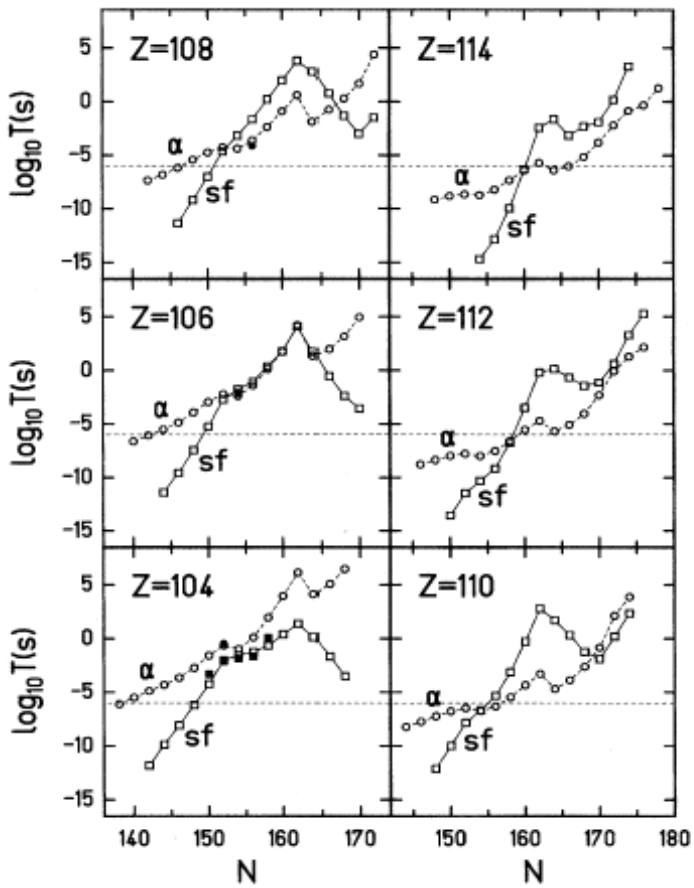

Below are some of ^{271}Mt's predicted alpha decay partial half lives.

Q_α (MeV)	$T_{1/2}$ (s)	Reference
9.91	~10^{-4}	I. Muntian, et al. [6]
10.14	~10^{-6}	G. Royer and R.A. Gherghescu [7]
9.3	26.92	P. Möller, et al. [8]
9.45	1.58	S. Cwiok, et al. [9]

Spontaneous fission may play a significant role in the decay of ^{271}Mt even though odd-A nuclides are hindered with respect to this decay mode as compared to their even even counterparts.

Lastly, discovery of a long-lived (> 1s) isotope of Mt would allow the first-ever chemistry experiment of this element. Presently, the highest Z atom to be studied chemically is Hs, in work that our group collaborated with colleagues in Europe [10], and extension of the Periodic Table to Mt would represent an important advance in basic science.

We expect to produce ^{271}Mt via the ^{238}U(^{37}Cl,4n) reaction. Our motivation for this target-projectile combination comes from recent work at Dubna [11] where they reported a 2.5pb cross section for the reaction ^{238}U(^{34}S,5n) ^{267}Hs, and the identification of three atoms of ^{267}Hs. We have run HIVAP (with the Schädel parameters) for our proposed reaction, shown below:

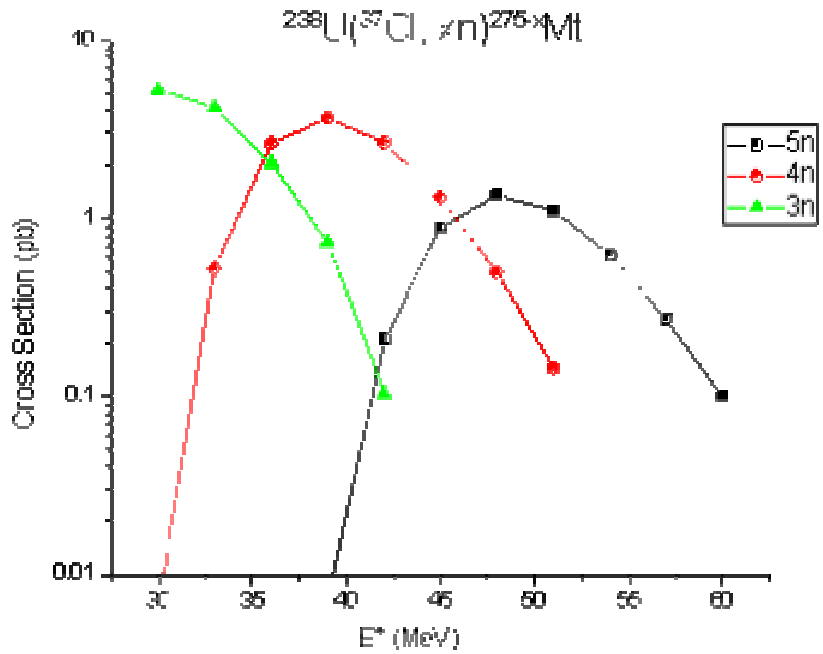

Lighter Mt isotopes were first synthesized in 1982 by Münzenberg and collaborators [12]. Meitnerium's chemistry has never been studied due to the fact that its two known isotopes (^{266}Mt and ^{268}Mt) have half-lives much less than one second. In order to perform the first-ever chemistry of Mt, one would first need to synthesize a longer-lived isotope. Hulet and collaborators attempted such an experiment [13], but were only able to establish a 1 nb cross section upper limit on the formation of ^{272}Mt.

Experimental

Uranium targets were produced at Oregon State University by evaporating a thin layer of UF_4 upon a 2 μm thick Al foil. Uranium thickness was measured by weighing, and uniformity and thickness were confirmed by counting small sections of a target in an α-chamber. For the third run, average target thickness was 400μgU/cm^2; the two earlier runs were similar.

Reaction products were separated in flight by the Berkeley Gas-filled Separator (BGS) and implanted in the focal plane detector. The focal plane detector consists of a five-sided box of vertical Si strips measuring 18cm x 6cm x 6cm; using this array of strips we can determine the horizontal and vertical position of the event in addition to the energy and elapsed time. The four box sides (referred to collectively as the upstream detectors) are used to record escape α's during our beam shutoff period. In addition, a multi-wire avalanche counter (MWAC) was mounted upstream of the focal plane detector, and a Si detector was mounted downstream of the focal plane as a punch-through detector. Both the MWAC and the punch-through detectors functioned to veto uninteresting events in the focal plane.

We employed an automated beam chopper in this experiment. During the experiment, should a correlated EVR-α event occur with certain time and energy windows, the beam would be deflected away from the target chamber for a set period of time. Should another correlated α be recorded, the beam shutoff would be continued for another set period of time. Deflecting the beam allows the upstream detectors to be utilized without the interference of scattered beam.

Discussion

A complicating factor encountered in carrying out this experiment as well as data analysis is that the evaporation residues lose most of their energy as they transit through the MWAC, resulting in implant energies below 1MeV (signals below 500keV). Indeed, steps were taken to reduce the amount of material encountered by the EVRs, especially in replacing the PPAC with an MWAC. We ran test reactions during this experiment, producing Fr and Es isotopes, to measure their range in the MWAC and confirm published range tables. We have concluded that our ranges were 15% less than published data. We plan to reduce the effective thickness of the MWAC from 3.3μm mylar to 2.4μm mylar in order to increase the EVR implant energy.

The Heavy Element Group at LBNL led an attempt to synthesize ^{271}Mt at the LBNL 88-inch cyclotron. The reaction of 195MeV (center of target) ^{37}Cl + ^{238}U was carried out in a series of three experiments during November 2002 & April/May 2003. Total beam dose delivered during these three experiments was 3.2 x 10^{18} particles. Data analysis is in progress, though no correlated decays attributable to the Mt-Bh-Db-Lr chain have been seen so far, leading to a single event upper limit cross section of 0.63pb. Future experiments at higher beam energy are planned to further explore the 4n and 5n exit channels with this beam and target combination.

References

[1] R. Smolanczuk, Phys. Rev **C56**, 812 (1997).
[2] S. Hofmann, Rep. Prog. Phys. **61**, 639 (1998).
[3] Yu. A. Lazarev *et al.* Phys. Rev. **C 54**, 620 (1996).
[4] A. Türler *et al.* Submitted to Eur. Phys. J. A
[5] W. Swiatecki, private communication
[6] I. Muntian, S. Hoffman, Z. Patyk, and A. Sobiczewski, Acta Phys. Pol. **B34**, 2073 (2003).
[7] G. Royer and R.A. Gherghescu, Nucl. Phys. **A699**, 479 (2002)
[8] P. Möller, J.R. Nix, and K.-L. Kratz, At. Dat. and Nucl. Dat. Tab. **66**, 321 (1997)
[9] S. Cwiok, S. Hoffman, and W. Nazarewicz, Nucl. Phys. **A573**, 356 (1994).
[10] C.E. Düllmann *et al.* Nature **418,** 859 (2002)
[11] Yu.A. Lazarev *et al.* Phys. Rev. Lett. **75**, 1903 (1995)
[12] G. Münzerberg *et al.* Z. Phys. **A309**, 89 (1982).
[13] E.K. Hulet, Lawrence Livermore National Laboratory E&TR, 17 (1988)

Random probability analysis of recent ^{48}Ca experiments

J.B. Patin[1], K.J. Moody[1], J.H. Landrum[1], C.A. Laue[1], D.A. Shaughnessy[1], M.A. Stoyer[1], J.F. Wild[1], V.K. Utyonkov[2], Y.T. Oganessian[2]

[1] Lawrence Livermore National Laboratory, Livermore, USA
[2] Joint Institute for Nuclear Research, Dubna, Russia

jbpatin@llnl.gov

A long experimental run was performed at the Dubna U400 Cyclotron Facility bombarding ^{249}Cf with ^{48}Ca aimed at producing isotopes of element 118. Recent independent data analysis of the information gathered during this experiment was performed at LLNL and shall be presented. Two interesting events shall be discussed in detail. The Monte Carlo random probability analysis developed at LLNL for such heavy element experiments was performed for these data and the implications from such analysis will be presented.

Much of the support for the LLNL scientists was provided by the US DOE under Contract W-7405-Eng-48.

Structure effects in photofission

N.N. Son[1], T.D. Thiep[1], P.V. Cuong[1]

[1] Institute of Physics, Vietnam

ngson@fpt.vn

We report on the fission experiments performed with bremsstrahlung beams. The mass distributions for a series of actinide nuclides from Th-232 to U-238 have been measured. The data were analysed in the framework of the statistical model which incorporates total statistical equilibrium between degrees of freedom at scission point and post fission dynamics and both shell effects in the fragments at the scission point and post-scission shell effects. The analysis allowed obtaining the systamatics on shell structure and odd-even effects in photofission of actinides and new understanding structure effects in photofission.

Chemical Theory

[This page was left blank intentionally.]

Progress in heavy-element research: results from relativistic quantum theory

V. Pershina[1]

[1] GSI, Germany

V.Pershina@gsi.de

The production of the heaviest elements was recently marked with new achievements: longer lived isotopes of elements 112 and 114 suitable for chemical investigations were produced in hot-fusion reactions [1]. This allowed for the first successful chemical identification of element 112 as a homolog of Hg with the use of the gas-phase chromatography technique [2,3]. Around the same time, elements 107 and 108 were chemically identified by studying volatility of their compounds with oxygen and chlorine [4,5] using the same approach. New experiments were conducted on aqueous chemistry separations of element 104 [6].

Traditionally, theoretical assistance was rendered to all those important experimental works: detailed predictions of the experimental behavior had been made on the basis of relativistic atomic and molecular calculations, as well as various physico-chemical models. In its turn, the relativistic quantum theory has further developed with respect to the accuracy of the calculated properties, as well as it moved to the description of various new systems of the heaviest elements not yet studied experimentally. Accurate calculations were performed for atoms till Z=122, molecules till Z=118 and very recently for the heaviest atoms interacting with metal clusters with the use of the best available modern quantum-chemical codes. A study of relativistic effects on the electronic structure and properties of these heaviest elements has been an indispensable aspect of those theoretical works. Results of the recent theoretical investigations of the electronic structures and properties of the heaviest elements and their homologs are overviewed in the presentation. A special attention is paid to the predictive power of those theoretical works for chemical experiments.

Atomic calculations. Electronic configurations have accurately been defined for elements up to Z=122 with the use of the Dirac-Fock-Breit Coupled Cluster Single Double excitations (DFB CCSD) method [7]. The multiconfiguration DF (MCDF) calculations for the ground and excited states were performed for elements 104 through 108 [8]. Both types of the calculations have shown that the relativistic stabilization of the 7s electrons of the transactinides results in the stability of the $7s^2$ electron pair in the ground and first ionized state over the entire 7th row of the Periodic Table, which is different from the states of some elements of the 6th row. The relativistic stabilization of the 8p electrons manifests itself in some ground states different than those of the lighter homologs: for example, the $8s^28p$ state of element 121 differs from the $8s^27d$ state of the lighter group-3 homologues, or the $8s^27d8p$ ground state of element 122 differs from the $7s^26d^2$ state of Th. These new DF CCSD results are in agreement with the old single-configuration DF and Dirac-Slater (DS) results of [9].

Ionization potentials (IP) were accurately defined by the DF CCSD calculations for elements up to Z=115, and 119 through 122. Multiple IPs were calculated using the MCDF method for elements 104 through 108 [8]. These calculations have shown the multiple IP to decrease within the transition element groups. The reason for that is the proximity of the relativistic valence 7s and 6d levels. This makes excitation energies of the 6d elements smaller than those of the lighter 4d and 5d homologues, resulting in an enhanced stability of the maximum oxidation states. Due to the same reason lower oxidation states at the beginning of the 6d series will be unstable.

Ionic radii (IR) of elements 104 through 108 have been defined on the basis of the MCDF calculations [8]. The values indicate that for the elements in the maximum oxidation state the IR of the transactinides

are about 0.05 – 0.06 Å larger than the IR of the lighter 5d homologs. The IR of the lighter 6d elements are, however, smaller than the IR of the actinides, since the latter undergo the actinide contraction of 0.030 Å which is mostly a relativistic effect. The calculated radii of the radial charge density R_{max} show that the maximum of the relativistic 7s orbital contraction falls on element 112.

Molecular calculations. Relativistic calculations have by now been performed for all the compounds of the heaviest elements studied experimentally. Two recent works on predictions of the electronic structure and volatility should be mentioned: on MO_3Cl (M=Tc, Re and Bh) [10] and MO_4 (M=Ru, Os and Hs) [11]. In those papers, volatility was predicted for specific gas-phase experiments on the basis of the fully relativistic (four-component) density function theory (DFT) calculations with the use of the physisorption models. It was shown that the volatility of the MO_3Cl species should change as Re > Tc > Bh due to increasing dipole moments in this row. The calculations for the group-8 tetroxides have shown that HsO_4 should be very similar in its electronic structure and properties to OsO_4. On the basis of these calculations using models of physisorption it was predicted that OsO_4 and HsO_4 should have similar adsorption enthalpies on a quartz surface of the chromatography column. Using thermodynamic models of adsorption, the temperature of the deposition of HsO_4 on the quartz surface was predicted to be slightly above that of OsO_4 [12]. Experiments [4] have confirmed the predicted behavior of the group-7 oxychlorides on adsorption, while they disagreed in the T_{ads} for the group-8 tetroxides [5]. The analysis of this disagreement will be given in the talk.

Due to the importance of experiments with element 112, predictions of its experimental behavior have been of a particular value. Early predictions of volatility were made via extrapolations over the lighter homologs in group 12 [13-15]. Predictions of adsorption behavior of element 112 on various metal surfaces from the electronic structure calculations have been of a particular importance. Recently, calculations of intermetallic compounds of element 112 and Hg (HgX and 112X, where X=Cu, Ag, Au, Pd and Pt) were performed using the DFT method [16]. Results of the calculations did not reveal an expected dramatic decrease in the binding energies from the Hg to the 112 compounds. They have shown that element 112 should form compounds with metals like Cu, Ag, Au and particularly Pd, with the bond strength being only 10-15 kJ/mol weaker than that of the respective Hg compounds. Results of the first calculations of adsorption energy of Hg and element 112 on metal clusters of Au and Pd [17] have shown about the same difference in the bond strength between Hg and 112 with gold clusters as that obtained from the dimer calculations [16].

A number of theoretical predictions were made for experiments with aqueous solutions of the heaviest elements. For Rf and its group-4 lighter homologs, predictions of hydrolysis and complex formation in the HF and HCl solutions were made on the basis of the DFT calculations [18]. It was shown that Rf should hydrolyse to a less extent than Zr and Hf. The complex formation in very diluted HF solutions was shown to change as Zr ≥ Hf > Rf, which will result in the following sequence Zr ≤ Hf < Rf by the extraction of the positively charged complexes of these elements by an AIX (anion exchange) column. Experiments [19] on the AIX separation of group-4 elements from HF solutions have confirmed those predictions.

For element 106, Sg, along with Mo and W, predictions of hydrolysis and complex formation in HF solutions were made on the basis of the DFT calculations [20]. Hydrolysis of Sg was shown to be a complex process depending on pH of the solution. At low pH, i.e. for the formation of positively charged complexes, the decreasing trend in hydrolysis of group-6 elements is continued with Sg, so that the trend in the complex formation is Mo > W > Sg. At higher pH, i.e. for the formation of negatively charged complexes, the trend in reversed in the group: Mo > Sg > W. The former trend proved to be in agreement with experiments on the separation of Sg from aqueous HNO_3 solutions by a cation exchange column: Sg having a positive change was sorbed on the column, while the neutral complex of W was not retained [21]. The complex formation of Sg in HF solutions was shown to be even a more complex process than hydrolysis and trends in group 6 were predicted to be different at various pH and HF concentrations.

Much attention was paid to the study of relativistic effects on the properties of the elements at the end of the 6d-series and at the 7p-series. A series of calculations using the relativistic pseudo-potential (PP) method was performed for compounds of elements 111 through 114 which are expected to have strong relativistic effects on their properties [22]. Energies of decomposition reactions of hydrides, fluorides and some chlorides of those elements were calculated. A most important conclusion of those works is that the relativistic stabilization and contraction of the 7s orbital in the 7th row results in the smallest bond lengths of the 111X and 112X compounds in groups 11 and 12, respectively. On the other hand, relativistic destabilization of the 6d orbitals leads to their larger involvement in bonding for high-coordination compounds, so that the stability of higher oxidation states increases in those groups, like for example of the 5+ state of element 111, or of the 4+ state of element 112. The calculations for the decomposition reactions of the 112 compounds have confirmed its inertness.

Molecular calculations with the use of the relativistic effective core potentials (RECP) for a series of hydrides of the 7p elements [23] have demonstrated a large influence of the 7p orbital spin-orbital (SO) splitting on molecular spectroscopic properties. A large bond contraction was observed in the compounds of element 113 with the predominant contribution of the relativistically contracted $7p_{1/2}$ orbital in bonding (for example in 113H), while for compounds of the other 7p elements, e.g. 115 through 118, the properties are influenced by a relativistically expanded $7p_{3/2}$ orbital. This results in an increase in the bond length of compounds of these elements. The calculations have confirmed a relative inertness of element 114 showing decreasing binding energies of compounds like 114X (X=F, Cl, Br, I, O, O_2) [24] in comparison with those of the lighter homologs. The PP calculations of the decomposition reactions of MX_4 and MX_2 (X=H, F, Cl) have shown a decreasing stability of the 4+ state and increasing stability of the 2+ state for element 114 [22].

The RECP calculations for the reactions $M + F_2 \rightarrow MF_2$ and $MF_2 + F_2 \rightarrow MF_4$, where M=Xe, Rn and element 118 [25] confirmed an increase in the stabilities of the 2+ and 4+ oxidation states in group 18. The SO effects were shown to stabilize $118F_4$ by a significant amount of about 2 eV, though they elongate the bond by 0.05 Å. Thus, increasing trends in bond length and bond strength are continued with element 118. The influence of the SO interaction on the geometry of MF_4 was also investigated [25,26]. It was shown that a D_{4h} geometrical configuration for XeF_4 and for RnF_4 becomes slightly unstable for $118F_4$. A T_d configuration was shown to be more stable than the D_{4h} in $118F_4$ by about 0.2 eV. The reason for that was the availability of only stereochemically active $7p_{3/2}$ electrons for bonding. Trends in molecular stability were predicted for a number of simple compounds of element 118 as compared to those of elements 112 and 114, as well as to those of Rn. So far, elements heavier than 118 were not studied at the MO level. For a complete review, the following references can be recommended [23,27-29]. Prospects for future theoretical studies are also presented in the talk.

References

[1] Oganessian, Yu. Ts., *et al*. Phys. Rev. C **63**, (2000) 011301 (R).
[2] Yakushev, A., *et al*. Radiochim. Acta, **89**, (2002) 743.
[3] Soverna, S., *et al*. Experiment at the GSI, March 2003.
[4] Eichler, R., *et al*. Nature **407**, (2000) 63.
[5] Düllmann, Ch., *et al.* Nature **418**, (2002) 859.
[6] Haba, H. *et al.* J. Nucl. Radiochem. Sci. **3**, (2002) 143.
[7] Kaldor, U. and Eliav, E. In: *Quantum Systems in Chemistry and Physics*, Ed. Hernandes-Laguna, v. II, (2000) 185.
[8] Johnson, E., *et al*. J. Phys. Chem. **116**, (2002) 1862.
[9] Fricke, B. Struct. Bond. **21**, (1975) 89.

[10] Pershina, V. and Bastug, T. J. Chem. Phys, **113**, (2000) 1441.
[11] Pershina, V., *et al*. J. Chem. Phys. **115**, (2001) 1.
[12] Pershina, V. Radiochim. Acta, submitted.
[13] Pitzer, K. J. Chem. Phys. **63**, (1975), 1032; J. Chem. Soc., Chem. Commun. (1975) 760.
[14] Eichler, B. Dubna Report JINR P12-7767 (1974).
[15] Eichler, B. and Rossbach, H. Radiochim. Acta **33**, (1983) 121.
[16] Pershina, V., *et al*. Chem. Phys. Lett., **365**, 176 (2002).
[17] Sarpe-Tudoran, C., *et al*. Eur. Phys. J., (2003) in print.
[18] Pershina, V. *et al*. Radiochm. Acta **90**, (2002) 869.
[19] D. Trubert, *et al*. In: Abstracts of the 1st Intern. Conf. on Chemistry and Physics of the Transactinides, Seeheim, September 26-30, 1999.
[20] Pershina, V. and Kratz, J.V. Inorg. Chem. **40**, (2001) 776.
[21] Schädel, M., *et al*. Nature (Letters) **388** (1997) 55.
[22] Schwerdtfeger, P. and Seth, M. In: *Encyclopedia on Calculational Chemistry*, Wiley, New York, (1998), Vol. 4, 2480-2499.
[23] Han, Y. K., *et al*. J. Chem. Phys. **112**, (2000) 2684; ibid, J. Chem. Phys. **110**, (1999) 8986; Choi, Y. J., *et al*. J. Chem. Phys. **115**, (2001) 3448.
[24] Liu , W. et al. J. Chem. Phys. **119**, (1999) 3730; Liu W, Adv. Quant. Chem. **39**, (2001) 325.
[25] Nash, C.S. and Bursten, B.E. J. Phys. Chem. A. **103**, (1999) 632.
[26] Han, Y.K. and Lee, Y.S. J. Phys. Chem. A **103**, (1999) 1104.
[27] Pershina, V. In: *The Chemistry of Superheavy Elements*, M. Schädel, ed., Kluwer, 2003, p. 31-94.
[28] Pershina, V. and Hoffman, D. C. In: *Theoretical Chemistry and Physics of Heavy and Superheavy Elements*, S. Wilson and U. Kaldor, eds., Kluwer (2003).
[29] Kratz, J. V. and Pershina, V. In: *Relativistic Effects in Heavy-Element Chemistry and Physics*, B. A. Hess, ed., Wiley, 2000, p. 219.

Improved density-functional calculations for molecules and calculation of adsorption of the heaviest elements on surfaces

B. Fricke[1]

[1] Universität Kassel, Germany

fricke@physik.uni-kassel.de

In 1964 Hohenberg and Kohn [1] were able to show that the total energy of any system in an external field can be described by a functional of its density only. This pioneer work is the basis of the Density Functional Theory (DFT) and provides an incentive for many theoreticians to find this functional. In the last three decades many approximations for the energy density functional were made which gave quite good results, but the 'exact' form of the functional is still unknown.

DFT calculations depend on the choice of the exchange-correlation functional and the treatment of the kinetic energy. The spectrum of the different approximations of the kinetic energy starts with a purely non-relativistic approach with or without spin-orbit interaction, continues with the Zeroth-Order Regular Approximation (ZORA) [2, 3] and ends with a full-relativistic description. A comparison of these approximations and corresponding results can be found in [4, 5].

An important difference between various density functionals is the treatment of the spin of the electrons. In the simplest form of non-relativistic density functionals spin is completely neglected. This approximation works quite well for closed-shell systems but leads to wrong results for open-shell molecular as well as atomic systems. A very important improvement was achieved by extending these functionals to spin-polarized (SP) forms [6]. In a relativistic description the spin should actually be included in the relativistic form of the density functionals, which directly depend on the four current density, but this approach is not yet suitable for practical applications. Alternatively, the spin can be included into the relativistic form of the density functionals in a theoretically consistent way via the magnetization density using a fictitious external magnetic field which is set to zero in the end formulas (for more details see [7, 8]).

In this case the exchange and/or correlation functionals depend not only on the density but also on the magnetization density (see details in [7, 8, 9]). The magnetization density at any point in space is defined as magnetic moment per volume [10]. Following this, it is a vector which, in general, points to different directions at different points in space. In order to simplify the calculations in most implementations the magnetization density is aligned to the axis of the highest symmetry (z-axis), which in the literature is called the collinear approximation. There are only few implementations of the non-collinear approximations for atoms and solids known in the literature [9, 11, 12]. Only one of them reports an implementation for molecules where the authors used a scalar-relativistic description [13]. In a recent letter [14] we were able to present the first four-component implementation of the non-collinear density functionals for the diatomic molecule Pt_2. The accuracy which is achieved with this method is better than 0.2 eV in contrast to the old type of calculations without the inclusion of the magnetization density.

In the context of the very first molecular calculations which include transactinide elements with this new method we present results for $RfCl_4$ and its homologues. Again the difference between the theoretical and the experimental results of $ZrCl_4$ and $HfCl_4$ indicate a maximal error of 0.2 eV. This gives us hope that this method can be used as calculational tool with chemical relevant accuracy.

A second improvement for future calculations of very heavy systems will be demonstrated in the adsorption of single atoms on surfaces. In order to detect a very heavy element atom like e.g.112 thermographic chromatography is a method which often is used. The physical quantity which determines the adsorption of the single atom on a surface is the binding energy. For this element 112 we present our first results where the surface is either determined by a cluster or alternatively by an embedding procedure which simulates the surface. Comparison with the homologue Hg leads to a good prediction of the adsorption energy of element 112.

References

[1] P. Hohenberg and W. Kohn, Phys. Rev. **136**, 864 (1964).
[2] E. van Lenthe, E. J. Baerends, and J. G. Snijders, J. Chem. Phys. **99**, 4597 (1993).
[3] E. van Lenthe, J. G. Snijders, and E. J. Baerends, J. Chem. Phys. **105**, 6505 (1996).
[4] S. Varga, E. Engel, W.-D. Sepp, and B. Fricke, Phys. Rev. A**59**, 4288 (1999).
[5] S. Varga, B. Fricke, H. Nakamatsu, T. Mukoyama, J. Anton, D. Geschke, A. Heitmann, E. Engel, and T. Bastug, J. Chem. Phys. **112**, 3499 (2000).
[6] U. von Barth and L. Hedin, J. Phys. **C5**, 1629 (1972).
[7] E. Engel, R. M. Dreizler, S. Varga, and B. Fricke, *Relativistic Effects in Heavy-Element Chemistry and Physics*, edited by B. A. Hess, John Wiley & Sons (2001).
[8] E. Engel, *Relativistic Electronic Structure Theory, Part 1: Fundamentals*, edited by P. Schwerdtfeger, Elsevier, Amsterdam (2002).
[9] H. Eschrig and V. D. P. Servedio, J. Comput. Chem. **20**, 23 (1999).
[10] J. D. Jackson, in *Klassische Elektrodynamik*, Walter de Gruyter, Berlin, New York (1983).
[11] L. Nordström and D. J. Singh, Phys. Rev. Lett. **76**, 4420 (1996).
[12] L. M. Sandratskii, Adv. Phys. **47**, 91 (1998).
[13] C. van Wüllen, J. Comput. Chem. **23**, 779 (2002).
[14] J. Anton, T. Jacob, B. Fricke and E. Engel, Phys. Rev. Lett. **89**, 213001 (2002).

Electronic properties for the superheavy elements 111 to 119 from relativistic ab-initio calculations

P. Schwerdtfeger[1], M. Seth[1]

[1] The University of Auckland, New Zealand

p.schwerdtfeger@auckland.ac.nz

Relativistic effects scale approximately with Z^2 (Z=nuclear charge), hence very large relativistic effects are expected for the trans-actinides, the elements beyond nuclear charge 103, the so-called superheavy elements. The heaviest element discovered so far is the superheavy element 116 with a half-life of about 33 ms for the isotope 289[1]. For chemical studies at an atom-at-a-time scale half-lives within at least the second range are required. The recent discoveries of superheavy isotopes in the second-range of stability open the way for atom-at-a-time chemistry of 108 (Hs), 110, 112 or even 114 [2]. A major drawback in the synthesis is the small production cross-section which drops rapidly with increasing nuclear charge. Thus, for the prediction of periodic trends and the chemical behaviour for elements including the 7th period of the periodic table and beyond, the use of theoretical methods are currently the only way to gain useful chemical information. This talk gives an overview on properties for the elements with nuclear charge 111 (eka-Au) to 119 (eka Fr) [3]. It is shown that relativistic effects significantly influence chemical properties of these elements (see figure below). In contrast, quantum electrodynamic effects are small and can be neglected for chemical properties. We also address the current problem of identifying new isotopes and suggest K-inversion spectroscopy as a useful tool [4].

[1] Y.T.Oganessian, *et al*., Eur. Phys. J. **A 15**, 201 (2002).
[2] C.E. Düllmann *et al*., Nature **418**, 859 (2002).
[3] P.Schwerdtfeger, M.Seth, in Encyclopedia of Computational Chemistry, ed. By P. von R.Schleyer et al., Wiley, NY(1997).
[4] N. Gaston, P. Schwerdtfeger, W. Nazarewicz, Phys. Rev. **A 66**, 062505 (2002).

High-accuracy calculations for heavy and superheavy elements

U. Kaldor[1], E. Eliav[1], A. Landau[1]

[1] Tel Aviv University, Israel

kaldor@jade.tau.ac.il

Accurate calculations for very heavy elements require high-order inclusion of both relativity and electron correlation. The framework of our method is the Dirac-Coulomb-Breit Hamiltonian, which includes relativistic terms up to second order in α, the fine-structure constant. This model is adequate for all atoms, as long as they are not highly ionized. The one-electron four-component Dirac-Fock-Breit spinors are obtained first, playing the same role as the Hartree-Fock orbitals in nonrelativistic quantum mechanics. Correlation is included via the coupled cluster method, which may be interpreted as infinite-order summation of large classes of perturbation terms, and has emerged as the most accurate approach for this purpose.

We are usually interested in studying a large number of states of a given atom. Since most of these states cannot be described, even approximately, by a single determinant, multireference coupled cluster methods are required. The essence of multireference methods is the partitioning of the function space into a small *P*, which comprises all the important determinants, and a large *Q*, the rest of the function space. The effect of *Q* is included by the CC scheme in an effective Hamiltonian constructed in *P*. This H_{eff} is then diagonalized, yielding the energies of all desired states simultaneously. Since the effect of *Q* is included approximately, whereas *P* is solved exactly by diagonalization, extending *P* will improve results. However, convergence of the CC iterations puts severe limitations on the structure and size of *P*. A new approach, the intermediate Hamiltonian coupled cluster, has recently been developed, allowing larger model spaces and greater flexibility in their construction, thereby extending the scope of the method and increasing its accuracy.

The method has been applied to many atoms, calculating energies of numerous states for each. Agreement with available experimental values was usually within a few hundredths of an eV. This makes the method a useful tool for reliable prediction of energy levels of superheavy elements.

Applications to transactinides include, *inter alia*:

- The ground state of Rf (E104) has been determined to be $7s^26d^2$, in contrast with previous predictions of $7s^27p^6d$. Correlation, which favors the d^2 configuration over dp, wins over relativity, which prefers the former configuration, leading to structure similar to that of Hf.
- E111 (eka-gold) is predicted to have a $6d^97s^2$ ground state, vs. the $(n-1)d^{10}ns$ structure of lighter coinage metals.
- The dication of E112 (eka-mercury), unlike Hg2+, shows very strong mixing of the d^8s^2, d^9s, and d^{10} levels in its low electronic states. The E112+ cation has the same electronic ground state as E111.
- E113 (eka-thallium) has a large (0.6eV) electron affinity, raising the possibility of $E113^-$ compounds. The d^9s^2 level of the dication is a mere 0.1 eV above the $d^{10}s$ ground state; this energy difference in Tl is over 8 eV. Di- and trivalent compounds of E113 with an open 6d shell could therefore exist.

- The ionization potential of E114 is 1.1 eV above that of Pb; in fact, it is higher than the IPs of all group-4 elements except carbon. This indicates that E114 will be less metallic and more inert than Pb.
- E118, a rare gas, is predicted to have positive electron affinity of 0.064(2) eV. QED effects on this value were calculated and found to decrease the EA by 9% or 0.0059(5) eV.
- The EA of E119 (eka-francium) is predicted to be 662 meV, much higher than for Cs (491 meV) or any other alkali atom.
- The ground state of E121 (eka-actinium) is $8s^2 8p$, vs. $ns^2(n-1)d$ of other group-3 elements.
- E122 (eka-thorium) will have an $8s^2 7d^8 p$ ground state, vs. the $7s^2 6d^2$ of Th.

These and other examples will be described.

Spin-orbit coupling in transactinide chemistry: secondary periodicity and effects in high-symmetry ligand fields

C.S. Nash[1]

[1] University of New England, USA

CNash@une.edu

Extreme spin-orbit coupling extant for the transactinides is known to have dramatic effects on the valence electronic structure of 6d-block and 7p-block elements. We will examine the consequences of these severe spin-orbit effects on the nature of the transactinide ligand field of 6d transactinide coordination compounds and discuss their implications on their structure, bonding, and spectra vis-à-vis analogs of lower periods. In addition, we will address the question of what constitutes a closed-shell or chemically satisfied valence in light of the secondry periodicity wrought by spin-orbit effects. In particular, we will discuss the effect of spin-orbit coupling on dispersion interactions in dimers of nominally closed-shell 7p-block elements. To further this end, we introduce a modified version of the Bernardi-Boys counterpoise-correction scheme which reduces the calculated overcorrection of the basis set superposition error typical of this method at the correlated level.

Valence-shell QED effects in heavy-element compounds

P. Pyykkö[1]

[1] University of Helsinki, Finland

pekka.pyykko@helsinki.fi

Valence-shell quantum-electrodynamical terms (QED), whose two leading terms, of opposite sign, are the self-energy (SE) and vacuum polarization (VP), are of interest for three different reasons: 1) To the extent that they are small, this smallness justifes the current Dirac-level models, 2) Actually the accuracy of present quantum chemistry, in the domain from water to the superheavies, is now approaching the level where not only relativistic, but QED effects will soon be seen in a head-on comparison between ab initio theory and experiments, 3) These terms may have been 'the last train from physics to chemistry' at the level of fundamental Hamiltonians.

A large number of careful studies of these effects exist for few-electron atoms. A few examples will be shown. The fundamental way of treating these terms is to first create a complete basis of one-particle states and to then evaluate the relevant Feynman diagrams. This can also be done for the SE of valence electrons in neutral, or nearly neutral atoms, to the extent that an effective one-electron potential is available [1]. For the lowest-order VP term, a local potential by Uehling and Serber in 1935 is available. Various approximate methods have also been tried [2].

To give an idea of the orders-of-magnitude, for heavy elements ($Z > 50$), the QED effects cance about -1% of the Dirac-level relativistic effects [1], for the energy shifts of *ns* valence electrons. For the ionization potential of the gold atom this means about -0.3% of the total value. Here it should be mentioned that the very first estimates for Cs and Fr were published by Dzuba et al. [3] already in 1983.

The VP part is to lowest order a local potential, a property of space, same for all elements. Would it be possible to find an effective potential, simulating the SE terms? For energy-only this can be done. Probably any 'broad δ-function' at the nucleus with a right norm will do the job. An example is the work by Fricke in 1971 [4]. For several simultaneous properties such an effective potential has not been attempted, to our knowledge, before Pyykkö and Zhao [5], who fitted the SE effects on the energy and the magnetic-dipole hyperfine integrals of 2s states. Note that both the relativistic and the QED effects are smaller for the 1*s* states than for the higher states. The V_{SE} used was a simple Gaussian, $B \exp(-\beta r^2)$. Finally, a quadratic fit of the height B and the width parameter β to the nuclear charge was made for the fitting range Z=29 - 83. The final results were tested over this range and above it, up to the superheavy alkali metal E119. Recent, more fundamental results are available for the hyperfine effects of the alkali metals Li-Fr by Sapirstein and Cheng [6]. For properties close to a threshold, the percental QED effects can become very large. An example is the electron affinity of eka-radon, E118, where a decrease of -9% is obtained [7]. The final calculated EA is -0.064(2) eV.

References

[1] L. Labzowsky, I. Goidenko, M. Tokman, P. Pyykkö, Phys. Rev. A**59**, 2707 (1999).
[2] P. Pyykkö, M. Tokman, L.N. Labzowsky, Phys. Rev. A**57**, R689 (1998).
[3] V. A. Dzuba, V. V. Flambaum, O. P. Sushkov, Phys. Lett.A**95**, 230 (1983); Novosibirsk Preprint 82-127.
[4] B. Fricke, Lett. Nuovo Cimento **2**, 293 (1971).
[5] P. Pyykkö, L.-B. Zhao, J. Phys. B: At. Mol. Opt. Phys. **36**, 1469 (2003).
[6] J. Sapirstein, K. T. Cheng, Phys. Rev. A**67**, 022512 (2003).
[7] I. Goidenko, L. Labzowsky, E. Eliav, U. Kaldor, P. Pyykkö, Phys. Rev. A**67**, 020101 (2003).

Electronic structure of molecules containing very heavy & superheavy elements

K. Balasubramanian[1,2]

[1] University of California, Davis
[2] Lawrence Livermore National Lab, USA

kbala@ucdavis.edu

Relativistic computations that include both relativistic and electron correaltion effects such as complete active space multi-configuration interaction (CAS-MCSCF) followed by multi-reference configuration interaction (MRSDCI) computations that included up to 50 million configurations of molecules containing very heavy and superheavy elements reveal surprising trends compared to their lighter analogs in the periodic table. We shal discuss these unusual features and trends concerning structure and properties of these very heay to superheavy molecules. We have computed not only the ground electronic states, but also several excited electronic states. It is shown that Jahn-Teller distortion is quenched by spin-orbit coupling in these very heavy species. We have carried out relativistic computations for the electronic states of the newly discovered superheavy elements and yet to be discovered elements such as 113 (eka-thallium) 114 (eka-lead) and 114+. Many unusual periodic trends in the energy separations of the electronic states of the elements 114, 113, 114+, (113)H, 114H, etc., and unusual features in electronic state compositions are found due to relativistic effects. The potential energy surfaces of $(114)H_2$ exhibit unusual trends compared to PbH_2 due to relativity and break-down of singlet and triplet features of the electronic states due to spin-orbit coupling. Unusual features have been computed for the Lawrencium and Nobelium compounds. All of these species will be considered with emphasis on unusual periodic trends.

Relativistic effects on the electronic structure and volatility of the group-8 tetroxides MO_4 (M=Ru, Os and Hs)

T. Bastug[1], V. Pershina[2]

[1] The Australian National University, Australia
[2] GSI, Germany

Turgut.Bastug@anu.edu.au

Element 108 was identified chemically by studying volatility of its tetroxide HsO_4 along with that of the osmium tetroxide, OsO_4 [1]. The MO_4 molecules were adsorbed on/desorbed from a quartz surface of a chromatography column and the temperatures of the 50% of the chemical yield of the products that passed through the column, $T_{50\%}$, provided an information about their volatilities in a comparative study. Theoretically, volatility, as the adsorption enthalpy, ΔH_{ads}, of the tetroxides on a quartz surface of the column, was predicted using a model of physisorption, with molecular spectroscopic properties being *ab initio* calculated using the fully relativistic (four-component) density functional theory (DFT) method [2]. On the basis of these predicted ΔH_{ads} with the use of thermodynamic models of adsorption, $T_{50\%}$ of HsO_4 was expected to be about 2 degrees lower than $T_{50\%}$ of OsO_4, which means that HsO_4 should be more volatile [3]. Experiments have, however, observed a larger $T_{50\%}$ for HsO_4, which was interpreted as HsO_4 having a lower volatility than that of OsO_4 [1]. The reasons for this disagreement will hopefully be found by the future research, while those from the theoretical point of view are analyzed in [3].

Theoretically, results of the DFT calculations [2] and the thermodynamic considerations [3] indicate that HsO_4 should be more volatile than OsO_4 due to its larger molecular size (i.e. large molecule-surface interaction distance) and a larger molecular weight. To investigate the influence of relativistic effects on the electronic structure and properties of MO_4 (M=Ru, Os and Hs), especially on volatility, non-relativistic calculations for these molecules have been performed by us in addition to our former relativistic calculations [2].

Comparison of the obtained non-relativistic with relativistic values shows that relativistic effects, as expected, increase binding energies and decrease bond lengths in those compounds, as they decrease molecular polarizabilities. Results of those recent investigations with respect to the influence of relativistic effects on molecular volatility and on the trend in Group-8 are discussed.

References

[1] Düllmann, Ch. *et al.* Nature, **418**, (2002) 859.
[2] Pershina, V., Bastug, T., Fricke, B., Varga, S. J. Chem. Phys. **115**, (2001) 1.
[3] Pershina, V., Radiochim. Acta, submitted.

Ionic radii of heavy actinide(III) cations

A. Bilewicz[1]

[1] Institute of Nuclear Chemistry and Technology, Poland

abilewic@orange.ichtj.waw.pl

Filling of the 4*f* orbitals in the lanthanide series and 5*f* orbitals in the actinide series is accompanied by a significant decrease in the atomic and ionic radii. This effect, called lanthanide (actinide) contraction, is the consequence of incomplete shielding of the outermost *p* orbitals from nuclear charge by the 4*f* and 5*f* electrons, respectively. In addition to the increase of the effective nuclear charge, relativistic effects contribute considerably to the actinide contraction[1,2]. Relativistic effects influence the contraction of the lanthanide(III) and actinide(III) ionic radii in two ways: by splitting the outermost *p* orbitals and stabilisation of $p_{1/2}$ orbitals, and by expanding the $f_{5/2}$ and $f_{7/2}$ orbitals. The latter results in less effective shielding from the nuclear charge. For the heaviest actinides this may lead to much smaller ionic radii than in the absence of relativistic effects. For example, in the case of Fm^{3+} the relativistic calculations give r_i 8 pm smaller than nonrelativistic, whereas in the case of Er^{3+} (homologue in the lanthanides series) - only 2.5 pm.

For the five heaviest members of the lanthanide series, the spacing between ionic radii of the adjacent elements decreases regularly from 1.3 to 1.0 pm (Table 1). Unexpectedly, in the case of end actinides the spacings between r_i of the neighbouring elements change irregularly. For example, the difference in r_i between Es^{3+} and Fm^{3+} is 1.7 pm, whereas that between Md^{3+} and No^{3+} only 0.2 pm.

Table 1. Ionic radii of heavy lanthanides and actinides, CN=6

Ln^{3+} ion	r_i , pm [3]	An^{3+} ion	r_i pm
Ho^{3+}	89.4	Es^{3+}	92.8
Er^{3+}	88.1	Fm^{3+}	91.1
Tm^{3+}	86.9	Md^{3+}	89.6
Yb^{3+}	85.8	No^{3+}	89.4
Lu^{3+}	84.8	Lr^{3+}	88.1

Ionic radii are usually obtained from X-ray diffraction data for oxides or fluorides [4]. In the case of heavy actinides from Bk^{3+} to Es^{3+} r_i were determined from lattice parameters of sesquioxides measured by electron diffraction [5]. Unfortunately, elements heavier than einsteinium are produced in non-weighable amounts, so that the experimental structural data for these elements are not available. For Fm^{3+}, Md^{3+}, No^{3+} and Lr^{3+}, the values of r_i were determined only by the chromatographic method [6,7,8]. The ionic radii of Fm^{3+}, Md^{3+} and Lr^{3+} were estimated by comparing their elution positions with the positions of rare earth tracers and of actinides of known ionic radii on strong acidic cation exchange resin with α-hydroxyisobutyrate solution as eluent [6,8]. In the case of No, which is unstable in the +3 oxidation state, r_i was also determined chromatographically but on the cryptomelane MnO_2 - inorganic ion exchanger which shows strong oxidizing properties. The HNO_3-H_5IO_6 solution was used both as oxidant and eluent [7].

In order to understand the sources of irregularity in the contraction of ionic radii of heavy actinides we compared the experimental r_i with the radii of the maximum charge density, R_{max}, of the outermost orbital radii in these cations. Linear correlations of r_i on R_{max} and on expectation values of orbital radii, $\langle r \rangle$, were found for cations of the same charge in many groups of the periodic table [9,10]. These

correlations are suitable to predict r_i of ions in case when experimental measurements are difficult or impossible [9,11,12].

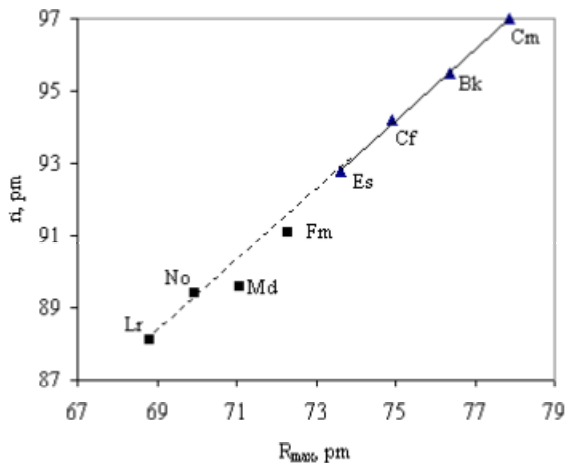

Figure 1. The ionic radius as a function of the 2j+1 weighted in the heavy actinides. Triangles present ionic radii determined from electron diffraction data, squares ionic radii from elution experiments.

Figure 1 presents the dependence of the ionic radius on R_{max} of the outermost shell in the ions of the heavy actinides. The orbital radii have been calculated by V.Pershina using the Dirac-Slater method [13]. As the outermost shell radii we used the 2j+1 weighted R_{max}. The ionic radii of Cm^{3+} Bk^{3+}, Cf^{3+} and Es^{3} are those of Templeton and Dauben radii [3], whereas the ionic radii of the last four actinides where obtained from elution experiments by comparing with Templeton and Dauben radii of lanthanides. As shown in Figure 1 a linear dependence of r_i on R_{max} of the outermost shell is observed for +3 actinides from Cm to Es. For these cations the experimental r_i were determined from electron diffraction on oxides. It is important to note that the chromatographically determined ionic radii of Lr^{3+} and No^{3+} also fit the extrapolated part of the straight-line plot. As shown in Table 2. large differences between the extrapolated and experimental radii are observed for Md^{3+} and Fm^{3+}.

Table 2. Experimental and extrapolated r_i for heaviest actinides, CN=6

An^{3+} ion	R_i(pm) experimental	r_i(pm) extrapolated
Fm^{3+}	91.1	91.5
Md^{3+}	89.6	90.3
No^{3+}	89.4	89.2
Lr^{3+}	88.1	88.1

As mentioned earlier the ionic radii of Fm^{3+}, Md^{3+} and Lr^{3+} were determined only by the chromatographic method. The linear dependence of the logarithm of distribution coefficients ,K_d, on r_i for the tripositive ions of heavy lanthanides and actinides in α-hydroxyisobutyrate solutions was the basis for the r_i determination of the heaviest actinides [6,8]. However, in complexing solutions strong deviations from linearity of the log K_d vs. r_i plot are observed [4,15]. This effect called double-double or tetrad consist in the division the lanthanide and actinide series into two subgroups by the f^7 configuration and futher division of each subgroup into two segments by the f^3-f^4 and f^{10}-f^{11} pairs [16]. Stabilization of the f^3, f^4, f^7 ,f^{10} and f^{11} configurations depends on the environment and decreases with increasing ability of the ligand to expand the *f* electrons cloud. In water, where the nepheloauxetic effect is very low the

delocalization of *f* electrons is insignificant. In α-hydroxyisobutyrate solution where water molecules in the solvation sphere are exchanged for the ligand which shows high nepheloauxetic effect, the cations with f^3, f^4, f^7, f^{10} and f^{11} configurations form less stable complexes than expected from ionic radii.

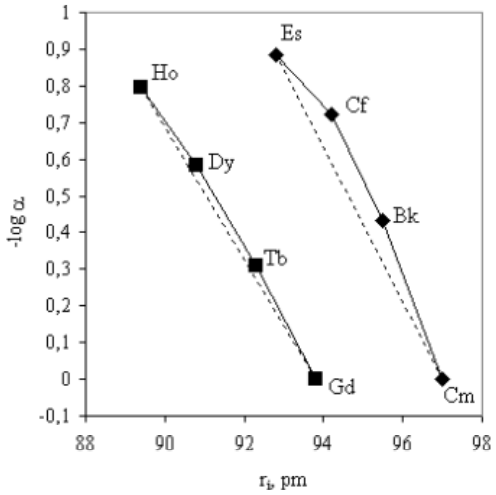

Figure 2. Dependence of the logarithm of the separation factor (α) on r_i for the third segment (f^7-f^{10}) in lanthanide (Gd^{3+}-Ho^{3+}) and actinide (Cm^{3+}-Es^{3+}) series in the α-hydroxyisobutyrate ~V strong acidic cation exchange resin system.

Figure 2 presents the dependence of the logarithm of the separation factor (α) on r_i for the third segment (f^7-f^{10}) in both lanthanide (Gd^{3+}-Ho^{3+}) and actinide (Cm^{3+}-Es^{3+}) series in the α-hydroxyisobutyrate ~V strong acidic cation exchange resin system. The separation factor α is defined as $K_d(Ln^{3+})/K_d(Gd^{3+})$ or as $K_d(An^{3+})/K_d(Cm^{3+})$ for lanthanides and actinides, respectively. Figure 2 shows that for the third segment the dependence of log α on r_i for lanthanides(III) does not deviate much from linear. However, in the case of actinides(III) strong deviations from linearity due to the tetrad effect are observed. This is because greater radial extent expansion of 5*f* in comparison with 4*f* orbitals results in stronger participation of 5*f* orbitals in metal to ligand bonding. Similar effect should be observed in the fourth segment (f^{11}-f^{14}) of the lanthanide (Er^{3+}-Lu^{3+}) and actinide (Fm^{3+}-Lr^{3+}) series. In the case of lanthanides(III) small deviations from linearity are indeed observed [17], whereas for Fm^{3+}- Lr^{3+} strong tetrad effect is to be expected. This means that ionic radii of the heaviest actinides can not be determined from linear dependence of log K_d or log α on r_i in experiments based on the α-hydroxyisobutyrate ~Vcation exchange system, as there is no way to get rid of the tetrad effect in the stability constants. The only way seems to be extrapolation of the linear dependence of r_i (ionic radius based on crystal data) on R_{max}, which is valid for the Cm-Es interval, to the Fm-Lr interval, see Figure 1. From this extrapolation one gets r_i equal to 91.5 and 90.3 pm for Fm^{3+} and Md^{3+}, respectively.

The question remains, why the ionic radii of Lr^{3+} and No^{3+}, determined from elution positions, are the same (Lr^{3+}) or almost the same (No^{3+}) as those calculated from orbital radii. In the case of Lr^{3+} participation of the *f* orbitals in the metal to ligand bonding is negligible because the 5*f* shell is filled and the nepheloauxetic effect in 5*f* electrons does not affect stability constant of the α-hydroxyisobutyrate complex. As far as the No^{3+} is concerned it should be noted that it has been determined chromatographically by comparison of its K_d with K_d of heavy lanthanides on cryptomelane-MnO_2 cation exchanger [7]. The selectivity of cryptomelane-MnO_2 for the cations is due to steric effects and depends on the radii of the cations and of the tunnel (280 pm) in the sorbent [18]. The hydrated +3 metal cations with diameters much larger than 280 pm must be dehydrated before entering the ion exchange phase.

Therefore, the selectivity of the cyptomelane MnO_2 depends nearly linearly on the free energy of hydration which, in turn, is a linear function of the reciprocal of the ionic radius. The linear dependence of the free energy of hydration on the reciprocal of the ionic radius for the whole Ln^{3+} series and for those actinides for which the ΔG_{hydr} is available, indicates that in the hydration energy the tetrad effect is, as expected, insignificant.

Conclusion

The tetrad effect in complexation of actinide(III) cations by α-hydroxyisobutyrate gives underestimated values for Fm^{3+} and Md^{3+} ionic radii comparing with the ionic radii obtained from the linear dependence of ionic radii on orbital radii. With the calculated r_i for Fm^{3+} 91.5 pm and Md^{3+} 90.3 pm, the ionic radii of An^{3+} at the end of the series decrease regularly like in the radii of the lanthanide (III) cations (Fig.3).

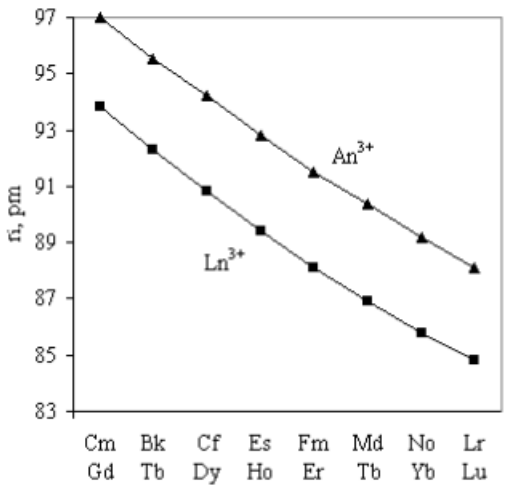

Figure 3. Contraction of ionic radii of the heavy lanthanides(III) and actinides(III). The radii of Fm^{3+} and Md^{3+} are calculated from R_{max} by extrapolation procedure.

Acknowledgments

The author thanks Prof. Slawomir Siekierski for helpful discussion and Dr. Valeria Pershina (GSI Darmstadt) for calculation of orbital radii of actinides cations. The research was supported by the grant from the State Committee for Scientific Research of Poland nr. 7 T09A 073 20.

References

[1] M.Seth, M.Dolg, P.Fulde, P.Schwerdtfeger, J.Am.Chem.Soc. 117, 6597 (1994).
[2] W.Kuchle, M.Dolg, H.Stoll, J.Phys.Chem.A, 101, 7128 (1997).
[3] D.H.Templeton, C.H.Dauben, J.Am.Chem.Soc. 76, 5237 (1954).
[4] R.D. Shannon, Acta Crystal. A32, 751 (1976).
[5] R.G.Haire, R.D.Baybarz, J.Inorg.Nucl.Chem. 35, 489 (1973).
[6] G.R.Chopin, R.J.Silva, J.Inorg.Nucl.Chem. 3, 153 (1956).
[7] A. Bilewicz J. Nucl.Radiochem.Sci. 3, 147 (2002).

[8] W.Brüchle, M.Schädel, U.W.Scherer, J.V.Kratz, K.E.Gregorich, D.M.Lee, M.J.Nurmia, R.M.Chasteler H.L.Hall, R.A.Henderson, D.C.Hoffman, Inorg.Chim.Acta **146**, 267 (1988).
[9] S.Siekierski, Comments Inorg.Chem. **19**, 121 (1997).
[10] S.Siekierski, J.Burges, Concise Chemistry of Elements, Harwood Publishing 2002.
[11] E.Johnson, V.Pershina, B.Fricke, J.Phys.Chem.A **103**, 8458 (1999).
[12] A.Bilewicz, Radiochim.Acta **88**, 833 (2000).
[13] V.Pershina Private information
[14] D.F.Peppard, G.W. Mason, S. Lewey, J.Inorg.Nucl.Chem. **31**, 2271(1969).
[15] S.Siekierski, J.Inorg.Nucl.Chem. **32**, 519 (1970).
[16] I.Fidelis, S.Siekierski, J.Inorg.Nucl.Chem. **28**, 185(1966).
[17] D.C.Hoffman J.Inorg.Nucl.Chem. **3**, 243 (1956).
[18] B.Barto, A.Bilewicz, R.Delmas, C.Neskovic, Solv.Extr.Ion Exch. **15**, 533 (1997).

Adsorption of element 112 on Au surface

C. Sarpe-Tudoran[1], J. Anton[1], W. Sepp[1], B. Fricke[1], V. Pershina[2]

[1] Universitat Kassel, Germany
[2] GSI, Germany

ctudoran@physik.uni-kassel.de

The adsorption of element 112 on a gold surface is studied using the full relativistic four– component ab initio density functional (DFT) cluster calculations. The binding energy and bond length is determined, as well the adsorption position relative to the surface atoms sites. The use of optimized numerical atomic wave functions in the MO-LCAO procedure in the DFT method offers a flexible basis for the expansion of the MO orbitals. Because the adsorption phenomenon is dominantly local, we use clusters of different sizes to approximate the surface. In addition we apply the embedded cluster method. This procedure uses an inner part of 22 and 28 atoms (depending of the symmetry of the adsorbate–cluster surface) which is made self consistently. The surrounding atoms which account for the environmental influences to the inner cluster, is divided in two parts (transition environment and external environment) which are treated in different ways in the description of the interaction with the inner part. Finally potential energy curves and diagrams for the density of states for the system under consideration are presented. The results from size convergent cluster calculations are compared with the results of the embedding calculations.

Relativistic mixed-sector intermediate hamiltonian coupled cluster method: theory and applications

E. Eliav[1], U. Kaldor[1], A. Landau[1]

[1] Tel Aviv University, Israel

ephraim@jade.tau.ac.il

Newly developed mixed-sector relativistic multireference Coupled Cluster (CC) scheme based on Intermediate Hamiltonian formulation is presented. This formulation widely extends possibilities of the traditional Fock-space and Hilbert–space CC approaches and could be regarded as a bridge between the two approaches. High-precision calculations of some heavy and super-heavy atomic systems are presented. The new method yields converged results for states not accessible by traditional Relativistic Fock-space coupled cluster approach. Moreover, states calculated by both methods exhibit much better accuracy in the mixed-sector intermediate Hamiltonian (MSIH) formulation.

Methods and Future Developments

[This page was left blank intentionally.]

Physical and chemical techniques to investigate the heaviest elements – Presence and future

H.W. Gaeggeler[1]

[1] Department of Chemistry and Biochemistry University of Bern, Bern, Switzerland and Paul Scherrer Institut, Villigen, Switzerland

heinz.gaeggeler@iac.unibe.ch

Early transactinide studies were much influenced by the assumption that isotopes of these elements decay predominantly by spontaneous-fission. As a consequence, rotating drums, wheels or tape systems were used to collect reaction products behind a target that were then transported in front of SF-detectors. Usually mica was applied for fission track counting. Also in the very first chemical investigation a frontal isothermal chromatography separation was coupled to a detection of SF-decaying nuclides by this technique. Clearly, these methods did not fulfil the stringent requirements of an unequivocal assignment of single-atoms to a given nuclide.

Later it turned out that not SF but α-decay is the dominant decay mode. Therefore, second generation experiments used event-by-event mode α detection systems, coupled to on-line physical separators in order to measure correlated decay chains. This approach immediately significantly reduced the random probability for an erroneous assignment of the decay of single atoms to a given nuclide.

Two physical separation techniques have been successfully applied in recent years: velocity filters (e.g. SHIP) and gas-filled magnetic separators (e.g. GNS). SHIP at GSI in Darmstadt was instrumental in the discovery experiments of the elements Bohrium through Darmstadtium, very likely also of the elements 111 and 112. Recently, experiments performed with the gas filled magnetic separator GNS at the FLNR in Dubna yielded evidence for the discovery of elements 113 through 116, possibly also of element 118. Both separation techniques are restricted to products from cold or "warm" fusion processes where evaporation residues have relatively high recoil energies. Current detection limits have reached the sub-pb level.

Chemistry studies of transactinides were much hampered by the technical challenge to couple fast and efficient on-line separations with high-resolution list-mode α-spectroscopy systems. In a first step, evaporation residues are collected in a thermalization chamber that are then continuously transported to a chemistry device. If the products are very volatile a pure gas (e.g. He) is used. For less volatile products solid aerosol particles (e.g. KCl) are added to the gas in order to serve as carrier particles for the adsorbed species (gas-jet technique).

So far, the following chemical techniques have been applied: for liquid phase investigations automated HPLC devices(e.g. ARCA) and continuous extraction systems (e.g. SISAK), and in the gas phase adsorption-chromatographic separators (e.g. OLGA). After chemical isolation, products are usually assayed for α or SF decay with conventional semiconductor detectors. In the SISAK device reaction products in an organic liquid are analysed in flow-through detector systems by liquid scintillation counting applying pulse-shape analysis. This method, however, is known to have a poor energy resolution. SISAK was therefore successful so far only if coupled to a physical separator (BGS at LBL). Promising are recent attempts to perform studies on chemically reactive surfaces (IVO/COLD for element 112 , CALLISTO for hassium). As yet, chemistry studies have been applied for transactinides up to hassium and very recently also for element 112. All these investigations are possible for nuclides with half-lives of a few seconds or longer.

Future success of transactinide research will much depend on, first, improvements in beam intensities (including duty cycles), second, novel target technologies, urgently needed to accumulate higher particles

doses in reasonable time, third, devices that are able to assign accurate mass numbers and/or atomic numbers to separated evaporation residues at a single atom level and, fourth, to next generation set-ups, able to perform physical and chemical studies with single atoms (ions) or molecules.

Several projects focus on these goals. Some examples are: at GSI a new high-intensity heavy ion superconducting CW-LINAC is evaluated and new chemical compounds are tested as future targets instead of metallic targets. At FLNR an on-line high-resolution mass separator (MASHA) is being built. At GSI the SHIPTRAP project focuses on the development of ion traps behind the velocity filter for detailed studies on single ions. PSI effort is currently devoted to the development of an ISOL target device that might be coupled to a physical separator (e.g. BGS). Such a system would enable novel investigations (e.g. of organo-metallic compounds).

Ion source developments for heavy element research

D. Leitner[1]

[1] Lawrence Berkeley National Laboratory, USA

DLeitner@lbl.gov

The low cross section experiments for the synthesis of new isotopes and elements in the transactinide and superheavy element region demand intense heavy ion beams (10^{13} particle/sec and higher on target). The duration of these experiments is long (> 200 hours), and frequently accelerated beams of neutron rich isotopes are required. These requirements present a challenge to accelerator injector systems. Therefore, a concentrated ion beam development program is necessary to be able to produce sufficient beam intensities for heavy element experiments.

In addition, high production efficiencies for those high intensity heavy ion beams are desired for various reasons: First, rare isotopes like ^{48}Ca, ^{36}S, or ^{85}Rb are very expensive (for example 250000$/g ^{48}Ca). Secondly, it is unpractical to reload the oven during long experiments for beams made from solid material. Third, it is desirable to minimize the contamination of the ion source for consecutive runs.

The production of heavy ion beams from solids and gases will be reviewed briefly. Electron cyclotron resonant ion source (ECRIS) development required for heavy element research is described in more detail. The development of an intense ^{48}Ca ion beam at LBNL is described as an example for methods to optimize ion source ionization efficiency.

Recoil separator capabilities for heavy element research and an opportunity for second generation chemistry studies

K.E. Gregorich[1]

[1] Lawrence Berkeley National Laboratory, USA

KEGregorich@lbl.gov

Compound nucleus recoil separators have become the tool of choice in the discovery and study of nuclear properties of transactinide isotopes. An overview of recoil separator principles, capabilities and limitations are presented. The recoil separators currently active in the study of heavy element isotopes are presented. An attempt is made to compare the efficiency, selectivity, sensitivity, and resolution of present-day separators for heavy element studies.

The factors limiting efficiency of recoil separators are dominated by energy loss and scattering of compound nucleus evaporation residues in the target material, together with the angular and velocity acceptance of the separators. Selectivity and sensitivity are closely related, with selectivity most dependent on the separator's ability to suppress unwanted nuclear reaction products, and sensitivity strongly dependent on the detection techniques used. Resolution refers to the ability of the separator/detector system to give information on the Z, A, and/or energy of the heavy element isotopes. The small cross sections and resulting low production rates for heavy element isotopes present the most fundamental limitation in transactinide science. Thus, the available integrated luminosity available to an accelerator-separator combination is as important as the capabilities of the separator itself. All of these factors are discussed for the existing separators, and options for future separator programs are presented.

The Berkeley Gas-filed Separator has been coupled with a gas-jet device to provide pre-separated isotopes for transactinide chemical studies. This technique is described, and the new capabilities it provides are discussed. An international effort to design and build a new separator specifically for transactinide chemical studies, "ChemSep," has begun.

Heavy element research with laser spectroscopy and traps

H. Backe[1]

[1] Institut für Kernphysik Universität Mainz, Germany

Backe@kph.uni-mainz.de

Recoil separators like the SHIP facility at GSI in Darmstadt open a great variety of new research opportunities in the heavy element research if combined with traps in which the fusion products can be stored.

The simplest conceivable trap is a buffer gas cell in which the fusion products come to rest either as atoms or singly charged ions. The capture time of the neutral atoms is determined by the diffusion process to the walls. This time of typically 50 ms is long enough to investigate the unknown atomic level schemes or determine the ionization potential of heavy elements by laser spectroscopy employing pulsed lasers with repetition rates of 20 Hz or more. Very powerful methods have been developed like the resonance ionisation spectroscopy with detection of the ionization process either by radioactive decay [1] or directly after mass analysis [2]. The combination of experimental search for atomic levels in the heavy actinide and transactinide region with theoretical level predictions based on Multi-Configuration-Dirac-Fock calculations may provide a critical test of such ab-initio calculations of electron configurations. Once excited atomic states are known, the hyperfine structure of suitable transitions can be studied as well enabling stringent tests of nuclear models applied to the heaviest nuclei.

The fraction of singly charged ions can be used to study gas phase ion chemical reactions with admixtures like O_2, H_2O, CH_4 … to the buffer gas in the stopping chamber. A measurement of the drift time of the ions or ionic compounds in the buffer gas chamber enables a determination of the ionic mobility and may open up new avenues in studies of relativistic effects on ionic radii and the bond length of simple molecular ions [3]. It is conceivable that such investigations can be extended to transactinides with lifetimes larger than 10 ms produced with cross-sections greater than about 100 pb.

A high-resolution Penning trap mass spectrometer as proposed for the SHIPTRAP facility [4] allows direct mass spectrometry of heavy actinide and transactinide isotopes. Traps with small amounts of reactive gases may also provide access to kinetic studies by investigating the loss rate of stored heavy ions and the formation of ion chemical compounds.

References

[1] H. Backe et al., Phys. Rev. Lett. **80**, 920 (1998).
[2] M. Sewtz et al., Phys. Rev. Lett. **90**, 163002 (2003).
[3] H. Backe et al., J. Nucl. Sci. Technol., Suppl. **3**, 86 (2002).
[4] J. Äystö et al., Proposal for SHIPTRAP, GSI 1998.

Status and future developments in the aqueous heavy element chemistry

J.V. Kratz[1]

[1] Institut fuer Kernchemie Universitaet Mainz, Germany

JVKratz@mail.kernchemie.uni-mainz.de

Recently, the status of the liquid-phase chemistry of the transactinide elements has been reviewed extensively in a number of reviews and book contributions [1-4]. In Table 1, an attempt is made to summarize the chemical systems studied with elements 104, 105, and 106, so far, and the pertinent references are given. The chemical techniques involved are briefly outlined. These include manual techniques, the multi-column technique (MCT), the automated rapid chromatography apparatus (ARCA), the on-line liquid-liquid extraction system SISAK in conjunction with liquid scintillation counting, and the automated ion-exchange separation apparatus coupled with the detection system for α-spectroscopy (AIDA). Critical comments [1] have been addressed to the results and conclusions presented in Refs. [8-12], and [14].

Technical developments are going on in several directions: The MCT has been coupled to the aerosol collection device ALOHA on which 2-s collection and dissolution cycles are performed so that the dissolved activity can be fed rapidly onto the sequence of chromatography columns in a quasi-continuous mode. The optimized conditions for on-line experiments with seaborgium are discussed in which Kd values on an anion exchange resin in 0.1 M HNO_3/5x10^{-3} M HF are planned to be measured via the long lived descendant of ^{265}Sg, 20-d ^{253}Es. It is also planned to reduce seaborgium to a lower oxidation state by contacting its aqueous solution with a hot aluminum surface and by distinguishing anionic seaborgium(VI) from cationic seaborgium (III) on a cation exchange column using the MCT.

Continuous efforts have been devoted to improvements of the on-line liquid-liquid extraction system SISAK coupled with liquid scintillation counting (LSC). Analog pulse-shape discrimination (PSD) has been used to reduce the β background in the α spectra by a factor of >1000. Without this technique, the β- and γ-induced background from activities produced in the target will interfere with the α spectrum to such an extent that it becomes useless. However, in the past, when feeding the He/KCl jet directly into the SISAK system, the PSD alone was insufficient to unequivocally identify transactinides with the SISAK - LSC system. Omtvedt et al. [17] have overcome this limitation by producing ^{257}Rf in the ^{208}Pb(^{50}Ti,1n) reaction, separating it in the Berkeley Gas-filled Separator (BGS), and transferring it to the gas jet using the Recoil Transfer Chamber (RTC). This was the first time that a transactinide was extracted and unequivocally identified by the SISAK - LSC system and also the first experiment to use preseparation in a transactinide chemistry investigation. Another improvement comes from the digital recording of the LSC pulses with a fast transient recorder and the pulse-shape analysis by an artificial neural network (PSD - NN) [29]. This has been proven to eliminate pileups to the extent that identification of transactinides even without preseparation becomes feasible. Its ability to recognize α-γ- and α-conversion-electron-coincidence summing which is known to cause shifted α energies may be used in the future to do nuclear spectroscopy [29].

Table 1.

Element	Isotope	Chemical technique	Chemical system studied	Ref.
104, rutherfordium	^{261m}Rf	manual	Cation exchange/α-hydroxyisobutyrate	5
	^{261m}Rf	manual	Aliquat 336/12 M HCl, 6 M HCl	6
	^{261m}Rf	manual	Tri-isooctyl amine/12 M HCl	7
	^{261m}Rf	manual	Thenoyltrifluoroacetone/0.05 - 0.24 M HCl	8
	^{261m}Rf	manual	Tributyl phosphate/8 M - 12 M HCl	9
	^{261m}Rf	manual	Tributyl phosphate/9 M - 12 M HBr	10
	^{261m}Rf	manual	Co-ferrocyanide/<6 M HCl	11
	^{261m}Rf	manual	Tri-isooctyl amine/0.4 M HF	12
	^{261m}Rf	MCT	Anion exchange/0.2 M HF	13
	^{261m}Rf	MCT	Anion exchange/0.27 M HF, 0.2 or 0.1 M HNO_3	14
	^{261m}Rf	ARCA	Tributyl phosphate/6 M HCl	15
	^{261m}Rf	ARCA	Cation exchange/0.1 M HNO_3, var. HF Anion exchange/0.1 M HNO_3, var. HF	16
	^{257}Rf	SISAK	Dibutyl phosphoric acid/6 M HNO_3	17
	^{261m}Rf	AIDA	Anion exchange/8 M HNO_3/4 M - 11.5 M HCl	18
	^{263}Rf	manual	Cation exchange/α-hydroxyisobutyrate and Tributylphosphate/9 M HCl	19
105, dubnium	^{262}Db	manual	Glass surfaces/fuming with HNO_3	20
	^{262}Db	ARCA	Tri-isooctyl amine/12 M HCl, 0.02 M HF/10 M HCl, 0.025 M HF/4 M HCl, 0.02 M HF/0.5 M HCl, 0.015 M HF	21, 22
	^{262}Db	ARCA	Diisobutyl carbinol/conc. HBr/6 M HCl, 0.0002 M HF/0.5 M HCl	23
	^{262}Db, ^{263}Db	ARCA	Cation exchange/α-hydroxyisobutyrate	24, 25
	^{262}Db	ARCA	Aliquat 336/10 M HCl/6 M HCl/6 M HNO_3, 0.015 M HF Aliquat 336/ 0.5 M HF/4 M HF/6 M HNO_3, 0.015 M HF	26
106, seaborgium	^{265}Sg	ARCA	Cation exchange/ 0.1 M HNO_3, $5x10^{-4}$ M HF	27
	^{265}Sg	ARCA	Cation exchange/0.1 M HNO_3	28

A new development in the field of liquid-liquid extraction is MicroSISAK based on the use of microsystem components [30]. Such a system provides separation times on the order of seconds at considerably reduced flow rates as compared to the conventional SISAK system. For mixing of the aqueous phase with the organic phase, a micro mixer is used where the phases are conducted through 2 mm long and 50 μm broad channels to a common outlet. The so-produced emulsion is subsequently separated in a filter apparatus on a filter membrane of 0.5 μm pore size. At a pressure differential of 10 mbar across the membrane and a flow rate of 0.5 ml min^{-1}, the aqueous phase is completely retained by

the hydrophobious membrane while the organic phase penetrates the filter. The goal is to eventually spray the organic phase onto a moving tape where it is evaporated to dryness and assayed for a activity by silicon detectors thus avoiding the drawbacks of LSC. In collaboration with the Institut für Mikrotechnik, Mainz, IMM, extraction yields are being optimized for flow rates below 0.1 ml min^{-1} [31].

For a future application to the spherical superheavy elements 112 and 114, the electrodeposition of these elements on certain electrode materials has been proposed [32]. It is well known that the electrochemical deposition of radionuclides in metallic form from solutions of extremely small concentrations depends strongly on the choice of the electrode material. The associated "underpotential" can deviate considerably from the Nernst potential. In a macroscopic model [32], the interaction between the microcomponent and the electrode material has been described by the partial molar adsorption enthalpy and -entropy. By combination with the thermodynamic description of the electrode process, a potential has been calculated that characterizes the process at 50% deposition. Model calculations for Ni-, Cu-, Pd-, Ag-, Pt-, and Au-electrodes and the microcomponents Hg, Tl, Pb, Bi, and Po have confirmed the decisive influence of the electrode material on the deposition potential. The experimental determination of "underpotentials" for some of these elements [33] is in qualitative agreements with the model predictions [32]. Plans for the application of this electrochemical technique to the spherical superheavy elements are presented.

References

[1] J.V. Kratz, Pure Appl. Chem. **75**, 103 (2003).
[2] J.V. Kratz, in *The Chemistry of Superheavy Elements*, edited by M. Schädel (Kluwer Academic Publishers, Dordrecht, 2003), p.159.
[3] J.V. Kratz and V. Pershina, in *Relativistic Effects in Heavy-Element Chemistry and Physics*, edited by B.A. Hess (Wiley, Chichester, 2003), p. 219.
[4] J.V. Kratz, in *Handbook of Nuclear Chemistry*, edited by Z. Klencsar, S. Nagy, and A. Vertes (Kluwer Academic Publishers, Dordrecht, 2003), in press.
[5] R.J. Silva, J. Harris, M. Nurmia, K. Eskola, A. Ghiorso, Inorg. Nucl. Chem. Lett. **6**, 871 (1970).
[6] E.K. Hulet *et al.* J. Inorg. Nucl. Chem. **42**, 79 (1980).
[7] K.R. Czerwinski *et al.* Radiochim. Acta **64**, 23 (1994).
[8] K.R. Czerwinski, PhD thesis, Lawrence Berkeley Laboratory Report LBL-32233 (1992).
[9] K.R. Czerwinski *et al.* Radiochim. Acta **64**, 29 (1994).
[10] C.D. Kacher *et al.* Radiochim. Acta **75**, 127 (1996).
[11] A. Bilewicz *et al.* Radiochim. Acta **75**, 121 (1996).
[12] C.D. Kacher *et al.* Radiochim. Acta **75**, 135 (1996).
[13] Z. Szeglowski *et al.* Radiochim. Acta **51**, 71 (1990).
[14] G. Pfrepper *et al.* Rasdiochim. Acta **80**, 7 (1998).
[15] R. Günther *et al.* Radiochim. Acta **80**, 121 (1998).
[16] E. Strub *et al.* Radiochim. Acta **88**, 265 (2000).
[17] J.P. Omtvedt *et al.* J. Nucl. Radiochem. Sci. **3**, 121 (2002).
[18] H. Haba *et al.* J. Nucl. Radiochem. Sci. **3**, 143 (2002).
[19] J.V. Kratz *et al.* Radiochim. Acta **91**, 59 (2003).
[20] K.E. Gregorich *et al.* Radiochim. Acta **43**, 223 (1988).
[21] J.V. Kratz *et al.* Radiochim. Acta **48**, 121 (1989).
[22] H.P. Zimmermann *et al.* Radiochim. Acta **60**, 11 (1993).
[23] M.K. Gober *et al.* Radiochim. Acta **57**, 77 (1992).
[24] J.V. Kratz *et al.* Phys.Rev. C **45**, 1064 (1992).

[25] M. Schädel *et al.* Radiochim. Acta **57**, 85 (1992).
[26] W. Paulus *et al.* Radiochim. Acta **84**, 69 (1999).
[27] M. Schädel *et al.* Radiochim. Acta **77**, 149 (1997).
[28] M. Schädel *et al.* Radiochim. Acta **83**, 156 (1998).
[29] G. Langrock, Doctoral thesis, University of Mainz (2002), see also G. Langrock et al., contribution to this Conference.
[30] W. Ehrfeld *et al.* Microreactors (Wiley-VCH, Weinheim, 2000).
[31] K. Eberhardt *et al.* Annual Report 2002, IKMz 2003 - 1, A4 (2003).
[32] B. Eichler and J.V. Kratz, Radiochim. Acta **88**, 475 (2000).
[33] H. Hummrich *et al.* contribution to this Conference.

The status and future of heavy element research at Dubna

S.N. Dmitriev[1], Yu.Ts. Oganessian[1], M.G. Itkis[1]

[1] Flerov Laboratory of Nuclear Reactions, Joint Institute for Nuclear Research, Russia

dmitriev@flnr.jinr.ru

Relatively long half-lives of isotopes of elements 105-116 produced in reactions between ^{48}Ca and ^{248,245}Cm, ^{244,242}Pu, ^{243}Am and ^{238}U and chemical properties of the SHE predicted theoretically provide possibilities of new experiments devoted to the chemical identification of SHE, study of their chemical properties, combination of chemical and physical methods for the SHE synthesis and search for SHE in Nature.

The FLNR programme of the heavy element research for 2004-05 includes the following main experiments:

- Chemistry of elements 112 and 114: the ^{244}Pu(^{48}Ca,xn) reaction will be used; the adsorption of E112 and E114 (if E114 will have an enhanced volatility) on the Au surface will be determined in a temperature interval 25^{0}C to –200^{0}C.
- Chemical separation of recoil nuclei produced in the ^{243}Am(^{48}Ca,xn) reaction will be carried out for the ^{268}Db identification.
- Test experiments at the new FLNR separator MASHA (Mass Analyzer of Super Heavy Atoms) will be completed. First experiments on the determination of masses of isotopes of 112 and 114 elements will be carried out.
- Preparation of an experiment on the search for SHE (Z=108) in nature (study of Os-samples with a low-background neutron multi-detector).

Development of an on-line hot catcher for volatile species

Z. Qin[1], R. Eichler[1], H. Gaeggeler[1], F. Haenssler[1], S. Soverna[1], R. Dressler[2], B. Eichler[2], A. Hohn[2], D. Piquet[2]

[1] University of Bern, Switzerland,
[2] Paul Scherrer Institute, Switzerland

zhi.qin@psi.ch

New isotopes of elements 112 and 114 have been produced in ^{48}Ca beam induced fusion reactions with ^{238}U and $^{242,\ 244}$Pu targets [1]. Their relatively long half-lives give chemists the possibility to investigate the chemical properties of these super heavy elements. The gas-phase chemical investigation of transactinides has gained remarkable progress during the last decade. Continuously operating gas-phase separations, e.g., some devices based on the On-Line Gas chromatographic Apparatus (OLGA), were instrumental to study the formation of halide, oxohalide and hydroxide compounds of transactinides from Rf through Bh. The In-situ Volatilization and On-line detection apparatus (IVO) was successfully applied to study the volatility of the tetroxide of HsO_4 [2]. For the heaviest element, calculations of the electron configurations predicted increasingly strong relativistic effects that may strongly influence their chemical behavior. Hence, the elements 112 and 114 are predicted to be chemically inert and volatile elements, similar to noble gases [3]. On the other hand, classical extrapolations along the groups of the periodic table predict elements 112 and 114 to behave similar to their homologues in the groups 12(Zn, Cd, Hg) and 14(Ge, Sn, Pb), respectively [4]. The expected *high volatility in elemental states* would allow us the chemical investigation of these elements with gas-phase chemical methods or even better at vacuum conditions. The differentiation between either a metallic or a noble-gas character of the heaviest elements could be achieved by vacuum thermochromatography, that provide very clean surfaces in the adsorption process. It also supplies crucial advantages for the experiment with short-lived isotopes: 1) fast separation under molecular flow condition; 2) no carrier gas; 3) a very stable temperature gradient due to the good heat isolation in vacuum; 4) vacuum chemical apparatus could be friendly coupled with a physical separator.

In order to transfer the fusion-reaction products from the target position to the chemical apparatus in vacuum, an on-line hot catcher system coupled to a vacuum thermochromatographic apparatus is now being developed at Paul Scherrer Institute, Switzerland.

The working principle is as follows: Products from heavy ion induced fusion reactions have a recoil momentum sufficiently high and forward-peaked in order to penetrate the target material (≈1mg/cm^2). Passing a thin carbon window (≈30 μg/cm^2), they are implanted into a solid catcher, which is heated up to 2000K. Due to thermo-diffusion, the implanted atoms drift towards the surface of the catcher and desorb from the catcher surface. Subsequently, they effuse inside of the surrounding crucible until they pass the inlet to the thermochromatographic device.

The yields and velocities of the described processes are closely related to the material constants of the solid catcher and of the crucible material, such as diffusion coefficients and adsorption enthalpies. Hence, in order to find the proper catcher material to release volatile metallic p-elements rapidly with high efficiency and also to investigate their adsorption behavior on different metal surfaces by means of vacuum thermochromatography, off-line experiments based on the long–lived isotopes of Tl, Pb, and Bi were performed. An off-line model set-up for "hot catcher" test experiments (see Fig.1) was developed. Isotopes of the p-elements Bi, Pb, Tl were produced by bombarding a $^{nat.}$W(9 μm) target foil with a ^{20}Ne beam (110 MeV on the target) at the PSI PHILIPS Cyclotron. The recoiling nuclei of the nuclear reactions with the W target were implanted in a He-atmosphere into variouscatcher foils just behind the target. Ta,

Ti, Pt, Rh, and C served as catcher materials in these experiments. Isotopes of other elements (Ag, As, Se, Te, Y, Ru, Nb, Mo, Ga) were produced due to the interaction of the beam particles with the catcher material. After the long term irradiation (~ 6 h), the catcher foil was placed into the Ta crucible, which was afterwards closed with a Ta-window. The tantalum crucible with an inner diameter of 1.8 cm and a length of 5 cm (model of a future recoil chamber) has a 2 mm hole, which was attached to the inlet of the chromatographic column by a Ta-connector. For the thermochromatographic separations a pure quartz tube or a quartz tube, which was covered inside by thin Au, Ag, Cu, Ni, Pt, and Pd metal foils (see Fig. 1) were used. The quartz tube was then applied to a copper tube. The whole set-up was evacuated by a turbo molecular pump to a pressure of about 5×10^{-5} mbar. An induction heating device was used to heat up the Ta-crucible to about 1800K. This temperature was measured applying an IR thermometer. Along the chromatography column a temperature gradient between 750°C and –170°C was forced by the gradient oven at the starting point and by the cold finger cooled with liquid nitrogen at the end.

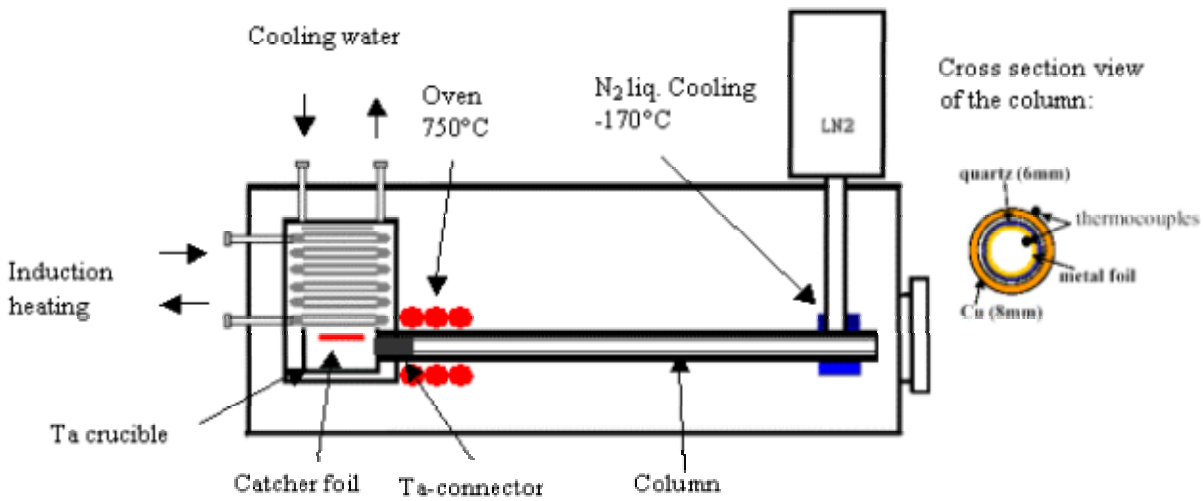

Figure 1. Schematic view of the set-up used for off-line release studies and vacuum thermochromatographic experiments.

Each experiment lasted about 30 min. Release efficiencies for volatile elements from the particular catcher material were determined by γ-activity measurement of the given catcher sample before and after heating. The distribution of the elements in the catcher system and their distribution along the chromatography column were determined with a HPGe-γ- detector with a 1 cm lateral resolution applying a lead collimator.

The determined release efficiencies of some volatile species from different catcher materials are compiled in Table 1. Generally, a higher release efficiency may be expected if the working temperature is close to the melting point of the catcher material. We observed a nearly complete release of Pb, Tl, and Bi from the Pt and Rh catcher at a working temperature of 1800K, whereas these elements partly remained in the catcher made of Ta, Ti, and graphite. Despite a He flushing during the irradiation the Ta and Ti catcher were always oxidized in the beam spot. For future applications, Rh was determined to be the best-suited catcher material, since in nuclear reactions of the heavy ion beams with the Pt catcher large amounts of interfering activities (e.g. ^{211,212}Po) are produced, which disturb the identification of transactinides. All of the released volatile species could be observed deposited in the quartz or metal chromatographic tube. Se was found in the crucible and in the connector, most probably because of the formation of very stable and not volatile Ta-Se compounds. The measured release efficiencies are well

correlated with the release enthalpies ΔH_f^M calculated from the sum and the formation enthalpy of solid solution based on the Miedema model [5] and of the desublimation enthalpy (see Tab. 1). These calculations seem to be very useful for a prediction of release efficiencies for unknown catcher-product combinations. The low release efficiencies for the Ta catcher originated probably from the very low diffusion velocities in a metal with an exceptionally high melting point or from the formation of a Ta_2O_5 layer on the surface of the catcher foil during the irradiation, which may remarkably disturb an efficient release.

Table 1. Release efficiency for some volatile species from different catcher materials.

% {ΔH_f^M, kJ/mol}	Catcher/ thickness (μm)	Pt/ 5	Rh/25	Ta/5	Ti/6	C/200	Fe/25
Element	Melting point (K)	2045	2239	3269	1941		1808
Pb		100{281}	88{228}	65{188}	81{298}	70{332}	100{100}
Tl		100{267}	100{211}	58{125}	86{224}	100{324}	{75}
Bi		100{319}	{266}	{237}	{352}	{368}	{138}
Ag		94{288}	30{247}	{225}	62{291}	{348}	{162}
Y		38{763}	67{675}	75{296}	76{350}	67{973}	{429}
Ru		56{661}	{652}	{808}	100{825}	{718}	{677}
Nb		10{986}	9{910}	12{722}	51{714}	41{1168}	{793}
Mo		0{764}	0{717}	0{676}	49{671}	16{900}	{665}
Te			39				
Se							96
As		{493}	{470}	{557}	{622}	{527}	90{433}
Ga		{465}	{421}	{361}	{418}	{531}	87{327}

Adsorption properties of Tl, Pb, Bi, and other volatile species on the metals Au, Ag, Cu, Pt, Pd, and Ni as well as on quartz were determined from the results of the of the vacuum thermochromatography (see Tab. 2). In order to obtain clean metal surfaces, each metal column was pre-treated with the mixture of He and H_2 gas flow at 850°C and then with a pure He gas at the same temperature just before the experiment. The deposition temperatures were determined from the peak maximum of element distribution along the tube. From the experimental parameters the adsorption enthalpies ($-\Delta H_{ads}^{TD}$) have been calculated using the thermodynamic model of vacuum thermochromatography from [6,7]. A Monte Carlo simulation based on kinetic model of mobile adsorption [8] was also used to evaluate the adsorption enthalpies ($-\Delta H_{ads}^{kin}$) from the experimental results.

Using different catcher materials several determinations of the adsorption enthalpies of Pb and Tl on quartz surfaces were performed. Reasonable reproducibility was found. The determined adsorption data are consistent with data from earlier vacuum thermochromatography experiments ($-\Delta H_{ads}^{Lit}$) [7]. In the Pd and Ag column, Pb and Tl were deposited at the starting point. Therefore, only an upper limit of the adsorption enthalpy is given. For the other metal columns, the adsorption enthalpies determined from the present experiment are well comparable with data obtained by gas thermochromatography ($-\Delta H_{ads}^{Lit}$) [9].

The developed coupling principle between a catcher system and vacuum thermochromatography was shown to work properly. The chemical inertness, the high release efficiencies at moderate temperatures and the absence of beam induced interfering α-decaying by-products make Rh the most attractive catcher material for future experiments with transactinides. Moreover, extremely stable compounds of Rh with actinide elements are known. Hence, the metal chemistry inside the catcher

material will be valuable for a chemical pre-separation already in the recoil chamber. Such separation effects can be predicted using calculated data of the release enthalpies ΔH_f^M. However, only on-line studies can provide information about the very important kinetics of the release. Therefore, on-line hot-catcher experiments with short-lived isotopes of Hg, Pb, Tl, and Bi using a similar experimental set-up are planned.

Table 2. Deposition temperatures and the evaluated adsorption enthalpies together with values given in literature [7,9]

Catcher / surface	Element	Deposition temperature (K)	$-\Delta H_{ads}^{TD}$ (kJ/mol)	$-\Delta H_{ads}^{kin}$ (kJ/mol)	$-\Delta S_{a,\,mob}$ (J/mol*K)	$-\Delta H_{ads}^{Lit}$ (kJ/mol)
Rh-02/quartz	Pb	550±25	146±7	154	166	142
Ta-06/quartz	Pb	541±25	142±7		166	
Ta-04/quartz	Pb	589±25	156±7		166	
Ti-02/quartz	Pb	589±25	155±7		166	
Rh_02/quartz	Tl	370±25	98±6	106	167	113
Ta-06/quartz	Tl	465±25	122±6		167	
Ta-04/quartz	Tl	413±25	109±6		167	
Ti-02quartz	Tl	475±25	125±6		167	
Rh_02/quartz	Bi	360±25	96±6	102	168	109
Rh_02/quartz	Ag	648±25	172±8	187	163	
Rh_02/quartz	Se	>1023±25	<271±10	<295	159	
Rh_02/quartz	Te	389±25	103±6	112	165	151
Pt/Au	Pb	931±25	247±12	260	163	229
Pt/Au	Tl	871±25	231±12	240	163	205
Pt/Ag	Pb	>961±25	<254±12	<250	164	
Pt/Ag	Tl	>961±25	<254±12	<250	164	
Pt/Pt	Pb	>1023±25	<271±12	<266	165	
Pt/Pt	Tl	871±25	231±12	226	165	
Pt/Pd	Pb	>1023±25	<271±12	<300	165	326
Pt/Pd	Tl	>1023±25	<271±12	<300	165	326
Pt/Cu	Pb	783±25	207±12	225	168	222
Pt/Cu	Tl	812±25	215±12	235	167	119
Pt/Ni	Pb	931±25	246±12	262	168	227;231; 243;272
Pt/Ni	Tl	389±25	103±6	115	172	117;149
Pt/Ni	Bi	>1023±25	<271±12	<300	168	252; 322; 328; 273
Pt/Ti	Pb	976±25	258±12	264	164	
Pt/Ti	Tl	948±25	250±12	251	164	
Pt/Ti	Zn	842±25	224±12	215	160	

References

[1] Yu. Ts. Oganessian *et al.*, Nucl. Phys. **A682,** 108 (2001).
[2] H.W. Gaeggeler and A. Tuerler, Ecole Internationale Joliot-Curie course, http://wwwcenbg.in2p3.fr.
[3] K. Pitzer, J. Chem. Phys. **63,** 1032 (1975).
[4] B. Eichler, Kernenergie **19,** 307 (1976).

[5] A.R. Miedema *et al*. Z. Metallkunde **69,** 183(1978).
[6] B.Eichler, Report ZfK-346 (1977).
[7] H.W. Gaeggeler, B. Eichler, N. Greulich *et al*., Radiochimca Acta **40,** 137 (1986).
[8] R.Eichler *et al*., J. Phys. Chem. **B106,** 5413 (2002).
[9] B. Eichler *et al*., Dubna Report P12-81-717 (1981).

Application of artificial neural networks in LSC for transactinide research

N. Wiehl[1], G. Langrock[1], K. Eberhardt[1], H.O. Kling[1], J.V. Kratz[1], M. Mendel[1], A. Nähler[1], U. Tharun[1], N. Trautmann[1]

[1] Institut fuer Kernchemie Universitaet Mainz, Germany

norbert.wiehl@uni-mainz.de

Introduction

In Liquid Scintillation Counting (LSC), α- or fission events can be distinguished from β- and γ- events by characteristic differences in their light curves. The reason is a predominant population of triplet states of the scintillator by strong ionizing particles. These triplet states are metastable which leads to a tailing in the light curve (Fig. 1a).

In a common experimental setup for α-LSC, analog pulse shape discrimination (PSD) is used to separate the β/γ- part of the spectrum. However, β/γ- pile up events in a time window of about 150 ns - 250 ns (Fig.1b) can simulate a heavier particle event in the PSD circuit. This leads to a pseudo α-background in the spectrum. Pile ups are occurring randomly at high count rates but can also be produced by decay cascades of a nuclide.

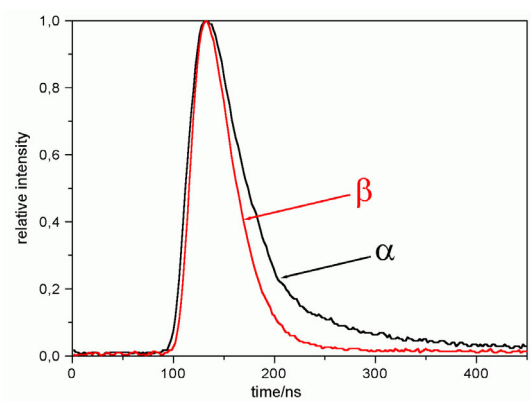

Figure 1a.

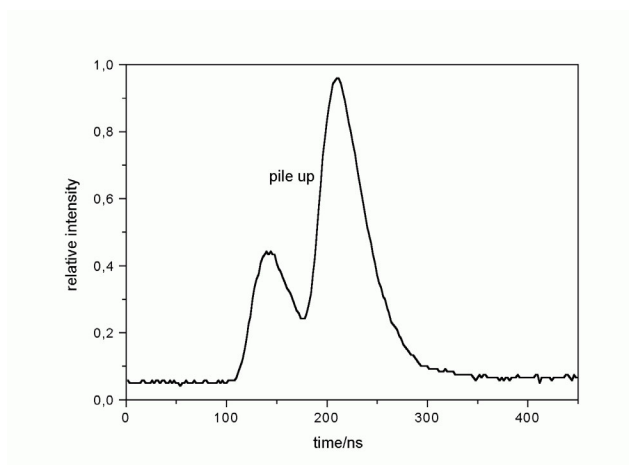

Figure 1b.

In transactinide research with the fast liquid-liquid extraction system SISAK-3 [1], the transactinide element under investigation is extracted into an organic phase containing a liquid scintillator. In these experiments, very few α- decays have to be identified at a high level of β/γ- events. Therefore, any pile up background makes the unambiguous identification of the transactinide nuclides difficult or impossible. In order to apply LSC also in those experiments, the analog PSD has been coupled with a digital pulse recorder. The digitally recorded pulses are off line analysed by an artificial neural network.

Electronics

The setup used is shown schematically in Fig. 2. The photomultiplier (PM), the charge sensitive preamplifier (CSPA), the PSD module, and the time to amplitude converter (TAC), are the standard modules for common LSC. From the built in single channel analyser of the TAC, a trigger signal for the digital pulse recorder is derived. The CSPA integrates the signal. Therefore, it has to be differentated by the timing filter amplifier (TFA) to get the original shape of the signal. As digital pulse recorder, the PC module acqiris DP110 is used. This module allows a maximum sampling rate of 1 GS/s at a bandwidth of 500 MHz. Besides the pulse also the time of the corresponding trigger event is recorded which allows the search for correlated events.

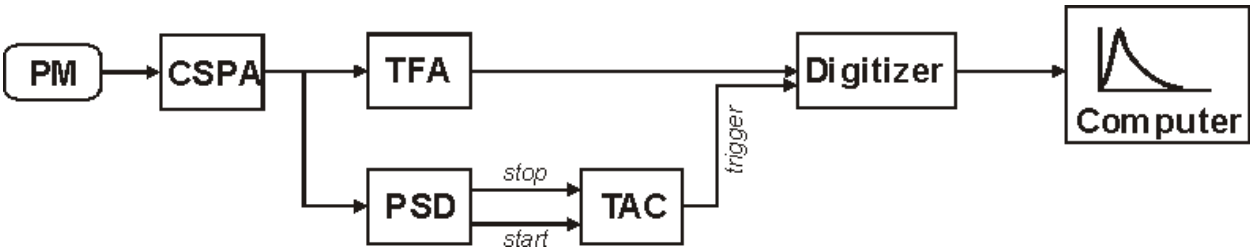

Figure 2.

Artificial neural network

Artificial neural networks are successfully used for pattern recognition especially if an analytical description of the characteristics of the patterns is difficult or impossible. The artificial model of a neuron is rather simple. Each input to a neuron is multiplied by a weighting factor. The weights are corresponding to the synaptic strength in a natural neural network. The output is some function, the so called transfer function, of the weighted sum of all inputs. The weights are initialized by some random values. Learning of the network means adjusting the weighting factors.

For the digital pulse shape discrimination with neural networks (PSD-NN), a 3 layer feed forward network was modeled with the program SMART [2]. The input layer has 175 neurons corresponding to 175 samples at every 2 ns of a pulse. The second (hidden) layer has 5 neurons, and the output layer has two neurons corresponding to an alpha event and any other type of event, respectively. Each output of a layer is connected to each neuron of the next higher layer. The sigmoid function is used as transfer function which gives output values between 0 and 1. The weights are adjusted during the training phase with the backpropagation algorithm [3]. In principle, the weights are corrected in proportion to the error of the network, i.e., the difference between the current and correct output for a given training pattern. This error is propagated backwards from the output layer to the inner layers in order to dertermine correction values for all weights of all layers. Taining patterns for α-events were recorded from a ^{219}Rn / ^{215}Po source. Training data for β-, γ-, and pile up events were recorded mostly from neutron irradiated dibutylphosphate (DBP) solved in toluene. All pulses are normalized to a fixed amplitude thus avoiding that the network learns an energy calibration. After each training cycle the network was tested with test data recorded from the same sources. Fig. 3 shows the error of the network with proceeding training. The errror decreases very rapidly and is almost constant after 600 iterations.

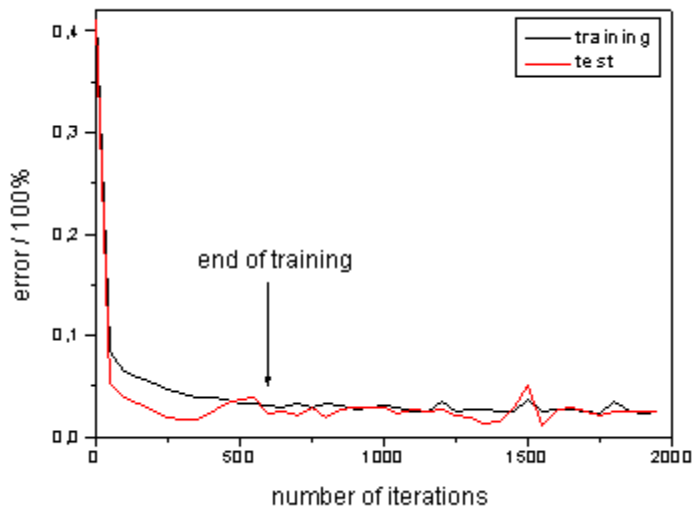

Figure 3.

Test experiment and results

The PSD-NN system was first tested in a SISAK experiment at the Paul Scherrer Institute in February 2000. In this experiment, rutherfordium was produced in the reaction $^{248}Cm(^{18}O,5n)^{261}Rf$ (E_a=8.8 MeV, $T_{1/2}$=78 s). Fig. 4 shows the setup schematically.

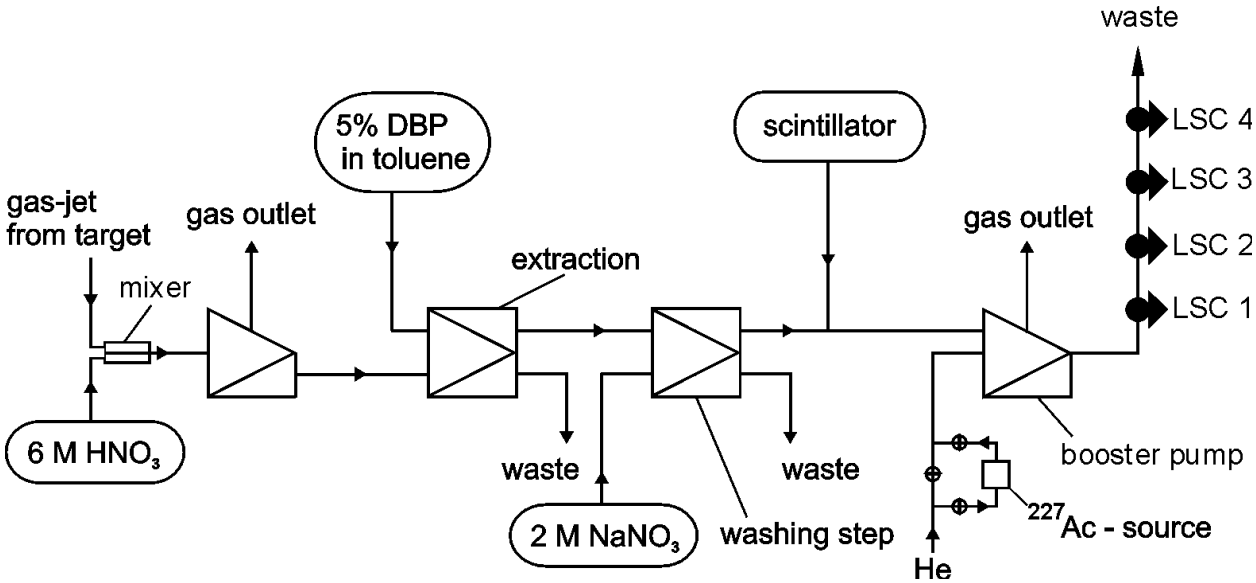

Figure 4.

The reaction products transported with a gas - jet are dissolved in 6M HNO_3. Group IV elements are then extracted with 5% DBP in toluene. In a washing step with 2 M $NaNO_3$ the remaining nitric acid is removed. Then, the scintillator consisting of dimethylPOPOP (3g/l) and methylnaphtalene (30vol%) dissolved in toluene is added. In this experiment, 4 detector cells of 5.5 ml each connected in series are used with the analog PSD electronics. The first detector was also connected to the digital pulse recorder.

The power of the artificial neural network is demonstrated in Fig. 5. Fig 5a shows a typical "α-spectrum" in the energy range of interest from the analog PSD. In Fig. 5b the same spectrum is shown after treatment with the neural network. In the total spectrum 95.8% of the events could be identified as pile up events. These results show that low level α-LSC can be significantly improved by the application of digital pulse recording in combination with artificial neural networks.

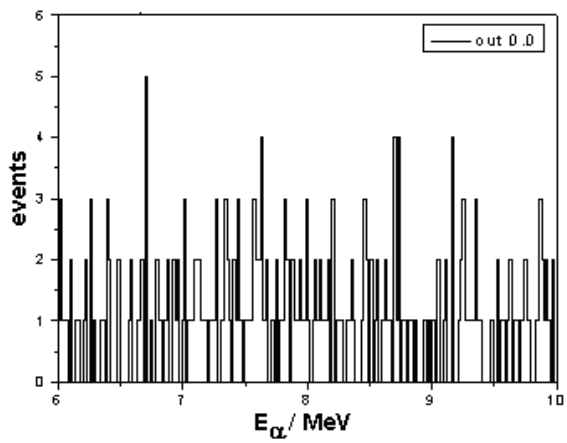

Figure 5a.

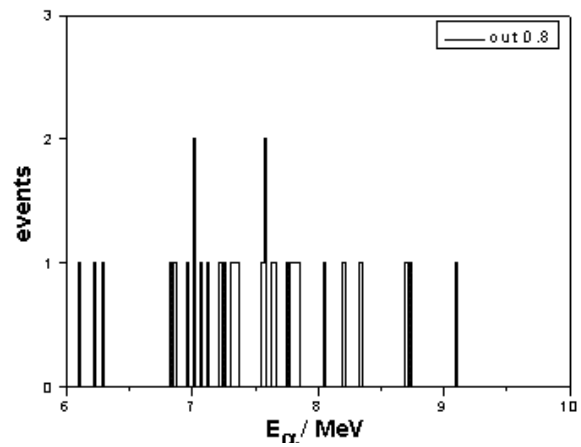

Figure 5b.

A new application of LSC with the digital recording of pulses is the determination of spectroscopic data. Pile ups are often associated with coincident nuclear transistions. If these transitions occur in the nanosecond regime, a pile up can be resolved such that the two radiations can be separated.This enables one to determine lifetimes of excited states. An example is given in Fig. 6 for a measurement of ^{241}Am. The α-decay of ^{241}Am populates the 5/2$^-$ level in ^{237}Np at 59.5 keV having a lifetime of 67 ns. This correlated α-γ decay produces pile ups in the scintillator. Fig. 6a gives an example. From the distance between the two peaks, a time difference Δt can be determined. The number of pile ups of a given Δt plotted vs. Δt is shown in Fig. 6b. From the fit of an exponential decay law to these data, the lifetime of the excited state can be determined to 67 ns in good ageement with published data. Thus, this application is promising as it allows the determination of hitherto unknown decay properties of short - lived nuclei.

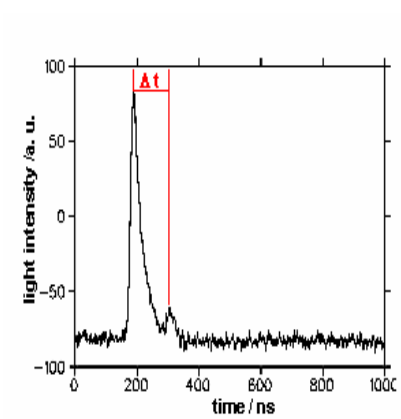

Figure 6a.

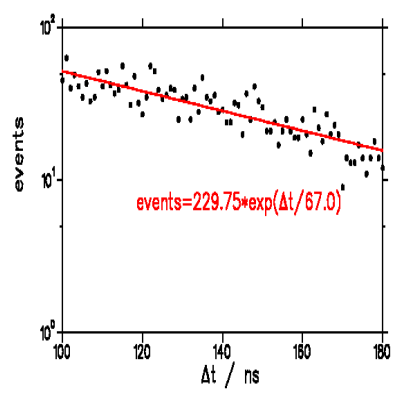

Figure 6b.

References

[1] H. Person et al., Radiochimica Acta **48**, 177 (1989).
[2] J. Meiler, www.jens-meiler.de, (1994-2000).
[3] P. Werbos, Proc. Int. Federation for Information Processes, 762, (Springer Verlag 1982).

Perspectives of the some computer methods using for the transactinide experimental and theory data treatment

M. Myagkova-Romanova[1], L.L. Makarov[1]

[1] Saint Petersburg State University, Russia

suna@mailbox.alkor.ru

Spontaneous radioactive decay of nuclear belongs to that category of the natural phenomena which reasons, by virtue of complexity of objects, have not received a strict scientific explanation yet. The advanced interest to this phenomena, as having major significance in human life, results, on the one hand, in accumulation of the comprehensive experimental material and, with another hand, in the plenty of theories about its physical nature. On the basis of theories the different mathematical models are created for experimental data processing and the nuclear behavior predicting. Computer modelling is modern and quickly developing method for the complicated physical and chemical processes studying, both for the treatment of the experimental data bulk, and for the theoretical researches. Therefore it seems to be useful to apply some computer methods to the radioactive decay processes investigating.

Spontaneous radioactive decay such as α -decay and spontaneous fission are the properties intrinsic in main to heavy nucleus: actinides and transactinides. One of the problem in modern nuclear physics and radiochemistry is to establish dependence between nuclear composition and half-life of radioactive isotopes and to predict stability of still undiscovered nucleus. Theoretical calculations of nucleus stability are based on the two main physical models: 'liquid -drop' and shell model [1]. The essence of these models is reduced to consideration of nuclear binding energy and calculations for α-particles or fragment particles after spontaneous fission of the potential barrier penetration probability that radioactive decay constant is depended on.

Properly process of nuclear disintegration is described by "liquid-drop" model. On analogy to a drop of a liquid any small distortion of the nuclear sphere will be associated with the surface tension and Coulomb energies increasing so the total nuclear binding decreasing. The main conclusion of this model was that fissionability of nucleus may be expected to correlate with parameter Z^2/A . By several semiempirical energy equations this parameter was calculated as 45-49. Thus all nuclei with $Z^2/A > 49$ are expected to undergo fission instantaneously and limit is set to the synthesis of transuranium elements at $Z \approx 110\text{-}120$.Thought the liquid-drop model explains many features of the nuclear disintegration process some of the experimentally facts could not be interpreted in this framework, especially the "magic numbers" of protons and neutrons at which nucleus are most stable and existence of heavy and superheavy elements. Dependence between number of the nucleons in nucleus and its stability is well described by the shell model, where shell structure in nuclei is proposed as analogous to the electron structure in atoms. The quantum calculations of energy levels showed that the filled shells have numbers of neutrons or protons equal to "magic numbers" and that nuclei are more stable which compositions are closer to the filled shells. Influence of the "shell effects" is important for all nuclei, however for the heaviest nuclei the most essentially. The introduction of the shell term in the formula for energy of a nucleus [2] has essentially improved the convergence between calculations and experimental data of the nuclear stability . Theoretical calculations using the unified "drop-shell" model has allowed to predict an opportunity of existence of unknown stable superheavy nuclei - "islands of stability", presumably in the area of Z=114. The experiments which have been carried out by scientists from Lawrence Berkeley National Laboratory (USA) , Flerov Laboratory in Dubna (Russia) and Research Center Rossendorf (Germany) have confirmed theoretical prediction [3] . Though the "island of stability" is not achieved yet, experimenters have precisely shown, that influence of neutron environment with N=162 (the next filled

shell predicted) on half-life of the synthesized nucleus already is observed [4] . Here interests of theorists closely adjoin to interests of experimenters as on the basis of theoretical predictions of "islands of stability" the new techniques of synthesis were development and new superheavy elements have been produced.

Nevertheless it seems to be noticed that functional dependence between nuclear composition (*Z* and *A*) and stability of isotopes is so complicated that in correspondence mathematical models semiempirical functions and parameters are usually used and sometimes experimental and calculation data are diverging. In this connection it seems to be useful to apply computer modelling methods to the treatment of the heavy elements experimental data and theoretical models complement and evolving.

For that purposes we selected database and interactive graphics computer methods and created the programs RADCHEM 1.0 and RADCHEMGRAF 1.0 presented here. RADCHEM 1.0 is the database containing as experimental data about isotopes (half-life, a kind of radioactive decay, decay energy characteristics, products of decay etc) as theoretical models explaining received experimental data. Submitting the data in such form is convenient for statistical and correlation analysis. So the investigations for actinides isotopes showed, that at the specified sampling of the unstable nucleus configurations by the probability theory and combinatorial numerical method the correlation between half-life and number of matching of protons and neutrons laid out above the last filled shell could be observed. RADCHEMGRAF 1.0 is the 3D-graphic program for the visual representation and analysis of several computed configurations of nuclei. As shown on the figure nucleus are imaged using mathematical model of “spheres density packing” (as more corresponded to nuclear “liquid drop –shells” model).

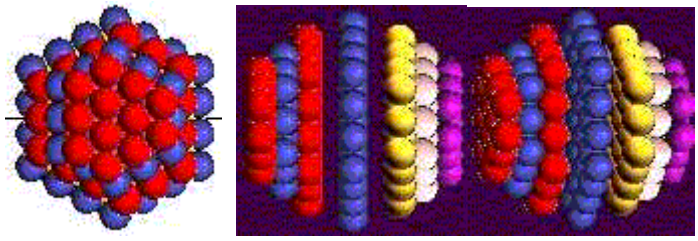

Figures 1-3. Surface energy differences for number of configurations for actinides isotopes calculated by the RADCHEMGRAF 1.0 also correlated with its stability.

We believe that the development of presented computer method lead to carry out more accurate calculations and to obtain further information, which could be supplement to the theoretical models. Then it will be perspective to apply RADCHEM 1.0 and RADCHEMGRAF 1.0 for education of specialists in radiochemistry as information resource and visual aids . For this purposes it seems to be very useful to replenish RADCHEM 1.0 with data for transactinides and we hope that TAN 03 Conference open up opportunities to make it.

References

[1] *G. Friedlander, J.W. Kennedy, J. M. Miller,* “Nuclear and Radiochemistry”, New York-London-Sydney, 1964.

[2]

[3] *Oganessian Yu. Ts.,* Nucl. Phys. **A583**. (1995).

[4] *Lazarev Yu. A., Lobanov Yu. V., Oganessian Yu. Ts., Utyonkov V. K., Abdullin F. Sh., Buklanov G. V., Gikal B. N., Iliev S., Mezentsev A. N., Polyakov A. N., Sedykh I. M., Shirokovsky I. V., Subbotin V. G., Sukhov A. M., Tsyganov Yu. S., Zhuchko V. E., Lougheed R. W., Moody K. J., Wild J. F., Hulet E. K., McQuaid J. H.,* Phys. Rev. Lett. **73**, 624 (1994).

[5] *H.Gould, J.Tobochnic* "An Introduction to Computer Simulation Methods Applications to Physical Systems", Addison-Wesley Publishing Company, 1988.

Optical spectroscopy of the heaviest elements

M. Sewtz[1], H. Backe[1], A. Dretzke[1], W. Lauth[1], P. Schwamb[1], K. Eberhardt[2], P. Thörle[2], N. Trautmann[2], P. Kunz[3], G. Passler[3], S. Fritzsche[4], R.G. Haire[5]

[1] Institut für Kernphysik Universität Mainz, Germany
[2] Institut fuer Kernchemie Universitaet Mainz, Germany
[3] Institut für Physik Universität Mainz, Germany
[4] University Kassel, Germany
[5] ORNL, USA

sewtz@kph.uni-mainz.de

The investigation of atomic, chemical and nuclear properties of heavy elements with charge numbers of Z > 100 is a real challenge. Heavy elements are produced in nuclear fusion reactions with rates of sometimes only a few atoms per week [1]. Their life-times are short, occasionally only in the order of milliseconds. At present, the most advanced method for the investigation of the properties of heavy elements is chemistry on single atoms in aqueous solutions [2] and in the gas phase [3]. This technique has already yielded detailed chemical information up to Z=108 [4]. Such experiments aid in the investigation of relativistic effects. For the heaviest elements these may result in alterations from expectations within a period of homologue elements. Relativistic effects, roughly speaking, originate from a shrinkage of the wave functions of inner shell electrons which, in turn, influence the binding energy of the valence electrons and thus the chemical properties. In the actinide region these are the 5f-, 6d-, 7p- and 7s- orbitals. Therefore, a more direct approach to investigate relativistic effects may be to study first ionization potentials (IP) or, even better, the atomic level schemes, both experimentally and by relativistic ab-initio multiconfiguration Dirac-Fock (MCDF) calculations or other methods [5-7]. However, any atomic spectroscopy, even with the most sensitive laser methods, is hampered by the fact that a broad band search for levels is limited due to the small number of atoms available for the studies. To obtain reliable information under these circumstances, it is necessary to incorporate theoretical level predictions in performing the experiments.

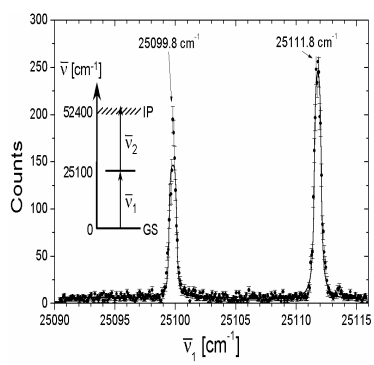

Figure 1. Observed levels in Fermium. The full line shows the best fit of a power broadened line profile to the data.

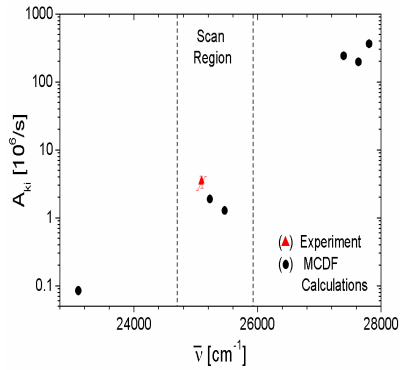

Figure 2. Partial transition rates to the $5f^{12}\,7s^2\,{}^3H^e_6$ ground state as function of the level energie $\bar{\upsilon}$.

In this contribution we report our successful search for predicted atomic levels for elemental fermium for which experimental information was not available previously. The experiments [8] were performed with only a sample of 2.7×10^{10} atoms of the isotope ^{255}Fm which was bred in the high flux isotope reactor at ORNL, USA. The atoms with a half-life of 20.1 h were evaporated at a temperature of about 1,000 °C from a filament and stored in the argon buffer gas of an optical cell [9]. Atomic levels were sought by the method of resonance ionization spectroscopy using an excimer-dye-laser combination. Two atomic levels were found at wave numbers (25,099.8 ± 0.2) cm^{-1} and (25,111.8 ± 0.2) cm^{-1}, see Fig. 1. Partial transition rates to the $5f^{12}\,7s^2\,{}^3H^e_6$ ground state have been determined from their saturation characteristics. By comparison of the absolute level energies, as well as the partial transition rates with Multiconfiguration-Dirac-Fock (MCDF) calculations, term assignments of the observed levels are proposed. The calculations suggest that the leading orders of these levels could be the $5f^{12}\,7s7p\,{}^5I^o_6$ and $5f^{12}\,7s7p\,{}^5G^o_5$ term.

In a follow up experiment the three optical transitions around 27,500 cm^{-1} with large Einstein-coefficients of about $3 \cdot 10^8$ /s were sought for. Five additional lines were found in the wave number region of 27,100 to 28,400 cm^{-1}, see Fig. 3. A possible term assignment will be discussed.

Due to the small samples which were available, the ionization potential of fermium could not be determined, so far. However, an upper limit of 52,140 cm^{-1} was deduced from the experiment. This is in agreement with extrapolations of spectral properties, which yield IP=52,400(600) [10] and MCDF calculations which yield IP=50,800(2400) cm^{-1} [11].

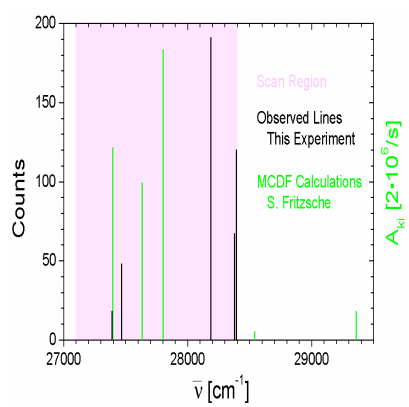

Figure 3. Wavenumber scan from 27,100 cm^{-1} to 28,4000 cm^{-1} and MCDF calculations.

References

[1] S. Hofmann and G. Münzenberg, Rev. Mod. Phys. **72**, 733 (2000).
[2] M. Schädel, Radiochim. Acta **89**, 721 (2001).
[3] A. Türler, Radiochim. Acta **72**, 7 (1996).
[4] Ch.E.Düllmann et al., Nature (London) **418**, 859 (2002).
[5] B. Fricke, E. Johnson, and G. M. Rivera, Radiochim. Acta **62**, 17 (1993).
[6] E. Eliav, U. Kaldor, and Y. Ishikawa, Phys. Rev. Lett. **74**, 1079 (1995).
[7] W. C. Martin and J. Sugar, Phys. Rev. **A 53**, 1911 (1996).
[8] M. Sewtz et al., Phys. Rev. Lett. **90**, 163002-1 (2003).
[9] H. Backe et al., Nucl. Instrum. Methods Phys. Res., **B 126**, 406 (1997).
[10] J. Sugar, J. Chem. Phys. **60**, 4103 (1974).
[11] S. Fritzsche. Proceedings of the International Workshop on Ion Chemical Aspects in Ion Guide Systems, Universität Mainz, 30.September-2.October 1999.

Development of a plutonium ceramic target for the MASHA separator

D.A. Shaughnessy[1], K.J. Moody[1], J.M. Kenneally[1], J.F. Wild[1], M.A. Stoyer[1], J.B. Patin[1], R.W. Lougheed[1], A.V. Yeremin[2], Y.T. Oganessian[2]

[1] Lawrence Livermore National Laboratory, USA
[2] Joint Institute for Nuclear Research, Russia

shaughnessy2@llnl.gov

We are currently working on the development of a solid Pu ceramic target for use in the MASHA (Mass Analyzer of Super Heavy Atoms) on-line mass separator in Dubna. Along with recent upgrades of the U400 Cyclotron, MASHA will provide for at least a ten-fold increase in the production and detection rate for element 114 atoms, and will allow us to measure their atomic weights precisely. The MASHA separator will employ a thick Pu ceramic target capable of tolerating temperatures in the range of 2000 °C without vaporizing the actinide target. Promising candidates for the Pu target include Pu carbides and nitrides, although more research into the thermodynamic properties of these compounds will be required. Reaction products will diffuse out of the target and will drift to an ECR ion source after which they will be transported through the separator and will impinge on a position-sensitive focal-plane detector array. Furthermore, operation of the MASHA hot target/ion source combination will provide chemical volatility information that will support our assignment of an atomic number of 114 to these nuclei. Taken together, we expect that experiments on MASHA will allow us to make measurements that will cement our identification of element 114 and provide for future experiments in which the chemical properties of the heaviest elements are studied.

Author Index

A

Abe, Y., 37
Ackermann, D., 132
Adams, J.L., 124
Afanasjev, A., 15
Ahmad, I., 4, 15
Akiyama, K., 20, 78, 85, 96
Aleklett, K., 138
Alstad, J., 81, 105, 113
Amzal, N., 15
An, T.T., 155
Angert, R., 88
Anton, J., 191
Asai, M., 20, 78, 85, 96
Asano, T., 55

B

Backe, H., 199, 218
Balasubramaniam, M., 50
Balasubramanian, K., 184
Bastug, T., 185
Belozerov, A.V., 149
Bilewicz, A., 186
Bouriquet, B., 37
Brandt, R., 31
Brüchle, W., 88, 108, 124
Bürger, S., 88
Butler, P.A., 15

C

Carpenter, M.P., 15
Chatillon, A., 154
Chepigin, V.I., 149
Chewter, A.J., 15
Cizewski, J.A., 15
Cloughesy, M., 158
Cuong, P.V., 170

D

Davids, C.N., 15
Dmitriev, S.N., 204
Do, N.V., 155
Dressler, R., 108, 124, 163, 205
Dretzke, A., 218
Drouart, A., 143
Düllmann, Ch.E., 67, 92, 108, 117, 124, 165

E

Eberhardt, K., 88, 108, 163, 210, 218
Eichler, B., 108, 124, 163, 205
Eichler, R., 63, 88, 108, 124, 163, 205
Eliav, E., 180, 192

F

Folden, C.M., III, 92, 108, 117, 165
Frauendorf, S., 15
Fricke, B., 177, 191
Fritzsche, S., 218

G

Gäggeler, H.W., 108, 124, 163, 195, 205
Gelber, S., 31
Gentry, R.V., 31
Ginter, T.N., 138
Goto, S.I., 78, 96
Greenlees, P.T., 15
Gregorich, K.E., 92, 108, 117, 124, 138, 165, 198
Greiner, W., 14
Gupta, P.K., 165
Gupta, R.K., 50

H

Haba, H., 78, 85, 96
Haenssler, F., 108, 163, 205
Hainzl, C., 19
Haire, R.G., 218
Hasegawa, H., 78
Hashimoto, K., 78
Heenen, P.H., 3
Heinz, A., 15, 42
Helariuta, K., 15
Herzberg, R.D., 15
Hessberger, F.P., 7
Hirai, T., 96
Hirata, M., 78, 85
Hoffman, D.C., 92, 113, 117, 124, 165
Hofmann, S., 149
Hohn, A., 205
Hübener, S., 124
Hummrich, H., 88, 100

I

Ichikawa, S.I., 20, 78, 96
Ishii, T., 20
Ishizu, H., 78

Itkis, M.G., 149, 204
Ito, M., 78

J

Jäger, E., 88, 108
Janssens, R.V.F., 15
Jera, R., 88
Jones, G., 15
Jones, G.D., 162
Jost, D.T., 124
Julin, R., 12, 15
Junghans, A.R., 42

K

Kabachenko, A.P., 149
Kaldor, U., 180, 192
Kaneko, T., 96
Kankaanpää, H., 15
Kasamatsu, Y., 24
Kawase, Y., 24
Kenneally, J.M., 221
Kettunen, H., 15
Khoo, T.L., 15
Kikunaga, H., 24, 78
Kimura, H., 24
Kinoshita, N., 78
Kirbach, U.W., 124
Kling, H.O., 88, 210
Kolb, D., 31
Kondev, F., 15
Kosenko, G., 37
Kratz, J.V., 78, 88, 100, 103, 108, 200, 210
Krille, U., 88
Kronenberg, A., 103
Kuczewski, B., 88
Kudo, H., 78, 96
Kumar, R., 50
Kunz, P., 218
Kuusiniemi, P., 15

L

Lalazissis, G.A., 15
Landau, A., 180, 192
Landrum, J.H., 169
Lane, M.R., 124
Langrock, G., 88, 210
Laue, C.A., 124, 169
Lauritsen, T., 15
Lauth, W., 218
Lavanchy, V.M., 124
Lee, D.M., 124
Lehr, G., 88, 100
Leino, M., 15
Leitner, D., 197
Lister, C.J., 15
Lougheed, R.W., 221
Loveland, W.D., 138, 158, 165

M

Mahmud, H., 165
Makarov, L.L., 215
Malyshev, O.N., 149
Marinov, A., 31
Mendel, M., 88, 100, 210
Miranda, P., 138
Mitsugashira, T., 24
Miyamoto, Y., 78
Mohapatra, P., 103
Moody, K.J., 169, 221
Morita, K., 137
Morrissey, D., 144
Myagkova-Romanova, M., 215
Myers, N., 138

N

Nagame, Y., 20, 78, 85, 96
Nähler, A., 88, 210
Nakahara, H., 78
Nakanishi, T., 24
Nash, C.S., 182
Nishinaka, I., 20, 78
Nitsche, H., 92, 113, 117, 124, 165
Nolen, J.A., 148

O

Oganessian, Yu.Ts., 131, 149, 169, 204, 221
Ohkubo, Y., 24
Ohta, M., 55
Ohtsuki, T., 24
Omtvedt, J.P., 81, 105, 113
Ono, S., 96
Osa, A., 20
Oura, Y., 20, 78

P

Pang, G.K., 92
Pape, A., 31
Passler, G., 218
Patin, J.B., 124, 138, 169, 221
Patyk, Z., 23
Peil, A., 88
Pershina, V., 88, 173, 185, 191
Péter, J., 143
Peterson, D., 138, 165
Pfrepper, G., 103
Piguet, D., 108, 124, 163
Poláková, D., 81, 105

Popeko, A.G., 149
Pyykkö, P., 183

Q

Qin, Z., 108, 205

R

Reddy, A.V.R., 103
Reiter, P., 15
Rieth, U., 88, 100

S

Sagaidak, R.N., 149
Saito, J., 78
Sakama, M., 20, 78
Saro, S., 149
Sarpe-Tudoran, C., 191
Sato, W., 24, 78
Schädel, M., 78, 88, 108, 124, 163, 165
Schausten, B., 88, 108
Schimpf, E., 88, 108, 163
Schmidt, K.H., 42
Schött, H.-J., 88, 108
Schwamb, P., 218
Schwantes, J.M., 165
Schwerdtfeger, P., 179
Sepp, W., 191
Seth, M., 179
Seweryniak, D., 15
Sewtz, M., 218
Shaughnessy, D.A., 124, 169, 221
Shen, C., 37
Shibata, M., 20
Shibata, S., 24
Shinohara, A., 24, 78
Shutov, A.V., 149
Siedentop, H., 19
Siem, S., 15
Singh, N., 50
Skarnemark, G., 81, 105
Smolańczuk, R., 13
Son, N.N., 155, 170
Sonzogni, A.A., 15
Soverna, S., 108, 163, 205
Stavsetra, L., 81, 105, 113
Stiel, E., 88
Stodel, C., 143
Stoyer, M.A., 169, 221
Strellis, D.A., 124
Sudowe, R., 92, 117, 165
Sueki, K., 20, 78, 85
Svirikhin, A.I., 149
Swiatecki, W., 41

T

Takamiya, K., 24
Tani, Y., 78
Taut, S., 124
Tharun, U., 210
Thiep, T.D., 155, 170
Thörle, P., 88, 100, 163, 218
Tobler, L., 124
Tomar, B.S., 103
Törle, P., 108
Toyoshima, A., 78, 85, 96
Trautmann, N., 88, 108, 163, 210, 218
Tripathi, R., 103
Tsukada, K., 20, 78, 85, 88, 96
Tsyganov, Y.S., 124
Türler, A., 59, 108, 124

U

Utyonkov, V.K., 169
Uusitalo, J., 15

V

Vahle, A., 124
Volkers, K.J., 120

W

Wada, T., 55
Wiedenhöver, I., 15
Wiehl, N., 88, 210
Wierczinski, B., 120
Wild, J.F., 169, 221
Wilk, P.A., 108, 124
Wirth, G., 88

Y

Yaita, T., 85
Yakushev, A.B., 73, 108, 124
Yamana, H., 24
Yasuda, K., 78
Yeremin, A.V., 149, 221
Yokoyama, A., 78
Yuki, H., 24

Z

Zagrebaev, V.I., 45
Zheng, L., 81, 105
Zielinski, P.M., 92, 117, 165
von Zweidorf, A., 88, 108